www.amonline.net.au/publications/ ISSN 0067-1975

RECORDS OF THE AUSTRALIAN MUSEUM

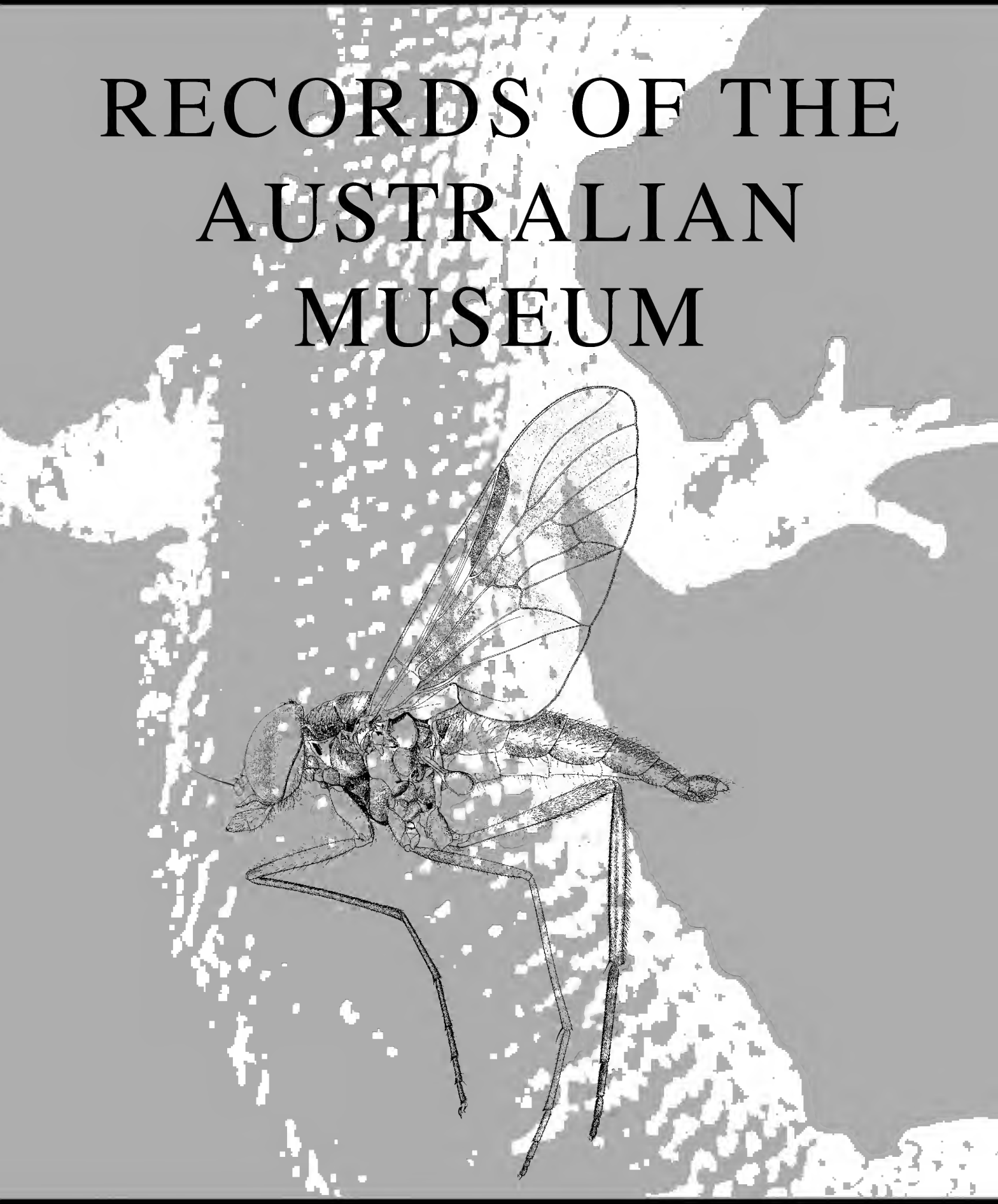

VOLUME 55 NUMBER 2 13 August 2003

RECORDS OF THE AUSTRALIAN MUSEUM

The Australian Museum, Sydney

Published 13 August 2003

Price: AU$50.00

Printed by RodenPrint Pty Ltd, Sydney

ISSN 0067-1975

The Australian Museum's mission is to research, interpret, communicate and apply understanding of the environments and cultures of the Australian region to increase their long-term sustainability. The Museum has maintained the highest standards of scholarship in these fields for more than 175 years, and is one of Australia's foremost publishers of original research in anthropology, geology and zoology.

The *Records of the Australian Museum* (ISSN 0067-1975) publishes the results of research on Australian Museum collections and of studies that relate in other ways to the Museum's mission. There is an emphasis on Australasian, southwest Pacific and Indian Ocean research. The *Records* is released annually as three issues of one volume, volume 54 was published in 2002. Monographs are published about once a year as *Records of the Australian Museum, Supplements*. Supplement 28 (ISBN 0 7347 2313 X) was published in June 2003. Catalogues, lists and databases have been published since 1988 as numbered *Technical Reports of the Australian Museum* (ISSN 1031-8062). *Technical Report* number 17 was published in March 2003. *Australian Museum Memoirs* (ISSN 0067-1967) ceased in 1983.

These three publications—*Records*, *Supplements* and *Technical Reports*—are distributed to libraries throughout the world and are now uploaded at our website six months after they are published. Librarians are invited to propose exchange agreements with the *Australian Museum Research Library*. Back issues are available for purchase direct from the *Australian Museum Shop*.

Authors are invited to submit manuscripts presenting results of their original research. Manuscripts meeting subject and stylistic requirements outlined in the *Instructions to Authors* are assessed by external referees.

www.amonline.net.au/publications/

Back issues may be purchased at the Australian Museum Shop or online at

www.amonline.net.au/shop/

The **cover illustration**—by Cape Town botanist and artist Dr John Manning—is of an athericid fly from the Claudie River and Jardine River systems in the north of Cape York Peninsula. The insect (*Suraginella macalpinei* Stuckenberg, 2000) was described in *Records of the Australian Museum* 52(2) and is thought to be blood-sucking. The faded impression (original photo by G.C. Clutton) of a Solomon Islands skink lizard—*Tribolonotus ponceleti* Kinghorn, 1937—which was also first described in an earlier issue of *Records of the Australian Museum* 20(1) provides background.

Since 1999 Australian Museum Scientific Publications have been released as PDF files, at our website, free of charge and six months after publication. The above description of the new genus *Suraginella* and the new species *macalpinei* can be viewed at www.amonline.net.au/pdf/publications/1312_complete.pdf or purchased as part of a bound issue (AU$33.00) from the Australian Museum Shop.

Records of the Australian Museum (2003) Vol. 55: 113–116. ISSN 0067-1975

A New Pygmy Seahorse (Pisces: Syngnathidae: *Hippocampus*) from Lord Howe Island

RUDIE H. KUITER

Ichthyology, Museum Victoria, Melbourne Victoria 3001, Australia

rudie.kuiter@zoonetics.com · syngnathiformes@zoonetics.com

ABSTRACT. A new species of seahorse, *Hippocampus colemani*, is described from Lord Howe Island off eastern Australia. It can be distinguished from congeners by the following combined features: very small size (to about 23 mm in height), very deep trunk (about 60% in its length), low number of tail rings (27–29) and most distinctly, a single gill opening, placed dorsally behind the head.

KUITER, RUDIE H., 2003. A new pygmy seahorse (Pisces: Syngnathidae: *Hippocampus*) from Lord Howe Island. *Records of the Australian Museum* 55(2): 113–116.

Seahorses are currently placed in a single genus: *Hippocampus* (family Syngnathidae). The Australian species were recently revised by Kuiter (2001), who recognized 24 species, two of which are diminutive, reaching less than 50 mm height. The two are collectively known as pygmy seahorses. These tiny species usually occur at depths of 30 m or more, but a third pygmy species was discovered at a depth of only 5 m in the lagoon at Lord Howe Island in the Tasman Sea. A description of the species, based on two specimens, is presented here.

Materials and methods

Methodology follows that of Kuiter (2001), except specimens were photographed and enlarged 20 times and proportional measurements recorded from the enlarged photos. Radiographs were used to confirm the number of tail rings. Sex was determined on the absence or presence of a pouch, however, in pygmy species this character is not as obvious as in the larger species. In all seahorse species, including pygmy species, the position of the anus in both sexes is at the same horizontal level in relation to the dorsal fin base. All males have a pouch and the anus is positioned further away from the body axis compared to the female. The pouch can look somewhat like a posterior extension of the trunk since the anus is often not obvious, especially when brooding. This is applicable to pygmy seahorses and sex can be determined by the posterior reach of their trunk and pouch combined in relation to the horizontal level with the dorsal-fin base, especially when working with photographs. The specimens are deposited in the Australian Museum, Sydney (AMS).

Hippocampus colemani n.sp.

Figs. 1, 2

Coleman's Pygmy Seahorse

Type material. HOLOTYPE: AMS I41181-001, height 22.1 mm, female, near Erscott's Hole, lagoon, Lord Howe Island, New South Wales (approximately 32°32.950'S 159°05.080'E), depth 5 m, collected by hand, Neville Coleman, January, 2002. PARATYPE: AMS I41181-002, height 21.4 mm, female, same data as holotype.

Diagnosis. Dorsal-fin rays 12–13; pectoral-fin rays 10; anal fin absent; trunk rings 11; tail rings 27–29; nose ridge well

www.amonline.net.au/pdf/publications/1382_complete.pdf
[includes a colour version]

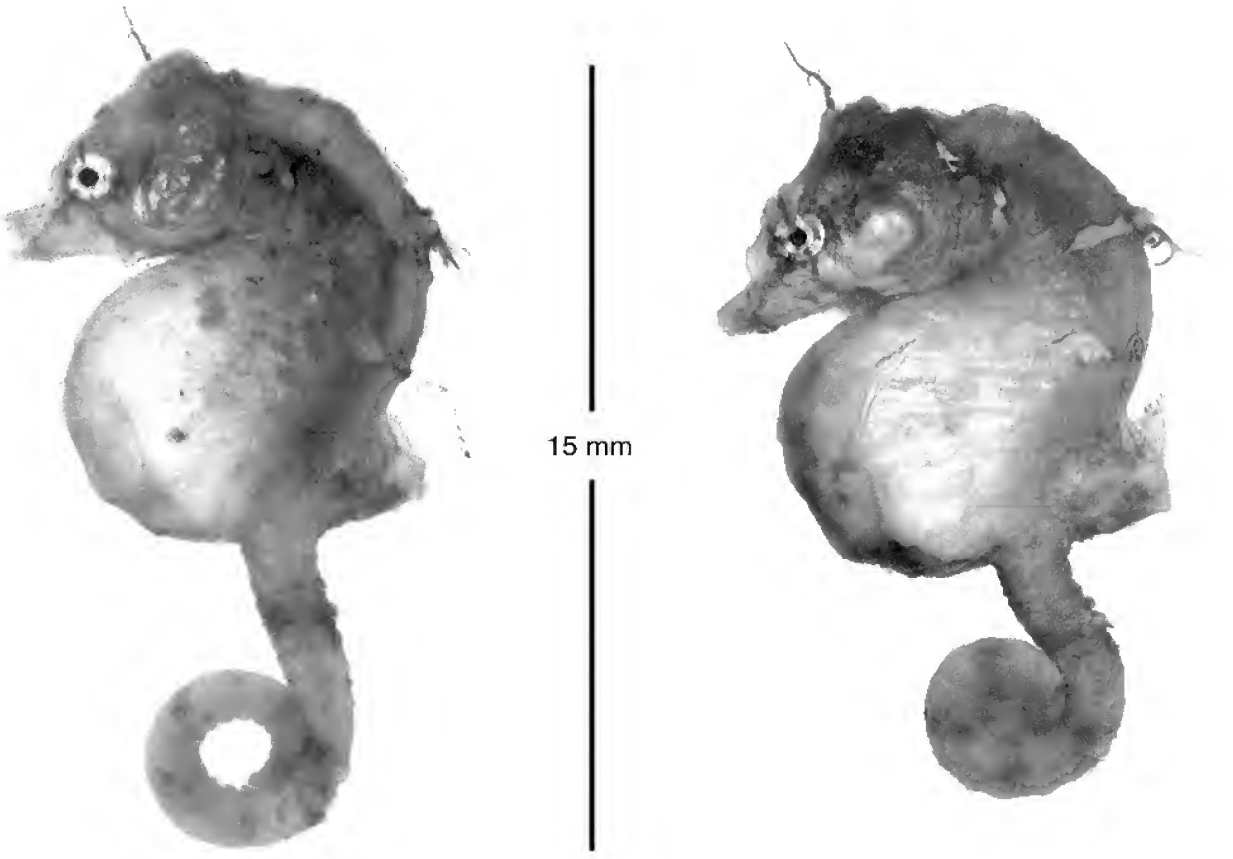

Fig. 1. *Hippocampus colemani*, holotype AMS I41181-001 (left) and paratype AMS I41181-002 (right), both female.

developed in front of eye; a single gill opening on the neck ridge, directly behind the head; base of dorsal fin greatly elevated posteriorly, forming a triangular hump on the back.

Description. Head small, c. 50% of trunk length and strongly angled down onto trunk; snout short, length about equal to eye diameter; trunk very deep, c. 60% of its length; tail thin, 1.3 times eye diameter, its greatest depth and width anteriorly, and its length 58% in height (overall, see fig. 3, Kuiter, 2001); dorsal fin with 12 rays (13 in paratype), its base greatly elevated posteriorly so that fin rays almost parallel with trunk axis, height of fin base at posterior end almost equal to its length; pectoral-fin rays 10; anal fin absent; trunk rings 11, obscured and smooth dorsally; tail rings 29 (27 in paratype); trunk and tail ridges poorly developed, mostly indistinguishable and only evident on lower two-thirds of trunk, as ventral and inferior ridges; all spines reduced to tubercles, those on back at 4th, 7th and 11th rings enlarged and most notable, largest below dorsal-fin base, and on head as lateral head spines, some with dermal appendages; coronet low and rounded with tentacle like dermal appendage anteriorly (also in paratype); nose spine present as well-developed ridge in front of eye; single relatively large gill opening, slightly raised by skin, and situated mid-dorsally on neck ridge, immediately behind head. Colour in life (paratype): body mostly pale golden-yellow; trunk with white circular or elliptical markings, each outlined with thin red lines, largest around tubercles on 4th and 7th rings; shoulder-ring tubercles white; head white on nape above eyes, extending over snout to tip of mouth, highlighting several dusky brown bands radiating from eye; tail slightly more brown with red markings, some expressed as elongate spots on same ring, suggesting a band. Colour in alcohol: pale brownish all over, some thin dark lines near tubercles on body and dusky bands radiating from eye.

Distribution and ecology. Only known from the types and two additional specimens photographed (Figs. 3, 4), but not collected at Lord Howe Island, off the New South Wales coast. All were found in the same general area at a depth of 5 m. The habitat is comprised of coarse sand with sparse *Zostera* and *Halophila* plants that have fine filamentous algae on their leaves. The same algae are present on the body of the seahorses, attached to their skin.

Remarks. This species is named *colemani* after Mr Neville Coleman, who discovered and photographed the species at Lord Howe Island, and then returned specifically to collect the type material. Only 4 specimens have been observed, the largest was collected and measured at 22.1 mm in height. Judging by its shape, it appears to be fully grown and would unlikely get much larger. At this stage it is the smallest known seahorse. Despite its small size, it is surprising that it has gone unnoticed until now. Several extensive fish surveys have been undertaken at Lord Howe Island, the largest and most comprehensive led by the

Fig. 2. *Hippocampus colemani*, paratype AMS I41181-002, in situ. Photo by Neville Coleman.

Fig. 3. *Hippocampus colemani*, this specimen not collected, sex not determined. The single gill opening is arrowed. Photo by Neville Coleman.

Fig. 4. *Hippocampus colemani*, this specimen not collected. A probable male as it appears to have a pouch. Photo by Neville Coleman.

Australian Museum in 1973. At the time, a team of 15 collectors, 8 of whom were ichthyologists, collected constantly for one month (Allen *et al.*, 1976), and did not find this seahorse.

The closest relative of *Hippocampus colemani* in Australian waters is *H. bargibanti* Whitley, a tropical species that lives on gorgonian corals. It has similar meristic values and shares the greatly elevated dorsal-fin base, but is quite different in its fleshy and lumpy appearance, and has a longer tail. From a global perspective, most similar in its morphology is a pygmy species from Japan (sp. 7, Kuiter, 2000) that is nearly identical in shape and has an almost identically formed nose ridge. Kuiter's *Hippocampus* sp. 7, however, has small but distinctive spines along the trunk and tail ridges. A further similar species that appears to be closely related (sp. 6, Kuiter, 2000) occurs on gorgonians in Papua New Guinea, but is only known from photographs. All share the unusually elevated dorsal-fin base that forms a large hump on their back. The feature of a single gill opening (see Figs. 2, 3) appears to be the same in the Japanese and the Papua New Guinea species (not clear in photographs). It is likely that the three species form a natural group, but until the relationship of all seahorses are understood the species will be retained together in the single genus *Hippocampus*.

ACKNOWLEDGMENTS. Martin Gomon, Museum Victoria provided the radiographs and commented on the manuscript. I thank Mr Geoff Kelly, Manager of the Lord Howe Island Marine Park, and Mr Patrick Tully, NSW Fisheries, for providing the collecting permit so quickly. I am most grateful to Neville Coleman who made a special trip and spent many long hours underwater just to find and collect the types plus taking the photographs in situ, and thanks to the Prodive-crew for their patience assisting Neville.

References

Allen, G.R., D.F. Hoese, J.R. Paxton, J.E. Randall, B.C. Russell, W.A. Starck, F.H. Talbot & G.P. Whitley, 1976. Annotated checklist of the fishes of Lord Howe Island. *Records of the Australian Museum* 30(15): 365–454.

Kuiter, Rudie H., 2000. *Seahorses, Pipefishes & Their Relatives*. Chorleywood (England): TMC Publications.

Kuiter, Rudie H., 2001. Revision of the Australian seahorses of the genus *Hippocampus* (Syngnathiformes: Syngnathidae) with descriptions of nine new species. *Records of the Australian Museum* 53(3): 293–340. www.amonline.net.au/pdf/publications/1350_complete.pdf

Manuscript received 25 February 2002, revised 4 August 2002 and accepted 22 August 2002.

Associate Editor: J.M. Leis.

Records of the Australian Museum (2003) Vol. 55: 113–116. ISSN 0067-1975

A New Pygmy Seahorse (Pisces: Syngnathidae: *Hippocampus*) from Lord Howe Island

RUDIE H. KUITER

Ichthyology, Museum Victoria, Melbourne Victoria 3001, Australia

rudie.kuiter@zoonetics.com · syngnathiformes@zoonetics.com

ABSTRACT. A new species of seahorse, *Hippocampus colemani*, is described from Lord Howe Island off eastern Australia. It can be distinguished from congeners by the following combined features: very small size (to about 23 mm in height), very deep trunk (about 60% in its length), low number of tail rings (27–29) and most distinctly, a single gill opening, placed dorsally behind the head.

KUITER, RUDIE H., 2003. A new pygmy seahorse (Pisces: Syngnathidae: *Hippocampus*) from Lord Howe Island. *Records of the Australian Museum* 55(2): 113–116.

Seahorses are currently placed in a single genus: *Hippocampus* (family Syngnathidae). The Australian species were recently revised by Kuiter (2001), who recognized 24 species, two of which are diminutive, reaching less than 50 mm height. The two are collectively known as pygmy seahorses. These tiny species usually occur at depths of 30 m or more, but a third pygmy species was discovered at a depth of only 5 m in the lagoon at Lord Howe Island in the Tasman Sea. A description of the species, based on two specimens, is presented here.

Materials and methods

Methodology follows that of Kuiter (2001), except specimens were photographed and enlarged 20 times and proportional measurements recorded from the enlarged photos. Radiographs were used to confirm the number of tail rings. Sex was determined on the absence or presence of a pouch, however, in pygmy species this character is not as obvious as in the larger species. In all seahorse species, including pygmy species, the position of the anus in both sexes is at the same horizontal level in relation to the dorsal fin base. All males have a pouch and the anus is positioned further away from the body axis compared to the female. The pouch can look somewhat like a posterior extension of the trunk since the anus is often not obvious, especially when brooding. This is applicable to pygmy seahorses and sex can be determined by the posterior reach of their trunk and pouch combined in relation to the horizontal level with the dorsal-fin base, especially when working with photographs. The specimens are deposited in the Australian Museum, Sydney (AMS).

Hippocampus colemani n.sp.

Figs. 1, 2

Coleman's Pygmy Seahorse

Type material. HOLOTYPE: AMS I41181-001, height 22.1 mm, female, near Erscott's Hole, lagoon, Lord Howe Island, New South Wales (approximately 32°32.950'S 159°05.080'E), depth 5 m, collected by hand, Neville Coleman, January, 2002. PARATYPE: AMS I41181-002, height 21.4 mm, female, same data as holotype.

Diagnosis. Dorsal-fin rays 12–13; pectoral-fin rays 10; anal fin absent; trunk rings 11; tail rings 27–29; nose ridge well

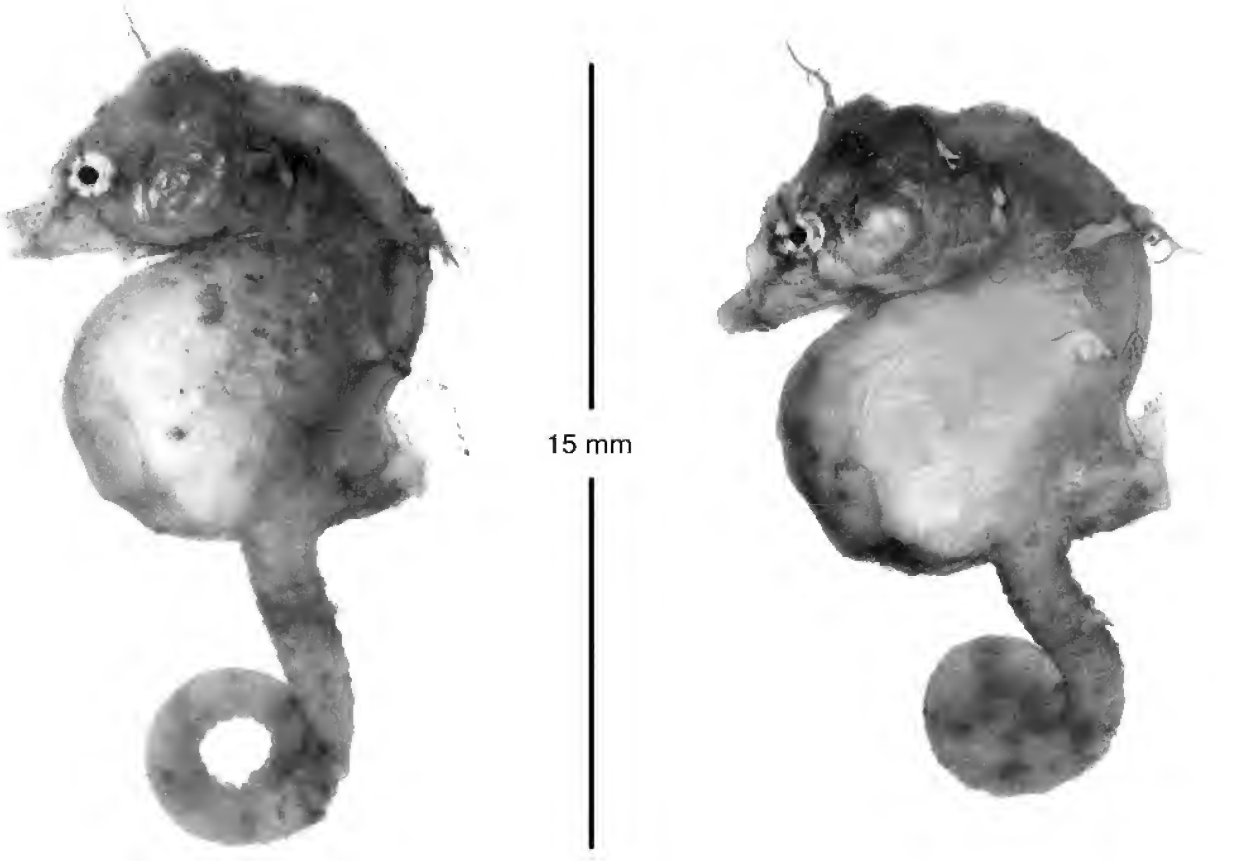

Fig. 1. *Hippocampus colemani*, holotype AMS I41181-001 (left) and paratype AMS I41181-002 (right), both female.

developed in front of eye; a single gill opening on the neck ridge, directly behind the head; base of dorsal fin greatly elevated posteriorly, forming a triangular hump on the back.

Description. Head small, c. 50% of trunk length and strongly angled down onto trunk; snout short, length about equal to eye diameter; trunk very deep, c. 60% of its length; tail thin, 1.3 times eye diameter, its greatest depth and width anteriorly, and its length 58% in height (overall, see fig. 3, Kuiter, 2001); dorsal fin with 12 rays (13 in paratype), its base greatly elevated posteriorly so that fin rays almost parallel with trunk axis, height of fin base at posterior end almost equal to its length; pectoral-fin rays 10; anal fin absent; trunk rings 11, obscured and smooth dorsally; tail rings 29 (27 in paratype); trunk and tail ridges poorly developed, mostly indistinguishable and only evident on lower two-thirds of trunk, as ventral and inferior ridges; all spines reduced to tubercles, those on back at 4th, 7th and 11th rings enlarged and most notable, largest below dorsal-fin base, and on head as lateral head spines, some with dermal appendages; coronet low and rounded with tentacle like dermal appendage anteriorly (also in paratype); nose spine present as well-developed ridge in front of eye; single relatively large gill opening, slightly raised by skin, and situated mid-dorsally on neck ridge, immediately behind head. Colour in life (paratype): body mostly pale golden-yellow; trunk with white circular or elliptical markings, each outlined with thin red lines, largest around tubercles on 4th and 7th rings; shoulder-ring tubercles white; head white on nape above eyes, extending over snout to tip of mouth, highlighting several dusky brown bands radiating from eye; tail slightly more brown with red markings, some expressed as elongate spots on same ring, suggesting a band. Colour in alcohol: pale brownish all over, some thin dark lines near tubercles on body and dusky bands radiating from eye.

Distribution and ecology. Only known from the types and two additional specimens photographed (Figs. 3, 4), but not collected at Lord Howe Island, off the New South Wales coast. All were found in the same general area at a depth of 5 m. The habitat is comprised of coarse sand with sparse *Zostera* and *Halophila* plants that have fine filamentous algae on their leaves. The same algae are present on the body of the seahorses, attached to their skin.

Remarks. This species is named *colemani* after Mr Neville Coleman, who discovered and photographed the species at Lord Howe Island, and then returned specifically to collect the type material. Only 4 specimens have been observed, the largest was collected and measured at 22.1 mm in height. Judging by its shape, it appears to be fully grown and would unlikely get much larger. At this stage it is the smallest known seahorse. Despite its small size, it is surprising that it has gone unnoticed until now. Several extensive fish surveys have been undertaken at Lord Howe Island, the largest and most comprehensive led by the

Fig. 2. *Hippocampus colemani*, paratype AMS I41181-002, in situ. Photo by Neville Coleman.

Fig. 3. *Hippocampus colemani*, this specimen not collected, sex not determined. The single gill opening is arrowed. Photo by Neville Coleman.

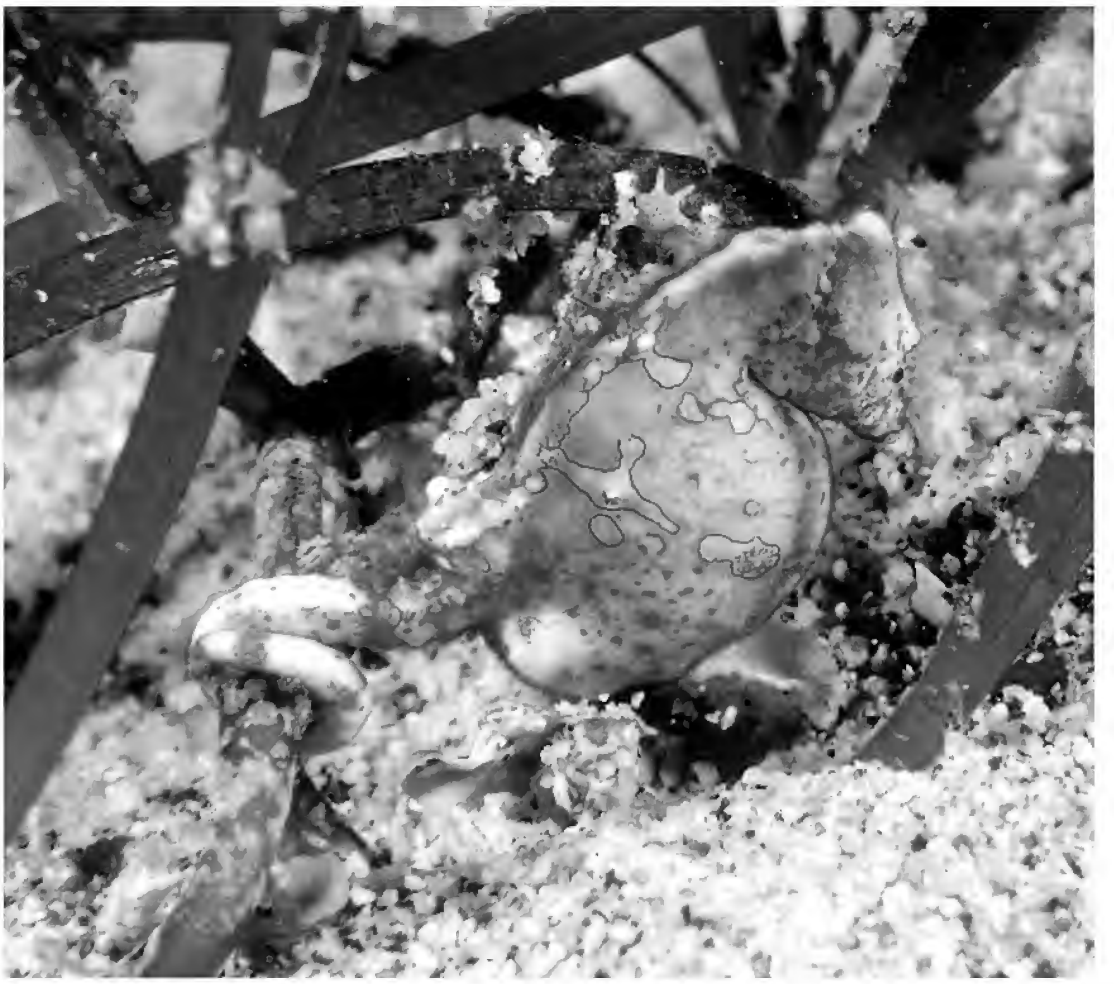

Fig. 4. *Hippocampus colemani*, this specimen not collected. A probable male as it appears to have a pouch. Photo by Neville Coleman.

Australian Museum in 1973. At the time, a team of 15 collectors, 8 of whom were ichthyologists, collected constantly for one month (Allen *et al.*, 1976), and did not find this seahorse.

The closest relative of *Hippocampus colemani* in Australian waters is *H. bargibanti* Whitley, a tropical species that lives on gorgonian corals. It has similar meristic values and shares the greatly elevated dorsal-fin base, but is quite different in its fleshy and lumpy appearance, and has a longer tail. From a global perspective, most similar in its morphology is a pygmy species from Japan (sp. 7, Kuiter, 2000) that is nearly identical in shape and has an almost identically formed nose ridge. Kuiter's *Hippocampus* sp. 7, however, has small but distinctive spines along the trunk and tail ridges. A further similar species that appears to be closely related (sp. 6, Kuiter, 2000) occurs on gorgonians in Papua New Guinea, but is only known from photographs. All share the unusually elevated dorsal-fin base that forms a large hump on their back. The feature of a single gill opening (see Figs. 2, 3) appears to be the same in the Japanese and the Papua New Guinea species (not clear in photographs). It is likely that the three species form a natural group, but until the relationship of all seahorses are understood the species will be retained together in the single genus *Hippocampus*.

ACKNOWLEDGMENTS. Martin Gomon, Museum Victoria provided the radiographs and commented on the manuscript. I thank Mr Geoff Kelly, Manager of the Lord Howe Island Marine Park, and Mr Patrick Tully, NSW Fisheries, for providing the collecting permit so quickly. I am most grateful to Neville Coleman who made a special trip and spent many long hours underwater just to find and collect the types plus taking the photographs in situ, and thanks to the Prodive-crew for their patience assisting Neville.

References

Allen, G.R., D.F. Hoese, J.R. Paxton, J.E. Randall, B.C. Russell, W.A. Starck, F.H. Talbot & G.P. Whitley, 1976. Annotated checklist of the fishes of Lord Howe Island. *Records of the Australian Museum* 30(15): 365–454.

Kuiter, Rudie H., 2000. *Seahorses, Pipefishes & Their Relatives*. Chorleywood (England): TMC Publications.

Kuiter, Rudie H., 2001. Revision of the Australian seahorses of the genus *Hippocampus* (Syngnathiformes: Syngnathidae) with descriptions of nine new species. *Records of the Australian Museum* 53(3): 293–340. www.amonline.net.au/pdf/publications/1350_complete.pdf

Manuscript received 25 February 2002, revised 4 August 2002 and accepted 22 August 2002.

Associate Editor: J.M. Leis.

Records of the Australian Museum (2003) Vol. 55: 117–140. ISSN 0067-1975

Spiophanes Species (Polychaeta: Spionidae) From Eastern Australia—With Descriptions of New Species, New Records and an Emended Generic Diagnosis

KARIN MEIßNER[1]* AND PAT A. HUTCHINGS

Marine Invertebrate Division, Australian Museum, 6 College Street, Sydney NSW 2010, Australia
k_meissner@web.de · path@austmus.gov.au

[1] Current address: Institut fuer Angewandte Oekologie,
Alte Dorfstraße 11, 18184 Neu Broderstorf bei Rostock, Germany

ABSTRACT. The *Spiophanes* fauna from Eastern Australia is described, and includes 5 new species (*S. modestus, S. viriosus, S. prestigium, S. pisinnus, S. dubitalis*) and 1 new record (*S. japonicum* Imajima, 1991). The generic diagnosis of *Spiophanes* is revised based on type and non-type material of all species in the genus, and a critical evaluation is also given of the characters previously used to distinguish *Spiophanes* species. A new diagnostic character, the appearance of gland openings exhibiting a chaetal spreader on the anterior chaetigers of the middle body region, is described. *Spiophanes japonicum* is removed from synonymy with *S. berkeleyorum* Pettibone, 1962. *Spiophanes urceolata* Imajima, 1991, is synonymized with *S. wigleyi* Pettibone, 1962. A key to all *Spiophanes* species known from Eastern Australia is given.

MEISSNER, KARIN, & PAT A. HUTCHINGS, 2003. *Spiophanes* species (Polychaeta: Spionidae) from Eastern Australia—with descriptions of new species, new records and an emended generic diagnosis. *Records of the Australian Museum* 55(2): 117–140.

The genus *Spiophanes* Grube, 1860, is a well-defined taxon within the Spionidae. It has been reviewed by Pettibone (1962) and more comprehensively by Foster (1971). Blake & Kudenov (1978) described the spionid fauna of southeastern Australia, including species of *Spiophanes*. Blake (1983, 1996) also provided detailed information for *Spiophanes* species from Californian, South American and Antarctic waters. Imajima (1991) studied material from Japan, resulting in the description of two new species. The most recent but brief overview of the taxonomic status and characters of *Spiophanes* species was by Maciolek (2000). The author also provides the latest description of a *Spiophanes* species, *S. abyssalis* from deep waters of the Atlantic Ocean, bringing the total number of species to 13, plus an additional subspecies. However, a careful analysis of the literature reveals the paucity of studies in which type material has been examined, especially when synonymies were being proposed or new species described. Serious confusion now exists about the reliability of described diagnostic characters for several species. In addition, characters used to distinguish species are often not useful, so the identification of most *Spiophanes* species is difficult.

The present study is based on *Spiophanes* material available from collections in Australia. Unfortunately only a restricted region, the coastal waters of Eastern Australia from Halifax Bay, near Townsville (Queensland) in the north

* author for correspondence

to Bass Strait (Victoria, Tasmania) in the south is represented by these collections. Because of the taxonomic problems arising from the literature, type material of all *Spiophanes* species and some additional material was included in this study. This approach made it possible to undertake comparative morphological studies, including SEM observations. As a result, new insights into the taxonomy of *Spiophanes* species were obtained and an emended generic diagnosis is given. A new character with significant implications for the taxonomy of several species in the genus is described and used for species identification. Diagnostic characters traditionally used for species identification are critically reviewed. For Australian waters, five new species are described and a key to *Spiophanes* species found in Eastern Australia is provided.

Material and methods

Specimens listed in this study are deposited in the following institutions:

AM	Australian Museum, Sydney
BMNH	The Natural History Museum, London
CAS	Californian Academy of Science, San Francisco
MNCN	Museo Nacional de Ciencias Naturales, Madrid
MV	Museum Victoria, Melbourne
NSMT	National Science Museum Tokyo
QM	Queensland Museum, Brisbane
	South African Museum, Cape Town
	South Australian Museum, Adelaide
SM	Senckenberg Museum, Frankfurt
USNM	Smithsonian Institution, National Museum of Natural History, Washington, D.C.
ZMH	Zoologisches Museum Hamburg
ZSRO	Zoologische Sammlung der Universität Rostock, Germany

For the observation of several characters, staining with methyl green is required. Specimens have to be transferred into water first and then dipped into a methyl green solution. The colouration fades quickly when specimens are returned to alcohol. If characters shown in the drawings are only visible after staining it is indicated in the legend. Sometimes location data given with the samples made precisely locating the sampling site difficult, e.g., 60 km South of Cape Conran. In these cases, longitude and latitude of an available reference point (e.g., Cape Conran) are set in brackets. Measurements of the body width refer to the distance between the most distal points of the parapodia seen from above on chaetiger 4 (chaetae and postchaetal lobes omitted). Information given under Remarks indicates the most important characters for identifying the species, always considering all currently known species in the genus. The synonymy lists presented in this study almost exclusively contain material checked by the authors themselves (exception only concerns *S. wigleyi* material marked *). This is explained by the fact that new characters essential for species identification are described for the first time in this study and other formerly used distinguishing characters are discounted. Therefore, previous studies naturally do not contain the necessary information for reliable species identification and the identity of species could not be determined from the literature.

A new diagnostic character

Studying the parapodial glandular organs of *Spiophanes* species in the middle body region in detail, it is apparent that two different forms of parapodial gland openings are present: a simple vertical slit usually observable from chaetiger 9 (Fig. 2D) or a gland opening exhibiting a species-specific structure called the "chaetal spreader", found on anterior chaetigers of this body region (Fig. 1A–E). The term chaetal spreader is a rough translation of the German term *Drüsenborstenspreiter* which Söderström (1920) applied to this structure. Söderström described the function of the chaetal spreader as forcing the bacillary chaetae into a defined position and thus preventing them from sticking together. Based on the material included in the present study, 5 different types of chaetal spreader have been found within *Spiophanes*: (*a*) the "2+3 type" with an undulate glandular opening (Fig. 1A), (*b*) the "1+2 type" with an undulate glandular opening (Fig. 1B), (*c*) the "0+1 type" with semicircular or subtriangular glandular opening (Fig. 1C), (*d*) the "0+1 type" with an undulate glandular opening (Fig. 1D) and (*e*) with a simple horizontal glandular opening (Fig. 1E). The terminology refers to the number of projections arising from the anterior and posterior margin of the gland opening, and the shape of the opening along which the bacillary chaetae emerge from inside the parapodial gland. After staining with methyl green it is usually easy to recognize which type of chaetal spreader is present, if the material is in good condition. The same type of chaetal spreader is developed in both juvenile and adult specimens. However, it may be difficult to observe in very small specimens, especially if bacillary chaetae are exposed. Chaetal spreaders can be present from chaetigers 5–7 or 5–8. In the species *S. tcherniai* Fauvel, 1950, they do not appear to be present, even when examined with SEM (Fig. 1F).

Systematic account

Genus *Spiophanes* Grube, 1860, emended

Spiophanes Grube, 1860: 88–89, pl. 5, fig. 1. Type species: *S. kroyeri* Grube, 1860, by monotypy.

Morants Chamberlin, 1919: 17. Type species: *M. duplex* Chamberlin, 1919, by monotypy. Junior synonym.

Diagnosis. Prostomium broad anteriorly; subtriangular, bell-shaped or rarely rounded; anterior margin often laterally extended, forming horns of different length; with or without occipital antenna (Fig. 2A,C). Eyes present or absent. Nuchal organ as 2 parallel ciliated bands along dorsum, maximally extending to chaetiger 16 (Fig. 2C) or as pair of dorsal loops not extending beyond chaetiger 4 (Fig. 2A). Peristomium moderately to well developed, forming lateral bulges or wings. Branchiae absent. Dorsal ciliated crests usually present. Body divided into 3 different regions: (*a*) Anterior region extending up to chaetiger 4: with parapodia 1–4 usually exhibiting well-developed neuro- and notopodial postchaetal lamellae compared to those of subsequent chaetigers, often positioned dorsally or dorsolaterally. (*b*) Middle body region: extending from chaetiger 5 to last chaetiger bearing capillary chaetae rather than hooks in neuropodia (chaetiger 13, 14 or 15 depending on species). Chaetigers usually with parapodial glandular organs: anterior organs exhibit a chaetal spreader in gland

Fig. 1. Chaetal spreader types in *Spiophanes* species. (*A*) "2+3 type" with wavy chaetal slit, *S. duplex* (ZSRO P1413); (*B*) "1+2 type" with wavy chaetal slit, *S. berkeleyorum* (USNM 81 750); (*C*) "0+1 type" with semicircular chaetal slit, *S. japonicum* (MV F90016); (*D*) "0+1 type" with wavy chaetal slit, *S. bombyx* (ZMH 14946); (*E*) type with a simple horizontal chaetal slit, *S. wigleyi* (MV F90009); (*F*) parapodium 5 of *S. tcherniai*, gland opening and chaetal spreader absent (AM W22463). Arrows point from anterior to posterior. Scales: *A*, 100 µm; *B–F*, 50 µm.

opening (Fig. 1A–E); from chaetiger 9, gland opens as simple vertical slit (Fig. 2D), often surrounded by pigmented cells. (*c*) Posterior region: indicated by presence of neuropodial hooks; largest number of hooks usually in first chaetigers of this region. Ventrolateral intersegmental genital pouches present or absent between neuropodia (Fig. 2H).

Notochaetae as capillaries, often limbate or hirsute, in middle body region usually in 3 rows. Neuropodia of chaetiger 1 with 1–2 conspicuous crook-like chaetae. Neurochaetae of chaetigers 1–4 simple, hirsute or limbate capillaries arranged in 2 rows. From chaetiger 5 neurochaetae short, broad, often bilimbate and distally pointed; arranged in 1–2 indistinct rows. Neuropodial hooks first present from chaetiger 14, 15 or 16; quadridentate, with main fang surmounted by single unpaired tooth and pair of smaller distal teeth, additional small teeth rarely present; hood absent or present (Fig. 2F,G). Bacillary chaetae may be exposed from chaetigers 5–8, emerging from inside the parapodium along slit between chaetal spreader and gland opening (Fig. 2E). One to 2 ventral sabre chaetae from chaetiger 4, or sometimes not present until neuropodial hooks appear; sabre chaetae accompanying the hooks often with cryptic ridge (easy to observe under the SEM, difficult to observe with light microscopy) (Fig. 2F). Stout, curved notochaetae often present in far posterior parapodia (Fig. 2B). Pygidium with 2 or more anal cirri.

Remarks. The present diagnosis is based on examinations of type and non-type specimens of every species in the genus. The major changes from past diagnosis concern chaetal arrangements along the body, and characters related to the glandular organs in the middle body region. The arrangement of neurochaetae on chaetigers 1–4 in two rows and of notochaetae on chaetigers of the middle body region in three rows has been found to be present in all species of *Spiophanes*. However, the interpretation of the chaetal arrangement may depend on the number of chaetae in a ramus; if small numbers of chaetae are present, their arrangement in rows may be difficult to discern. In the neuropodia of the middle body region, a large number of chaetae are present in two indistinct rows, whereas smaller numbers of chaetae usually appear to be arranged in a single row. Therefore, the arrangement of chaetae in a specific number of rows is not a useful specific character.

In the middle body region, different forms of gland openings occur. Useful taxonomic information is given by the gland openings presenting a chaetal spreader, the type of which is species specific. The description of the different types and explanations concerning their terminology was given earlier. According to Söderström (1920), the chaetal spreader function is closely related to the function of the bacillary chaetae. Therefore, it is suggested that bacillary chaetae may be present only in parapodia where chaetal spreaders are developed, rather than potentially being present in the entire glandular region (compare, e.g., Foster, 1971; Imajima, 1991; Blake, 1996; Maciolek, 2000). This assumption is supported by our own observations that, in cases where bacillary chaetae are exposed, they are only present in chaetigers with chaetal spreaders developed. From chaetiger 9, glands are obviously producing material similar to bacillary chaetae, which in preserved material resembles a sort of white fibre wool. The appearance of bacillary chaetae probably cannot serve as a useful diagnostic character. Observed differences in the appearance of the chaetal tip or in the arrangement of fine hairs of varying or constant length covering the shafts of the bacillary chaetae have previously been considered as species specific. Based on our observations, the observed differences may just represent a different state of condition.

From chaetiger 9, parapodial glands often have associated pigmented cells which also appear to be useful for species identification.

SEM studies revealed that all known species in the genus possess quadridentate hooks. Previous reports of bi- or tridentate hooks might be due to teeth being worn down or a slightly lateral position of the uppermost pair of small teeth, e.g., in *S. bombyx* Claparède, 1870, which is usually positioned clearly above the unpaired tooth surmounting the main fang and hence allows easier recognition of all four denticles when viewed with light microscopy.

Spiophanes modestus n.sp.

Figs. 2D, 3

Spiophanes cf. *kroeyeri*.–Blake & Kudenov, 1978: 225, fig. 27, in part.

Spiophanes bombyx.–Blake & Kudenov, 1978: 224, in part.–Hutchings & Murray, 1984: 62, in part.

Spiophanes sp. 1.–Wilson & McDiarmid, 2003.

Type material. HOLOTYPE: Australia, New South Wales, Hawkesbury River, Juno Head–Hungry Beach, 33°34.5'S 151°16.5'E, in 10 m, 5 May 1977 (AM W28192). PARATYPES: Australia, New South Wales, Hawkesbury River: Juno Head–Hungry Beach, 33°34.5'S 151°16.5'E, in 10 m, 5 May 1977, 5 specimens (AM W196361, AM W196355, AM W196359), in 4 m, 1 specimen (AM W196350) and 3 Aug 1977, 4 specimens (AM W196352, AM W196358, AM W196360).

Non-type material. Australia, QUEENSLAND: Halifax Bay, N of Townsville, 19°10'S 146°37'E, in 2–5 m, Jan 1977, >80 specimens (AM W202313, AM W202314, AM W202316, AM W202317); Pallarenda Beach, N of Townsville, 19°12'S 146°46'E, 27 Aug 1977, 1 specimen (AM W18103); Gladstone, Calliope River, in 8 m, Jan 1983, 1 specimen (AM W198054); Moreton Bay, Middle Banks, 27°12'S 153°32'E, Nov 1975, 2 specimens (QM G11594), Nov 1983–Nov 1984, >50 specimens (QM G218423). NEW SOUTH WALES: Burwood Beach, 32°57.52'S 151°44.72'E, Apr 1975, 1 specimen (AM W8947); Pittwater: 33°35.9'S 151°18.26'E, in 15 m, 6 May 1994 and 9 Oct 1995, 3 specimens (AM W23699, AM W23702); E of Malabar: 33°57.49'S 151°16.14'E, in 30 m, 17 Apr 1989, 1 specimen (AM W20704); Botany Bay: Yarra Bay, 33°58.9'S 151°12.1'E, 12 Feb 75, 5 specimens (AM W18978, AM W19017, AM W195473), W of Frenchmans Bay, 33°59.3'S 151°13.1'E, 16 Jan 1975, 8 specimens (AM W195508), NE of Dolls Point, 33°59.5'S 151°09.6'E, 17 Jan 1975, 1 specimen (AM W19030), W of La Perouse, 33°59.5'S 151°13'E, in 12 m, 21 Jan 1976, 1 specimen (AM W14632), N of Kurnell, 33°59.52'S 151°12.55'E, in 13 m, 10 Mar 1977, 19 specimens (AM W14638–W14640), W of La Perouse, 33°59.52'S 151°12.55'E–34°S 151°13.5'E, in 15–19 m, Jan–Feb 1977, 9 specimens (AM W14633–W14637), W of Bare Island, 33°59.6'S 151°12.2'E, 2 Feb 1975, 1 specimen (AM W195438).

Other species examined. *Spiophanes bombyx*: NORTH ATLANTIC OCEAN: North Sea, German Bight, 54°20.01'N 7°20.01'E, in 43 m, 26 May 1987, several specimens (SM 4950); 55°54'N 3°27.6'E, in 65 m, 10 Aug 1990, 2 specimens (SM 6476); 55°46.93'N 3°52.38'E–55°53.09'N 3°28.8'E, in 48.4 m, 10 Aug 1990, 3 specimens (SM 6480); 53°41.46'N 6°59.58'E, in 3.5 m, 13 Mar 1989, 8 specimens (SM 6527). MEDITERRANEAN: Spain, between Cape San Antonio and Valencia harbour, 29 Apr 1996, two specimens (MNCN 16.01/2648, 2661). INDIAN OCEAN: 34°16.8'S 18°42.8'E, in 60 m, 25 Feb 1959, several specimens (South African Museum A20779). PACIFIC OCEAN: Alaska, Bering Sea, 58°46.36'N 164°14'W, in 35 m, 23 May 1976, 2 specimen (CAS 23887); Alaska, Chukchi Sea, 67°44.29'N 164°33.45'W, in 5.7 m, 17 Aug 1976, 1 specimen (CAS 1675); California, 37°49.27'N 122°25.55'W, in 58–67 m, 24 Sep 1973, several specimen (CAS 1915); 37°46'N 122°41.5'W, in 31 m, 14 Aug 1973, several specimen (CAS 123655).

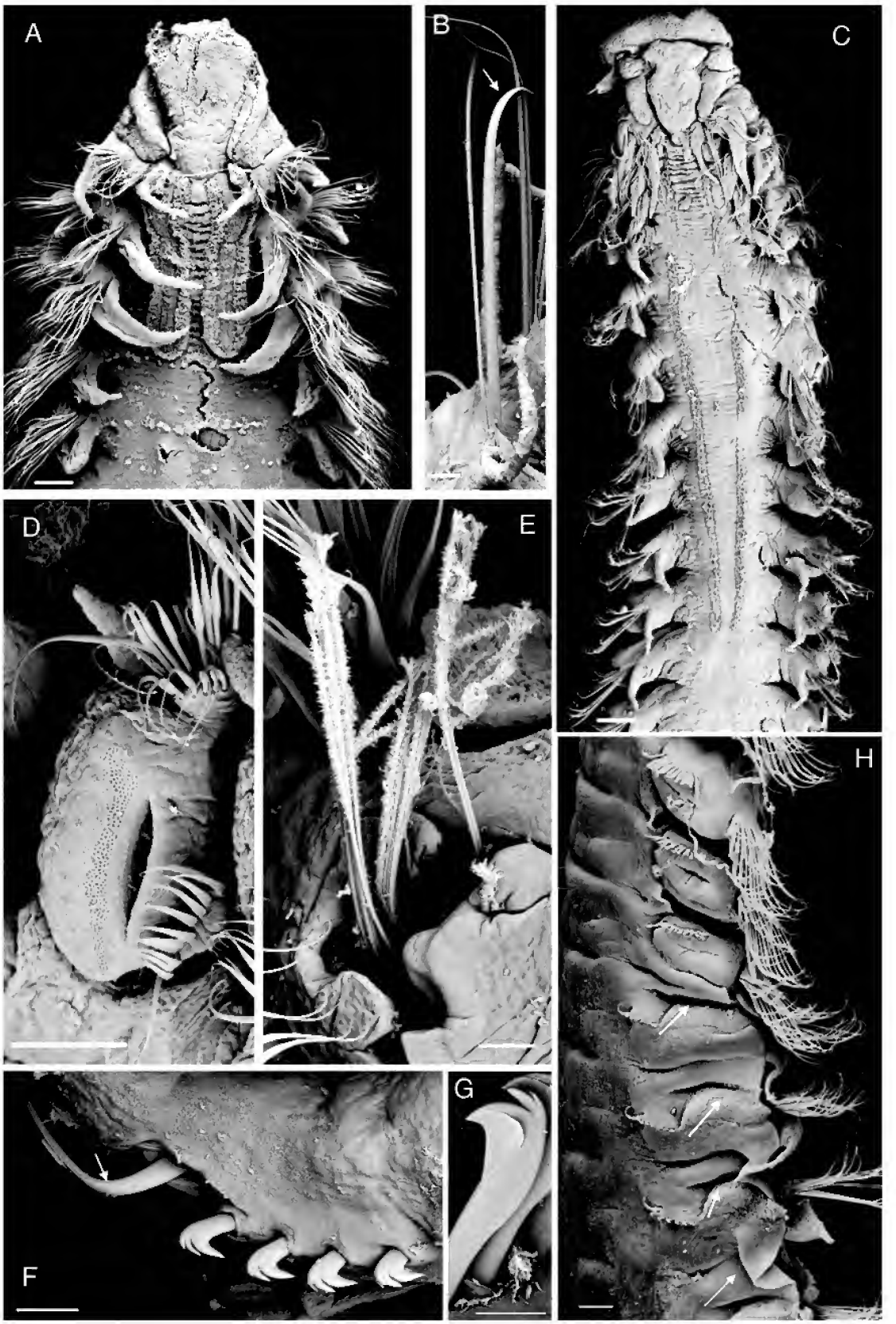

Fig. 2. General characters of the genus *Spiophanes*. (*A*) anterior end with nuchal organ as pair of ciliated dorsal loops up to the beginning of chaetiger 4, *S. wigleyi* (AM W22948), scale 100 µm; (*B*) stout notochaeta of posterior chaetigers; *S. japonicum* (MV F90004), scale 20 µm; (*C*) anterior end with nuchal organ as 2 parallel ciliated lines, *S. japonicum* (MV F90016), scale 100 µm; (*D*) gland opening without chaetal spreader from the middle body region, *S. modestus* (QM G218423), scale 50µm; (*E*) bacillary chaetae, *S. viriosus* (QM G218424), scale 20 µm; (*F*) non-hooded hooks and sabre chaeta with cryptic ridge, *S. japonicum* (MV F90016), scale 20 µm; (*G*) hooded hook, *S. wigleyi* (AM W22948), scale 10 µm; (*H*) intersegmental genital pouches, *S. viriosus* (QM G218424), scale 100 µm.

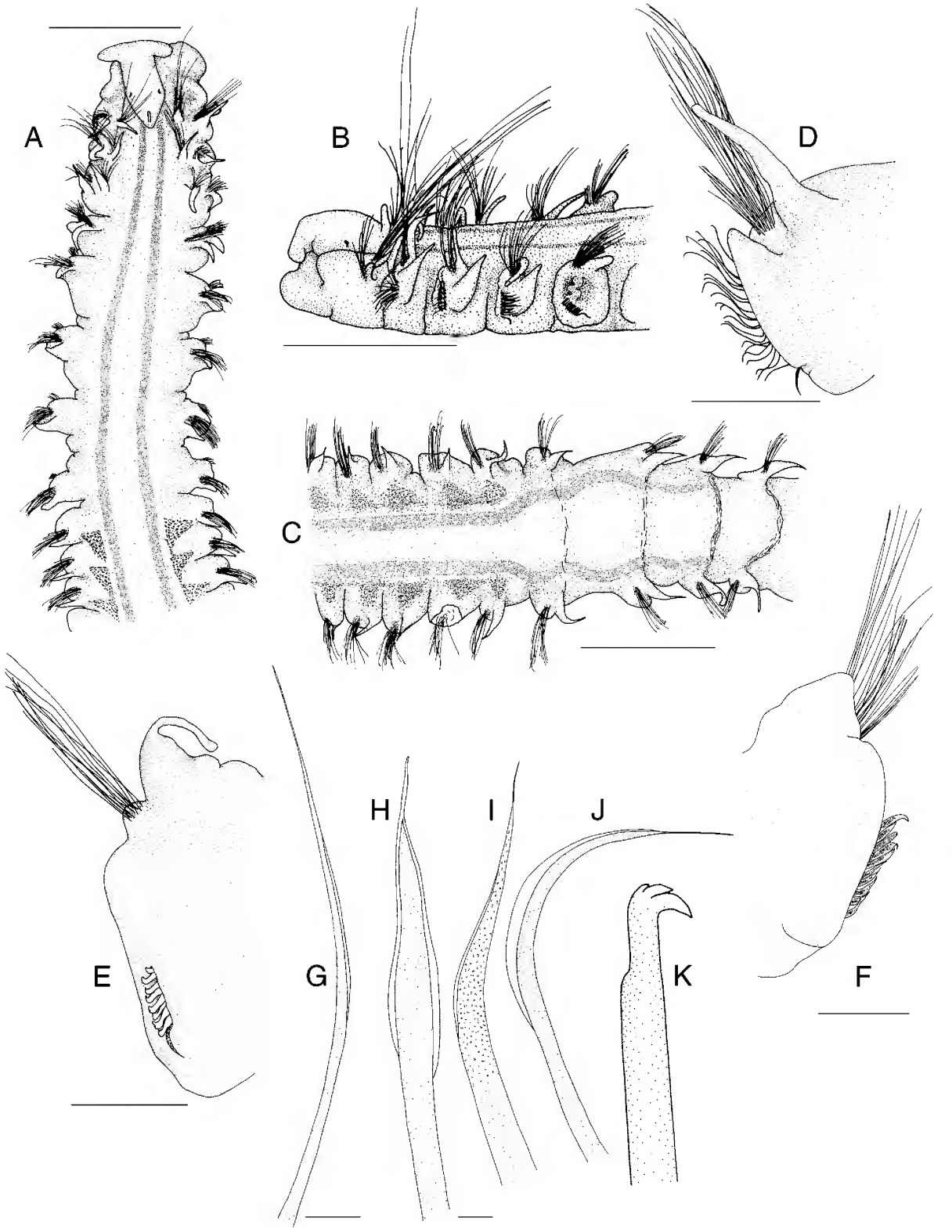

Fig. 3. *Spiophanes modestus* n.sp. (*A*) anterior end, dorsal view, methyl green-stained nuchal organ and glandular patches; (*B*) anterior end, lateral view, methyl green-stained nuchal organ and chaetal spreader of parapodium 5; (*C*) chaetigers 10–18, dorsal view, methyl green-stained nuchal organ and glandular patches; (*D*) left parapodium from chaetiger 4; (*E*) left parapodium from chaetiger 15; (*F*) right parapodium from chaetiger 8, sabre chaeta lacking; (*G*) notochaeta from chaetiger 4, lateral view; (*H*) neurochaeta from chaetiger 5, frontal view; (*I*) sabre chaeta from chaetiger 8; (*J*) neurochaeta from chaetiger 5, lateral view; (*K*) neuropodial hook from chaetiger 16, lateral view. Scales: *A–C*, 0.5 mm; *D–F*, 0.1 mm; *G* 10 µm; *H–K*, 5 µm. All QM G218423.

Description. Holotype complete specimen (posterior region regenerated) with 50 chaetigers, 12 mm total length, about 0.9 mm wide. Other specimens between 0.5–0.9 mm wide. Body slender, subcylindrical. *Prostomium* broad anteriorly, bell-shaped, with distinct anterolateral horns (Fig. 3A). Occipital antenna short. Two pairs of eyes sometimes present, anterior pair further apart and crescent-shaped, posterior pair as small black spots. Nuchal organs as two straight, parallel bands along dorsum, becoming divergent, undulate bands between chaetigers 15–17 (Fig. 3C). Peristomium moderately developed as lateral bulges. Parapodium of chaetiger 1 oriented dorsally; postchaetal lamellae cirriform, equal in length. Postchaetal lamellae of parapodia 2–4 cirriform, but those of neuropodia becoming gradually broader at base (Fig. 3B,D). Chaetigers 5–8 each with rounded notopodial and reduced neuropodial postchaetal lamella (Fig. 3F). From chaetiger 9, notopodial lamella with small triangular base and tapered slender tip; neuropodial lamella reduced (Fig. 3E). *Chaetal spreader* "2+3 type" with undulate glandular opening well developed in chaetigers 5–7; glandular opening absent in chaetiger 8; glandular organ of chaetigers 9–13 opens as lateral vertical slit (Fig. 2D). Ventrolateral intersegmental genital pouches absent. Dorsal ciliated crests apparent from chaetiger 15 (Fig. 3C). *Chaetiger 1* with 1–2 stout, crook-like chaetae in neuropodium, remainder of chaetae simple capillaries; notochaetae very long, reaching back to chaetiger 4 or 5, arranged in a tuft; neurochaetae arranged in 2 rows. Chaetigers 2–4 with simple and unilimbate capillaries (Fig. 3G), the latter becoming more numerous and sheaths becoming more distinctive from chaetigers 2–4; notochaetae in tufts, neurochaetae arranged in 2 rows. Chaetigers 5–13 with stout, bilimbate neurochaetae, distally pointed (Fig. 3J,H), arranged in 1–2 rows; notochaetae each with broad distal sheath, arranged in 3 rows. From chaetiger 14, notopodial capillaries with narrower sheath, arranged in tuft; neuropodial hooks quadridentate without hoods (Fig. 3K), initially 6–8 hooks arranged in 1 row, smaller numbers in more posterior chaetigers. Bacillary chaetae are thin, hirsute bristles with brush-like tips, may be exposed on chaetigers 5–7. Ventral sabre chaetae from chaetiger 4, appearing granulated near tip when viewed with light microscopy, each with cryptic ridge (Fig. 3I). Few stout, curved notochaetae in far posterior parapodia. *Pygidium* with 2 dorsolateral anal cirri.

Pigmentation. Conspicuous pigmentation absent.

Methyl green staining pattern. Intensely stained glandular patches visible in dorsal region of chaetigers 9–14, if specimens in good condition (Fig. 3A,C).

Biology. Species inhabits shallow water areas down to 30 m depth. All sediment types. Gravid specimens observed from January to March (AM W14635; W14638).

Remarks. The species is characterized by the presence of hooks without hoods from chaetiger 14. It clearly differs from *S. bombyx* Claparède in the presence of a short occipital antenna instead of lacking one, and having non-hooded hooks rather than hooks with hoods being present.

Etymology. *modestus*—Latin for modest; referring to the sparse development of parapodial postchaetal lobes in anterior chaetigers, the small antenna and generally fairly small size.

Geographical distribution. Australia: Queensland, New South Wales.

Spiophanes viriosus n.sp.

Figs. 1A, 2E,H, 4, 5

Spiophanes cf. *kroeyeri*.–Blake & Kudenov, 1978: 225, fig. 27, in part.
Spiophanes sp. 2.–Wilson & McDiarmid, 2003.

Type material. HOLOTYPE: Australia, Queensland, Moreton Bay, Peel Island, 27°3'S 153°21'E, in 7.93 m, Mar 1970, (QM G10387). PARATYPES: Australia, Queensland: Moreton Bay: Middle Banks, 27°12'S 153°32'E, Nov 1983–Nov 1984, >50 specimens (QM G218424), 27°15'S 153°15'E, Sep 1976, 6 specimens (MV F42850) and Sep 1976, 3 specimens (MV F42849), Bramble Bay, 27°18'S 153°06'E, Sep 1972, 2 specimens (QM G10631), Peel Island, 27°3'S 153°21'E, in 4.7 m, Jun 1970, 1 specimen (QM G10415), in 3.35 m, Jun 1970, 1 specimen (QM G10399), in 9.5 m, Jun 1970, 1 specimen (QM G10353).

Description. Holotype incomplete, with 63 chaetigers; total length 28 mm, width 1.5 mm. Paratypes between 0.8–1.7 mm wide. Body slender, subcylindrical. *Prostomium* broad anteriorly, bell-shaped to subtriangular, with distinct anterolateral projections (Fig. 4A). Occipital antenna long, slender. Up to 2 pairs of eyes. Nuchal organs as two straight, parallel lines along dorsum; when fully developed, lines slightly diverging posteriorly terminating between chaetigers 17–18 (Fig. 4G). Peristomium well developed. Parapodia of chaetiger 1 orientated dorsolaterally; postchaetal lamella cirriform, neuropodial one more robust (Fig. 4A). Postchaetal notopodial lamellae of parapodia 2–4 long, cirriform; lamellae of neuropodia shorter, subulate, tapering to slender tip (Fig. 4A,C). Chaetigers 5–8 with short, rounded notopodial and reduced neuropodial postchaetal lamellae (Fig. 4E). From chaetiger 9, each notopodial lamella with small triangular base and long slender tip; neuropodial lamellae reduced (Fig. 4D,F). *Chaetal spreader* "2+3 type" with undulate glandular opening in chaetigers 5–7 (Figs. 1A, 4B); glandular opening in chaetiger 8 absent; glandular organ of chaetigers 9–14 opens as lateral, vertical slit. Fully developed ventrolateral intersegmental genital pouches present between chaetigers 14–15 (Figs. 2H, 5A). Dorsal ciliated crests apparent from chaetiger 18 (Fig. 5A). *Chaetiger 1* usually with 1 stout, crook-like chaeta in each neuropodium; remainder of chaetae capillaries; notochaetae arranged in a tuft; neurochaetae in 2 rows. Notopodia 2–4 with simple capillaries and capillaries with narrow sheaths, arranged in a tuft (Fig. 5F); neurochaetae capillaries with narrow sheaths, arranged in 2 rows (Fig. 5H). Notopodial capillaries of first 4 chaetigers longer than those in subsequent chaetigers. Chaetigers 5–14 with stout, bilimbate neurochaetae, distally pointed (Fig. 5D), in 1–2 indistinct rows; notochaetae with distinct sheath (Fig. 5G,I), in 3 rows. From chaetiger 15, notopodial limbate capillaries arranged in tuft; neuropodia with quadridentate hooks without hoods (Fig. 5B), initially with 5–7 hooks in 1 row, often smaller numbers in more posterior chaetigers. Bacillary chaetae as thin, hirsute bristles with brush-like tips (Figs. 2E, 5C), may be exposed on chaetigers 5–7. Ventral sabre chaetae with cryptic ridge from chaetiger 4, appearing granulated near tip under the light microscope (Fig. 5E). *Pygidium* unknown.

Pigmentation. Specimens usually with dark brownish pigment posteriorly along vertical slit of glandular organs of chaetigers 9–12; most conspicuous on chaetiger 9, gradually fading on the following parapodia (Fig. 5A).

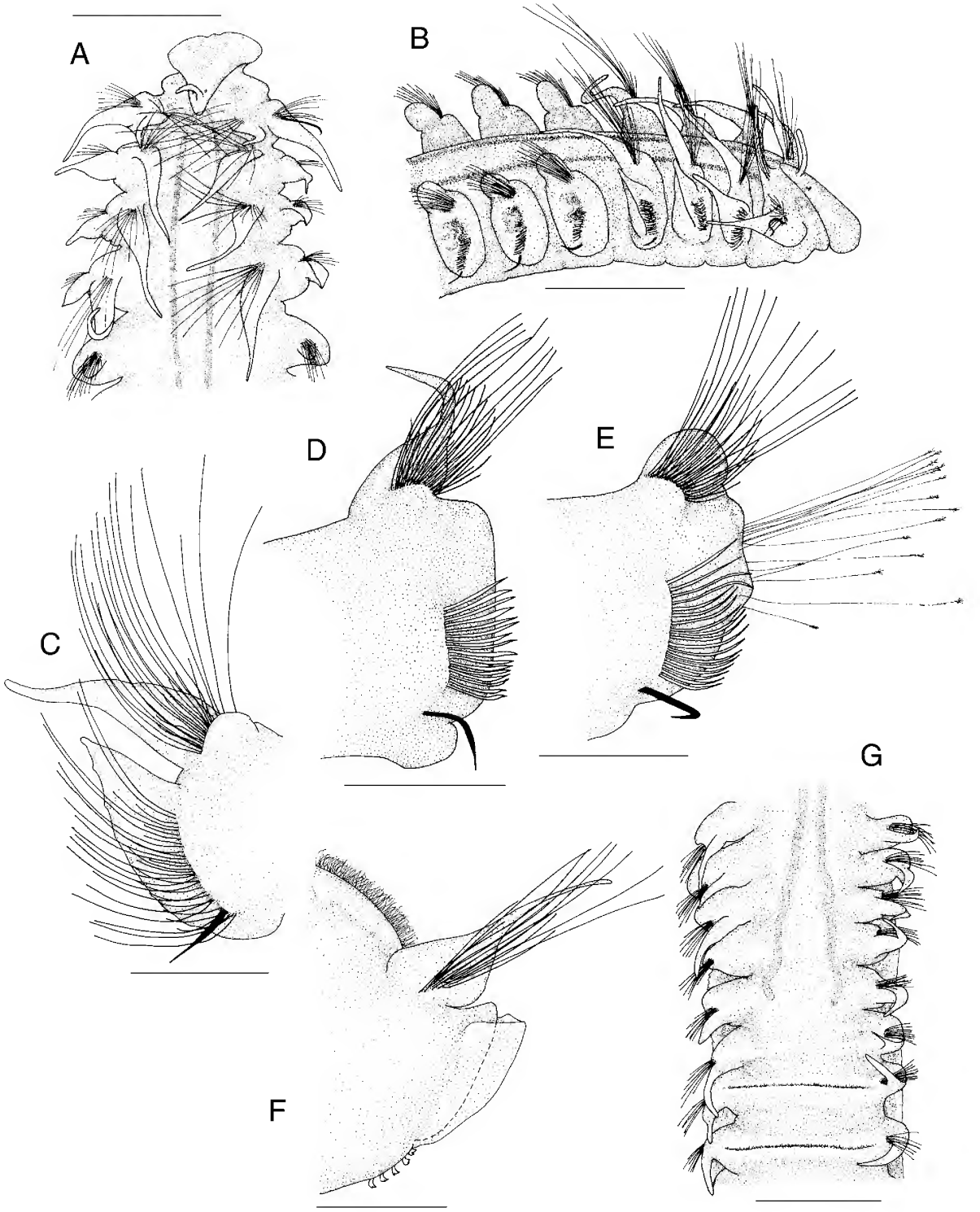

Fig. 4. *Spiophanes viriosus* n.sp. (*A*) anterior end, dorsal view, methyl green-stained nuchal organ; (*B*) anterior end, lateral view; (*C*) right parapodium from chaetiger 4; (*D*) left parapodium from chaetiger 10; (*E*) left parapodium from chaetiger 6; (*F*) left parapodium from chaetiger 19; (*G*) chaetiger 13–20, dorsal view, methyl green-stained nuchal organ. Genital pouches visible laterally from chaetiger 14. Scales: *A,B,G* 1 mm; *C–F* 0.3 mm. *A,B,G* holotype (QM G10387), all others QM G218424.

Methyl green staining pattern. In chaetigers 5–7, the chaetal spreader region, in particular the 2 lobes arising from the anterior margin, stainable (Fig. 4B). In addition, on chaetigers 8–14, the neuropodial region and sometimes proximal part of the respective parapodia seen dorsally stainable, but not appearing well defined compared to the surrounding tissue.

Biology. Species occurs in shallow water areas in different sediment types. Gravid specimen found in May (holotype).

Remarks. The species can be readily recognized by the following combination of characters: presence of an occipital antenna, presence of genital pouches from chaetigers 14–15 and chaetal spreaders in chaetigers 5–7 of the "2+3" type with wavy glandular opening.

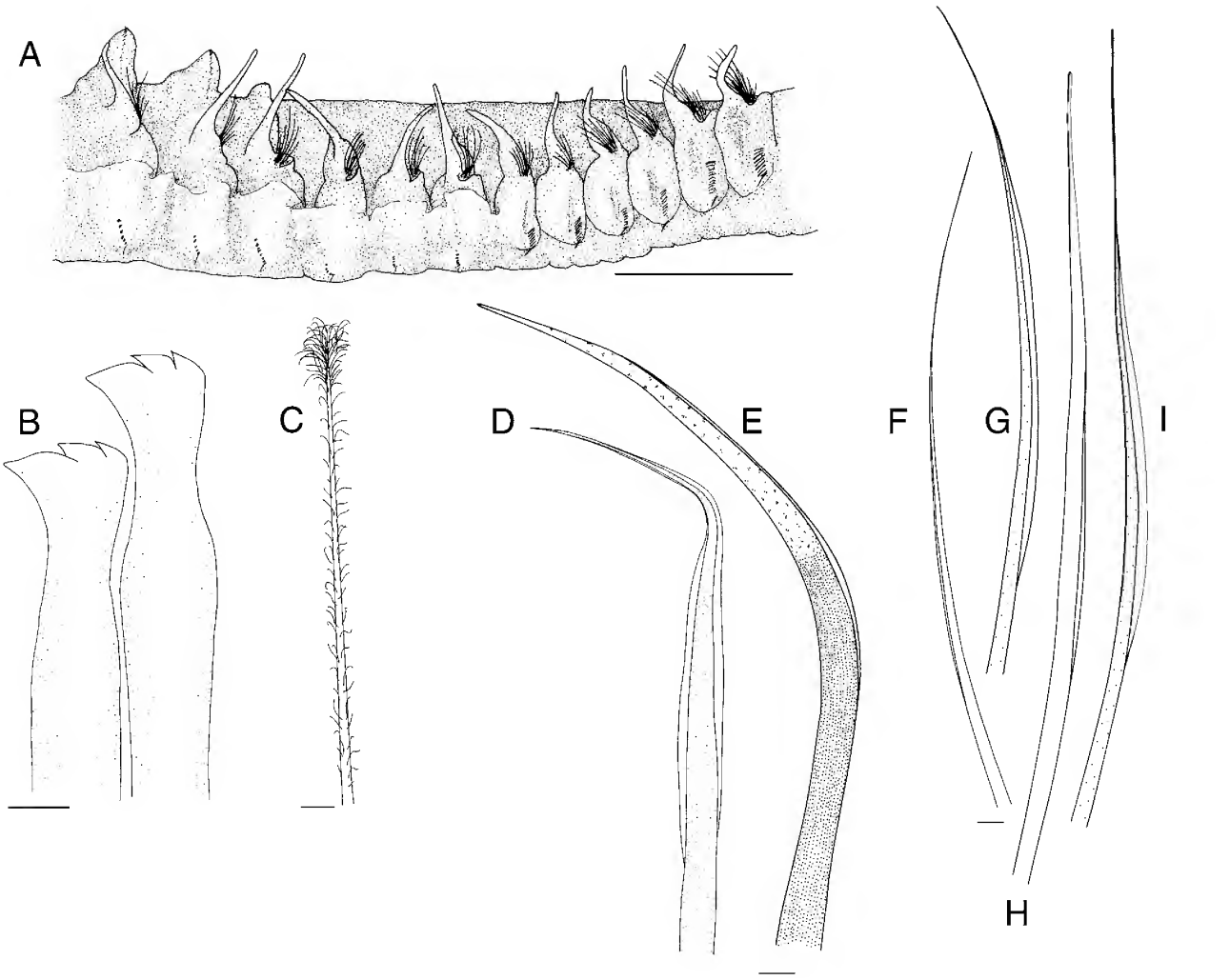

Fig. 5. *Spiophanes viriosus* n.sp. (*A*) chaetiger 9–20, lateral view. Inconspicuous pigmentation along vertical slit of glandular opening on chaetigers 9–12. Genital pouches starting between chaetiger 14–15; (*B*) hooks from chaetiger 19; (*C*) bacillary chaeta from chaetiger 6; (*D*) neurochaeta from chaetiger 6; (*E*) sabre chaeta from chaetiger 4; (*F*) notochaeta from chaetiger 4, semi-long chaeta; (*G*) notochaeta from chaetiger 10; (*H*) neurochaeta from chaetiger 4; (*I*) notochaeta from chaetiger 6; Scale: *A*, 1 mm; *C*, 5 µm; *B,D–I*, 10 µm. *A* holotype, all others QM G218424.

Japanese specimens recorded as this species may have been incorrectly identified as *Spiophanes kroeyeri* = *Spiophanes kroyeri* by Imajima (1991). Since the author has not given information about the appearance of the chaetal spreader and material listed in his article was not available, his identifications require verification.

Etymology. *viriosus*—Latin for robust, strong; referring to the comparatively large size of the species.

Geographical distribution. Australia: Queensland.

Spiophanes japonicum Imajima, 1991

Figs. 1C, 2B,C,F, 6, 7

Spiophanes japonicum Imajima, 1991: 123–128, figs. 5–7.
Spiophanes cf. *kroeyeri*.–Blake & Kudenov, 1978: 225, fig. 27, in part.

Type material. HOLOTYPE: Japan, 35°12.3'N 139°33.2'E–35°13.0'N 139°33.0'E, in 73 m, Sep 1979 (NSMT-H 333).

Non-type material. Australia: NEW SOUTH WALES: Sydney, Malabar: 33°58.0'S 151°16'E, in 28 m, 22 May 1972, 5 specimens (AM W6500); 3.5 km E of Little Bay, 33°58.9'S 151°17.1'E, in 75 m, 16 May 1972, >10 specimens (AM W6499); E of Port Hacking, 34°04.2'S 151°12.8'E, in 60 m, 31 Jul 1989, 1 specimen (AM W24332); Bass Point, 34°36'S 150°54'E, in 50 m, 1 Feb 1990, 1 specimen (AM W22945). VICTORIA: 60 km S of Cape Conran [37°49'S 148°44'E], in 1463 m, May 1969, 1 specimen (AM W13020);112 km S of Lake Entrance [37°53'S 148°00'E], in 95 m, May 1969, 1 specimen (AM W13021); Central Bass Strait: 38°39.8'S 144°18.2'E, in >79 m, 19 Nov 1981, 1 specimen (MV F90012), 38°45.9'S 145°33.5'E, in 74 m, 13 Nov 1981, 6 specimens (MV F90013, MV F90079). TASMANIA: Eastern Bass Strait: 39°02.4'S 146°30.6'E, in 120 m, 15 Nov 1981, many specimens (MV F90004), 39°02.4'S 148°30.6'E, in 120 m, 15 Nov 1981, many specimens (MV F92138), 39°44.8'S 146°40.6'E, in 124 m, 14 Nov 1981, 35 specimens (MV F91985), 40°14.4'S 148°30.0'E, in 60 m, 14 Nov 1981, 1 specimen (MV F90012). Central Bass Strait: 39°43.5'S 146°18.8'E, in 80 m, 13 Nov 1981, >20 specimens (MV F92137), 39°46.0'S 146°18.0'E, in 80 m, 13 Nov 1981, >15 specimens (MV F90008), 39°48.6'S 145°44.3'E, in 75 m, 13 Nov 1981, >20 specimens (MV F90016), 39°49.5'S 146°18.5'E, in 82 m, 13 Nov 1981, 7 specimens (MV F91984), 40°10.75'S 145°43.2'E–40°14.25'S 145°42.8'E, in 76 m, 3 Feb 1981, 1 specimens (MV F90014), 40°10.9'S 145°44.3'E, in 75 m, 13 Nov 1981, >55 specimens (MV F90076), 40°10.9'S 146°18.8'E, in 82 m, 13 Nov 1981, >20 specimens (MV F90077), 40°33.07'S 145°44.7'E–40°36.22'E 145°48.7'S, in 68 m, 4 Feb 1981, 1 specimen (MV F90019).

Other species examined. *Spiophanes berkeleyorum* Pettibone, 1962, North Pacific Ocean: Canada, British Columbia, Vancouver Island, Departure Bay Beach, 25 Apr 1936, 6 paratypes, (USNM 30400).

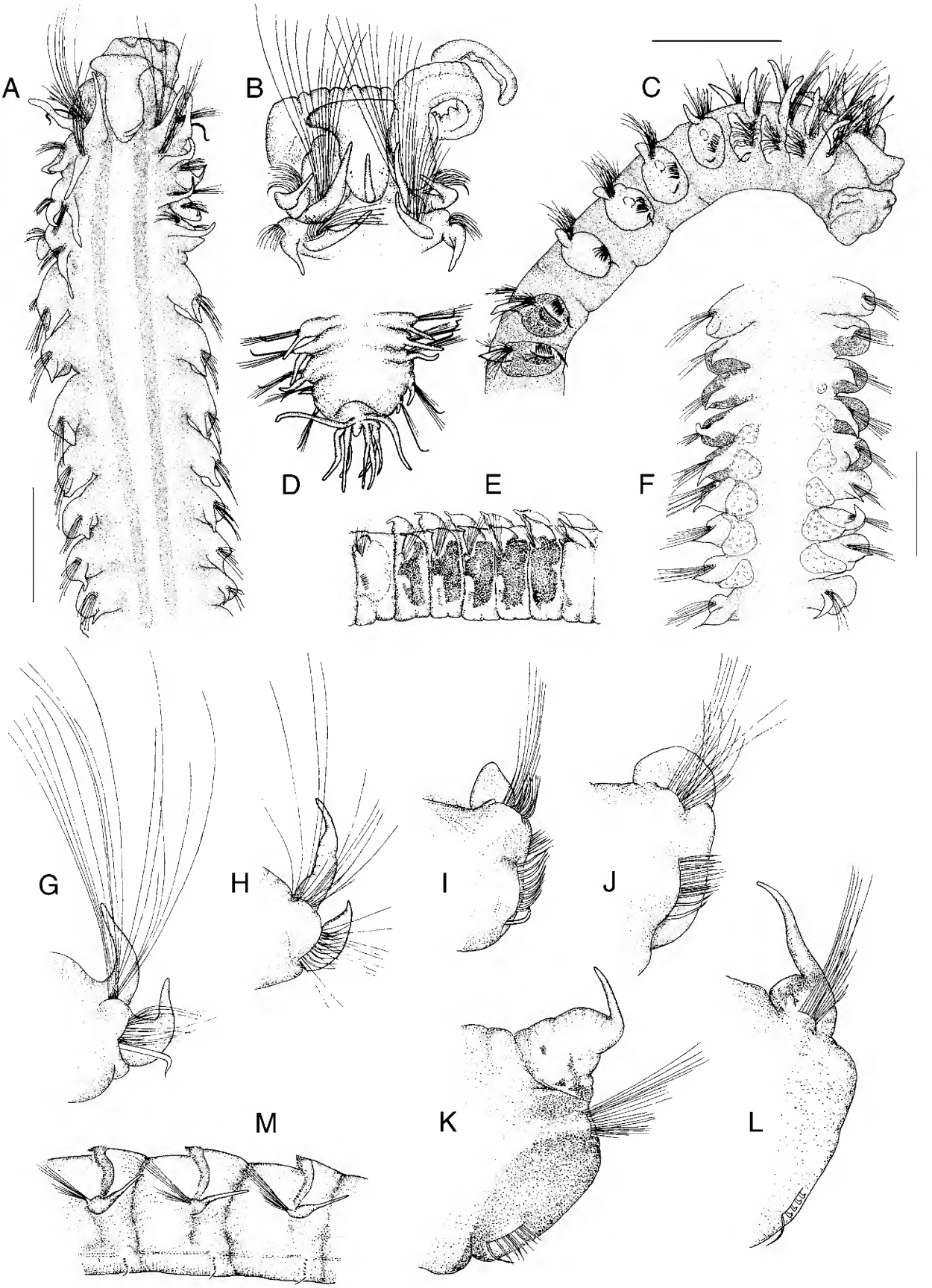

Fig. 6. *Spiophanes japonicum* Imajima, 1991. (*A*) anterior end, dorsal view, methyl green-stained nuchal organ; (*B*) anterior end with right palp, dorsal view, 40×; (*C*) anterior end, lateral view, methyl green-stained chaetal spreader in parapodia 5–7; (*D*) posterior end, dorsal view, 47×; (*E*) chaetigers 8–14, left lateral view, showing glandular region with dark glands, 32×; (*F*) chaetigers 8–16, dorsal view, showing glandular region with dark pigment laterally on chaetigers 9–13 and pink pigment (represented by light stippling) …

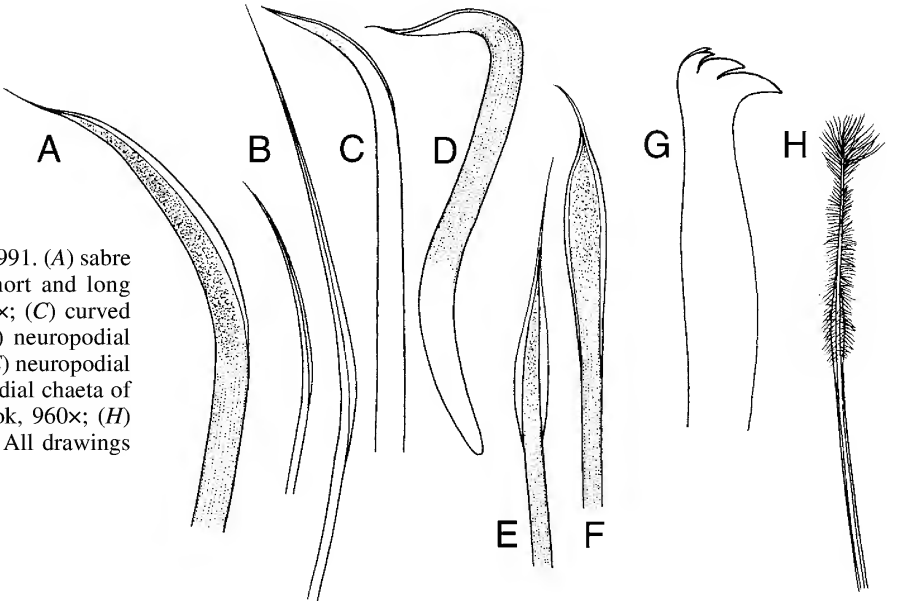

Fig. 7. *Spiophanes japonicum* Imajima, 1991. (*A*) sabre chaeta from chaetiger 11, 680×; (*B*) short and long notopodial chaetae of chaetiger 10, 255×; (*C*) curved chaeta of posterior chaetiger, 375×; (*D*) neuropodial crook-like chaeta of chaetiger 1, 255×; (*E*) neuropodial chaeta of chaetiger 5, 255×; (*F*) neuropodial chaeta of chaetiger 11, 680×; (*G*) neuropodial hook, 960×; (*H*) bacillary chaeta from chaetiger 5, 680×. All drawings after Imajima (1991).

Description. Holotype complete, with 102 chaetigers, total length 29 mm, about 1 mm wide. Australian specimens up to 1.2 mm wide. Body slender, subcylindrical. *Prostomium* broad anteriorly, bell-shaped, with short but distinct anterolateral projections (Fig. 6A,B); anterior margin slightly convex, sometimes with minor median incision. Cirriform occipital antenna. Up to 2 pairs of eyes present. Nuchal organs as two straight, parallel bands along dorsum, terminating between chaetigers 10–12 (Fig. 6A). Peristomium moderately developed as lateral bulges. Parapodia of chaetiger 1 oriented dorsally; postchaetal lamellae cirriform, equal in length (Fig. 1A,C,G). Postchaetal notopodial lamellae of parapodia in chaetigers 2–4 cirriform, lamellae of neuropodia subulate, becoming gradually broader at base (Fig. 6C,H). Chaetigers 5–8 with subtriangular to rounded notopodial and reduced neuropodial postchaetal lamellae (Fig. 6C,I,J). From chaetiger 9, notopodial lamellae with small triangular base and tapered slender tip; neuropodial lamellae reduced (Fig. 6K,L). *Chaetal spreader* of "0+1 type" with semicircular glandular opening well developed in chaetigers 5–7 (Figs. 1C, 6C); glandular opening in chaetiger 8 absent; glandular organ of chaetigers 9–14 opens as lateral vertical slit. Ventrolateral intersegmental genital pouches absent. Dorsal ciliated crests apparent from chaetiger 18. *Chaetiger 1* usually with 1 stout, crook-like chaeta in neuropodium (Fig. 7D); remainder of chaetae simple, hirsute capillaries (hirsute character clearly observable only with SEM); notochaetae arranged in tuft; neurochaetae arranged in 2 rows. Chaetigers 2 and 3 each with simple hirsute capillaries; notochaetae in tufts, neurochaetae in 2 rows. In chaetiger 4, arrangement of chaetae same as in previous segments, but hirsute character of capillaries gets lost whereas narrow sheaths are visible. Notopodial capillaries of first 4 chaetigers slightly longer than those of subsequent chaetigers. Chaetigers 5–14 with stout, bilimbate neurochaetae, distally pointed (Fig. 7E, F), arranged in 1–2 rows; notochaetae with broad sheath (Fig. 7B), arranged in 3 rows. From chaetiger 15, capillaries with narrow sheath in notopodia, arranged in tufts; neuropodia bearing quadridentate hooks without hoods (Figs. 2F, 7G), initially with 4–7 hooks in single row, often smaller numbers in more posterior chaetigers. Bacillary chaetae thin, hirsute, with brush-like tips (Fig. 7H), can be present on chaetigers 5–7. Ventral sabre chaetae from chaetiger 4, granulated near tip when viewed with light microscopy (Fig. 7A); sabre chaetae in hook-bearing neuropodia with cryptic ridge (Fig. 2F). Single, stout, curved notochaeta with sheath in each far posterior parapodium (Figs. 2B, 7C). *Pygidium* with 6 anal cirri; one pair dorsoterminal and second pair dorsolateral; cirri sometimes bifurcate (Fig. 6D).

Pigmentation. Conspicuous dark brownish pigmentation on parapodia in chaetigers 9–13 encompasses the neuropodium as well as the interramal region, particularly dark region observable along the vertical slit of the gland opening (Fig. 6C,E). In addition, a second glandular region is detectable dorsally at the bases of notopodia 10–15, most conspicuous on chaetigers 13–15, white in colour on the Japanese holotype, in Australian specimens usually bright orange or pink (Fig. 6F).

Methyl green staining pattern. Stain is taken up best in pigmented areas of parapodia 9–13.

Biology. Species mostly found at depths between 50–125 m, exceptionally in 28 m or 1463 m, in mud and fine sand.

Remarks. *Spiophanes japonicum* had been erroneously synonymized with *S. berkeleyorum* by Blake (1996). Blake's decision was obviously based on information from the literature since type specimens of *S. japonicum* were not examined. The species can be easily distinguished by the type of chaetal spreader present on parapodia 5–7: *S. japonicum* has a chaetal spreader of the "0+1 type" with a semicircular glandular opening, whereas *S. berkeleyorum* exhibits a chaetal spreader of the "1+2 type" with a wavy

[Fig. 6, continued] ... dorsally on chaetigers 10–15; (*G*) left parapodium 1, 58×; (*H*) left parapodium 3, 58×; (*I*) left parapodium 5, 88×; (*J*) left parapodium 8, 88×; (*K*) left parapodium13, 88×; (*L*) left parapodium 15, 88×; (*M*) chaetigers 47–49, left lateral view, 40×. *A,C,F* original drawings, scale 0.5 mm, MV F90077; others after Imajima (1991).

glandular opening. *Spiophanes japonicum* is the only currently known species with the following combination of characters: presence of an occipital antenna, chaetal spreader of "0+1 type" with semicircular glandular opening, and the absence of genital intersegmental pouches. The disjunct distribution pattern may only reflect the lack of samples from other regions.

Geographical distribution. Japan; Australian waters from Sydney to the Bass Strait.

Spiophanes wigleyi Pettibone, 1962

Figs. 1E, 2A,G, 8–10

Spiophanes wigleyi Pettibone, 1962: 83, figs. 5,6.–*Hartman, 1965: 153, pl. 28, figs. e,f.–*Foster, 1971: 43–46, 76–85.–Blake & Kudenov, 1978: 224, fig. 26.–*Johnson, 1984: 6–11, fig. 6(4).

Spiophanes urceolata Imajima, 1991: 132–136, figs. 10–12 **new synonymy**.

Type material. PARATYPES: North Atlantic Ocean, 40°0.9'N 68°58'W, Georges Bank Area, off Massachusetts, in 70–135 m, 22 Aug 1957, 2 specimens (USNM 30402).

Non-type material. NORTH ATLANTIC OCEAN: Norwegian Sea, 60°47.74'N 3°26.85'E, in 333 m, 14 May 1998, 1 specimen (ZSRO P716); 60°45.04'N 3°26.85'E, in 330 m, 13 May 1998, 1 specimen (ZSRO P717). SOUTH ATLANTIC OCEAN/INDIAN OCEAN: South Africa, off Cape Town, 34°16'S 18°38'E, in 59 m, 1967, 9 specimens (South African Museum A20781); mixture of 9 stations off South Africa J.H. Day, 29 Nov 1960, 1 specimen (BMNH 1961.19.596/634). SOUTH PACIFIC OCEAN: Milne-Edwards Deep: 8°21'S 81°25'W, in 1296–1317 m, 14 Oct 1965, several specimens (LACM-AHF ABII-94); 7°59'S 80°37'W, in 991–1015 m, 14 Oct 1965, 4 specimens (LACM-AHF ABII-90). AUSTRALIA: NEW SOUTH WALES: E of Providential Head, Wattamolla, 34°0.8'S 151°08.5'E, in 50 m, 1 Feb 1990, 1 specimen (AM W22948). VICTORIA: S of Lakes Entrance [37°53'S 148°00'E], May 1969, 2 specimens (AM W13018); Tasman Sea: eastern slope, 38°06.2'S 149°45.5'E, in 188 m, 14 Oct 1984, 8 specimens (MV F90017), 38°10.3'S 149°57.2'E, in 592 m, 14 Oct 1984, 3 specimens (MV F90010); Bass Strait: 38°08'S 148°35'E, May 1969, 1 specimen (AM W13016), 38°59'S 148°34'E, in 466 m, May 1969, 3 specimen (AM W13017); Western Bass Strait: 39°0.5'S 142°33'E, in 207 m, 9 Oct 1980, 1 specimen (MV F90025), 39°0.6'S 142°29'E, in 630 m, 9 Oct 1980, 1 specimen (MV F90026). TASMANIA: Eastern Bass Strait: 38°57.8'S 148°26.5'E, in 130 m, 15 Nov 1981, 5 specimens (MV F90023), 39°00'S 148°25'E, in 92 m, 14 Oct 1984, 1 specimen (South Australian Museum E3199); 39°02.4'S 148°30.6'E, in 120 m, 15 Nov 1981, 32 specimens (MV F90078), 39°31.2'S 148°24.4'E, in 40 m, 15 Nov 1981, 1 specimen (MV F90020), 39°44.8'S 146°40.6'E, in 124 m, 14 Nov 1981, 3 specimens (MV F90018); Central Bass Strait, 39°43.5'S 146°18.8'E, in 80 m, 13 Nov 1981, 2 specimens (MV F90075); Western Bass Strait: 40°06'S 143°16'E, in 187 m, 11 Oct 1980, 1 specimen (MV F90022), 40°06'S 143°17'E, in 158 m, 11 Oct 1980, 2 specimens (MV F90024); Tasman Sea: 55 km E of Babel Island, 40°00.0'S 148°58.0'E, in 1130 m, 11 Oct 1984, 10 specimens (MV F90015), 20 km E of Falmouth, 41°32.9'S 148°35'E, in 122 m, 10 Oct 1984, 11 specimens (MV F90003), 30 km NNW of Cape Sorell, 42°10.9'S 144°48.9'E, in 160 m, 20 Oct 1984, 1 specimen (MV F90007), Maria Island, 42°37'S 148°20'E, in 102 m, 9 Oct 1984, 7 specimens (MV F90009).

Additional material. *Spiophanes urceolata*, North Pacific Ocean: Japan, 35°10.5'N 139°34.3'E–35°11'N 139°34.4'E, in 92 m, Sep 1979, holotype (NSMT H335).

Description. Specimens up to 1.5 mm wide. Incomplete paratype from Massachusetts with 38 chaetigers, 0.8 mm wide, 9.0 mm long. Incomplete large Australian specimen with 28 chaetigers, 1.1 mm wide, 7.5 mm long. Body slender, subcylindrical. *Prostomium* broad anteriorly, bell-shaped to subtriangular or almost oval-shaped, with or without blunt, very short anterolateral projections; tapered posteriorly to elevated, sometimes pigmented tip (Fig. 8A,C). Occipital antenna absent. Usually 2 pairs of eyes, anterior pair slightly further apart. Nuchal organs as pair of dorsal loops, extending from posterior prostomium margin to beginning of chaetiger 4 (Figs. 2A, 8A). Peristomium well developed. Parapodia of chaetiger 1 in dorsolateral position; postchaetal lamellae cirriform, equal in length (Figs. 2A, 8A,D). Parapodia of chaetigers 2 and 3 also dorsolateral, parapodium of chaetiger 4 lateral. Postchaetal notopodial lamellae of parapodia of chaetigers 2–4 cirriform to subulate, longest at notopodium in chaetiger 3; neuropodial postchaetal lamellae subulate (Fig. 8B,E,F). Chaetigers 5–8 with subtriangular notopodial lamellae, gradually increasing in size, reaching significant size in chaetiger 8; neuropodial postchaetal lamellae reduced (Fig. 8G). From chaetiger 9, notopodial lamellae subulate, with slender tips; neuropodial lamellae reduced (Fig. 8H,I). *Parapodial glands* of chaetigers 5–8 with indistinct, crescent-shaped, horizontal glandular openings (Fig. 1E); glandular organs of chaetigers 9–14 open as lateral vertical slits. Ventrolateral intersegmental genital pouches absent. Dorsal ciliated crests from chaetigers 15 or 16. *Chaetiger 1* usually with 1 stout, crook-like chaeta in neuropodia; other chaetae all capillaries (Fig. 9A,C,K); notochaetae arranged in tuft; neurochaetae in 2 rows. Notopodia of chaetigers 2–4 with capillaries with narrow sheaths (Fig. 9B), arranged in tuft; neurochaetal capillaries with narrow and broad sheaths (Fig. 9G,H), arranged in 2 rows. Notopodial capillaries of first 4 chaetigers only slightly longer than those of subsequent chaetigers. Chaetigers 5–14 with stout, bilimbate neurochaetae, distally pointed (Fig. 9F,J), in 1–2 indistinct rows; notochaetae with narrow sheath, in 3 rows. From chaetiger 15, notopodial capillaries with narrow sheath, arranged in tuft; neuropodia with quadridentate hooded hooks (Figs. 2G, 9I), initially with 10 or 11 hooks in single row in Australian specimens, up to 14–16 hooks in specimens from Japan; hooks usually in smaller numbers in more posterior chaetigers. Bacillary chaetae thin, hirsute, with brush-like tips, can be present on chaetigers 5–8. One or sometimes 2 thin capillaries in the position of ventral sabre chaetae from chaetiger 4 (Figs. 9D, 10A,B). Stout ventral sabre chaeta and usually additional thin capillary present from chaetiger 15 accompanying the hooks (Fig. 10C), sabre chaeta appearing granulated near tip (Fig. 9E). Single stout, bent chaetae with broad sheath in far posterior notopodia. *Pygidium* with 4–6 anal cirri.

Pigmentation. Notopodial postchaetal lamellae of chaetigers 9–15 with reddish-brown pigment in proximal region, darkest on chaetigers 12–15 (Fig. 8A).

Methyl green staining pattern. No distinct methyl green staining pattern: areas most intensively stained are pigmented notopodial lamella of chaetigers 9–15; also posterior tip of the prostomium appears to be darker than surrounding area after staining.

Biology. Species recorded from depths of 40–1130 m in all sediments. Gravid specimen found in May (Australia, Victoria: Bass Strait, AM W13016).

Remarks. *Spiophanes wigleyi* is the most readily recognized species in the genus and is characterized by the

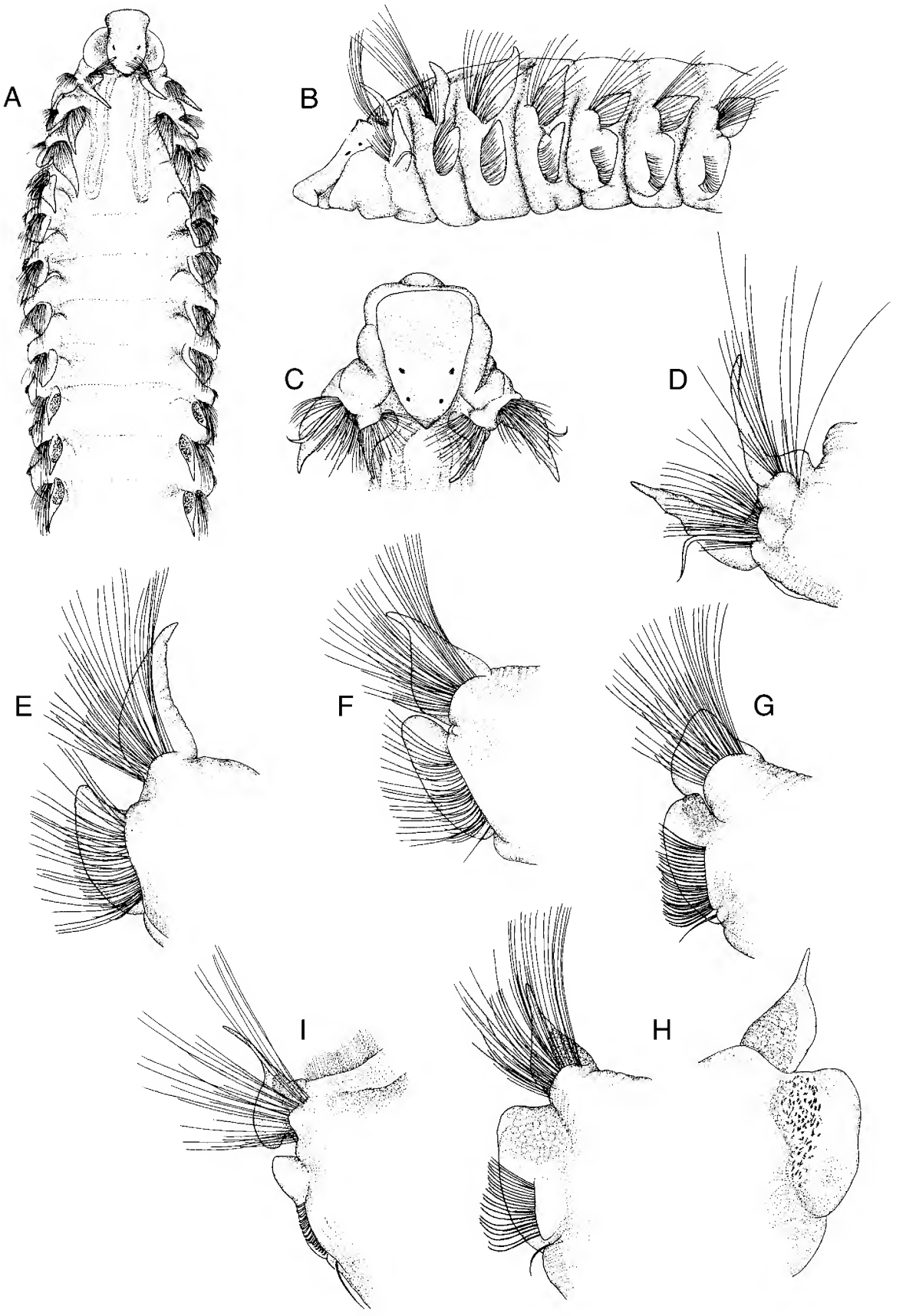

Fig. 8. *Spiophanes wigleyi* Pettibone, 1962. (*A*) anterior end, dorsal view, 20×; (*B*) anterior end, lateral view, 35×; (*C*) prostomium and chaetiger 1, dorsal view, 35×; (*D*) right parapodium from chaetiger 1; (*E*) right parapodium from chaetiger 3; (*F*) right parapodium from chaetiger 4; (*G*) right parapodium from chaetiger 5; (*H*) right parapodium from chaetiger 9, anterior and posterior view, in the latter one chaetae omitted; (*I*) right parapodium from chaetiger 20. *D–I* all 47×. All drawings after Imajima (1991).

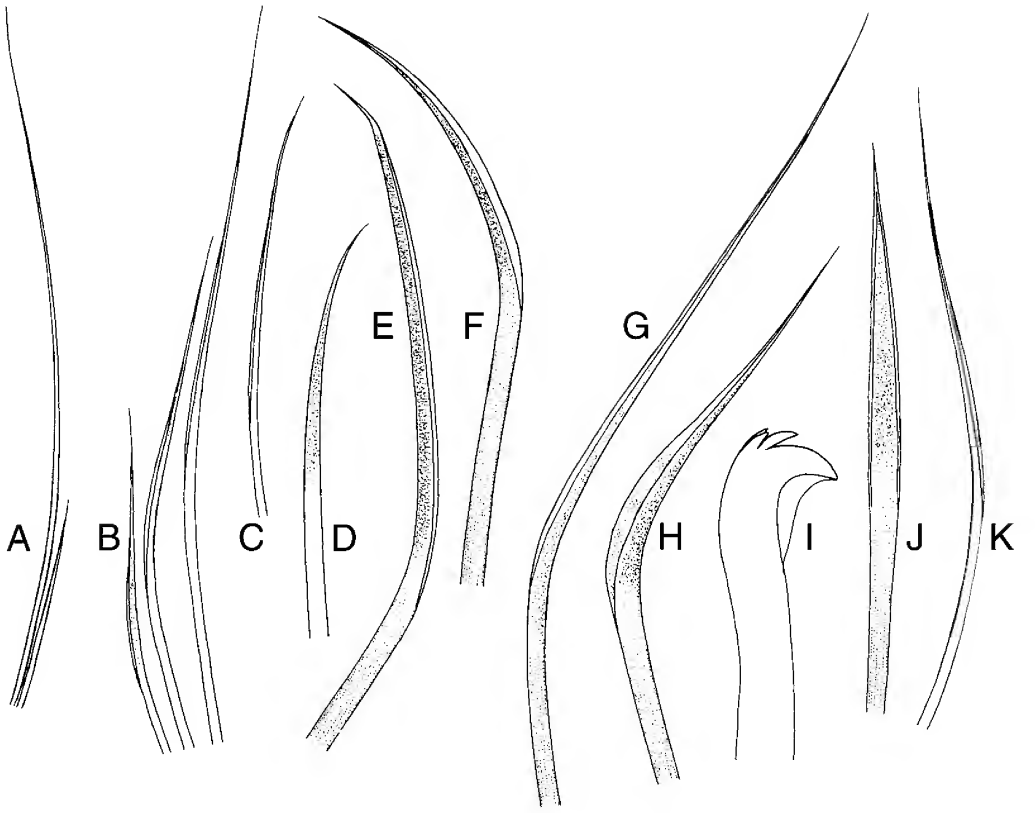

Fig. 9. *Spiophanes wigleyi* Pettibone, 1962. (*A*) short and long notochaeta from chaetiger 1, 130×; (*B*) short to long notochaetae from chaetiger 4, 192×; (*C*) short capillary from neuropodium 1, 255×; (*D*) inferiormost neurochaeta from chaetiger 4, 375×; (*E*) sabre chaeta from chaetiger 20, 375×; (*F*) neurochaeta from chaetiger 9, lateral view, 375×; (*G*) long neurochaeta from chaetiger 4, 375×; (*H*) short neurochaeta from chaetiger 4, 375×; (*I*) hooded hook, 960×; (*J*) neurochaeta from chaetiger 9, frontal view, 375×; (*K*) long capillary from neuropodium 1, 255×. All drawings after Imajima (1991).

rounded shape of the prostomium together with the presence of large numbers of hooded hooks and a nuchal organ forming a pair of dorsal loops extending to chaetiger 4. The pigmentation of notopodial lamellae of chaetigers 9–15 and size and shape of the postchaetal lamellae in chaetiger 8 notopodia are also characteristic. The development of glandular openings in chaetigers 5–8 is unique among currently described *Spiophanes* species; unfortunately, these openings are difficult to observe under the light microscope. Imajima (1991) described the species *S. urceolata* as differing from *S. wigleyi* in (*a*) the shape of the prostomium being triangular to bell-shaped, with a rounded or truncate anterior margin, rather than somewhat ovum-shaped with a rounded anterior margin, (*b*) the arrangement of notopodial capillary chaetae in three rows throughout rather than two rows, and (*c*) ventral sabre chaetae being present from chaetiger 4 rather than 9. Examination of specimens from Australia, South Africa, and the holotype of *S. urceolata* from Japan, and two *S. wigleyi* paratypes from Massachusetts revealed that the arrangement of notopodial capillary chaetae in 3 distinct rows can only be observed on chaetigers 5–14 on all specimens and, furthermore, it seems to be a character which can be attributed to all species in the genus. The above mentioned differences in the shape of the prostomium match well with the variability of this character in *S. wigleyi*. However, the most confusing character listed by Imajima (1991) was the first appearance of sabre chaetae in the neuropodia of chaetiger 4. Blake (1996) reported for Californian specimens of *S. wigleyi* sabre chaetae to be first present from chaetigers 15–16, accompanying the hooks. Pettibone (1962) observed them first in chaetiger 9 in material from the North Atlantic. Usually the stout sabre chaetae are easy to observe in dissected parapodia or even on entire specimens. In the case of *S. wigleyi*, the situation is more complicated. The stout bilimbate neurochaetae on chaetigers 4–14 closely resemble sabre chaetae and thus make it difficult to detect unambiguously the first appearance of sabre chaetae. Examination of material included in this study confirmed the presence of 1–2 chaetae in the inferiormost position slightly apart from remaining neurochaetae, regarded to be the position of a sabre chaetae, from chaetiger 4 (Fig. 10A,B). These chaetae vary in thickness, but usually are thinner than other chaetae in the respective neuropodia. This observation is also partly reflected in the drawings by Imajima (1991) and Pettibone (1962). Since these thin chaetae are present in hook-bearing neuropodia, now accompanying the normal sabre chaetae (Fig. 10C), we regard them as chaetae different from sabre chaetae and consider sabre chaetae in *S. wigleyi* to first appear from chaetiger 15.

Geographical distribution. Cosmopolitan. North and South Pacific Ocean: Australia, Japan, California; North and South Atlantic Ocean: off Massachusetts, off Ireland and Norway, off South Africa; Indian Ocean.

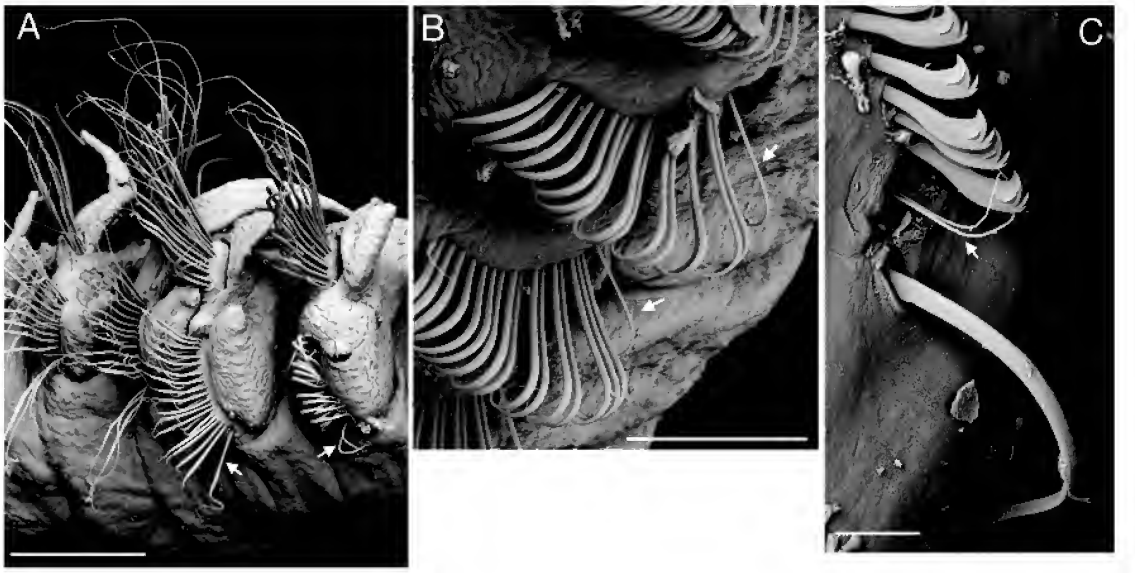

Fig. 10. *Spiophanes wigleyi* Pettibone, 1962. (*A*) parapodia 2–5, lateral oblique view (MV F90009); (*B*) neuropodia of chaetigers 7–8, anterior oblique view (MV F90018); (*C*) detail of a posterior neuropodium (AM W22948). Scales: *A,B* 100 µm; *C* 20 µm. Arrows point to thin neurochaetae in inferiormost position, usually regarded to be the position of the sabre chaeta.

Spiophanes prestigium n.sp.

Fig. 11

Spiophanes sp. 3.–Wilson & McDiarmid, 2003.

Type material. HOLOTYPE: Australia, Tasmania, Central Bass Strait, 40°31.1'S 145°04'E, in 29 m, 3–XI 1980 (MV F92141). PARATYPES: Australia, Tasmania, Central Bass Strait, 40°31.1'S 145°04'E, in 29 m, 3–XI 1980, 3 specimens (MV F90006); Tasmania, 41°09.68'S 146°27.38'E, in 3 m, May 1939, 1 specimen (MV F90027).

Other species examined. *Spiophanes tcherniai* Fauvel, 1950, SOUTHERN OCEAN: 45°59.8'S 49°58.3'E, in 210–217 m, 14 Apr 1976, 2 specimens (South African Museum A20308); South Shetlands, King George Island, Ardley Bay, 62°12'S 58°58'E, in 15 m, 9 Feb 1987, 1 specimen (ZSRO P1257) and Fildes Strait, 62°14'S 58°58'E, in 50 m, 18 Jan 1986, 1 specimen (ZSRO P1256); Wedell Sea, 20 Mar 1998, several specimens (ZMH P23931); Ross Island, McMurdo Sound, 77°13.08'S 166°26.4'E, in 54 m, 4 Jan 1971, several specimens (AM W22463).

Description. Holotype incomplete, with 27 chaetigers, 6.0 mm long and about 0.8 mm wide. Paratypes between 0.7–0.9 mm wide. Body slender, subcylindrical. *Prostomium* broad anteriorly, subtriangular, with elongate, digitiform anterolateral horns (Fig. 11A). Occipital antenna absent. Up to 2 pairs of eyes present. Nuchal organs as short ciliated bands, extending from posterior prostomium margin to beginning of chaetiger 3 (Fig. 11A). Peristomium poorly developed. Parapodia of chaetiger 1 oriented dorsally; postchaetal lamellae cirriform, notopodial lamellae slightly longer than neuropodial lamellae (Fig. 11A). Postchaetal notopodial lamellae of parapodia of chaetigers 2–4 cirriform, lamellae of chaetiger 3 usually longest (Fig. 11A,C,D). Neuropodial postchaetal lamellae of parapodia of chaetiger 2 subulate, tapered; in chaetiger 3 subulate with rounded tip; in chaetiger 4 short and rounded. In subsequent chaetigers, notopodial postchaetal lamellae subtriangular, with tapered tips becoming gradually thinner in middle and posterior body region; neuropodial lamellae reduced (Fig. 11E,F). *Chaetal spreader* not observed; glandular organ of chaetigers 9–15 opens as lateral vertical slit (Fig. 11B). Ventrolateral intersegmental genital pouches absent. Inconspicuous dorsal ciliated crests mostly present from chaetiger 4. *Chaetiger 1* usually with 1 stout, crook-like chaeta in neuropodium; remainder of chaetae capillaries; notochaetae arranged in tuft; neurochaetae arranged in 2 rows. Chaetigers 2–4 with capillaries with narrow sheath (Fig. 11L,M); notochaetae in tuft, neurochaetae in 2 rows. Notopodial capillaries of first 4 chaetigers not much longer than those in subsequent chaetigers. Notochaetae of chaetigers 5–13 capillaries with narrow sheath, arranged in 3 rows. From chaetigers 14–19, special spatulate chaetae with fine tips (mucro) present in addition to small number of capillaries with narrow sheath (Fig. 11G,I); spatulate chaetae number 12–25, most numerous on chaetigers 16 and 17. From chaetiger 20, notochaetae capillaries with narrow sheath, arranged in tuft. Neurochaetae of chaetigers 5–15 stout, bilimbate, distally pointed (Fig. 11J), arranged in 1–2 rows. From chaetiger 16 neuropodia with quadridentate, hooded hooks (Fig. 11K); initially with 5–7 hooks in 1 row, less numerous in more posterior chaetigers. Bacillary chaetae not emergent. Ventral sabre chaetae from chaetiger 4, very long, appearing granulated (Fig. 11H). *Pygidium* unknown.

Pigmentation. Conspicuous dark brownish pigmentation in chaetigers 9–15 encompasses the neuropodium as well as interramal region (Fig. 11B), absent in some alcohol-preserved material.

Methyl green staining pattern. Pigmented areas of parapodia 9–15 take up stain most intensely; if pigmentation is lost, respective area becomes visible by staining. In addition, small round stained patches detectable between noto- and neuropodia of chaetigers 5–8, in region where chaetal spreader usually occurs.

Biology. Species found in shallow water, between 3–29 m; in sandy substrates.

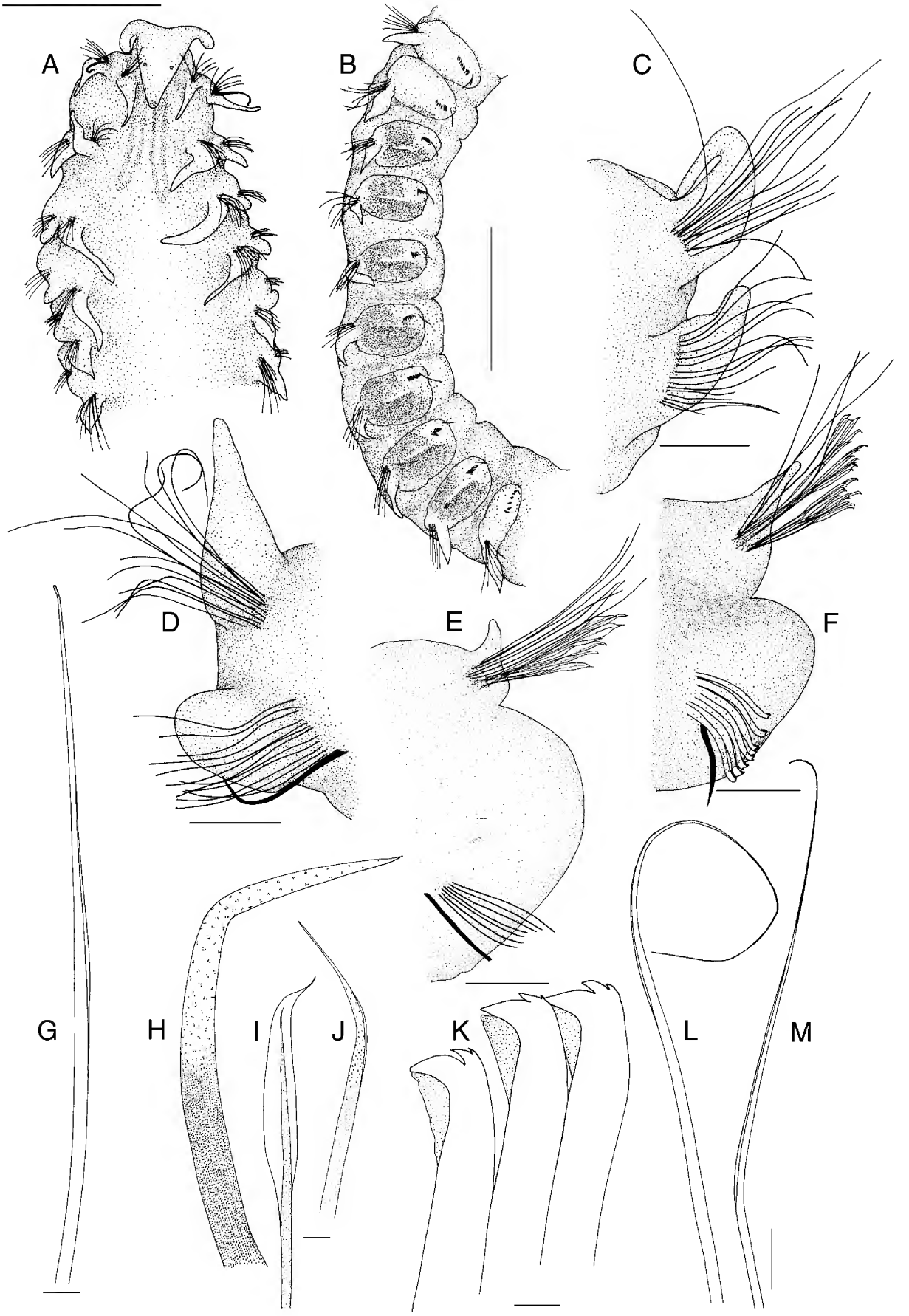
A
B
C
D
E
F
G
H
I
J
K
L
M

Remarks. *Spiophanes prestigium* is similar to *S. tcherniai* Fauvel, 1950 with regard to the structure of the nuchal organs, the shape of the prostomium, in having spatulate notochaetae in median segments, and the first appearance of hooks in chaetiger 16. However, *S. tcherniai* differs from *S. prestigium* in exhibiting spatulate notochaetae on chaetigers 15–18 instead of chaetigers 14–19; the number of spatulate chaetae in a tuft is considerably lower: ≤12 in *S. tcherniai* compared to up to 25 in *S. prestigium*; hooks in *S. tcherniai* are accompanied by thin simple capillaries which are absent in *S. prestigium*. In addition, the anterior row of chaetae in the neuropodia of chaetiger 3 consists of special geniculate chaetae in *S. tcherniai* but are simple capillaries in *S. prestigium*. *Spiophanes tcherniai* is known from Antarctic and Subantarctic waters only.

The diagnosis should be enhanced if material for SEM studies becomes available.

Etymology. *prestigium*—Latin for illusion, deception; referring to the close resemblance to *S. tcherniai*.

Geographical distribution. Australia: Bass Strait (Tasmania/Victoria).

Spiophanes pisinnus n.sp.

Fig. 12

Spiophanes sp. 4.–Wilson & McDiarmid, 2003.

Type material. HOLOTYPE: Australia, New South Wales, Pittwater, Longnose Point, 33°37.3'S 151°18.2'E, in 15 m, Apr 1992, (AM W24085). PARATYPE: Australia, New South Wales, Pittwater, 33°35.77'S 151°18.29'E, in 15.9 m, Jun 1995, 1 specimen (AM W23683).

Description. Holotype complete, with 31 chaetigers; total length about 4 mm, 0.3 mm wide. Incomplete paratype with 25 chaetigers, about 0.4 mm wide. Body slender, subcylindrical. *Prostomium* broad anteriorly, bell-shaped; anterior margin convex, with rounded, short anterolateral projections (Fig. 12A). Occipital antenna absent. Up to three single small eye spots forming 2 larger pigmented spots on the posterior part of the prostomium (Fig. 12A). Nuchal organs as pair of dorsal loops, extending from posterior prostomium margin to beginning of chaetiger 4 (Fig. 12A). Peristomium poorly developed. Parapodia of chaetiger 1 in dorsolateral position; postchaetal lamellae cirriform, about equal in length in both rami. Parapodia of chaetiger 2 also dorsolateral, parapodia 3–4 situated laterally (Fig. 12A). Notopodial postchaetal lamellae of parapodia of chaetigers 2–4 cirriform to subulate; neuropodial postchaetal lamella of chaetigers 2–3 subulate, in chaetiger 3 with rounded tip, postchaetal neuropodial lamellae of chaetiger 4 rounded (Fig. 12B). Chaetigers 5–8 with subtriangular, distally rounded notopodial lamellae; neuropodial postchaetal lamellae reduced (Fig. 12C). From chaetiger 9, notopodial lamellae subulate to subtriangular, with elongate tips; neuropodial lamellae reduced (Fig. 12D,E). *Chaetal spreader* of "0+1 type" with semicircular glandular opening well developed on chaetigers 5–7 (Fig. 12C); opening of glandular organs of chaetigers 9–14 present as lateral vertical slits. Ventrolateral intersegmental genital pouches absent. Dorsal ciliated crests indistinct. *Chaetiger 1* with 1–2 stout, crook-like chaetae in the neuropodium; remainder of chaetae capillaries. Notopodia of chaetigers 2–4 with capillaries, most with long, fine tips and narrow sheaths; neurochaetae stouter, bilimbate capillaries with narrow sheaths (Fig. 12M). Notopodial capillaries of chaetigers 1–4 longer than those in subsequent chaetigers. Arrangement of chaetae not determined. Chaetigers 5–14 with very stout bilimbate neurochaetae, distally pointed (Fig. 12J,O), arranged in 1 irregular row; notochaetae bilimbate capillaries of different lengths, with distinct sheaths, tips pointed and elongate to a varying degree (Fig. 12H,I,K,N), arranged in 3 indistinct rows. From chaetiger 15, notopodia with bilimbate capillaries with narrow sheaths (Fig. 12G,P), arranged in tuft; neuropodia with quadridentate hooks without hoods (Fig. 12F), initially with 3–4 hooks in single row. Bacillary chaetae not emergent in specimens examined. Sabre chaetae begin on chaetiger 4, very long in first parapodia compared to most other species of the genus (Fig. 12L). Single stout, bent capillary chaetae without sheath in posterior notopodia. *Pygidium* with two robust anal cirri, attached terminally in a ventrolateral position.

Pigmentation. Patch with reddish-brown pigment on prostomium, anteriorly to eyes (Fig. 12A).

Methyl green staining pattern. No discernible staining pattern.

Biology. Species occurs in mud and muddy sand, 15–16 m.

Remarks. This species is most similar to *S. wigleyi* in having the same type of nuchal organs, a pair of dorsal loops on the first 4 anterior chaetigers. However, *S. pisinnus* can be clearly distinguished by having non-hooded hooks rather than hooded hooks as well as the chaetal spreader of "0+1 type" with a semicircular glandular opening as opposed to exhibiting a short horizontal glandular opening. The shape of the neuropodial chaetae of chaetigers 5–14 is unique among *Spiophanes* species.

Etymology. *pisinnus*—Latin for small, little; referring to the small size of the species.

Geographical distribution. Species known only from the type locality.

Fig. 11 [facing page]. *Spiophanes prestigium* n.sp. (*A*) anterior end, dorsal view, methyl green-stained nuchal organ; (*B*) chaetigers 7–16, lateral view; (*C*) left parapodium from chaetiger 3; (*D*) right parapodium from chaetiger 4; (*E*) left parapodium from chaetiger 14; (*F*) left parapodium from chaetiger 16; (*G*) notochaeta from chaetiger 14; (*H*) sabre chaeta from chaetiger 4; (*I*) spatulate chaeta with mucro from notopodium 16; (*J*) neurochaeta from chaetiger 14; (*K*) hooded hooks from neuropodium 16; (*L*) notochaeta from chaetiger 4; (*M*) neurochaeta from chaetiger 4. Scales: *A,B* 0.5 mm; *C–F* 0.1 mm; *L,M* 10 µm; *G–K* 5 µm. *A,B* holotype, all others paratype MV F90027.

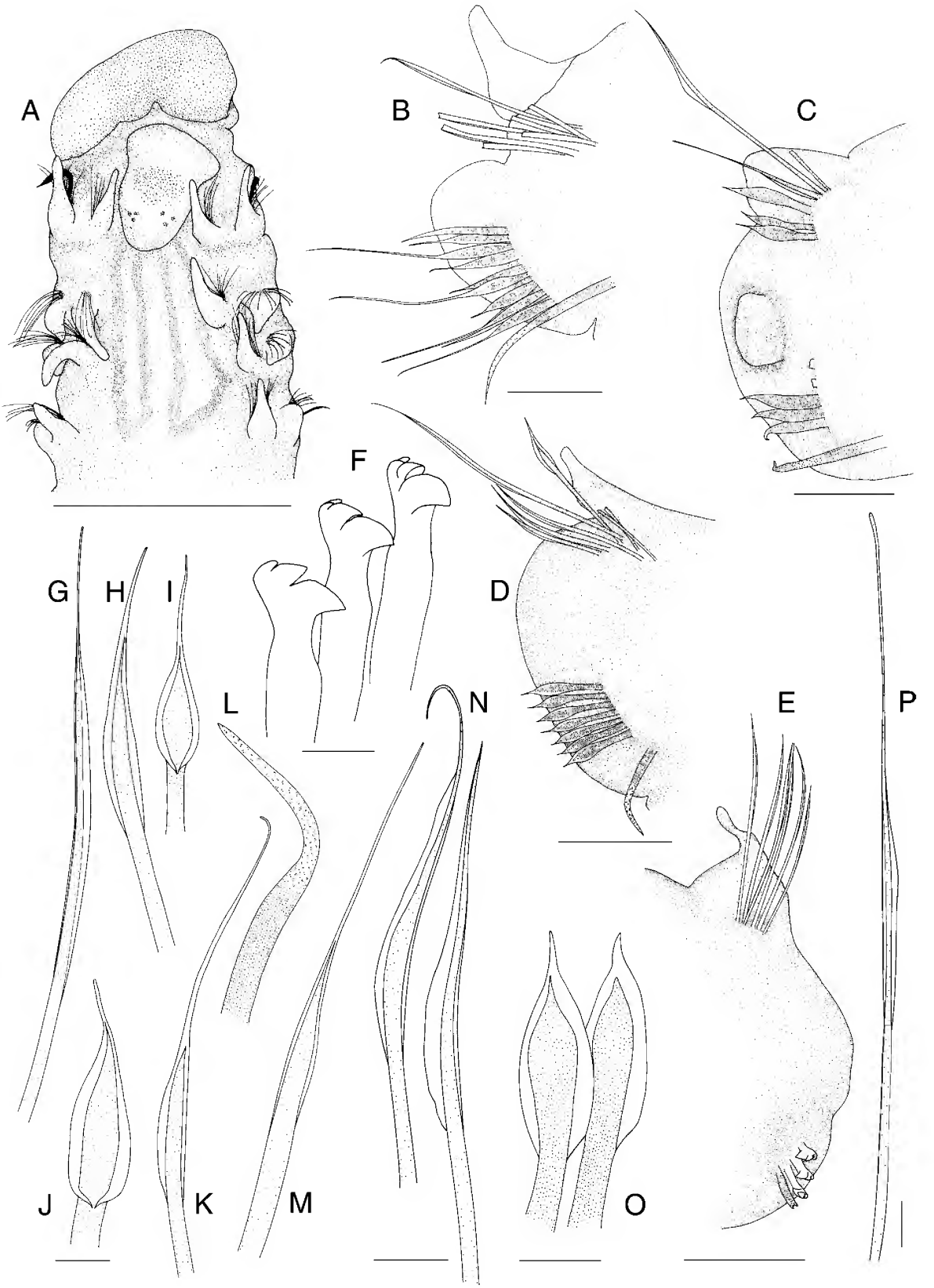

Fig. 12. *Spiophanes pisinnus* n.sp. (*A*) anterior end, dorsal view, methyl green-stained nuchal organ; (*B*) right parapodium from chaetiger 4; (*C*) right parapodium from chaetiger 7; (*D*) right parapodium from chaetiger 9; (*E*) left parapodium from chaetiger 15; (*F*) unhooded hooks neuropodium 15; (*G*) notochaeta from chaetiger 15; (*H*) notochaeta from chaetiger 9, frontal view; (*I*) short notochaeta from chaetiger 7; (*J*) neurochaeta from chaetiger 7; (*K*) long notochaeta from chaetiger 7; (*L*) sabre chaeta from chaetiger 9; (*M*) neurochaeta from chaetiger 4; (*N*) notochaetae from chaetiger 9, lateral view; (*O*) neurochaetae from chaetiger 9; (*P*) notochaeta from chaetiger 20. Scales: *A* 0.4 mm; *B–E* 50 μm; *F–P* 10 μm. All paratype AM W23683.

Spiophanes dubitalis n.sp.

Fig. 13

Spiophanes sp. 5.–Wilson & McDiarmid, 2003.

Type material. HOLOTYPE: Australia, Victoria, Central Bass Strait, 66 km S of Rodondo Island, 39°49.5'S 146°18.5'E, in 82 m, 13 Nov 1981, (MV F90005).

Other species examined. *Spiophanes bombyx*: NORTH ATLANTIC OCEAN: North Sea, German Bight, 54°20.01'N 7°20.01'E, in 43 m, 26 May 1987, several specimens (SM 4950); 55°54'N 3°27.6'E, in 65 m, 10 Aug 1990, 2 specimens (SM 6476); 55°46.93'N 3°52.38'E–55°53.09'N 3°28.8'E, in 48.4 m, 10 Aug 1990, 3 specimens (SM 6480); 53°41.46'N 6°59.58'E, in 3.5 m, 13 Mar 1989, 8 specimens (SM 6527). MEDITERRANEAN: Spain, between Cape San Antonio and Valencia harbour, 29 Apr 1996, two specimens (MNCN 16.01/2648, 2661). INDIAN OCEAN: 34°16.8'S 18°42.8'E, in 60 m, 25 Feb 1959, several specimens (South African Museum A20779). PACIFIC OCEAN: Alaska, Bering Sea, 58°46.36'N 164°14'W, in 35 m, 23 May 1976, 2 specimen (CAS 23887); Alaska, Chukchi Sea, 67°44.29'N 164°33.45'W, in 5.7 m, 17 Aug 1976, 1 specimen (CAS 1675); California, 37°49.27'N 122°25.55'W, in 58–67 m, 24 Sep 1973, several specimen (CAS 1915); 37°46'N 122°41.5'W, in 31 m, 14 Aug 1973, several specimen (CAS 123655).

Spiophanes tcherniai: SOUTHERN OCEAN: 45°59.8'S 49°58.3'E, in 210–217 m, 14 Apr 1976, 2 specimens (South African Museum A20308); South Shetlands, King George Island, Ardley Bay, 62°12'S 58°58'E, in 15 m, 9 Feb 1987, 1 specimen (ZSRO P1257) and Fildes Strait, 62°14'S 58°58'E, in 15 m, 18 Jan 1986, 1 specimen (ZSRO P1256); Wedell Sea, 20 Mar 1998, several specimens (ZMH P23931); Ross Island, McMurdo Sound, 77°13.08'S 166°26.4'E, in 54 m, 4 Jan 1971, several specimens (AM W22463).

Description. Holotype incomplete, with 27 chaetigers; about 3 mm long, 0.15 mm wide. Body slender, subcylindrical. *Prostomium* broad anteriorly, bell-shaped to subtriangular, with distinct anterolateral projections (Fig. 13A,B). Occipital antenna absent. Eyes not observed. Nuchal organs as indistinct pair of dorsal loops or kind of short ciliated band, extending from posterior prostomium margin to beginning of chaetiger 3 (Fig. 13A,B). Peristomium poorly developed. Parapodia of chaetiger 1 oriented dorsally; postchaetal lamellae subulate, more or less equal in length in both rami (Fig. 13A). Parapodia of chaetigers 2–4 positioned laterally; notopodial postchaetal lamellae subulate, those of chaetiger 2 longest; neuropodial postchaetal lamellae subulate to rounded (Fig. 13A,C). Chaetigers 5–8 with ovoid notopodial postchaetal lamellae; neuropodial lamellae reduced (Fig. 13D). From chaetiger 9, notopodial lamellae short, digitiform to subulate; neuropodial lamellae reduced (Fig. 13E,F). *Chaetal spreader* of "0+1 type" with semicircular glandular opening on chaetigers 5–7 (Fig. 13A); glandular opening absent in chaetiger 8; glandular organ of chaetigers 9–14 opens as lateral, vertical slit. Ventrolateral intersegmental genital pouches absent. Dorsal ciliated crests indistinct. *Chaetiger 1* with 1–2 stout, crook-like chaetae in the neuropodia; remainder of chaetae capillaries; notochaetae arranged in tuft; neurochaetae arranged in 2 rows. Chaetigers 2–4 notopodia with capillaries with narrow sheaths (Fig. 13K,M), arranged in tuft; neurochaetae capillaries with narrow and broad sheaths (Fig. 13L,N), arranged in 2 rows. Notopodial capillaries of chaetigers 1–4 only slightly longer than those of subsequent chaetigers. Chaetigers 5–14 with stout, bilimbate neurochaetae, distally pointed (Fig. 13H,I), arranged in 1 irregular row; notochaetae with narrow sheath (Fig. 13P), arranged in 3 rows. From chaetiger 15, notopodial capillaries with narrow sheaths (Fig. 13 O), arranged in tuft; neuropodia with quadridentate hooded hooks (Fig. 13G), initially with 5 hooks in 1 row, smaller number of hooks in more posterior chaetigers. Bacillary chaetae not present in the holotype. Sabre chaetae from chaetiger 4, long, granulated, without sheath (Fig. 13J). *Pygidium* unknown.

Pigmentation. Orange-brown pigment on chaetigers 10–13; encompasses neuropodia and lateral side of the body.

Methyl green staining pattern. Posterior tip of the prostomium and postchaetal lamellae stain dark blue (Fig. 13B).

Biology. Substrate at the sampling locality was described as "sand-silt-mud".

Remarks. This species resembles *S. prestigium* n.sp., *S. tcherniai* and *S. bombyx* with regard to the appearance of nuchal organs, being a short ciliated band or kind of ciliated loop on the dorsum, extending to the beginning of chaetiger 3, the presence of hooded hooks, and the absence of an occipital antenna. However, *S. prestigium* and *S. tcherniai* clearly differ from *S. dubitalis* in having spatulate notochaetae in the middle body region, which are absent in *S. dubitalis*, and bearing neuropodial hooded hooks from chaetiger 16 rather than 15. *Spiophanes bombyx* is readily distinguished from *S. dubitalis* by its long anterolateral horns compared to only short anterolateral horns in *S. dubitalis*, the presence of sabre chaetae only accompanying the neuropodial hooks rather than being present from chaetiger 4, and its chaetal spreaders of the "0+1 type" with a wavy glandular opening in chaetigers 5–8 rather than chaetal spreaders of the "0+1 type" with a semicircular glandular opening on chaetigers 5–7. *Spiophanes tcherniai* has not been reported from Australian waters; previous records of *S. bombyx* were found to be incorrect (this paper) and the occurrence of this species could not be substantiated from investigating all *Spiophanes* material available from Australian collections.

Etymology. *dubitalis*—Latin for dubious, to be doubted; referring to the unfortunate situation of having only one specimen for establishing a new species which shares several of its characters with other species in the genus but still has a clearly different character combination.

Geographical distribution. Species only known from the type locality.

Spiophanes sp. A

Material. AUSTRALIA, VICTORIA, 53 km S of Cape Conran, 38°8'S 148°39'E, in 750 m, May 1969, 1 specimen (AM W13019).

Other species examined. *Spiophanes lowai* Solís-Weiss, 1983, NORTH PACIFIC OCEAN: MÉXICO, Sinaloa, Sinaloa coast S of Mazatlan, 23°38.3'N 106°55.3'W, in 37 m, 25 Aug 1981, 1 paratype (USNM 80467).

Description. Specimen incomplete, with 25 chaetigers; 1.8 mm wide, about 8 mm long. Body slender, subcylindrical. *Prostomium* broad anteriorly, bell-shaped, with distinct anterolateral projections. Occipital antenna long, slender.

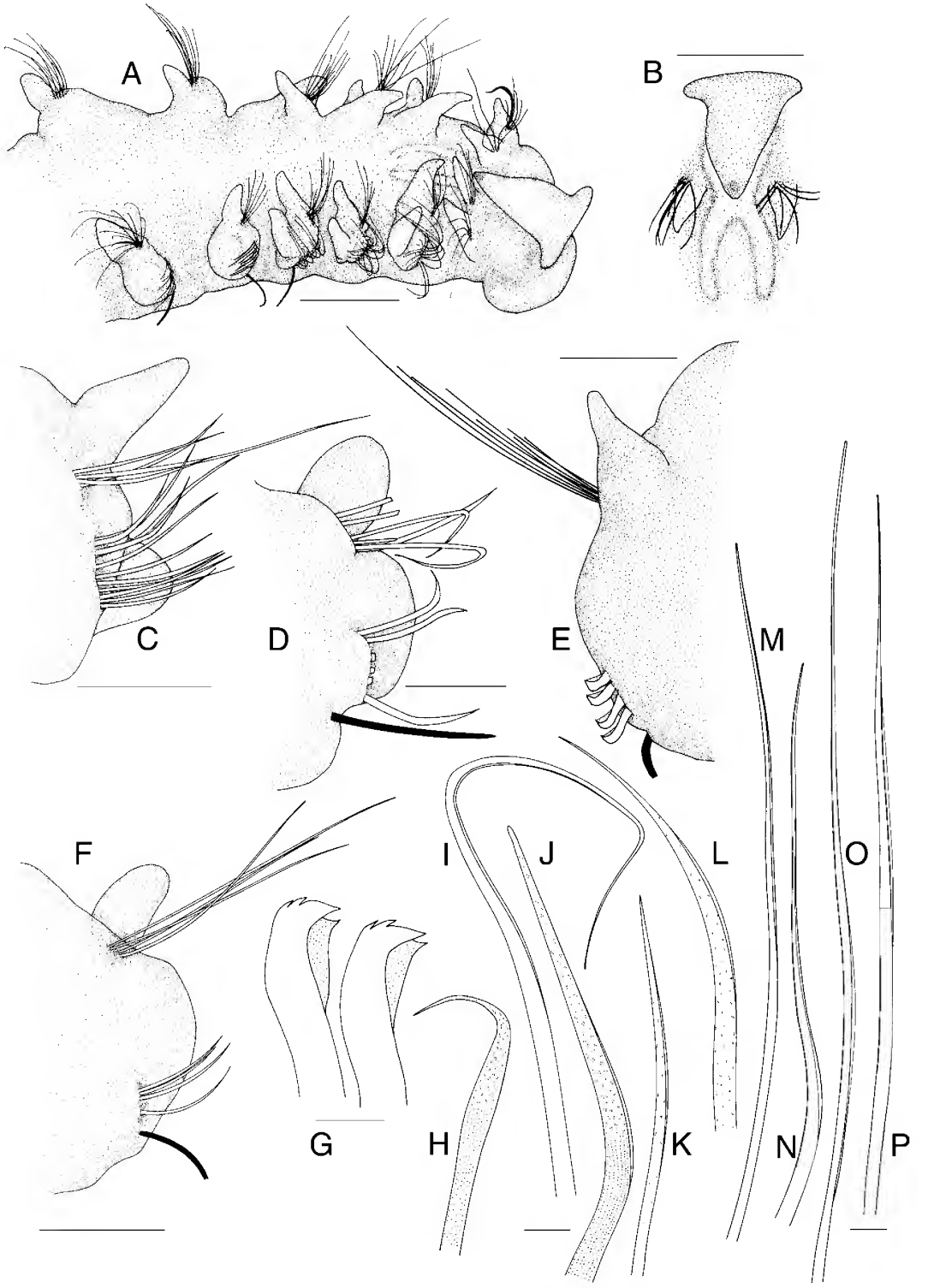

Fig. 13. *Spiophanes dubitalis* n.sp. (*A*) anterior end, lateral view, methyl green-stained nuchal organ; (*B*) prostomium and nuchal organ, dorsal view, stained; (*C*) left parapodium from chaetiger 3; (*D*) left parapodium from chaetiger 5; (*E*) left parapodium from chaetiger 16; (*F*) left parapodium from chaetiger 10; (*G*) hooded hooks from neuropodium 16; (*H*) neurochaeta from chaetiger 10; (*I*) neurochaeta from chaetiger 5; (*J*) sabre chaeta from chaetiger 15; (*K*) short notochaeta from chaetiger 3; (*L*) short granulated neurochaeta from chaetiger 3; (*M*) long notochaeta from chaetiger 3; (*N*) long neurochaeta from chaetiger 3; (*O*) notochaeta from chaetiger 15; (*P*) notochaeta from chaetiger 10. Scales: *A,B* 0.1 mm; *C–F* 50 μm; *G–P* 5 μm. All holotype MV F90005.

Eyes absent. Nuchal organs as two ciliated bands along dorsum; starting posterior to prostomium as two parallel, dorsolateral lines to chaetiger 6, bands converge between chaetigers 7–9, continuing posteriorly as two close parallel bands middorsally to chaetiger 15. Peristomium well developed. Parapodia of chaetiger 1 dorsolateral; postchaetal lamellae cirriform, neuropodial more robust. Postchaetal notopodial lamellae of parapodia of chaetigers 2–4 long, cirriform, neuropodial lamellae shorter, subulate in chaetigers 3 and 4. Chaetigers 5–8 with short, rounded

notopodial and reduced neuropodial postchaetal lamellae. From chaetiger 9, notopodial lamellae subtriangular with short slender tip, in posterior chaetigers slender tip elongate; neuropodial lamellae reduced. *Chaetal spreader* "0+1 type" with well-developed semicircular glandular openings on chaetigers 5–7; glandular opening on chaetiger 8 absent; glandular organ of chaetigers 9–14 opens as lateral, vertical slit. First fully developed ventrolateral intersegmental genital pouches present between chaetigers 14–15. Dorsal ciliated crests from chaetiger 20. *Chaetiger 1* usually with 1 stout, crook-like chaetae in neuropodium; remainder of chaetae capillaries; notochaetae arranged in tuft; neurochaetae in 2 rows. Notochaetae of chaetigers 2–4 with simple capillaries and capillaries with narrow sheaths, arranged in tuft; neurochaetae capillaries with narrow sheaths, arranged in 2 rows, anterior row appearing granulated. Notopodial capillaries of chaetigers 1–4 longer than those of subsequent chaetigers. Chaetigers 5–14 with stout bilimbate neurochaetae, distally pointed, arranged in 1–2 indistinct rows; notochaetae with distinct sheath, in 3 rows. From chaetiger 15, limbate capillaries in notopodia, their sheaths becoming narrower, notochaetae in tuft; neuropodia bearing quadridentate hooks without hoods, initially with 6–7 hooks in 1 row. Bacillary chaetae not emergent. Ventral sabre chaetae with cryptic ridge from chaetiger 4, appearing granulated distally. *Pygidium* unknown.

Pigmentation. Brownish pigment from chaetigers 9–14; encompasses entire parapodium except for distal parts of postchaetal notopodial lamellae and distal-most region of neuropodium. Brownish pigment in notopodial postchaetal lamellae of chaetigers 15–19.

Methyl green staining pattern. Pigmented areas take up stain most intensely.

Remarks. The described specimen, an anterior fragment, is in good condition. It is clearly different from all other species in the Australian museum collections in presenting the following character combination: presence of an occipital antenna, chaetal spreader of "0+1 type" with well-developed semicircular glandular opening on chaetigers 5–7, presence of intersegmental genital pouches from between chaetigers 14–15, and pigmented parapodia on chaetigers 9–14. Among Australian species, it is most similar to *S. viriosus* n.sp., which also has an occipital antenna on a bell-shaped prostomium with short anterolateral projections and intersegmental genital pouches from between chaetigers 14–15. However, *Spiophanes* sp. A clearly differs from *S. viriosus* in having a chaetal spreader of the "0+1 type" with semicircular glandular opening rather than a chaetal spreader of the "2+3 type" with wavy glandular opening. In addition, *Spiophanes* sp. A has a pigmented region on chaetigers 9–14 and pigmented notopodial lamellae on chaetigers 15–19 instead of having a smaller pigmented region in neuropodia of chaetigers 9–12 as present in *S. viriosus*. Considering species known world-wide, the specimen closely resembles a paratype of *S. lowai* (USNM 80467), described from the Pacific coast of México. Only minor differences concerning the pigmentation of these two specimens can be found, but it also has to be mentioned that the nuchal organs cannot be observed in the specimen from México since the cuticula of the dorsum is damaged. However, all other characters appear to match. The problem is that several significant characters of the examined *S. lowai* paratype are different from the species description of *S. lowai*: the occipital antenna is described as small rather than large, brown pigment is supposed to occur from chaetigers 10–15 rather than 9–14, and sabre chaetae to begin on chaetiger 5 rather than 4. Intersegmental genital pouches Solís-Weiss (1983) describes to begin on chaetiger 15 rather than between chaetiger 14 and 15. Apart from these discrepancies, it also has to be stressed that the differentiation between *S. kroyeri* and *S. lowai* is also problematical. Under these circumstances it did not seem to be appropriate to assign the single Australian specimen to either a new or a known species.

Summary

In the present study, five new *Spiophanes* species from Australian waters are described. *Spiophanes japonicum*, is newly reported for Australia. Blake's (1996) synonymy of *S. japonicum* with *S. berkeleyorum*, was found to be incorrect and has been rescinded. The species *S. urceolata*, is synonymized with *S. wigleyi*. Previous records of *S. kroyeri* and *S. bombyx* for Australian waters (e.g., Blake & Kudenov, 1978; Hutchings & Murray, 1984) could not be substantiated. Hence, eight species are presently reported for Eastern Australia. Species can be assigned to two major groups; one comprising mostly larger species possessing an occipital antenna and nuchal organs with two parallel ciliated bands running along the dorsum to chaetigers 10–18 and bearing neuropodial hooks without hooks (*S. modestus, S. viriosus, S. japonicum, Spiophanes* sp. A); the other group includes mostly small species without an occipital antenna and nuchal organs consisting of a pair of ciliated loops on the dorsum extending up to chaetiger 4 (*S. wigleyi, S. prestigium, S. pisinnus, S. dubitalis*) (Table 1). Among species of the first group, *S. modestus* differs in exhibiting anterolateral horns rather than short anterolateral projections and having neuropodial hooks from chaetiger 14 rather than from 15. In the second group, *S. wigleyi* stands out due to its moderate size compared to the small size of the other species and the undeveloped anterolateral horns.

Table 1. Important taxonomic characters of *Spiophanes* species from eastern Australia.

species	occipital antenna; prostomial shape	chaetal spreader (type; chaetigers where exposed)	nuchal organ	neuropodial hooks (first appearance; number in one row)	intersegmental genital pouches	pigment	remarks
S. modestus n.sp.	short antenna present; bell-shaped with distinct horns	"2+3 type" with wavy glandular opening; chaetigers 5–7	2 parallel lines, terminating as divergent wavy lines on chaetigers 15–17	from chaetiger 14; without hood; 6–8	absent	inconspicuous	—
S. viriosus n.sp.	present; bell-shaped with short antero-lateral projections	"2+3 type" with wavy glandular opening; chaetigers 5–7	2 parallel lines, diverging at the end, until chaetigers 17–18	from chaetiger 15; without hood; 5–7	present, first fully developed between chaetigers 14–15	in parapodia (posteriorly along vertical slit) of chaetigers 9–12	—
S. japonicum Imajima, 1991	present; bell-shaped with short antero-lateral projections	"0+1 type" with semi-circular glandular opening; chaetigers 5–7	2 parallel lines extending to chaetigers 10–12	from chaetiger 15; without hood; 4–7	absent	neuropodia 9–13 and dorsally on chaetigers 10–15	removed from synonymy of *S. berkeleyorum* Pettibone, 1962
S. wigleyi Pettibone, 1962	absent; slightly bell-shaped, subtriangular to oval	indistinct crescent-shaped, horizontal glandular opening on chaetigers 5–8	pair of dorsal loops extending to chaetiger 4	from chaetiger 15; hooded; 10–11	absent	notopodial postchaetal lamella of chaetigers 9–15	includes *S. urceolata* Imajima, 1991
S. prestigium n.sp.	absent; subtriangular with distinct horns	not visible	pair of dorsal loops extending to the beginning of chaetiger 3	from chaetiger 16; hooded; 5–7	absent	parapodia of chaetigers 9–15	special spatulate notopodial chaetae from chaetiger 14–19
S. pisinnus n.sp.	absent; bell-shaped with short antero-lateral projections	"0+1 type" with semi-circular glandular opening; chaetigers 5–7	pair of dorsal loops extending to chaetiger 4	from chaetiger 15; without hood; 3–4	absent	on the prostomium anteriorly to the eyes	—
S. dubitalis n.sp.	absent; bell-shaped with distinct horns	"0+1 type" with semi-circular glandular opening; chaetigers 5–7	pair of dorsal loops extending to the beginning of chaetiger 3	from chaetiger 15; hooded; 4–5	absent	neuropodia and lateral side of the body on chaetigers 10–13	—
Spiophanes sp. A	present; bell-shaped with short antero-lateral projections	"0+1 type" with semi-circular glandular opening; chaetigers 5–7	2 mostly parallel lines up to chaetiger 15; see description for details	from chaetiger 15; without hood; 6–7	present, first fully developed between chaetigers 14–15	parapodia of chaetigers 9–14 and postchaetal lamella of notopodia 15–19	most similar to *S. lowai* Solís-Weiss, 1983

Key to species of *Spiophanes* from Eastern Australia

Methyl green staining will be required for observation of most characters.

1 Occipital antenna present, nuchal organs as parallel lines along dorsum, neuropodial hooks without hoods 2

—— Occipital antenna absent, nuchal organ short or as a pair of dorsal loops up to chaetigers 2–4, hooks with or without hoods 5

2 Neuropodial hooks starting on chaetiger 14, occipital antenna short, prostomium bell-shaped with distinct anterolateral horns, chaetal spreader of the "2+3 type" with wavy glandular opening developed on chaetigers 5–7, pigment inconspicuous in alcohol preserved specimens ..... *S. modestus*

—— Neuropodial hooks starting on chaetiger 15, occipital antenna of moderate length, prostomium bell-shaped with short anterolateral projections 3

3 Chaetal spreader of the "2+3 type" with wavy glandular opening developed on chaetigers 5–7, brown pigment in parapodia of chaetigers 9–12 posteriorly along vertical slit, intersegmental genital pouches first present between chaetigers 14–15 ..... *S. viriosus*

—— Chaetal spreader of the "0+1 type" with semicircular glandular opening developed on chaetigers 5–7, pigment different, intersegmental genital pouches present or absent 4

4 Intersegmental genital pouches present, brown pigment in parapodia of chaetigers 9–14 and in postchaetal lamella of notopodia of chaetigers 15–19 ..... *Spiophanes* sp. A

—— Intersegmental genital pouches absent, brownish pigment in neuropodia of chaetigers 9–13 and additional glandular region (usually with pink or bright orange pigment) dorsally on chaetigers 10–15 close to the bases of the notopodia ..... *S. japonicum*

5 Neuropodial hooks without hoods, prostomium bell-shaped with short anterolateral projections and reddish pigment anteriorly to the eyes, nuchal organ as a pair of dorsal loops extending to chaetiger 4 ..... *S. pisinnus*

—— Neuropodial hooks with hoods 6

6 Prostomium slightly bell-shaped, subtriangular or oval; nuchal organ as a pair of dorsal loops extending to chaetiger 4, up to 10–11 neuropodial hooks in one row; reddish pigment in notopodial postchaetal lamella of chaetigers 9–15 ..... *S. wigleyi*

—— Prostomium subtriangular or bell-shaped with distinct anterolateral horns; not more than 7 neuropodial hooks in one row; nuchal organ short extending to the beginning of chaetiger 3 7

7 Neuropodial hooks starting on chaetiger 16; special spatulate chaetae in notopodia of chaetigers 14–19 ..... *S. prestigium*

—— Neuropodial hooks starting on chaetiger 15; orange-brown pigment in neuropodia and lateral side of the body in chaetigers 10–13 ..... *S. dubitalis*

ACKNOWLEDGMENTS. We would like to thank the following curators and polychaete workers for finding and providing material, especially type material, from the collections of their institutions: Chris Rowley and Robin Wilson, Museum Victoria; Mal Bryant and Lester Cannon, Queensland Museum; Thierry Laperousaz, South Australian Museum; Minoru Imajima and Masatsune Takeda, National Science Museum Tokyo; William Moser and Kristian Fauchald, Smithsonian Institution; Angelika Brandt and Gisela Wegener, Zoologisches Museum Hamburg; Birger Neuhaus, Naturkundemuseum Berlin; Andreas Bick, Zoologische Sammlung Rostock; Dieter Fiege and Marie-Luise Tritz, Senckenberg Museum; Miguel Villena Sánches Valero, Museo Nacional de Ciencias Naturales; Ardis Johnson, Museum of Comparative Zoology, Harvard University Cambridge; Leslie Harris, Los Angeles County Museum-Allan Hancock Foundation; Elizabeth Kools, Californian Academy of Science; Harry A. ten Hove, Zoological Museum of Amsterdam University; Michelle van der Merwe and Elizabeth Hoenson, South African Museum; Miranda Lowe, The Natural History Museum, London; Stefan Lundberg, Swedish Museum of Natural History; and Vasily Radashevsky, who provided specimens from his personal collection. We would also wish to thank Sue Lindsay, who assisted in the SEM lab, and Shane Ahyong for helpful discussions. We also wish to thank the two anonymous reviewers for their critical review of the manuscript. The study was funded by the Postdoctoral Fellowship Program of the German Academic Exchange Service (Deutscher Akademischer Austauschdienst—DAAD) and generously supported by the Australian Museum, Sydney.

References

Blake, J.A., 1983. Polychaetes of the family Spionidae from South America, Antarctica and adjacent seas and islands. *Biology of the Antarctic Seas* XIV (*Antarctic Research Series*) 39(3): 205–288.

Blake, J.A., 1996. Family Spionidae Grube, 1850. Including a review of the genera and species from California and a revision of the genus *Polydora* Bosc, 1802. In *Taxonomic Atlas of the Benthic Fauna of the Santa Maria Basin and the Western Santa Barbara Channel*, ed. J.A. Blake, B. Hilbig & P.H. Scott. Santa Barbara: Santa Barbara Museum of Natural History. The Annelida Part 3—Polychaeta: Orbiniidae to Cossuridae 6: 81–223.

Blake, J.A., & J.D. Kudenov, 1978. The Spionidae (Polychaeta) from southeastern Australia and adjacent areas with a revision of the genera. *Memoirs of the National Museum of Victoria* 39: 171–280.

Chamberlin, R.V., 1919. New polychaetous annelids from Laguna Beach, California. *Pomona College Journal of Entomology and Zoology* 11: 1–23.

Claparède, E., 1870. Les Annélides Chétopodes du Golfe de Naples. Troisième partie. *Mémoires de la Société de Physique et d'Histoire naturelle de Genève* 20(2): 365–542.

Fauvel, P., 1950. Mission de batiment polaire «Commandant-Charcot». Récoltes faites en Terre Adélie (1950) par Paul Tchernia. Annélides polychètes. *Bulletin du Muséum National d'Histoire naturelle, Paris*, sér. 2, 22(6): 753–773.

Foster, N.M., 1971. Spionidae (Polychaeta) of the Gulf of Mexico and the Caribbean Sea. *Studies on the Fauna of Curaçao and other Caribbean Islands* 36: 1–150.

Grube, A.E., 1860. Beschreibung neuer oder wenig bekannter Anneliden. *Archiv der Naturgeschichte* 26: 71–118.

Hartman, O., 1965. Deep-water benthic polychaetous annelids off New England to Bermuda and other North Atlantic areas. *Allan Hancock Foundation Publications. Occasional Paper* 28: 1–378.

Hutchings, P., & A. Murray, 1984. Taxonomy of polychaetes from the Hawkesbury River and the southern estuaries of New South Wales, Australia. *Records of the Australian Museum* 36(3): 1–119.

Imajima, M., 1991. Spionidae (Annelida, Polychaeta) from Japan VII. The genus *Spiophanes*. *Bulletin of National Science Museum Tokyo* Ser. A (Zoology) 17: 115–137.

Johnson, P.G., 1984. Family Spionidae Grube, 1850. In *Taxonomic guide to the polychaetes of the northern Gulf of Mexico*, Vol. 2. Uebelacker, ed. J.M. & P.G. Johnson, 245 pp. Mobile, Alabama: Barry A. Vittor & Associates, Inc.

Maciolek, N.J., 2000. New species and records of *Aonidella, Laonice*, and *Spiophanes* (Polychaeta: Spionidae) from shelf and slope depths of the western North Atlantic. *Bulletin of Marine Science* 67(1): 529–547.

Pettibone, M.H., 1962. New species of polychaete worms (Spionidae: *Spiophanes*) from the east and west coast of North America. *Proceedings of the Biological Society of Washington* 75: 77–88.

Söderström, A., 1920. *Studien über die Polychaetenfamilie Spionidae*. PhD thesis, Uppsala, 286 pp.

Solís-Weiss, V., 1983. *Parandalia bennei* (Pilargidae) and *Spiophanes lowai* (Spionidae), new species of polychaetous annelids from Mazatlan Bay, Pacific coast of Mexico. *Proceedings of the Biological Society of Washington* 96(3): 370–378.

Wilson, R.S., & H. McDiarmid, 2003. Spionidae (Polychaeta)—A DELTA database of genera, and Australian species. In *Polychaetes: Interactive Identification and Information Retrieval*, ed. R.S. Wilson, P.A. Hutchings & C.J. Glasby. Melbourne: CSIRO Publishing.

Manuscript received 7 May 2002, revised 1 December 2002 and accepted 20 March 2003.

Associate Editor: G.D.F. Wilson.

Records of the Australian Museum (2003) Vol. 55: 141–152. ISSN 0067-1975

Basalts from Rose Atoll, American Samoa

K.A. RODGERS[1], F.L. SUTHERLAND[2]* AND P.W.O. HOSKIN[3]

[1] Research Associate, Australian Museum, 6 College Street, Sydney NSW 2010, Australia

[2] Geodiversity Research Centre,
Australian Museum, 6 College Street, Sydney NSW 2010, Australia
lins@austmus.gov.au

[3] Institut für Mineralogie, Petrologie und Geochemie,
Albert-Ludwigs Universität Freiburg, Albertstrasse 23b, D-79104 Freiburg in Breisgau, Germany

ABSTRACT. Three specimens of lava float collected in 1939 from Rose Atoll consist of three distinct basalt types: holocrystalline olivine tholeiite, coarse vesicular picrite basalt and olivine-poor transitional basalt; the tholeiite contains coarser, late-stage segregations with a glassy, silicic mesostasis. In mineralogy and chemistry these basalts most closely resemble Ta'u Group lavas of the neighbouring Manu'a Islands. Differences exist that do not suggest their transport to Rose Atoll, even though no in situ basalts are known there. Incompatible primitive mantle-normalized trace element plots show strong depletion in K and Sr and enrichment in U, Pb and La. In Ba/Nb versus La/Nb plots Rose basalts lie between normal mid-ocean ridge basalt (N-MORB) and low $^{87}Sr/^{86}Sr$ oceanic island basalt (OIB) fields. They lie outside many plume-related OIB fields, including plume-related Samoan basalts. Trace element ratios for the Rose samples show little correspondence with end member MORBs and OIBs. This, and temporal and geographic plume reconstructions, indicate that the Rose basalts are derived from melting of unusual or mixed lithospheric sources. They seem unrelated to the main phases of Samoan plume activity, now located at Vailulu'u Seamount.

RODGERS, K.A., F.L. SUTHERLAND & P.W.O. HOSKIN, 2003. Basalts from Rose Atoll, American Samoa. *Records of the Australian Museum* 55(2): 141–152.

Basalts found on Rose Atoll, American Samoa, present an enigma. To date petrologists have overlooked the seemingly conflicting reports of infrequent expeditions to the island (Sachet, 1954, 1955; Keating, 1992; Rodgers *et al.*, 1993). Yet, given the geographic position at the eastern end of the Samoan chain, the age and nature of any basalts there are important in constraining the tectono-volcanic evolution of this chain. Only one brief description of a thin section of Rose basalt exists (Sachet, 1954). Here we present petrographic descriptions and chemical data for three samples from Rose held by the Smithsonian Institution (NMNH no. 102227) —the only known captive samples. From this we offer an assessment of their possible provenance.

Rose Atoll

Rose Atoll (14°32'S 168°08'W) lies 240 km ESE of Pago Pago at the eastern end of the Samoan Islands, part of a 1700 km long chain of seamounts, shallow banks and submerged atolls (Fig. 1). These volcanic features show an orientation consistent with their potential generation by

* author for correspondence

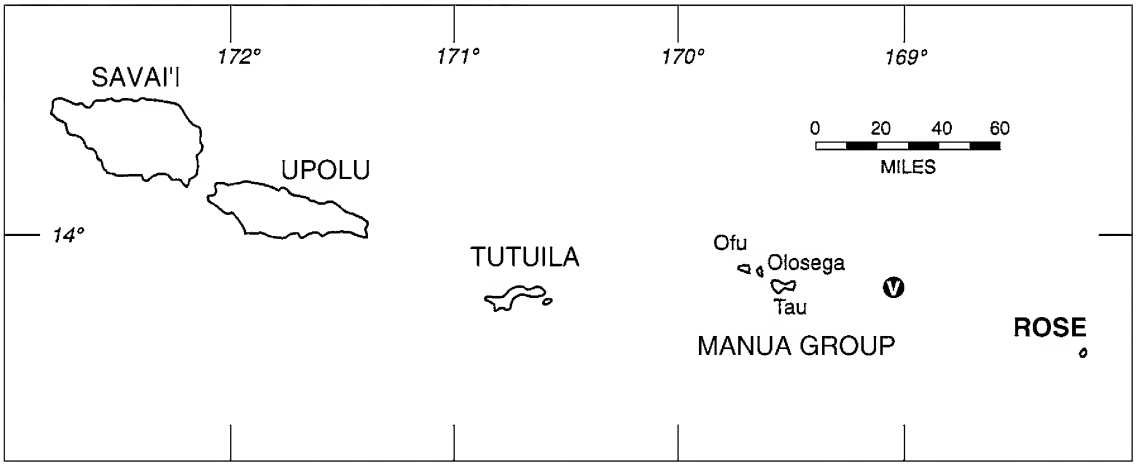

Fig. 1. Location map of Rose Atoll within the Samoan Island Chain. Vailulu'u submarine volcano (V) is located at 14°13'S 169°04'W.

Pacific plate motion over a fixed thermal anomaly (e.g., Natland, 1980; Menard, 1986). Island size and proportion covered with Quaternary lava flows increases to the west, in contrast to the Hawaiian, Society and Marquesas lineaments. There, submerged volcanic mounds, both drowned and capped by atoll reefs, occur at their western end. In contrast to mature submerged atolls and banks of the Samoan chain, Rose lacks wide offshore banks. It appears very young. The fetch of the lagoon is only 2 km and with the fringing reef and lagoon together covering just 640 ha, the atoll is among the smallest in the world. No in situ basalt is known on Rose Island.

The United States Exploring Expedition of 1839 reported loose boulders of vesicular lava ranging from 20 to 200 pounds in weight, scattered on the reef flat and in the lagoon (Couthouy, 1842; Wilkes, 1844; Dana, 1849, 1851; Pickering, 1876). In the absence of in situ basalt, Dana (1849, p. 309) suggested these boulders may have "been carried there by floating logs, or as ballast of some canoe." In 1920, Mayor (1921, 1924) looked for but failed to find volcanic rocks. He and Setchell (1924) dismissed the earlier reports as incorrect identifications of dark coloured, weathered limestone that abounds on the reef. However, in June 1939, Schultz (1940) sampled from a dozen boulders of lava lying on the reef flat and Dr Gilbert Corwin of the Smithsonian Institution subsequently confirmed these as olivine basalt (Sachet, 1954).

In evaluating these accounts, Keating (1992) cites a personal report from Dr Balzas, a herpetologist, that the only volcanic rocks he observed during several visits to Rose in the 1980s were float he attributed to transport by Samoans for use in traditional cooking. While this interpretation could account for some smaller boulders, it is implausible for larger masses, and fails to account for their reported number, variations in the observations and scattered distribution across the fringing reef and within the lagoon. These all strongly suggest basalt is being released from adjacent underwater sources, perhaps during large storms.

Material and methods

The rocks described here are those collected by Schultz and identified by Corwin in Sachet (1954). The suffixes A, B & C, added here, distinguish each specimen. No thin sections could be located in the Smithsonian collection from the three samples and a fresh polished thin section was prepared from each specimen. Each consists of a distinct basalt textural type, albeit with related petrographic affinities.

Electron microprobe analyses (EMPA) were made at the Geology Department, University of Auckland using a JEOL JXA-5A instrument operating at an accelerating voltage of 15 kV and an adsorbed sample current of c. 650 pA, with a Link Systems LZ-5 EDS detector. Raw data were corrected using a QX 2000 processor and ZAF-4/FLS quantification software version QX 20-24F-1291.

Chemical compositions of the three rocks were analysed by standard x-ray fluorescence (XRF) of Norrish fusion discs (majors) and pressed boric acid pellets (minors) after Parker (1994). The laser ablation analyses were performed using a 193 nm wave length ultraviolet Excimer laser facility in the Research School of Earth Sciences, Australian National University, Canberra, ACT, as outlined in Hoskin (1998).

Petrography

102227A. Holocrystalline olivine basalt. Partially resorbed olivine phenocrysts (<5%) and microphenocrysts of clinopyroxene and plagioclase (15%), and sparse ferromagnesian intergrowths are set in a pilotaxitic to intergranular, microporphyritic groundmass of feldspar laths (>40%), pyroxene (>20%), and ilmenite (s.l.) and magnetite (s.l.) granules (15%). Apatite needles, potash feldspar laths and quartz are scarce.

In composition olivine ranges Fo_{76-72}; feldspar groundmass laths and microphenocrysts An_{60-55}, inclusions An_{65-55}; clinopyroxene $Ca_{46-41}Mg_{47-41}Fe_{15-11}$. Fe-Ti oxides occur as flakes, cubes, octahedra, irregular grains and in intimate intergrowths in skeletal intergrowths. Pyroxene grains are generally angular, anhedral, and rarely rounded, colourless and rarely pleochroic (weak yellow). Elongated, twinned laths and irregular feldspar microlites have abundant inclusions. Some ferromagnesian minerals show oxidized rims.

Rounded, coarse-crystallized (doleritic or micrograbbroic) clots, up to 10 mm diameter, from 15–20% of the rock and are commonly enclosed by a discontinuous rim of euhedral-subhedral ulvöspinel (s.l.). Intergrown bladed plagioclase An_{61-55} (40–55%), subhedral olivine $\approx Fo_{75}$ (<5%), anhedral orthopyroxene $Ca_{2-5}Mg_{74-71}Fe_{23-28}$, clinopyroxene $Ca_{37-42}Mg_{43-47}Fe_{15-16}$, (15–20%), and coarse, acicular aggregations of Fe-Ti oxides (<10%), are ophitically enclosed by a mesostasis of brownish glass (10–30%) riddled with fine radiating needles, possibly rutile. In some smaller masses the silicate crystals radiate towards the centre. In others, small elongate feldspars at margins surround a coarser interior. Several of the clots appear linked through an incipient coarsening of the enclosing basalt. All resemble coarse segregations within the basalt, rather than cognate xenoliths of earlier crystallized rock. Similar "glomeroporphyritic clots of olivine and feldspar with subophitic pyroxene" appear in the Salani Volcanics of Upolu (Brothers, 1959, p. 40).

102227B. Coarse, altered, vesicular picrite basalt with a weathered outer rim, 5–10 mm thick, in which bioclastic carbonate infills vesicles.

Abundant olivine (>35%) phenocrysts and microphenocrysts, up to 5 mm diameter, are commonly subhedral. Most are partially resorbed and marginally altered, particularly the larger grains, with orange-stained iddingsitic rims and fractures. Many crystals show zoning and/or lamellae. Some (<5%) form in glomerocrysts with pyroxene and, rarely, plagioclase. Olivine compositions range Fo_{88-75}, but mostly Fo_{78-75}, without noticeable differences between phenocrysts, megacrysts, or in lamellated crystals. Zoned crystals show slight variations (e.g., core Fo_{83}, rim Fo_{76}), but some large phenocrysts show cores up to Fo_{88}. Rare crystals show Fo_{44-41}.

Clinopyroxene forms glomerocrysts (e.g., $Ca_{45}Mg_{45}Fe_{10}$), phenocrysts (e.g., $Ca_{44}Mg_{45}Fe_{11}$) and intersertal grains (15–20%), where it accompanies stubby, irregular laths of plagioclase (35–45%), Fe-Ti oxides (5–10%), and murky (chloritized) glass (5–10%). The oxide phase(s) are too intergrown with both primary and secondary silicates for satisfactory electron microprobe analysis.

Plagioclase laths and rare feldspar microphenocrysts (zoned An_{53-66}) form an unoriented mat but are locally moulded about large olivines and glomerocrysts.

102227C. Fine-grained, vesicular, olivine-poor (<4%) basalt with 5% pyroxene, and <5% plagioclase phenocrysts and microphenocrysts and aggregations in a pilotaxitic to hylaopilitic groundmass. The latter forms a felt of ill-defined plagioclase laths (15%), microcrystalline Fe-Ti oxides (20%), fine granular pyroxene (10%), and dark glass and irresolvable material (40%). Numerous, small (<1 mm), feldspar-poor glomerocrysts of coarse ferromagnesian phases (8–12%) are seamed by the host basalt, but show irregular, angular and unresorbed margins.

Olivine (Fo_{78-76}) shows minimal zoning. It forms large (up to 2 mm) scattered, slightly resorbed euhedral crystals, smaller (0.05–0.2 mm) euhedral to anhedral phenocrysts and microphenocrysts, and rare glomerocrysts.

Clinopyroxene ranges from tabular, <1 mm diameter, euhedral phenocrysts ($Ca_{45-41}Mg_{46-39}Fe_{17-11}$), through microphenocrysts (e.g., $Ca_{46}Mg_{41}Fe_{13}$), to an intergranular microcrystalline groundmass phase (e.g., $Ca_{46}Mg_{43}Fe_{11}$) and is common in glomerocrysts (e.g., $Ca_{45}Mg_{44}Fe_{11}$). It is most iron-rich in some phenocryst rims.

Plagioclase is common as groundmass laths. Rare, large phenocrysts include one with an internal irregular reaction rim of opaque oxide. The laths show weak alignment, range in composition An_{60-70} and rarely to An_{35}. Minor feldspar in glomerocrysts (<20%) ranges An_{65-70}.

Vesicle coatings include silicates as straw-coloured, flat subhedral and tabular euhedral clinopyroxene, possibly orthopyroxene, euhedral plagioclase and stumpy, subhedral anorthoclase (?). Other phases are dark bladed subhedral Fe-Ti oxides, white rosettes of a subhedral silica, possibly tridymite, and undetermined colourless, abundant, radiating, trigonal needles.

Table 1. Representative analyses and structural formulae of olivines from Rose Atoll basalts.

	1Ac	2Bc	2Br	3Bc	4Bc	5Br	6Br	7Br	8Bc	10B	11B	14Cc	15Cr
SiO_2	39.17	39.42	38.73	39.95	38.71	38.77	39.71	34.24	39.23	38.51	38.80	38.86	39.16
FeO	21.40	18.21	20.96	13.20	21.11	20.53	16.59	46.31	18.40	21.47	19.52	20.84	20.15
MnO	0.35	0.24	0.28	—	0.37	0.21	0.23	0.74	0.21	0.35	—	0.23	0.24
MgO	39.16	42.09	39.77	45.59	38.88	39.50	42.65	18.44	42.02	39.51	40.49	39.07	39.81
CaO	0.12	0.37	0.43	0.34	0.38	0.38	0.36	0.54	0.39	0.46	0.42	0.28	0.35
Total	100.20	100.33	100.17	99.08	99.45	99.39	99.54	100.27	100.25	100.30	99.23	99.28	99.71
Structural formulae on basis of 4(O)													
Si	0.994	1.001	1.000	1.003	1.010	1.005	1.012	1.011	0.996	0.996	1.002	1.010	1.010
Fe	0.454	0.387	0.453	0.277	0.461	0.445	0.354	1.143	0.196	0.465	0.422	0.463	0.435
Mn	0.008	0.007	0.007	—	0.009	0.005	0.013	0.019	0.005	0.008	—	0.005	0.006
Mg	1.481	1.795	1.530	1.705	1.512	1.513	1.620	0.812	1.590	1.523	1.559	1.514	1.531
Ca	0.003	0.010	0.012	0.009	0.011	0.011	0.010	0.017	0.001	0.013	0.012	0.008	0.010
X	2.01	2.00	2.00	1.99	1.99	1.99	2.00	1.99	2.00	2.01	1.99	1.98	1.98
Fo	76.5	80.5	77.2	86.0	75.9	77.4	81.2	40.8	80.3	76.6	78.7	76.5	77.3
Fa	23.5	19.5	22.8	14.0	24.1	22.6	18.8	59.2	19.7	23.4	21.3	23.5	22.7

A, B, C = specimens 102227A, 102227B, 102227C
c, core; *r*, rim; FeO = total iron as FeO (or Fe^{II}); *Fo*, forsterite; *Fa*, fayalite

Table 2. Representative analyses and structural formulae of pyroxenes from Rose Atoll basalts.

	Phenocrysts		Microphenocrysts			Groundmass	Glomerocrysts	Intergrowth	Dolerite clots				
	1Bct	**2Cc**	**4Cr**	**5A**	**7C**	**9B**	**11C**	**13A**	**14A-B1**	**16A-B1**	**18A-B2**	**19A-B2**	**20A-B3**
SiO_2	50.64	50.20	49.75	50.67	46.40	50.51	49.41	54.51	50.87	54.09	51.39	53.10	53.26
TiO_2	1.08	1.34	1.72	1.51	3.00	1.35	1.86	—	1.31	0.62	1.18	0.52	0.73
Al_2O_3	2.87	3.88	4.29	2.87	6.37	3.53	4.21	0.72	2.73	1.52	2.00	1.75	1.70
Cr_2O_3	0.62	—	—	—	—	—	—	—	—	—	—	—	—
FeO	6.49	5.79	6.60	8.92	7.65	6.65	6.33	17.30	10.03	14.60	8.56	14.95	14.69
MnO	—	0.24	—	0.34	—	0.23	—	0.77	0.40	0.47	0.24	0.63	0.43
MgO	15.50	15.66	15.22	15.77	13.53	14.72	15.18	25.73	14.62	27.04	16.14	26.65	27.06
CaO	20.92	21.62	21.25	20.27	21.41	21.58	21.57	1.41	19.89	2.19	19.73	1.96	1.90
Total	98.12	98.73	98.83	100.35	98.36	98.57	98.56	100.44	99.85	100.53	99.24	99.56	99.77
Structural formulae on basis of 6(O)													
Si	1.898	1.872	1.853	1.883	1.754	1.897	1.854	1.982	1.900	1.946	1.920	1.934	1.933
Ti	0.031	0.038	0.049	0.042	0.085	0.038	0.052	—	0.037	0.017	0.033	0.014	0.020
Al^{iv}	0.071	0.090	0.098	0.075	0.161	0.065	0.094	0.018	0.063	0.037	0.047	0.052	0.047
Al^{vi}	0.058	0.080	0.090	0.051	0.123	0.091	0.093	0.013	0.057	0.027	0.041	0.023	0.026
Cr	0.019	—	—	—	—	—	—	—	—	—	—	—	—
Fe	0.203	0.181	0.206	0.277	0.242	0.209	0.199	0.526	0.313	0.440	0.268	0.455	0.446
Mn	—	0.008	—	0.011	—	0.007	—	0.024	0.013	0.014	0.008	0.019	0.013
Mg	0.866	0.871	0.845	0.874	0.763	0.824	0.848	1.394	0.814	1.451	0.899	1.448	1.463
Ca	0.841	0.864	0.852	0.807	0.868	0.868	0.867	0.055	0.796	0.085	0.790	0.007	0.074
X+Y	1.985	2.004	1.993	2.020	1.996	1.999	2.007	2.012	1.993	2.017	2.006	2.022	2.022
Wo	44.0	44.9	44.8	41.0	46.4	45.7	45.3	2.8	41.1	4.3	40.4	3.8	3.7
En	45.3	45.3	44.4	44.4	40.7	43.3	44.3	69.7	42.1	72.9	45.9	71.7	73.8
Fs	10.7	9.8	10.8	14.6	12.9	11.0	10.4	27.5	16.8	22.8	13.7	24.5	22.5

A, B, C, = 102227A, 102227B, 102227C; *t*, twinned grain; *c*, core; *r*, rim; *B1, B2, B3*, different doleritic clots; *Wo*, wollastonite; *En*, enstatite; *Fs*, ferrosilite.

Mineralogical observations

Representative EMP analyses of the major phases in the three samples are given in Tables 1–4.

Olivines (Table 1). The representative olivine analyses are typical of alkali basalts in Samoan rocks (Macdonald, 1944; Stice, 1968; Natland & Turner, 1985). Compositions mostly lie between Fo_{82} and Fo_{72} with samples A and C showing restricted resorption and compositional zoning in their crystals (analyses 1,14–15).

In contrast, the picrite, 102227B, shows wider olivine compositions (analyses 2–8, 10–11). Most range within $Fo_{88-75,}$ zoning is common (analyses 2,3,5,6). This is typical in Samoan basalts, along with Fe-rich crystals (Fo_{44-41}) e.g., analyses 7 (cf. Macdonald, 1944; Natland & Turner, 1985). Thus olivine in 102227B indicates a complex crystallization; both the lamellar olivines and the iron-rich varieties may represent xenocrysts.

Pyroxenes (Table 2). The clinopyroxene compositions cluster in the quadrilateral $Ca_{47}Mg_{43}Fe_{10}$-$Ca_{47}Mg_{36}Fe_{17}$-$Ca_{40}Mg_{43}Fe_{17}$-$Ca_{40}Mg_{50}Fe_{10,}$ as is typical in the alkalic and tholeiite basalts of the Fagaloa shield volcano of Upolu (Natland & Turner, 1985). However, more Ca-rich pyroxenes from Fagaloan lavas contain less Fe than some Rose analyses.

Groundmass pyroxenes in 102227B (analysis 9) are Ca-rich ($\geq Ca_{45}$) and range from Fe_{10} to Fe_{14}, as are some microphenocrysts from A and C, cores of phenocrysts, and glomerocrysts, from samples B and C (analyses 1–2, 11). Phenocryst cores of augite ($\approx Ca_{41}$) in C and microphenocrysts in A are less common, but also display Fe-values similar to the main compositional range (analysis 5). Only rims of some phenocrysts in A are more extreme (analysis 4Cr). Although titanaugites are known in Samoan lavas (e.g., Macdonald, 1944; Brothers, 1959; Stice, 1968; Natland & Turner, 1985), in only one spot Rose analysis (analysis 7) did TiO_2 exceed 1.9 wt%. The negligible Na in the Rose clinopyroxenes is an unusual feature, but is recorded in rare tholeiitic lavas in Upolu basalts (Natland & Turner, 1985). Chromium was detected in only two clinopyroxene crystals from Rose samples.

A rare intergrowth of orthopyroxene in clinopyroxene in A gave $Ca_3Mg_{70}Fe_{27}$ (analysis 13). No pigeonite was found (cf. Natland & Turner, 1985). The clinopyroxenes of the coarser clots in B all plot at or beyond the Ca_{40} margin of the main field (analyses 14A,18A). In composition (Ca_{40-41} Mg_{42-46} Fe_{14-17}), they coexist with orthopyroxenes (Mg_{71-74} Fe_{22-26} Ca_{3-4}) with significant Ca (analyses 16, 19–20). Calculated Wood & Banno (1973) temperatures for these coexisting pyroxene compositions range 1021–1088°C; Wells (1977) temperatures are 1030–1126°C.

Feldspars (Table 3). Plagioclase in the three rocks ranges from $An_{70}Ab_{29}Or_1$ to $An_{53}Ab_{43}Or_3$. Those in A lie at the Na- and K-rich end (analysis 1), those in B span the entire range and those in C are skewed towards the middle and Ca-rich end (analyses 5–7, 16–17). Microphenocrysts in A (analyses 8,9) and the feldspars in its clots (analyses 10–12) overlap the groundmass feldspar compositions. However, the microphenocrysts are the most Ca-rich feldspars, while feldspars in the clots tend towards the Na- and K-rich end of the range. Most feldspars are inhomogeneous and Fe and a little Ti may partly reflect minute Fe-Ti oxide inclusions.

K-rich oligoclase is common as an interstitial phase in some Samoan lavas (Macdonald, 1944; Brothers, 1959), but only one such composition was found herein ($Ab_{36}An_{51}Or_{12}$).

Table 3. Representative analyses and structural formulae of feldspars from Rose Atoll basalts.

	Groundmass laths				Microphenocrysts			Ex dolerite inclusions			Ex glomerocrysts		
	1A	**2B**	**5C**	**6C**	**7C**	**8A**	**9A**	**10A**	**11A**	**12A**	**16C**	**17C**	**18B**
SiO_2	54.24	54.09	51.70	52.51	50.34	54.67	52.22	54.74	53.36	54.84	51.03	50.69	60.46
TiO_2	0.19	0.25	0.19	0.23	—	0.22	—	0.18	—	0.18	—	—	0.26
Al_2O_3	27.36	27.72	29.29	28.83	30.50	27.47	29.44	28.23	28.35	27.48	29.67	30.44	23.07
FeO	0.87	0.91	1.00	1.05	0.81	0.85	0.97	0.87	1.14	0.80	0.61	0.64	0.61
CaO	10.96	10.76	12.82	12.23	14.08	10.65	13.02	11.37	12.11	10.88	13.64	14.21	5.16
Na_2O	4.64	4.79	3.71	4.32	3.28	4.44	3.73	4.51	3.96	4.61	3.70	3.08	5.85
K_2O	0.69	0.57	0.24	0.38	0.17	0.74	0.47	0.63	0.51	0.77	0.18	0.16	3.49
Total	98.95	99. 09	98.95	99.55	99.18	98.98	99.85	100.53	99.43	99.56	98.83	99.22	98.90
Structural formulae on basis of 32(O)													
Si	9.952	9.898	9.520	9.613	9.267	9.997	9.530	9.875	9.760	9.987	9.437	9.315	
Ti	0.026	0.035	0.026	0.032	0.013	0.032	0.019	0.026	0.013	0.026	0.003	0.019	
Al	5.917	5.981	6.358	6.221	6.618	5.907	6.333	6.003	6.112	6.898	6.404	6.592	
Fe	0.134	0.138	0.154	0.160	0.125	0.128	0.147	0.131	0.173	0.122	0.093	0.992	
Ca	2.157	2.109	2.531	2.397	2.778	2.086	2.547	2.198	2.374	2.125	2.701	2.800	
Na	1.651	1.699	1.325	1.533	1.171	1.574	1.318	1.578	1.402	1.626	1.325	1.098	
K	0.160	0.134	0.054	0.090	0.042	0.173	0.109	0.147	0.118	0.179	0.045	0.035	
Z	16.03	15.91	16.05	16.03	16.03	16.06	16.03	16.03	16.06	16.03	15.94	16.02	
X	3.97	3.94	3.91	4.02	3.99	3.83	3.97	3.93	3.89	3.93	4.07	3.93	
An	54.4	53.5	64.8	59.6	69.6	54.4	64.1	56.0	61.0	54.1	66.4	71.2	
Ab	41.6	43.1	33.8	38.2	29.3	41.1	33.2	40.2	36.0	41.4	32.5	27.9	
Or	4.0	3.3	1.4	2.2	1.1	4.5	2.7	3.8	3.0	4.5	1.1	0.9	

A, B, C = 102227A, 102227B, 102227C. *An*, anorthite; *Ab*, albite; *Or*, orthoclase normative components.

Fe-Ti oxides (Table 4). Two groups of Fe-Ti oxides occur in the samples: a Ti-poor Fe-rich spinel phase, presumably magnetite, and a Ti-rich ulvöspinel phase with Fe^{2+}»Fe^{3+} (based on stoichiometry). Only the Fe-Ti oxides in A gave consistent electron microprobe results. Representative examples in Table 4 have the structural formulae recalculated after Droop (1987) to partition total iron between Fe^{2+} and Fe^{3+}. An alternative method by Carmichael (1967) gives a magnetite-rich phase with 20.9 to 16.7 mol % ulvöspinel and a Ti-rich oxide phase with from 15.6 % R_2O_3 in 2du, through 2.1% R_2O_3 in 1bl, to zero in 5d.

Natland & Turner (1985) report two opaque oxide solid solutions in the tholeiitic and alkalic basalts of Fagaloa, Upolu: an ilmenite-hematite solid solution and a magnetite-ulvöspinel solid solution. However, these differ from those in 102227A. In particular the alkalic Fagaloa lavas show a complete gradation in Fe^{3+} and Ti, between phenocrystalline magnesiochromite and groundmass magnetite-ulvöspinel solid solution; Cr_2O_3 (and V_2O_3) is negligible in the Rose sample. Further, among Fagaloa analyses, with comparable TiO_2 levels to the Ti-rich Rose oxides (only 4 out of 19 analyses), Al_2O_3 was markedly lower, although MgO and MnO were similar or less. In contrast, a single Fagaloa analysis with a similar TiO_2 level to the Ti-poor Rose oxides, showed a far greater Al_2O_3, a lower MgO, but ≈15 wt% Cr_2O_3. The remaining 14 Fagaloa analyses all had TiO_2 values well above those in 102227A. Nevertheless 102227A, like many of the Fagaloa lavas (Natland & Turner, 1985) has crystallized abundant Ti-bearing oxides, albeit of different composition, rather than incorporating Ti in the clinopyroxene.

Coexisting magnetite-ulvöspinel and hematite-ilmenite in a multiphase crystal in 102227A were analysed (2du, 2br). The results give ≈720°C and fO_2 ≈10^{-15} atm when plotted on the experimentally determined curves of Buddington & Lindsley (1964, fig. 5). In the coarser clots both Ti-poor and Ti-rich oxide phases are present but textural relations indicate separate crystallization; the spinels occur at the clot rims as reaction products, while the ulvöspinel-rich phases lie within the clots, where siliceous liquid could have afforded an oxygen buffer (cf. Carmichael, 1967).

Table 4. Representative analyses and structural formulae (after Droop, 1987), Fe-Ti oxides from Rose Atoll basalt 102227A.

	1bl	**2du**	**5d**	**6d**	**2br**	**8d†**
SiO_2	0.47	0.42	0.41	0.44	0.56	0.45
TiO_2	52.30	46.33	51.49	31.88	6.72	5.75
Al_2O_3	1.56	0.22	1.33	0.50	3.87	2.87
Fe_2O_3	*	15.64	*	33.03	42.10	43.59
FeO	37.59	28.89	37.79	29.65	40.41	43.64
MnO	0.25	0.51	—	—	0.42	0.50
MgO	3.34	7.67	3.27	2.50	3.73	2.62
CaO	—	—	0.13	0.13	—	—
Total	95.51	99.68	94.42	98.13	97.81	99.42
Structural formulae on basis of 24 cations						
Si	0.144	0.108	0.132	0.132	0.163	0.132
Ti	12.036	10.032	12.036	7.329	1.488	1.268
Al	0.564	0.072	0.480	0.179	1.343	0.992
Fe^3	*	3.396	*	7.599	9.322	9.626
Fe^2	9.624	6.972	9.828	7.582	9.943	10.709
Mn	0.060	0.120	—	—	0.105	0.126
Mg	1.560	3.300	1.512	1.136	1.635	1.146
Ca	—	—	—	0.042	—	—

bl, bladed grain; *du*, least reflectant area of composite skeletal gain; *br*, most reflectant area of skeletal composite grain; *d*, grains from doleritic clots; † grains from clot rims; * total iron as FeO (or Fe^2).

Chemistry

The XRF analyses, and CIPW norms, for the three samples are given in Table 5. Semiquantitative analysis for chlorine showed some 2200 ppm in 102227B point to slight seawater contamination. This rock also contains small amounts of encrusting bioclastic carbonate debris in its vesicles.

The three samples represent contrasting basalt types: 102227A is gradational to quartz tholeiite, with 21% normative Hy and 1% Q, slightly evolved *mg* value (60), and a *DI* of 21; 102227B plots as a picrobasalt (Le Maitre, 1984) with high normative Ol (23%), minor Hy (<1%), an *mg* value typical of primitive or cumulate basalts (70), and a *DI* of 18; 102227C is transitional olivine basalt with normative Ol (6%) and Hy (7%), a moderately evolved *mg* value (57), and *DI* of 26. Electron microprobe analysis of tholeiite A glass (Agl Table 6) shows it to be potash- and silica-rich, and rhyolitic in normative composition with 27–39% Q. The glass shows low totals suggesting 4–6% volatiles (Table 6) and strong Rb, Th, U, K, La, Zr enrichment and Ba, Ti, Sr depletion relative to the host basalt (Table 7).

The three samples resemble other Samoan basalts and to date are closest to Ta'u island lavas (Stice, 1968; Hubbard, 1971) from the nearest volcano in the adjacent Manu'a Group (Table 8, Figs. 2, 3). Importantly, both Rose and Ta'u basalts differ from western Manu'a Group basalts of the Ofu and Olosega islands, which are more enriched in Ti relative to Al (Hubbard, 1971). The Al_2O_3/TiO_2 ratios of the Rose samples are typical of most Samoan chain basalts (cf. Macdonald, 1968; Hawkins & Natland, 1975; Natland & Turner, 1985; Johnson, *et al.*, 1986). Only examples from the Lalla Rookh Bank (Johnson *et al.*, 1986) show the lower Al_2O_3/TiO_2 found in western Manu'a islands lavas.

Yet, despite geochemical similarities between Rose and Ta'u basalts (Table 8, Figs. 2, 3), some differences exist, particularly in Sr vs P_2O_5 and Ni vs MgO (Figs. 4, 5). Although this could reflect sampling bias, no rock corresponding to 102227A was reported from the Manu'a islands by Stice (1968) despite prominent tholeiites among Samoan shield basalts west of Manu'a (Natland & Turner, 1985). One picrite basalt no. 131 from Ta'u (Stice, 1968) has transitional tholeiitic affinities, but higher SiO_2 and Hy

Table 5. Analyses and CIPW norms Rose Atoll basalts and averaged glass (*Agl*) from within doleritic clots of sample A (Tables 6 and 7).

	A	B	C	Agl*
SiO_2	46.77	44.29	46.40	70.59
TiO_2	3.93	2.97	3.92	0.85
Al_2O_3	12.83	10.22	13.89	13.07
Fe_2O_3t	13.41	14.09	13.05	0.69
MnO	0.19	0.18	0.18	—
MgO	8.24	13.56	6.89	0.01
CaO	10.65	11.33	11.20	0.99
Na_2O	1.75	1.59	2.51	2.10
K_2O	0.86	0.70	0.81	6.48
P_2O_5	0.70	0.36	0.47	—
Total	99.33	99.30	99.32	95.08
t, total Fe as Fe_2O_3 * includes 0.30 Cl				
CIPW normative composition				
Q	1.01	—	—	34.45
C	—	—	—	1.23
Or	5.12	4.17	4.82	40.24
Ab	14.91	13.55	21.38	16.70
An	24.78	18.82	24.41	5.16
Mt	3.91	4.12	3.81	—
Hm	—	—	—	0.18
Il	7.51	5.68	7.50	—
Ru	—	—	—	0.18
Ap	1.67	0.86	1.12	—
Di	19.23	28.41	23.06	—
Hy	20.81	0.43	6.97	0.03
Ol	—	22.85	5.91	—
Hl	—	—	—	0.43
mg	60.3	70.4	56.6	2.8
DI	21.0	17.7	26.2	91.4

	A	B	C	Agl
Sc	29	30	33	<8
V	337	310	344	<3
Cr	357	884	200	<3
Ni	131	366	93	61
Cu	25	69	89	24
Zn	118	115	120	nd
Ga	23	17	24	nd
Rb	29	13	14	240
Sr	484	390	521	80
Y	42	25	37	41
Zr	365	195	274	638
Nb	57	29	36	60
Ba	273	165	211	509
La	57	24	35	79
Pb	6	4	3	nd
Ce	128	54	73	158
Th	6	1	5	23
U	3	7	2	6
Normative mineralogy				
Clinopyroxene				
Wo	51.7	42.1	51.5	—
En	33.2	35.6	31.9	—
Fs	15.1	12.4	16.6	—
Orthopyroxene				
En	68.6	74.2	65.7	100.0
Fs	31.4	25.8	34.3	—
Olivine				
Fo	—	73.2	3.5	—
Fa	—	27.7	65.0	—
Plagioclase				
Ab	37.6	29.6	3.3	76.4
An	62.4	70.4	6.7	23.6

Normative symbols after Hutchison (1974), with norms calculated from anhydrous analyses recalculated to 100% with $Fe_2O_3/(FeO+Fe_2O_3)$ set to 0.20. *mg*, $Mg/(Mg+Fe^{2+})\times100$. *DI*, Differentiation Index (Σ Q, Or, Ab).

Table 6. EMP analyses of glassy mesostasis, doleritic clots in 102227A.

	inclusion 1		inclusion 2		inclusion 3	
	1	2	3	4	5	6
SiO_2	70.27	71.89	69.98	71.06	70.37	70.01
TiO_2	0.77	0.70	1.04	0.92	0.78	0.91
Al_2O_3	12.87	13.08	13.27	12.20	13.54	13.47
FeO*t*	0.91	0.74	0.71	0.49	0.59	1.15
MgO	—	—	—	0.05	—	—
CaO	0.77	0.81	1.72	0.77	0.84	1.01
Na_2O	2.22	2.21	2.96	1.68	1.94	1.56
K_2O	6.03	6.23	4.54	6.46	7.06	8.53
Cl	0.34	0.28	0.23	0.30	0.35	—
P_2O_5	—	—	—	—	—	—
Total	94.18	95.94	94.45	93.93	95.47	96.64
t, total Fe as FeO.						
CIPW norms						
Q	36.48	36.66	34.80	38.68	33.57	27.13
Or	37.84	38.88	28.41	40.67	43.70	52.16
Ab	17.28	17.33	24.72	12.78	14.48	13.66
An	4.06	4.19	9.03	4.07	4.36	4.72
C	1.89	1.70	0.73	1.57	1.76	—
Wo	—	—	—	—	—	0.20
Mt	0.12	—	—	—	—	0.34
Hm	0.13	0.17	0.17	0.12	0.14	0.03
Il	1.55	1.30	1.27	0.88	1.04	1.79
Ru	—	0.04	0.43	0.52	0.27	—
Hl	0.60	0.48	0.40	0.53	0.60	—
Hy	—	—	—	0.13	—	—

Norms calculated from anhydrous analyses recalculated to 100% with $Fe_2O_3/(FeO+Fe_2O_3)$ set to 0.20.

than the Rose picrite basalt B. Intriguingly, the alkalis and silica of 102227A are in similar proportions to the recalculated composition of Stice's picrite basalt no. 131, if all normative Ol is subtracted from the original composition. Further, both the total alkalis and titania of A are lower than in comparable picrites from Manu'a. Only 102227C bears some chemical comparison with Manu'a lavas (e.g., Stice, 1968; no. 117), but direct resemblances between Manu'a and Rose basalts are not clear.

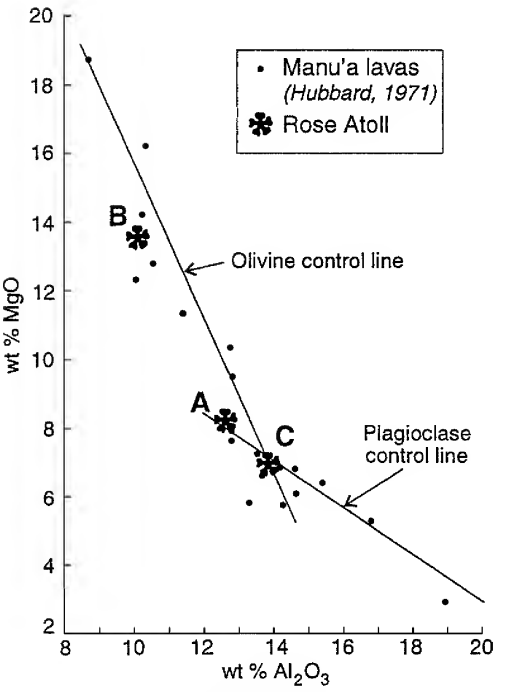

Fig. 2. Al_2O_3 vs MgO for Manu'a lavas and Rose Atoll samples. The olivine and plagioclase control lines are those of Hubbard (1971).

Incompatible elements in Rose basalts are compared in a mantle normalized diagram (Fig. 6). The elements are normalized to primitive mantle (PM) values and compared with enriched mid ocean ridge basalt (E-MORB) and low $^{87}Sr/^{86}Sr$ ocean island basalt (OIB), after Sun & McDonough (1989). The Rose basalts are relatively depleted in K and Sr and relatively enriched in U, Pb and La; they show variable enrichment in Rb, Ba, Th and P. The Ba/Nb and La/Nb ratios are compared in Fig. 7, which relates OIB fields to their $^{87}Sr/^{86}Sr$ isotope levels with increasing sedimentary crustal components in their source (Sun *et al.*, 1989). Rose basalts plot from near the N-MORB field towards E-MORB (Ba/Nb 6.86 La/Nb 0.76) and low $^{87}Sr/^{86}Sr$ OIB (Ba/Nb 7.29, La/Nb 0.77) values, but do not intersect any major plume related OIB field.

Table 7. Laser ablation ICP-MS analyses of glass in doleritic clots in basalt 102227A.

	spot-1	spot-2	spot-3		spot-1	spot-2	spot-3
Li	< 6	< 2	< 8	La	80(10)	28(4)	128(18)
Sc	< 10	< 3	< 12	Ce	164(21)	55(7)	255(31)
V	< 4	< 1	< 5	Pr	19(3)	6.4(0.9)	28(4)
Cr	< 4	< 1	< 5	Nd	72(12)	24(4)	103(16)
Ni	62(16)	26(6)	95(42)	Sm	12(4)	5(1)	18(5)
Rb	234(23)	75(10)	411(50)	Eu	1.9(0.7)	1.0(0.3)	2(1)
Sr	50(7)	100(11)	90(14)	Gd	10(3)	4(1)	14(4)
Y	44(5)	14(3)	65(9)	Tb	1.4(0.4)	0.5(0.2)	2.2(0.8)
Zr	625(67)	227(28)	1061(123)	Dy	9(2)	2.7(0.8)	13(3)
Nb	56(10)	22(4)	101(15)	Ho	1.4(0.5)	0.6(0.2)	2.5(0.9)
Ba	458(50)	200(25)	869(96)	Er	5(1)	1.6(0.5)	6(2)
Ta	4.2(0.8)	1.4(0.3)	6(1)	Tm	0.7(0.3)	0.2(0.1)	0.8(0.4)
Th	22(2)	8(1)	38(5)	Yb	4(2)	1.6(0.5)	6(2)
U	5.6(0.9)	1.9(0.4)	10(1)	Lu	0.5(0.2)	0.2(0.09)	0.9(0.4)

Precision for ICP-MS laser ablation analyses given in brackets.

Table 8. Comparative Rose Atoll and Manu'a Islands (Ta'u) basalt compositions.

	Rose av.	Manu'a[a] av.	Manu'a[b]
SiO_2	45.8	45.5	45.8
TiO_2	2.6	3.5	3.4
Al_2O_3	12.3	12.3	12.7
FeO*t*	13.5	12.5	12.0
MnO	0.2	—	0.2
MgO	9.6	10.5	9.5
CaO	11.1	10.8	11.5
Na_2O	1.9	2.5	2.3
K_2O	0.8	0.8	0.9
P_2O_5	0.5	0.5	0.4
Ni	197	373	315
Sr	465	468	400
Zr	278	230	232
Rb	19	17	16
t, total Fe as FeO.			
Ranges			
La	24–57	27–40?	
Sr	390–521	330–510	
Ce	54–128	54–76	
Ni	93–366	88–755	
Zr	195–365	175–440	
Rb	13–29	9–27	
K/Rb	245–479	350–?	

[a] excluding hawaiites; [b] basalt with similar MgO to Rose av. (Ab > An).

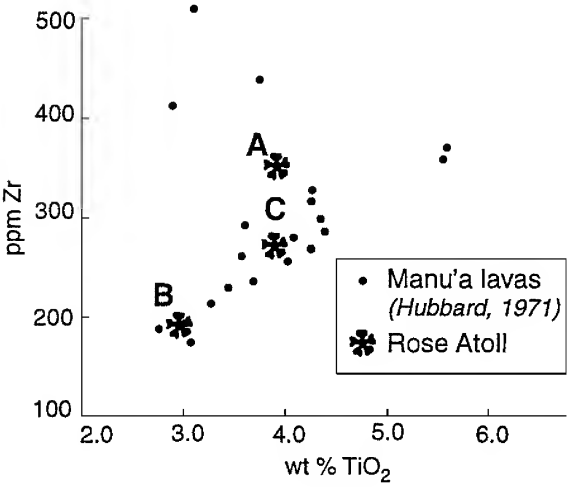

Fig. 3. TiO_2 vs Zr for Manu'a lavas and Rose Atoll samples.

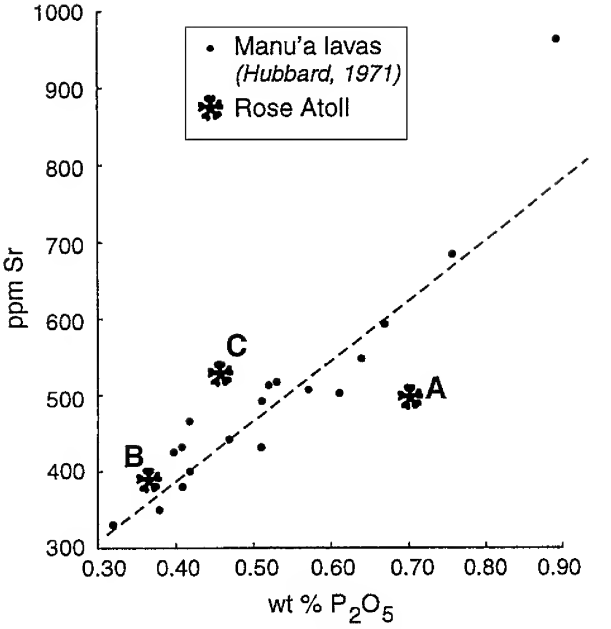

Fig. 4. Sr vs P_2O_5 for Manu'a lavas and Rose Atoll samples. Trend line from Hubbard (1971).

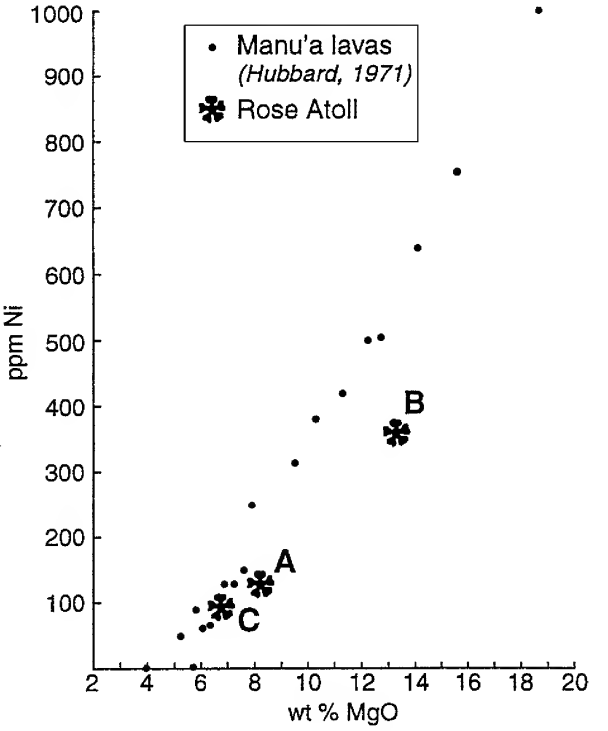

Fig. 5. Ni vs MgO for Manu'a lavas and Rose Atoll samples.

Table 9. Comparative trace element ratios for Rose Atoll basalts, N- and E-type MORB, low $^{87}Sr/^{86}Sr$ OIB, EM-OIB and HIMU basalts.

	Nb/Pb	Ce/Pb	Nb/U	K/U	K/Nb	Nb/Th
Rose Atoll A	9.5	21.3	19.0	2367	125	9.5
Rose Atoll B	7.3	13.5	3.4	829	200	29.0
Rose Atoll C	12.0	12.0	18.0	3350	186	7.2
N-MORB	7.5	25	50	12766	258	19.4
E-MORB	13.8	25	46	11677	253	13.8
Low $^{87}Sr/^{86}Sr$ OIB	15	25	47	11765	250	12.0
EM-OIB (Range)	8.3–15.9	14.5–31	40–43	5660–13700	270–430	6.3–11.5
HIMU (Range)	18–23	29–33	43–88	6000–8000	160–180	10–17

Data compiled from this paper and Sun & McDonough (1989).

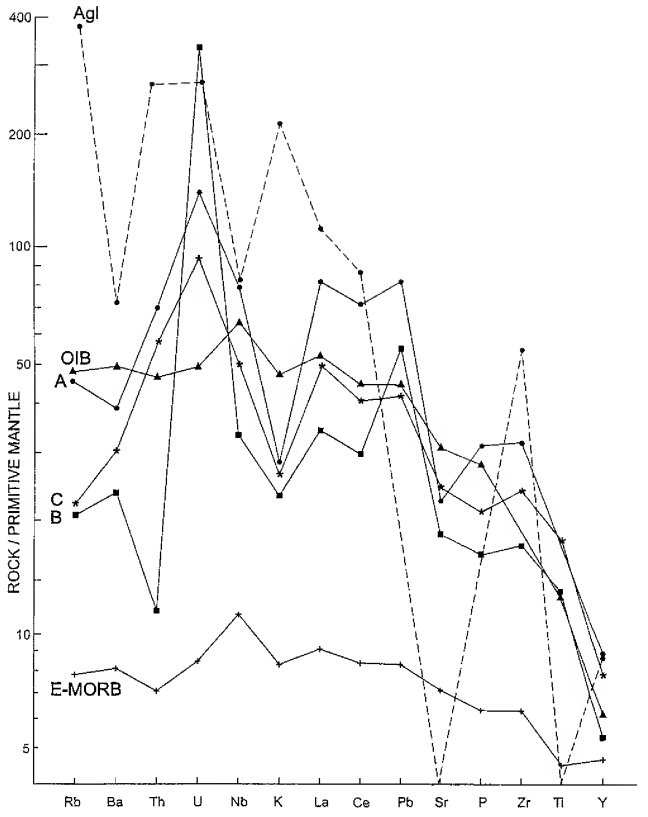

Fig. 6. Incompatible trace element plots of Rose Island basalts (A, B, C) normalized to primitive mantle, using normalization factors and data after Sun & McDonough (1989). Plots for enriched-type MORB and low $^{87}Sr/^{86}Sr$ OIB are shown for comparison.

Petrogenesis

Average Rose Island basalt shows lower MgO (1%), TiO_2 (0.9%) and Na_2O (0.6%) and higher FeO* (1%) than average Manu'a's Island's (Ta'u) basalt and TiO_2, FeO and Na_2O remain higher at equivalent MgO contents (Table 8). A more magnesian Manu'a's Islands parent would explain the higher Ta'u Ni contents. Petrologically, however, both Rose and Ta'u transitional to tholeiitic basalts suggest greater degrees of partial mantle melting than for basanites and nephelinites that characterize the young post-erosional Samoan volcanoes and seamounts (Hawkins & Natland 1975). The question then arises as to whether these young easternmost volcanoes reflect the asthenospheric/lower mantle plume activity of the older Samoan shields and Vailulu'u undersea volcano (Hart *et al.*, 2000).

Samoan plume magmatism is considered responsible for:

- the observed linear age progression in the shield volcanism for several Samoan islands (Natland & Turner, 1985; McDougall, 1985; Hart *et al.*, 2000);
- the isotopic character of shield basalts, where Sr, Nd and Pb isotopes are consistent with isotopic values of other Pacific island chains assigned to plume sources (Hedge *et al.*, 1972; Wright & White, 1987);
- a primitive helium isotopic mantle component in shield basalts (Farley *et al.*, 1992);
- mantle carbonatitic metasomatism identified in peridotite xenoliths contained in post-shield lavas (Hauri *et al.*, 1993).

The Rose basalts partly overlap the alkali basalt compositional range of the present plume-related Vailulu'u seamount (Hart *et al.*, 2000) in SiO_2 and MgO, but are distinctly lower in alkalis (Na_2O+K_2O 2.6–3.3 cf 3.5–5.9 wt %). This may reflect greater degrees of partial melting for Rose basalts. Rose basalts overlap and show a similar fractionation trend to other Samoan island basalts for Nb vs Zr (Fig. 8), except for the late-stage groundmass fractionation to silicic glass in the tholeiitic basalt (102227A) and both groups differ from the Combe Bank trend, which show elevated Nb/Zr. In Ba vs. Zr plots, Rose basalts differ in their fractionation trend to Samoan islands, Lalla Rookh Bank, Wallis Island, Combe Bank and Alexa Bank fields (Fig. 8).

No overlap in Ba/Nb vs. La/Nb exists between Rose basalts and the plume-related Samoan, Hawaiian or Atlantic fields (Fig. 7). In this respect Rose basalts differ from Wallis Island basalts, which fall within the Samoan plume field. Rose Ba/Nb and La/Nb values do not suggest high levels of crustal sedimentary components, while late-stage fractionation trends in tholeiite (102227A) to silicic glass (Agl) mostly increases La/Nb values.

A present Samoan plume position near Manu'a Group islands some 100km to 150km east of Tutuila was deduced on migration rates from shield volcano ages (Duncan, 1985; Natland & Turner, 1985; McDougall, 1985). Reconstructed plate motion tracks for two extreme plume positions relative to Manu'a and Rose islands (Fig. 9) are based on revised plate motion relative to Pacific "hotspots" (Gaina *et al.*, 2000; R.D. Müller, pers. comm., 2000). A Manu'a plume position more closely matches shield ages along the Samoan islands and the postulated plume at Vailulu'u submarine volcano, 45 km E of Ta'u Island. A Rose Atoll plume position gives ages 2 myr older than observed ages. Clearly, Rose Atoll lacks temporal or geochemical evidence for a Samoan plume input. Isotope data are not available for Rose basalts, but Sr isotopes for Ta'u ($^{87}Sr/^{86}Sr$ 0.7042–0.7050) are among the lowest recorded for Samoan basalts, while Ta'u and Vailulu'u record the highest $206Pb/^{204}Pb$ (192–194) values (Hart *et al.*, 2000). These values extend towards other Samoan shield values, but most shield and in particular "post-erosional" lavas show higher $^{87}Sr/^{86}Sr$ and lower $^{206}Pb/^{204}Pb$ values (Wright & White, 1987; Hart *et al.*, 2000).

Rose trace element ratios show little correspondence to end member MORB and OIB values (Table 9) perhaps reflecting an unusual or mixed lithospheric source. The Zr/Nb ratios for Rose basalts follow the Samoan shield crystal fractionation differentiation trend (Fig. 8), but initial Zr/Nb may stem from binary mixing of depleted MORB and other more enriched end members (Kamber & Collerson, 2000). Other element ratios for Rose basalts (Rb/Sr 0.027–0.060, U/Pb 0.50–1.75, Th/Pb 0.25–1.64) generally overlap typical Hawaiian tholeiitic data (Rb/Sr 0.278, U/Pb 0.56–2.11, Th/Pb 2.09); this precludes an abnormal, overwhelming Mid-Ocean Ridge imprint, as found in the Detroit seamount along the Hawaiian plume trace (Keller *et al.*, 2000).

Discussion

Of the different basalt types documented from the Samoan Island chain, the three Rose Atoll samples collected by Schultz conform most closely to the Ta'u Island basalts of the neighbouring Manu'a Group. However, differences exist and any similarities in petrography and chemistry are typical

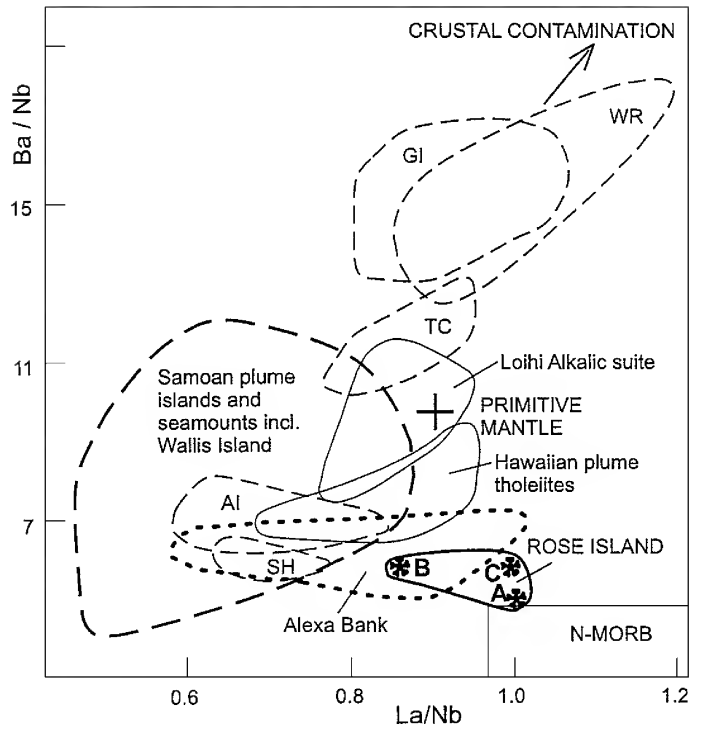

Fig. 7. Ba/Nb vs La/Nb diagram of Rose Atoll basalt plots related to N-MORB, Primitive Mantle (cross) and fields of Pacific and Atlantic plume basalts (based on Sun & McDonough, 1989). Solid thick line: Rose Atoll basalt field; thick dotted line: Alexa Bank field; solid thin line: Hawaiian plume tholeiites and Loihi alkalic to transitional basalt fields; thin dashed lines: Atlantic plume basalt fields (St Helena SH, Ascension Island AI, Tristan da Cunah TC, Gough island GI, and Walvis Ridge WR). Rose Atoll data (A, B, C and Agl) from this paper. Samoan plume islands and seamount fields (9 analyses) from Johnson *et al.* (1986) and Wallis Island (12 analyses) from Price *et al.* (1991). Hawaiian plume tholeiites (19 analyses, excluding Koolau and other separate source basalts) from Norman & Garcia (1999). Loihi alkalic to transitional basalts (20 analyses) from Garcia *et al.* (1995).

of those to be expected among geographically contiguous basalts formed within a single evolving petrographic province. Only one Rose sample shows distinct affinities with any of the rock types documented from the eastern Manu'a Group. As such, no unambiguous evidence presently exists that the three described rocks might have been transported to Rose; an inference consistent with the large size of some specimens recorded by Wilkes (1844) and Dana (1849). The chemistry of the rocks generally conforms with that expected from a young volcano in the Samoan chain but their precise characters pose a number of questions.

Both Rose and Ta'u basalts lie near the eastern plume limits for Samoan activity. Both resemble Wallis Island basalts in age (<1Ma) and petrological spectrum, except that Wallis lavas display the presence of a plume component that reflects their island's position within the previous Samoan plume path (Stice, 1968; Natland & Turner, 1985; Price *et al.*, 1991). Wallis Island activity is attributed to a thermal disturbance in the lithosphere some 9 myr after plume passage, possibly from tectonism near a Pacific-Australian transform boundary. Rose Atoll is distant from this tectonic feature and hence its origin is enigmatic. Its activity may stem from late differential flexure and rifting and volcanic loading along the Samoan chain (Savi'i, Upolu, Tutuila) that involved production of "post-erosional" eruptives (Natland & Turner, 1985), although the height of the atoll and its petrological span may be too large for such an exclusive origin. Adjustments in the stress field beyond this zone however, may have focused melting in lithosphere beneath the Manu'a and Rose region, prior to resurgence of the Samoan plume at Vailulu'u seamount.

Origin of the Samoan chain has been controversial due to its limited migratory progression, complex eruptive pattern and its unusual mantle geochemical signatures (Natland, 1980; White & Hofmann, 1982). However recent studies support plume input (Hart *et al.*, 2000). Removal of Rose (and Ta'u) volcanism from plume input suggests plume activity has become more sporadic since earlier more western Samoan plume volcanism. One possibility is for a fast plume, as modelled by Larsen & Yuen (1997). Such plumes last for less than 8 myr and are initiated when subducted slabs grade into horizontal flow in the lower mantle. However subduction and downthrusting along the Pacific-Australian plate margin is away from the Samoan chain in this region, which presents a difficulty for a fast plume origin. A recent study has proposed that linear Pacific volcanic chains may show progressive plume eruptive ages mixed with non-progressive activity (Hieronymous & Bercovici, 1999). In these cases the volcano spacing and irregular infillings are controlled by tectonic and flexural stresses on magma transport. Whether such a model applies to the Samoan Islands needs more detailed age dating and dynamic modelling studies of the volcanic evolution.

The basalt float sampled from Rose Atoll shows petrological attributes that link the rocks generally with neighbouring Ta'u Island. Some petrological distinctions, however, are known and this with size and distribution of such rocks on Rose does not favour their transport to Rose. Even if transport to Rose Atoll were to be demonstrated, knowledge of the particular characters of these rocks, along with those of known Ta'uan representatives, is important to decipher the petrogenetic evolution of this eastern end of the Samoan chain. Despite an enigmatic trace, the Samoan plume resembles other main deep plumes in their seismic anomalies (Ritsema & Allen, 2003).

ACKNOWLEDGMENTS. Particular thanks are due to Leslie Hale for recovering the three basalt samples from the Smithsonian petrology collection and to Dr Sorena Sorensen for authorising their loan and analysis. Support was provided by the Auckland University Research Committee and by a Visiting Fellowship awarded by the Smithsonian Institution to KAR. Thanks are also due to Dr Dietmar Müller, Geology Department, University of Sydney, for providing reconstruction of plate motion tracks in the Samoan region, and to Louise Cotterall, Barry Curham, Svetlana Danilova, Dr Ritchie Sims and John Wilmshurst who assisted with analytical and technical expertise. Dr Ian McDougall, Research School of Earth Sciences, Australian National University, examined thin sections for potential for age dating but considered the rocks unsuitable for accurate K-Ar determination. The script was read by Dr Jane Barron, Sydney. Comments on the script were made by Dr B.J. Keating, School of Ocean and Earth Science and Technology, University of Hawaii, while petrological aspects were reviewed by Dr M.O. Garcia, Dept of Geology and Geophysics, University of Hawaii, Honolulu.

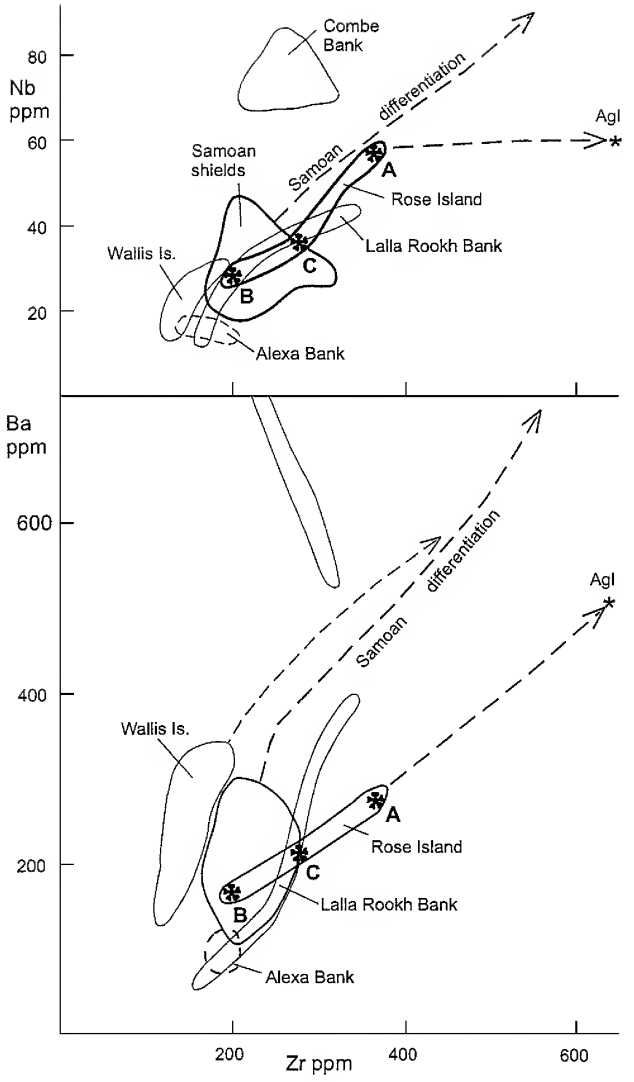

Fig. 8. Nb and Ba related to Zr for Samoan shields, islands and submarine banks. Thick lines: Rose Atoll and Samoan shields; thin lines: Combe Bank, Lalla Rookh bank, Alexa Bank and Wallis Island. Stars: Rose Atoll analyses, this paper. Other data from Natland & Turner (1985), Johnson *et al.* (1986), Price *et al.* (1991).

References

Brothers, R.N., 1959. Petrography. In D. Kear & B.C. Wood. The geology and hydrology of Western Samoa. *New Zealand Geological Survey Bulletin* 63: 38–48.

Buddington, A.F., & D.H. Lindsley, 1964. Iron-titanium oxide minerals and synthetic equivalents. *Journal of Petrology* 5: 310–357.

Carmichael, I.S.E., 1967. The iron-titanium oxides of salic volcanic rocks and their associated ferro-magnesian silicates. *Contributions to Mineralogy and Petrology* 14: 36–64.

Couthouy, J.P., 1842. Remarks upon coral formations in the Pacific; with suggestions as to the causes of their absence in the same parallels of latitude on the coast of South America. *Boston Journal of Natural History* 4: 66–105, 137–162.

Dana, J.D., 1849. *United States Exploring Expedition. During the Years 1838, 1839, 1840, 1841, 1842. Under the Command of Charles Wilkes, U.S.N., v. X. Geology*. C. Sherman, Philadelphia, 309 pp.

Dana, J.D., 1851. On coral reefs and islands. *American Journal of Science and Arts* 61: 357–72, ser. 2, 62: 25–51.

Droop, G.T.R., 1987. A general equation for estimating Fe^{3+} concentrations in ferromagnesian silicates and oxides from microprobe analyses, using stoichiometric criteria. *Mineralogical Magazine* 51: 431–435.

Duncan, R.A., 1985. Radiometric ages from volcanic rocks along the New Hebrides—Samoa lineament. In *Geological Investigations of the Northern Melanesian Borderland*, ed. T.M. Brocker, pp. 67–76. Houston, Texas: Circum-Pacific Council for Energy and Resources.

Farley, K.A., J.H. Natland & H. Craig, 1992. Binary mixing of enriched and undegassed (primitive?) mantle components (He, Sr, Nd, Pb) in Samoan lavas. *Earth and Planetary Science Letters* 111: 183–199.

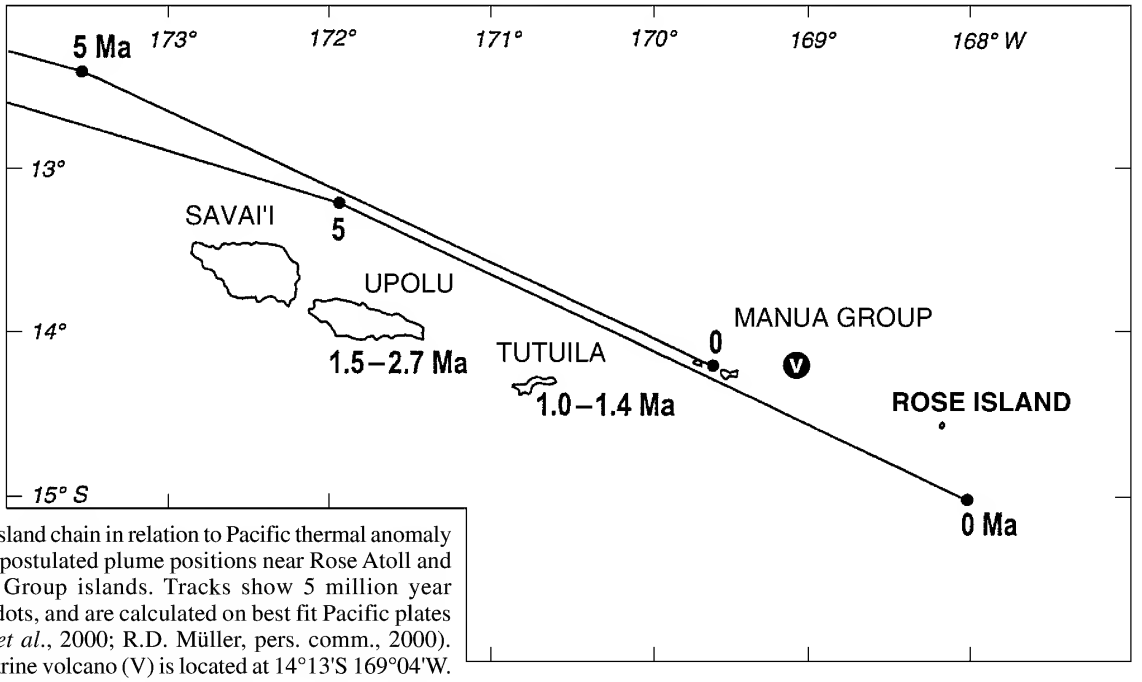

Fig. 9. Samoan Island chain in relation to Pacific thermal anomaly tracks based on postulated plume positions near Rose Atoll and in the Manu'a Group islands. Tracks show 5 million year intervals, solid dots, and are calculated on best fit Pacific plates motion (Gaina *et al.*, 2000; R.D. Müller, pers. comm., 2000). Vailulu'u submarine volcano (V) is located at 14°13'S 169°04'W.

Gaina, C., R.D. Müller & S. Cande, 2000. Absolute plate motion, mantle flow and volcanism at the boundary between the Pacific and Indian Ocean mantle domains since 90Ma. In *The History and Dynamics of Global Plate Motions*, ed. M.A. Richards, R.G. Gordon & R.D. van der Hilst, vol. 121, pp. 189–210. American Geophysical Union Monograph.

Garcia, M.O., D.J.P. Foss, H.B. West & J.J. Mahoney, 1995. Geochemical and isotopic evolution of Loihi Volcano, Hawaii. *Journal of Petrology* 36: 1647–1674.

Hart, S.R., H. Staudigel, A.A.P. Koppers, J. Blusztajn, E.T. Baker, R. Workman, M. Jackson, E. Hauri, M. Kurz, K.Sims, D. Fornari, A. Saal & S. Lyons, 2000. Vailulu'u undersea volcano: the new Samoa. *Geochemistry, Geophysics Geosystems Research Letter* 1: 1–13.

Hauri, E.H., N. Shimizu, J.J. Dieu & S.R. Hart, 1993. Evidence for hotspot-related carbonatite metasomatism in the oceanic upper mantle. *Nature* 365: 221–227.

Hawkins Jr., J.W., & J.H. Natland, 1975. Nephelinites and basanites of the Samoan linear volcanic chain: their possible tectonic significance. *Earth and Planetary Science Letters* 24: 427–439.

Hedge, C.E., Z.E. Peterman & W.R. Dickinson, 1972. Petrogenesis of lavas from Western Samoa. *Geological Society of America Bulletin* 83: 2709–2714.

Hieronymous, C.F., & D. Bercovici, 1999. Discrete alternating hotspot islands formed by interaction of magma transport and lithospheric flexure. *Nature* 397: 605–607.

Hoskin, P.W.O., 1998. Minor and trace element analyses of natural zircon ($ZrSiO_4$) by SIMS and laser ablation ICPMS: a consideration and comparison of two broadly competitive techniques. *Journal of Trace Microprobe Techniques* 16: 301–326.

Hubbard, N.J., 1971. Some chemical features of lavas from the Manu'a Islands, Samoa. *Pacific Science* 25(2): 178–187.

Hutchison, C.S., 1974. *Laboratory Handbook of Petrographic Techniques*. New York: John Wiley & Sons.

Johnson, K.T.M., J.M. Stinton & R.C. Price, 1986. Petrology of seamounts northwest of Samoa and their relation to Samoan volcanism. *Bulletin of Volcanology* 48: 225–235.

Kamber, B.S., & K.D. Collerson, 2000. Zr/Nb systematics of ocean island basalts reassessed—the case for binary mixing. *Journal of Petrology* 41: 1007–1021.

Keating, B.H., 1992. The geology of the Samoan Islands. In *Geology and Offshore Mineral Resources of the Central Pacific Basin*, ed. B.H. Keating & B.R. Bolton, vol. 14, pp. 127–178. Circum-Pacific Council for Energy and Mineral Resources Earth Science Series.

Keller, R.A., M.R. Fisk & W.M. White, 2000. Isotopic evidence for Late Cretaceous plume-ridge interaction at the Hawaiian hotspot. *Nature* 405: 673–676.

Larsen, T.B., & D.A. Yuen, 1997. Ultrafast upwelling bursting through the upper mantle. *Earth and Planetary Science Letters* 146: 393–399.

Le Maitre, R.W., 1984. *A Classification of Igneous Rocks and Glossary of Terms*. Oxford: Blackwell, 193 pp.

Macdonald, G.A., 1944. Petrography of the Samoan Islands. *Bulletin of the Geological Society of America* 55: 1333–1362.

Macdonald, G.A., 1968. A contribution to the petrology of Tutuila, American Samoa. *Sonderuck aus der Geologischen Rundschau* 57: 821–837.

McDougall, I., 1985. Age and evolution of the volcanoes of Tutuila, American Samoa. *Pacific Science* 39: 311–320.

Mayor, A.G., 1921. Rose Atoll, American Samoa. *Proceedings of the American Philosophical Society* 60(2): 62–70.

Mayor, A.G., 1924. Rose Atoll, American Samoa. *Carnegie Institution of Washington Publication* 340: 73–79.

Menard, H.W., 1986. Islands. Scientific American, New York. 230p.

Natland, J.H., 1980. The progression of volcanism in the Samoan linear volcanic chain. *American Journal of Science* 280: 709–735.

Natland, J.H., & D.L. Turner, 1985. Age progression and petrological development of Samoan shield volcanoes: evidence from K-Ar ages, lava compositions, and mineral studies. In *Geological Investigations of the Northern Melanesian Borderland*, ed. T.M. Brocher, vol. 3, pp. 139–171. Circum-Pacific Council for the Energy and Mineral Resources Earth Science Series.

Norman, M.D., & M.O. Garcia, 1999. Primitive magmas and source characteristics of the Hawaiian plume: petrology, geochemistry of shield picrites. *Earth and Planetary Science Letters* 168: 27–44.

Parker, R.J., 1994. *Major Element Analysis: Methods and HP-86 Computer Programs*, version 3.0. Department of Geology, University of Auckland Report 3: 1–32.

Pickering, C., 1876. *United States Exploring Expedition. During the Years 1838, 1839, 1840, 1841, 1842 Under the Command of Charles Wilkes, U.S.N. v. XV. The Geographical Distribution of Animals and Plants. Part II, Plants in their Wild State*. Salem, Massachusetts: Naturalists Agency, 524 pp.

Price, R.C., P. Maillet, I. McDougall & J. Dupont, 1991. The geochemistry of basalts from the Wallis Islands, Northern Melanesian Borderland: evidence for a lithospheric origin for Samoan-type basaltic magmas? *Journal of Volcanology and Geothermal Research* 45: 267–288.

Ritsema, J., & R.M. Allen, 2003. The elusive mantle plume. *Earth and Planetary Science Letters* 207: 1–12.

Rodgers, K.A., I. McAllan, C. Cantrell & B. Ponwith, 1993. Rose Atoll: an annotated bibliography. *Technical Reports of the Australian Museum* 9: 1–37.

Sachet, M.-H., 1954. A summary of information on Rose Atoll (Samoa Islands). *Atoll Research Bulletin* 29: 1–25.

Sachet, M.-H., 1955. Pumice and other extraneous volcanic material on coral atolls. *Atoll Research Bulletin* 37: 1–27.

Schultz, L.P., 1940. The Navy surveying expedition to the Phoenix and Samoan Islands. Smithsonian Institution Exploration and Fieldwork in 1939, pp. 45–50.

Setchell, W.A., 1924. American Samoa, part III, vegetation of Rose Atoll. *Carnegie Institution of Washington Publication* 341: 225–261.

Stice, G.D., 1968. Petrography of the Manu'a Islands, Samoa. *Contribution to Mineralogy and Petrology* 19: 343–357.

Sun, S.-s, & W.F. McDonough, 1989. Chemical and isotopic systematics of oceanic basalts: implications for mantle compositions and processes. In *Magmatism in the Ocean Basins*, ed. D.A. Saunders & M.J. Norry, vol. 42, pp. 313–345. Geological Society Special Publication.

Sun, S.-s, W.F. McDonough & A. Ewart, 1989. Four component model for East Australian basalts. In *Intraplate Volcanism in Eastern Australia and New Zealand*, ed. R.W. Johnson, pp. 333–347. Cambridge: Cambridge University Press.

Wells, P.R.A., 1977. Pyroxene thermometry in simple and complex systems. *Contributions to Mineralogy and Petrology* 62: 129–139.

White, W.M., & A.W. Hofmann, 1982. Sr and Nd isotope geochemistry of oceanic basalts and mantle evolution. *Nature* 296: 821–825.

Wilkes, C., 1844. *Narrative of the United States' Exploring Expedition During the Years 1838, 1839, 1840, 1841, 1842*. Vol. 2, xvi. Philadelphia: C. Sherman, 505 pp.

Wood, B.J., & S. Banno, 1973. Garnet-orthopyroxene and orthopyroxene-clinopyroxene relationships in simple and complex systems. *Contributions to Mineralogy and Petrology* 42: 109–121.

Wright, E., & W.M. White, 1987. The origin of Samoa: new evidence from Sr, Nd and Pb isotopes. *Earth and Planetary Science Letters* 81: 151–162.

Manuscript received 13 August 2001, revised 22 August 2002 and accepted 30 August 2002.

Associate Editor: G.D. Edgecombe.

Records of the Australian Museum (2003) Vol. 55: 153–168. ISSN 0067-1975

Redescription of Four Species of Lagenophryid Peritrichs (Ciliophora) from Australia and New Guinea, With Descriptions of Two New Species

JOHN C. CLAMP[1]* AND JOHN R. KANE[2]

[1] Department of Biology, North Carolina Central University, Durham, North Carolina, United States of America
jclamp@wpo.nccu.edu

[2] 33 Prunda Pde, Raceview Queensland 4305, Australia
john_r_kane@hotmail.com

ABSTRACT. Four insufficiently described species of ectosymbiotic peritrich ciliates in the family Lagenophryidae that occur on crustacean hosts in Australia and New Guinea are redescribed. These include two species of *Operculigera* from phreatoicid isopods, one species of *Setonophrys* from a phreatoicid isopod, and one species of *Lagenophrys* from a palaemonid shrimp. Two undescribed species of *Operculigera*, also found on phreatoicid isopods, are described for the first time. Australian species of *Operculigera* appear to be restricted to phreatoicid hosts. This is unusual because a diverse array of other lagenophryids occur on parastacid crayfish in Australia. Furthermore, species of *Operculigera* are conspicuous symbionts of parastacids and various freshwater crabs in Chile and Madagascar. In addition to this peculiarity of distribution, the Australian species of *Operculigera* appear to comprise a morphologically distinct group within the genus.

CLAMP, JOHN C., & JOHN R. KANE, 2003. Redescription of four species of lagenophryid peritrichs (Ciliophora) from Australia and New Guinea, with descriptions of two new species. *Records of the Australian Museum* 55(2): 153–168.

All but one of the species of peritrich ciliates in the family Lagenophryidae Bütschli, 1889 are specialized ectocommensals of crustaceans. Lagenophryids do not have the familiar bell-, barrel-, or trumpet-shaped, radially symmetrical bodies typical of other peritrichs. Instead, they are grossly flattened and laterally distorted, with a discoid, bilaterally symmetrical shape that fits closely against the host's surface. Unlike most peritrichs, they do not secrete a cylindrical stalk for attachment but, instead, cement themselves to the host's exoskeleton with the rim of their protective lorica.

Lagenophryid loricae are usually hemispheroidal, with the flat side adherent to the host; some species, however, have a narrower, pyriform to ovoid lorica that is adapted for clinging to setae. Lagenophryids protrude only the central, epistomial disk of the peristome (expanded oral area) from the lorica aperture during feeding. Other loricate peritrichs (e.g., all vaginicolids) project the entire oral end of the body through the lorica aperture when feeding. The aperture of a lagenophryid lorica is a complex structure that shuts tightly when the epistomial disk is retracted. Part of the peristomial margin is attached around the base of the lorica aperture in lagenophryids and closes it forcefully, using an enlarged version of the contractile, myonemal sphincter that closes the peristomial lip over the retracted epistomial disk in other peritrichs. Lagenophryids are like other peritrichs in being suspension feeders that capture particulate food such as bacteria and phytoplankton. They may associate with crustaceans because these hosts generate

* author for correspondence

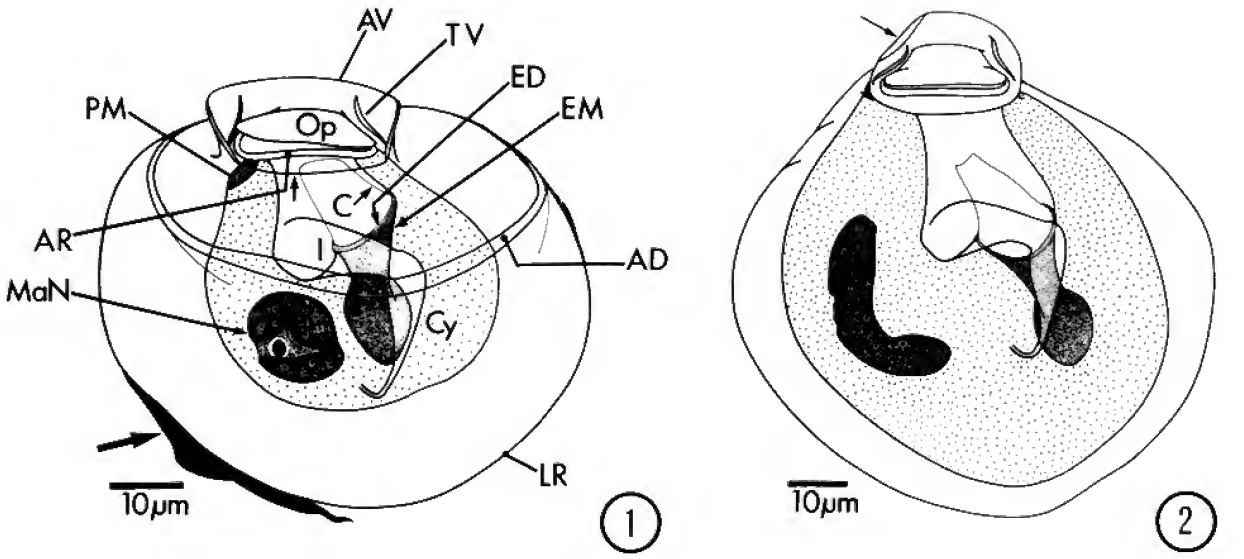

Figs. 1, 2. (*1*) *Operculigera montanea*, Erlich's hematoxylin preparation. Dorsal view of lectotype individual from the type locality and host, AM P62810. (*AD*) thickened ridge that bounds anterior depression in dorsal surface of lorica; (*AR*) rim of lorica aperture; (*AV*) anterior and lateral parts of vallum; (*C*) peristomial cilia originating from epistomial disk (shown in outline only); (*Cy*) cytoplasm (sparsely stippled areas—food vacuoles and other taxonomically irrelevant structures are omitted); (*ED*) epistomial disk; (*EM*) myonemes that retract epistomial disk (densely stippled column anchored to ED); (*I*) infundibulum—this is a passageway through which food particles pass to reach the cytostomal area (the bulbous ampulla leading to a tubular cytopharynx that lies beyond the constriction at the end of the infundibulum); (*LR*) rim of lorica—the localized areas with large accumulations of lorica material (large arrow) are not typical; (*MaN*) macronucleus—the micronucleus is the small, dense, darkly stained body nestled in the central area of the macronucleus; (*Op*) operculum (the slightly displaced left side of the closed operculum is an artefact); (*PM*) myoneme in edge of peristomial lip that effects closure of the operculum; (*TV*) thickened strip in the anterolateral wall of the vallum; small arrow, vestigial posterior part of the vallum—to see species of *Operculigera* with this part of the vallum fully developed, consult Clamp (1991). (*2*) *Operculigera zeehanensis*, Erlich's hematoxylin preparation. Dorsal view of lectotype individual from the type locality and host, AM P62813. The folding over of the left edge of the vallum (small arrow) is an artefact. The micronucleus was hidden underneath the macronucleus and is therefore not shown. The unfolded macronucleus indicates that this individual was probably approaching cell division when it was fixed. Most individuals in the sample examined had the ends of the macronucleus folded together.

currents of water, mainly respiratory or locomotory, which convey a steady supply of particles to their suspension-feeding symbionts (Fenchel; 1965; Clamp, 1973, 1988a).

The genera of lagenophryids with the most species are, in descending order, *Lagenophrys* Stein, 1852, *Operculigera* Kane, 1969, and *Setonophrys* Jankowski, 1986. They differ mainly with respect to the structure of the lorica aperture. In *Lagenophrys*, the aperture is closed by a pair of flexible lips that are the edges of an invaginated collar of lorica material to which the posterior edge of the peristomial lip is attached, and only the posterior half of the peristomial sphincter is enlarged (Figs. 17, 18, 22). The aperture of *Setonophrys* is superficially similar to that of *Lagenophrys*; the anterior lip of the aperture, however, is rigid in *Setonophrys*, a flexible posterior lip is folded against this rigid anterior lip to effect closure, and the entire peristomial sphincter is enlarged (Fig. 16). The lorica aperture of *Operculigera* is markedly different from that of the other two genera. Its aperture is a simple opening that is closed by a flat operculum, and only the anterior half of the peristomial sphincter is enlarged (Fig. 1). Unlike other lagenophryid genera, *Operculigera* has a thickened wall of lorica material, the vallum, which at least partially encircles the lorica aperture (Fig. 1). Some species of *Lagenophrys* have a thickened ridge of lorica material around the anterior half of the lorica aperture, but this ridge is never developed into an actual wall as it is in species of *Operculigera* (Clamp, 1991).

Lagenophryid peritrichs have been reported from all continents except Antarctica on a wide variety of crustaceans living in many kinds of marine, brackish-water, and freshwater habitats. Kane (1969) described several lagenophryid species from hosts collected in Australia and South Africa. The descriptions, unaccompanied by figures, were published in an extended abstract in the proceedings of the 3rd International Congress of Protozoology with the intention of publishing them in more complete form soon afterward. Personal circumstances prevented Kane from doing this, however. Although brief, the descriptions in this abstract meet the minimum requirements for publication of new taxa given in Article 8 of the current, fourth edition of the International Code of Zoological Nomenclature and are not excluded under Article 9.9 because the published proceedings were widely available in book form for purchase by persons other than attendees (ICZN, 1999). Fuller accounts are desirable, however, especially since one species (*Operculigera montanea* Kane, 1969) is the type species of its genus (Clamp, 1991).

Fortunately, Kane saved permanent preparations of the species named in the 1969 publication, and additional material of two species was obtained from the Australian Museum (hereafter abbreviated AM) and the Crustacean Collection of the National Museum of Natural History, Smithsonian Institution (hereafter abbreviated NMNH-CC). This material was sufficient for redescription of four of the Australian species, adding a record from New Guinea for one of them. Two of the species that we will redescribe in this paper are species of *Operculigera* occurring on phreatoicid isopods, and a third is a species of *Setonophrys*

that also associates with phreatoicids. The fourth is a species of *Lagenophrys* found on palaemonid shrimp in northern Australia and Papua New Guinea. *Lagenophrys jacobi* (Kane, 1969), a fifth Australian species described in the 1969 abstract, apparently comprises a complex of different species (Clamp, unpublished observations), and its redescription must be deferred because it requires examination of far more material than we possess at present. The two South African species of *Lagenophrys* named by Kane (1969) will be treated in a separate paper. One new species of *Operculigera*, originally identified (Kane, 1969) as a variant of *O. montanea*, was discovered among the permanent preparations saved by Kane and another was discovered on material from the NMNH-CC. Both are described for the first time in this paper.

Materials and methods

The majority of the material used in this study consisted of slides made by J.R. Kane in the early 1960s. These slides were made by fixing infested portions of host exoskeleton in Bouin's fluid and staining with Erlich's hematoxylin or Delafield's hematoxylin. As is typical for lagenophryids, most ciliates on the slides were still in good, well-stained condition comparable to recently collected and fixed material (Clamp, 1990a). Unlike other sessiline peritrichs, taxonomically important features of lagenophryids are not affected by fixation, and it is customary to use fixed material alone when describing them (Clamp, 1989, 1990a, 1991, 1992). Four samples of infested body parts removed from phreatoicid isopods in museum collections also were included in our study. Three were from the NMNH-CC, and one was from the AM. The fixative for this material was unknown but was probably formalin since cellular features were preserved well and the vacuolate cytoplasm characteristic of alcohol fixation was not evident.

Permanent preparations of museum material were made by staining with Heidenhain's iron hematoxylin or protargol. For protargol, the quick method (Wicklow & Hill, 1992) was used with a staining time of 12–13 min at 70°C. Pieces of host exoskeleton with attached ciliates were carried through both staining processes in capsules approximately 1 cm in length made of polyethylene tubing (outside diameter 9.5 mm) sealed on one end with fine-mesh bolting silk melted into the edge of the tubing with a heated spatula. Protargol preparations were made of *Lagenophrys turneri* only. Material for protargol preparations of other species treated in this paper was either unavailable or of insufficient quantity to obtain usable views of the buccal infraciliature.

Measurements were done at 970× magnification using a filar micrometer. Height of loricae was measured by using the calibrated scale on the fine focusing knob of the microscope to determine the focal distance from the edge of the lorica base to the dorsal surface of the lorica. Phase-contrast microscopy was used for this measurement because loricae are usually too transparent for their dorsal surface to be ascertained accurately by bright-field microscopy. All individuals measured were ones oriented with the dorsal surface of the lorica uppermost and the flattened, ventral surface approximately parallel to the plane of the slide.

Drawings were made using a graticule inscribed with a grid (1 mm squares covering entire field) mounted in one objective of the microscope as a guide. A matching, printed grid was placed under a sheet of tracing paper on which the drawing was done. The microscope used for drawings had a circular stage that could be rotated to align each ciliate with the axes of the grid. Photographs of stained ciliates were made with a Minolta X-700 camera mounted on an Olympus CH-2 microscope using Kodak T-Max film.

Full literature citations for the authorship of species of lagenophryids listed in each genus treated below are given in Kahl (1935), Jankowski (1986, 1993), or Clamp (1989, 1990a, 1991, 1992, 1993, 1994) or in the Reference section of this paper. Nicholls (1943) is a source for full literature citations for the authorship of phreatoicid species.

Results

Operculigera Clamp, 1991

Diagnosis. Solitary, loricate, with lorica aperture consisting of simple opening without either folded lips at its anterior and posterior edges or invaginated collar of lorica material (loricastome). Aperture closable by means of a flat operculum of lorica material and usually surrounded partially or completely by thickened wall of lorica material (vallum) that projects vertically from dorsal surface of lorica. Edge of peristomial lip of trophont associated with anteroventral edge of operculum. Anterior part of myonemal band within peristomial lip thickened. Macronucleus cylindroid, either long or short, often folded compactly, and varying in shape and location between species.

Type species. *Operculigera montanea* Kane, 1969 by designation (Clamp, 1991).

Generic Composition. The following species are currently assigned to *Operculigera*: *O. asymmetrica* Clamp, 1991; *O. carcini* Clamp, 1992; *O. haswelli* n.sp.; *O. inornata* n.sp.; *O. insolita* Clamp, 1991; *O. madagascarensis* Clamp, 1992; *O. montanea* Kane, 1969; *O. obstipa* Clamp, 1991; *O. parastacis* Jankowski, 1986; *O. seticola* Clamp, 1991; *O. striata* Jankowski, 1986; *O. taura* Clamp, 1991; *O. velata* Jankowski, 1986; *O. zeehanensis* Kane, 1969.

Operculigera montanea Kane, 1969

Figs. 1, 8–11; Tables 1, 6

Operculigera montanea Kane, 1969: 369.–Jankowski, 1986: 82, 83; Clamp, 1991: 365.

Redescription. Lorica hemispheroidal, suboval in dorsal view, moderately wider than long. Lorica asymmetrical in dorsal view; width of right half from midline to edge noticeably greater than width of left half from midline to edge. Rim of lorica moderately thickened. Dorsal surface of lorica with prominent, curved ridge extending across entire width of lorica and encircling concave depression in surface surrounding lorica aperture. Because of dorsal ridge, lorica with acuminate, nearly triangular profile in lateral view. Posterior part of vallum reduced to slightly thickened ridge. Anterior and lateral parts of vallum moderately tall, sloping abruptly to posterior part of vallum; posterior edges of lateral parts nearly vertical. Vallum symmetrical in height; free edge straight, even, lacking projections of any sort. Long strip near base of inner wall of each anterolateral part of vallum heavily thickened to form slightly protruding fold. Rim of lorica aperture moderately thickened. Operculum subcuneate in dorsal view. Anterior edge of operculum moderately thickened to form narrow, ventral shelf; ventral shelf smooth, lacking processes.

Macronucleus short, cylindroid; ends flexed upon centre to create compact, folded shape. Macronucleus located in left half of body. Micronucleus ovoid, located more frequently near centre of macronucleus than near either end.

Etymology. The specific name refers to the montane habitat of the type host.

Type material. LECTOTYPE, AUSTRALIA, Victoria, summit of Mt Baw Baw (1850 m elevation); 13 Oct 1963, J.R. Kane; on *Colubotelson searlei* Nicholls, 1944, pleopods. Lectotype slide with lectotype organism marked by inscribed circle (Erlich's hematoxylin), AM P62810. PARALECTOTYPE slide (Erlich's hematoxylin), International Protozoan Type Collection (hereafter abbreviated IPTC) USNM 1004287. AUSTRALIA, Victoria, Kiewa; J.R. Kane; on *Colubotelson* sp., pleopods. Paralectotype slide (Erlich's hematoxylin), AM P62811.

Other material examined. Victoria, Mt Buffalo; Feb 1926, G.E. Nicholls; on *C. joyneri* (Nicholls, 1926), pleopods (AM Z6189). Voucher slides (3 Heidenhain's hematoxylin, 2 protargol) AM P62812, P62880, P62881, P62882, P62883.

Nomenclatural note. No type species was explicitly fixed for *Operculigera* in Kane (1969); consequently, this name was not yet available because such fixation was required for genus-group names published after 1930 (ICZN, 1999). Clamp (1991) designated *O. montanea* as the type species of the genus, making the name *Operculigera* available and (inadvertently as it turned out) becoming the author of the genus. The authorship of species of *Operculigera* described in Kane (1969) and Jankowski (1986) was not affected by this action (Article 11.9.3.1 of the current Code).

Remarks. The curved ridge in the dorsal surface of the lorica (Figs. 1, 9) is a distinctive characteristic of *O. montanea* that does not occur, even in reduced form, in any other known species within the genus (Jankowski, 1986; Clamp, 1991). Indeed, this ridge has no real equivalent in any other lagenophryid species.

Operculigera montanea has a simple vallum (Fig. 1), lacking the spines or other processes so characteristic of most other species in the genus (Jankowski, 1986; Clamp, 1991). Its shape resembles that of *O. zeehanensis* Kane, 1969, *O. inornata* n.sp., and *O. obstipa* Clamp, 1991; nevertheless, its distinctive proportions make it relatively easy to recognize. The vallum of *O. montanea* is markedly shorter in relation to its width than those of either *O. zeehanensis* or *O. inornata* (Figs. 1, 2, 14, 15; Tables 1, 2, 4–6). The vallums of *O. montanea* and *O. obstipa* are both short in relation to their widths but the vallum of the former is uniform in height compared to that of the latter, which diminishes in height from left to right (Table 6; Clamp, 1991).

Approximately 50% of the ciliates in the sample of *O. montanea* from the type locality contained one or more individuals of an unknown type of spherical, unicellular parasite in their cytoplasm (Fig. 10). Neither of the other samples examined showed any evidence of infection. The mean diameter of a sample of 15 parasites was 9.5±3.2 μm (4.8–13.9 μm). Each parasite had a single, dense nucleus (Fig. 10), eliminating the possibility that they could be ciliates of any kind, such as the suctorians that parasitise some peritrich ciliates. In addition, none of the distinctive stages in the life cycle of parasitic suctorians (Lynch & Noble, 1931; Matthes, 1971) were evident.

A closely fitting, thin-walled cyst or cell wall encapsulated the cell body of the parasite. Several ruptured, empty examples of these capsules were seen (Fig. 11), and a sample of 5 of them was measured. They had a mean diameter of 14.0±0.9 μm (12.7–15.3 μm). All empty capsules were in hosts that appeared either moribund or dead and disintegrating. One such capsule had a cluster of 16 small, oval cells nearby that may have been recently escaped swarmers of some kind. Each of these small cells had a single, dense, spherical nucleus similar to that of larger, encysted cells. A sample of 5 of the small cells had a mean length of 8.2±0.5 μm (7.4–8.7 μm) and a mean width of 5.7±0.6 μm (5.0–6.3 μm). The general appearance of the parasites suggests that they are either a species of chytrid fungus or amoeboid protozoan; however, positive identification will require more material than we had and observation of living parasites to elucidate their life cycle.

Note on the lorica aperture of *Operculigera*. Until now, functioning of the lorica aperture has not been described in living individuals of any species of *Operculigera*. Clamp

Table 1. Measurements and proportions (expressed as ratios of attributes to one another) of *Operculigera montanea* from the type locality and host (n=9).

Attribute	Mean (μm)	S.D. (μm)	C.V. (%)	Range (μm)
Height of lorica	37	±3	7.1	34–41
Length of lorica	59.4	±2.8	4.7	54.2–62.3
Width of lorica	66.5	±4.2	6.3	57.5–71.1
Width of dorsal concavity	56.4	±4.2	7.5	47.4–60.8
Width of vallum	25	±1.2	5	23.4–26.8
Width of operculum	19.6	±0.8	4.1	18.2–21.0
Width of epistomial disk	13.1	±1.0	7.5	11.9–14.4
Length of micronucleus	3.8	±0.4	9.2	3.4–4.5
Width of micronucleus	3.1	±0.2	5.8	2.8–3.4
Length/width of lorica	0.89	±0.04	4.3	0.85–0.94
Height/width of lorica	0.56	±0.05	9.1	0.48–0.63
Width of vallum/width of lorica	0.38	±0.02	6	0.35–0.41
Width of operculum/width of lorica	0.3	±0.02	5.9	0.28–0.32
Width of epistomial disk/width of lorica	0.2	±0.02	12.2	0.18–0.25
Length/width of micronucleus	1.22	±0.15	12.1	1.03–1.48

Table 2. Measurements and proportions (expressed as ratios of attributes to one another) of *Operculigera zeehanensis* from the type locality and host (n=11). All individuals measured were on the holotype slide.

Attribute	Mean (μm)	S.D. (μm)	C.V. (%)	Range (μm)
Height of lorica	31	±1	4.1	29–33
Length of lorica	77.8	±2.9	3.7	73.6–82.2
Width of lorica	84.6	±3.2	3.7	77.6–89.4
Width of vallum	24.9	±1.1	4.5	23.5–27.4
Width of operculum	21.2	±0.7	3.1	20.2–22.3
Width of epistomial disk	17.2	±0.7	4.3	15.9–18.2
Length of micronucleus	3.6	±0.1	3	3.5–3.8
Width of micronucleus	2.9	±0.1	4.7	2.7–3.1
Length/width of lorica	0.92	±0.05	5.3	0.86–1.03
Height/width of lorica	0.36	±0.02	4.3	0.35–0.40
Width of vallum/width of lorica	0.29	±0.01	4.5	0.27–0.32
Width of operculum/width of lorica	0.25	±0.01	4.1	0.24–0.27
Width of epistomial disk/width of lorica	0.2	±0.01	5.4	0.19–0.22
Length/width of micronucleus	1.25	±0.06	4.5	1.16–1.32

(1991) described the operculum as being attached to the anterior edge of the aperture, based on sections of fixed material, and as opening toward the anterior, based on a short statement in Kane (1969). In this paper, we are able to draw on Kane's personal observations of living *O. montanea* that were more fully described and illustrated in his MSc thesis (Kane, 1964) than in the 1969 publication. In *O. montanea*, the operculum opens toward the posterior to lie against the dorsal surface of the lorica posteriad of the aperture. This allows the epistomial disk to protrude from the aperture anteriad of the reflected operculum instead of posteriad to it if Clamp (1991) were correct. To accomplish this, the operculum would have to be attached to the dorsum of the cell immediately posteriad of the peristomial lip instead of to the anterior edge of the aperture. The sagittal sections of two species of *Operculigera* illustrated in Clamp (1991) do not show this, but the lack of contact between the cell body and the operculum could have been a fixation artefact. Further observations of living material and sections of freshly fixed material are needed to resolve this ambiguity.

Operculigera zeehanensis Kane, 1969

Fig. 2; Tables 2, 6, 7

Operculigera zeehanensis Kane, 1969: 369.–Jankowski, 1986: 82; Clamp, 1991: 365.

Redescription. Lorica hemispheroidal, suboval in dorsal view, slightly wider than long. Lorica asymmetrical in dorsal view; width of right half from midline to edge noticeably greater than width of left half from midline to edge. Rim of lorica not thickened. Dorsal surface of lorica without curved ridge. Posterior part of vallum reduced to slightly thickened ridge. Anterior and lateral parts of vallum moderately tall; posterior edges of lateral parts sloping moderately to posterior part of vallum, giving anterior and lateral parts symmetrically rounded profile as a whole. Free edge of vallum smooth, even, lacking projections of any sort. Long strip near base of inner wall of each anterolateral part of vallum moderately thickened and projecting inward to form prominent, protruding fold. Rim of lorica aperture moderately thickened. Operculum subcuneate in dorsal view. Anterior edge of operculum moderately thickened to form narrow, ventral shelf; ventral shelf smooth, lacking processes.

Macronucleus elongate, cylindroid, usually folded to make compact mass. Macronucleus located in left half of body. Micronucleus ovoid, located almost always near centre of macronucleus rather than near either end.

Etymology. The specific name refers to the locality from which the type host was collected.

Type material. LECTOTYPE, AUSTRALIA, Tasmania, near Zeehan; W. Drummond; on *Phreatoicoides longicollis* Nicholls, 1943, pleopods. Lectotype slide with lectotype organism marked by inscribed circle (Erlich's hematoxylin), AM P62813.

Operculigera haswelli n.sp.

Figs. 3–7, 12; Tables 3, 6

Description. Lorica hemispheroidal, suboval in dorsal view, moderately wider than long. Lorica more or less symmetrical in dorsal view; width of right half from midline to edge not noticeably greater than width of left half from midline to edge. Rim of lorica not thickened. Dorsal surface of lorica without curved ridge. Posterior part of vallum reduced to slightly thickened ridge. Anterior and lateral parts of vallum moderately tall; posterior edges of lateral parts sloping abruptly to posterior part of vallum and flaring outward. Free edge of vallum smooth, even, usually with spine on left margin. Spine varying from absent to as long as width of body of vallum. Long strip near base of inner wall of each anterolateral part of vallum moderately thickened and projecting inward to form prominent, protruding fold. Rim of lorica aperture heavily thickened. Operculum subcuneate in dorsal view. Anterior edge of operculum moderately thickened to form narrow, ventral shelf; ventral shelf smooth, lacking processes. Macronucleus elongate, cylindroid, usually folded to make compact mass. Macronucleus located in left half of body. Micronucleus ovoid, almost always located near centre of macronucleus rather than near either end.

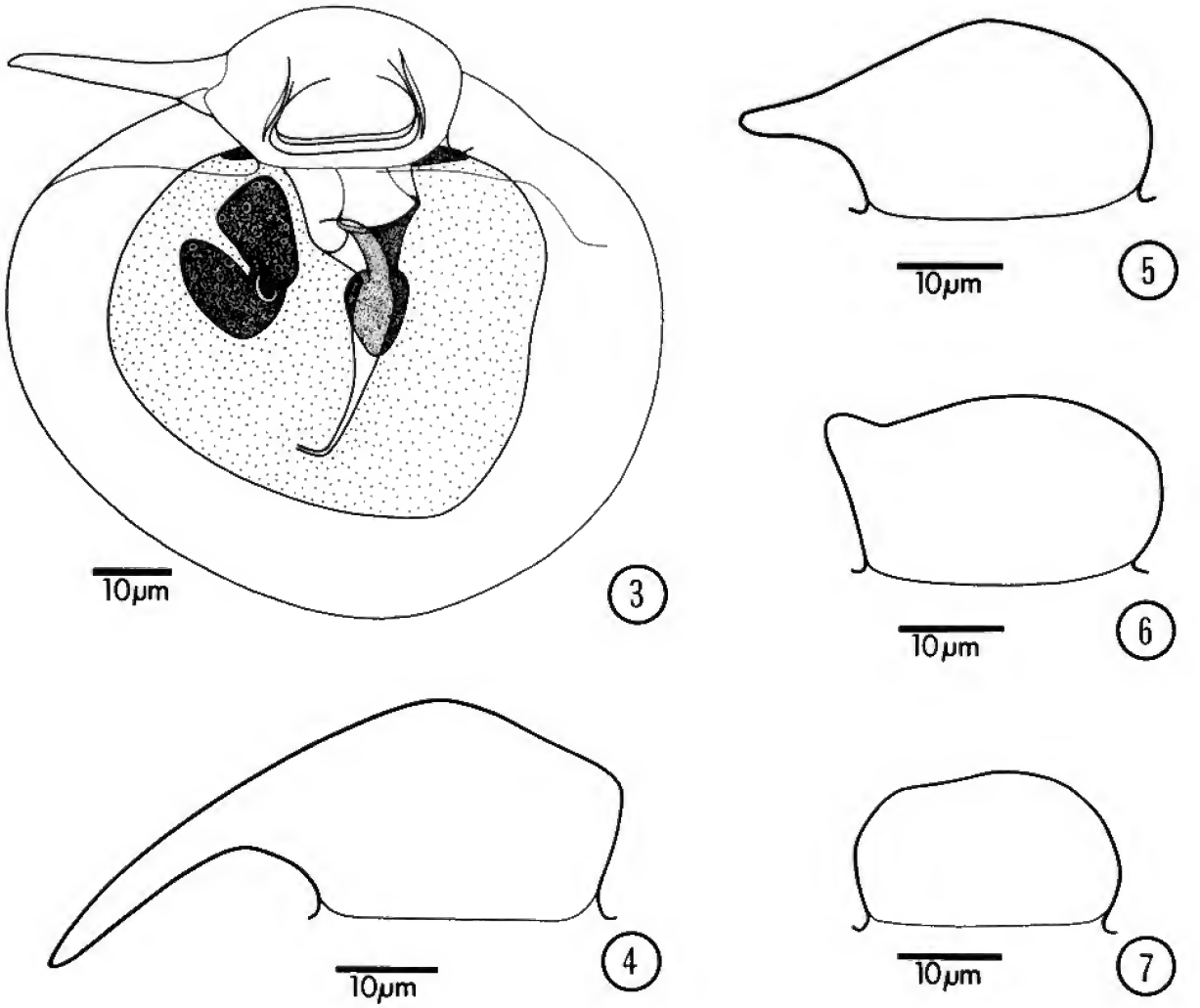

Figs. 3–7. *Operculigera haswelli* n.sp. from the type locality and host; Heidenhain's hematoxylin preparations, AM P62814 and P62815. (*3*) Dorsal view of holotype individual with maximally developed spine. (*4*) Vallum with maximally developed spine curving posteriad. (*5*) Vallum with partially developed spine. (*6*) Vallum with minimally developed spine reduced to blunt process. (*7*) Vallum lacking spine.

Etymology. This species is named in honour of William A. Haswell, who published the first mention of lagenophryid peritrichs on Australian crustaceans in 1901.

Type material. HOLOTYPE, AUSTRALIA, Tasmania, Great Lake; 1914, W.M. Tattersall; on *Mesacanthotelson tasmaniae* (Thomson, 1894), pleopods (NMNH-CC USNM 60658). Holotype slide with holotype organism marked by inscribed circle (Heidenhain's hematoxylin), AM P62814. PARATYPE slides (Heidenhain's hematoxylin), AM P62815 and IPTC USNM 1004288.

Remarks. The spine on the left margin of the vallum of *O. haswelli* is unique within the genus. *Operculigera taura* Clamp, 1991 has a long, slender spine on each side of the anterior part of the vallum, but they project anteriad at a very different angle (Clamp, 1991) to the laterally projecting spine of *O. haswelli*, the tip of which curves toward the posterior in maximally developed examples (Fig. 4). *Operculigera velata* Jankowski, 1986 has a single, long, pointed process on the left margin of the vallum, but it is broad and bladelike rather than being a slender spine.

The spine on the vallum was extremely variable in its development among individual ciliates in the single sample of *O. haswelli* that was examined. Most individuals had a spine of some sort (Figs. 3–6, 12), but the spine was completely absent in some (Fig. 7). When present, the spine varied from extremely long and acuminate (Figs. 3, 4, 12) to short, barely visible, blunt processes (Figs. 5, 6).

Operculigera inornata n.sp.

Figs. 13–15; Tables 4–7

Description. Lorica hemispheroidal, suboval to subcircular in dorsal view, slightly longer than wide. Lorica asymmetrical in dorsal view; width of right half from midline to edge noticeably greater than width of left half from midline to edge. Rim of lorica not thickened. Dorsal surface of lorica without curved ridge. Posterior part of vallum reduced to slightly thickened ridge. Anterior and lateral parts of vallum moderately tall; posterior edges of lateral parts sloping abruptly to posterior part of vallum, posterior edges nearly vertical. Free edge of vallum smooth, even, lacking projections of any sort. Long strip near base of inner wall of each anterolateral part of vallum moderately thickened and projecting inward to form prominent, protruding fold. Rim of lorica aperture moderately thickened. Operculum

Table 3. Measurements and proportions (expressed as ratios of attributes to one another) of *Operculigera haswelli* n.sp. from the type locality and host (n=20).

Attribute	Mean (μm)	S.D. (μm)	C.V. (%)	Range (μm)
Height of lorica	17	±2	12.3	14–21
Length of lorica	74.4	±3.4	4.6	69.8–83.1
Width of lorica	82.9	±4.5	5.4	73.7–89.1
Width of vallum	24.5	±1.3	5.4	22.0–27.2
Width of operculum	19.5	±1.0	5.2	16.7–21.3
Width of epistomial disk	12.7	±0.6	4.4	11.3–13.6
Length of micronucleus	5.1	±0.6	12.4	3.6–5.9
Width of micronucleus	3.3	±0.5	14.3	2.7–4.2
Length/width of lorica	0.91	±0.04	3.9	0.85–0.96
Height/width of lorica	0.22	±0.04	15.8	0.17–0.28
Width of vallum/width of lorica	0.3	±0.02	6.1	0.27–0.32
Width of operculum/width of lorica	0.24	±0.02	6.8	0.22–0.26
Width of epistomial disk/width of lorica	0.15	±0.01	7.7	0.13–0.17
Length/width of micronucleus	1.52	±0.17	11	1.23–1.79

subcuneate in dorsal view. Anterior edge of operculum moderately thickened to form narrow, ventral shelf; ventral shelf smooth, lacking processes. Macronucleus short to moderately elongate, cylindroid, usually folded to make compact mass. Macronucleus located in left half of body. Micronucleus ovoid, located more frequently near centre of macronucleus rather than near either end.

Etymology. The specific name (Latin: unadorned, simple) refers to the plain appearance of the lorica and its vallum.

Type material. HOLOTYPE, AUSTRALIA, Victoria, Otway Range; 24 Dec 1963, J.R. Kane; on *Phreatoicopsis terricola* Spencer & Hall, 1896, pleopods. Holotype slide with holotype organism marked by inscribed circle (Delafield's hematoxylin), AM P62816. PARATYPE slide (Delafield's hematoxylin), IPTC USNM 1004289. Victoria, Grampian Range, swamp near Fyan's Creek; 20 Nov 1963, J.R. Kane; on *Phreatoicopsis* sp., pleopods. Paratype slides (Delafield's hematoxylin), AM P62817 and IPTC USNM 1004290. Tasmania, Great Lake, 1914, W.M. Tattersall; on *Colubotelson chiltoni* (Sheppard, 1927), pleopods (NMNH-CC USNM 60657). PARATYPE slides (Heidenhain's hematoxylin), AM P62818 and IPTC USNM 1004291 (the latter comprises 2 slides).

Remarks. The vallum of *O. inornata* lacks the spines or other types of processes so characteristic of some other species of *Operculigera* (Jankowski, 1986; Clamp, 1991), but so do three other species of *Operculigera* that are hosted by various species of phreatoicid isopods (Figs. 1, 2; Table 6; Clamp, 1991). At first glance, this appears to create the potential for taxonomic confusion; however, two of these species, *O. obstipa* Clamp, 1991 and *O. montanea* (Fig. 1), are easily distinguished from *O. inornata* (Figs. 14, 15) by differences in shape and symmetry of the anterolateral part of the vallum, proportions of the lorica, and (in the case of *O. montanea*) presence of a prominent ridge in the dorsal surface of the lorica (Table 6).

The third species with a plain vallum, *O. zeehanensis* (Fig. 2), is much closer to *O. inornata* (Figs. 14, 15) in appearance but is separated from it by differences in the shape of the anterolateral part of the vallum and, especially, proportions of the lorica (Table 6). The lorica of *O. inornata* is subcircular to moderately longer than wide in dorsal view (Figs. 13–15; Tables 4, 5, 7). Only four individuals in the sample of *O. inornata* from Tasmania and none in the sample from Victoria had loricae that were slightly wider than they were long. By contrast, all but one individual in the sample of *O. zeehanensis* had loricae that were at least 5% wider than they were long

Table 4. Measurements and proportions (expressed as ratios of attributes to one another) of *Operculigera inornata* n.sp. from the type locality and host (n=25).

Attribute	Mean (μm)	S.D. (μm)	C.V. (%)	Range (μm)
Height of lorica	20	±2	9.6	15–23
Length of lorica	65.3	±2.0	3.1	59.5–69.1
Width of lorica	61.9	±2.9	4.8	53.5–67.1
Width of vallum	21.8	±0.8	3.7	19.0–23.3
Width of operculum	16.1	±0.7	4.6	13.7–17.1
Width of epistomial disk	12.9	±0.6	4.7	11.3–14.1
Length of micronucleus	3.1	±0.2	6.9	2.7–3.4
Width of micronucleus	2.2	±0.1	6.1	1.9–2.5
Length/width of lorica	1.06	±0.03	2.5	1.02–1.12
Height/width of lorica	0.32	±0.04	12.5	0.23–0.39
Width of vallum/width of lorica	0.35	±0.01	2.9	0.34–0.37
Width of operculum/width of lorica	0.26	±0.01	3.7	0.24–0.28
Width of epistomial disk/width of lorica	0.21	±0.01	6.1	0.19–0.24
Length/width of micronucleus	1.4	±0.11	7.9	1.25–1.59

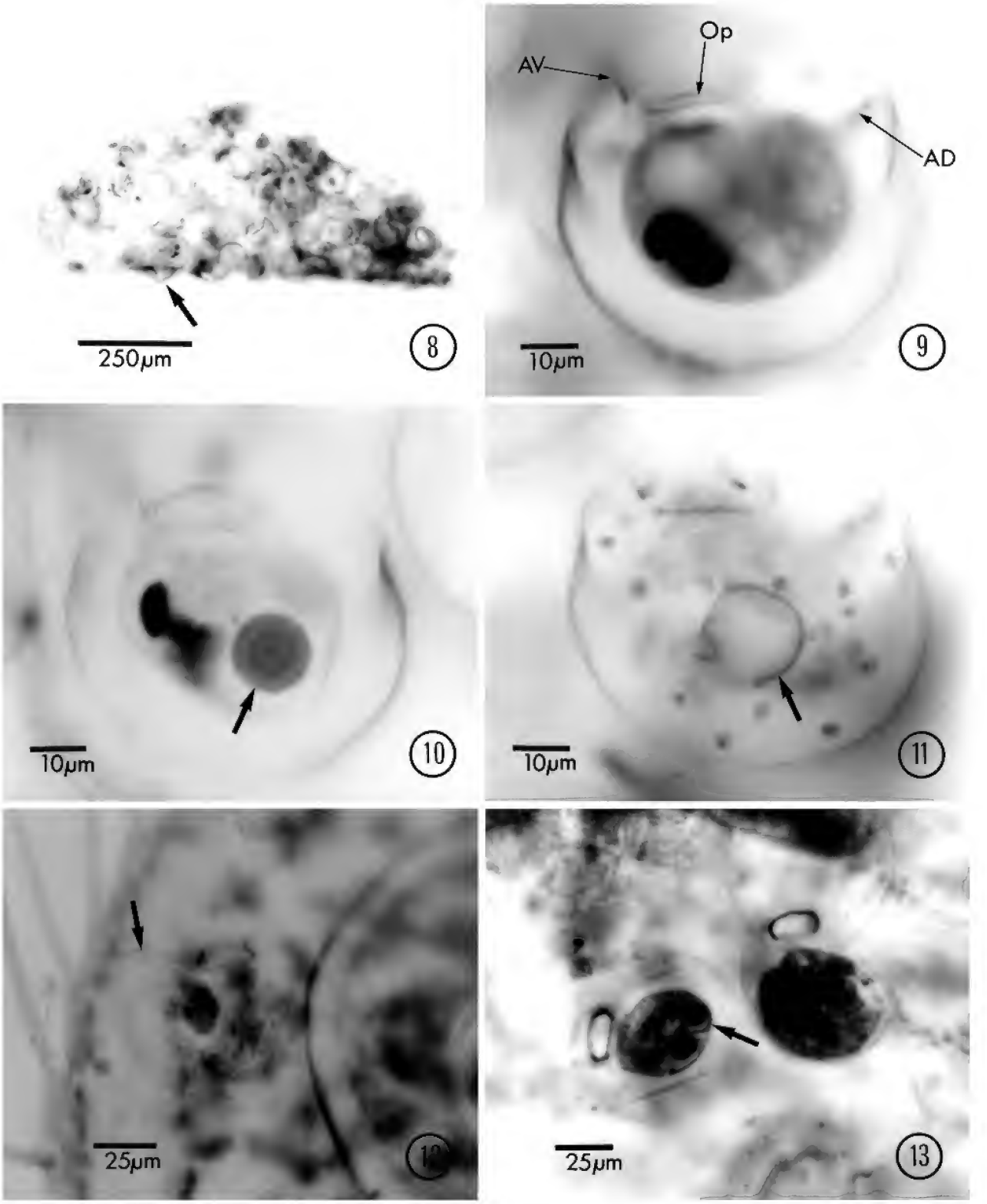

Figs. 8–13. (*8–11*) *Operculigera montanea* from the type locality and host; Erlich's hematoxylin preparations, AM P62810. (8) Heavily infested pleopod of host at low magnification. Arrow, lateral view showing triangular profile of lorica. (9) Dorsal view of single individual. See Fig. 1 for explanation of symbols. (*10*) Dorsal view of individual with intracellular parasite (arrow). (*11*) Dorsal view of individual with empty, ruptured cyst of intracellular parasite (arrow). (*12*) Dorsal view of *Operculigera haswelli* n.sp. from the type locality and host; Heidenhain's hematoxylin preparation, AM P62814. Arrow, spine on left margin of vallum. (*13*) Dorsal view of two individuals of *Operculigera inornata* n.sp. from Great Lake, Tasmania; Heidenhain's hematoxylin preparation, IPTC USNM 1004291. Arrow, intracellular parasite.

Table 5. Measurements and proportions (expressed as ratios of attributes to one another) of *Operculigera inornata* n.sp. from Great Lake, Tasmania (n=19).

Attribute	Mean (μm)	S.D. (μm)	C.V. (%)	Range (μm)
Height of lorica	19	±1	7.3	17–22
Length of lorica	66.3	±4.9	7.3	58.9–76.4
Width of lorica	65.2	±4.6	7	59.3–75.8
Width of vallum	23.4	±1.1	4.9	21.3–25.1
Width of operculum	17.4	±0.7	4	15.9–19.0
Width of epistomial disk	13.2	±0.5	4	12.0–13.9
Length of micronucleus	3.9	±0.6	16	3.2–5.7
Width of micronucleus	2.6	±0.3	11.1	2.2–3.6
Length/width of lorica	1.02	±0.03	3.3	0.93–1.07
Height/width of lorica	0.3	±0.02	7.6	0.24–0.35
Width of vallum/width of lorica	0.36	±0.02	6	0.30–0.41
Width of operculum/width of lorica	0.27	±0.02	5.8	0.24–0.31
Width of epistomial disk/width of lorica	0.2	±0.02	7.4	0.18–0.23
Length/width of micronucleus	1.48	±0.15	10	1.25–1.93

(Table 7). In addition, the width of the vallum in comparison to the width of the lorica was markedly greater in both samples of *O. inornata* than in the single sample of *O. zeehanensis* (Table 7). Only one individual in the sample of *O. inornata* from Tasmania fell within the range seen in *O. zeehanensis* in regard to this proportion. Otherwise, the two species did not overlap. Finally, one characteristic of the cell body clearly differed between *O. inornata* and *O. zeehanensis*. The epistomial disk of *O. zeehanensis* was, on the average, 30% wider than the epistomial disk of *O. inornata* (Figs. 2, 14, 15; Tables 2, 4, 5).

The same type of intracellular parasite that was found in one sample of *O. montanea* was observed in the sample of *O. inornata* from Tasmania (Fig. 13); the percentage of infected individuals (approximately 8%), however, was much lower in the latter. No parasites were seen in the samples of *O. inornata* from Victoria.

Setonophrys Jankowski, 1986

Diagnosis. Solitary, loricate, with lorica aperture bounded by and closable by two opposing lips formed from folds of lorica material. Anterior lip of aperture thick-walled, rigid, usually with one or more spines on edge. Posterior lip thin-walled, flexible, pulled into lorica and pressed against anterior lip to effect closure of aperture. Vallum absent. Loricastome present, consisting of tubular passageway of lorica material that extends into interior of lorica from ventral edges of aperture lips. Edge of peristomial lip of trophont adherent to posterior surface of loricastome. Entire circumference of myonemal band within peristomial lip thickened. Macronucleus elongate, located in approximate centre of body, with same distinctive shape in all species. Medial portion of macronucleus extremely slender, straight or slightly curved, parallel to transverse axis of body or

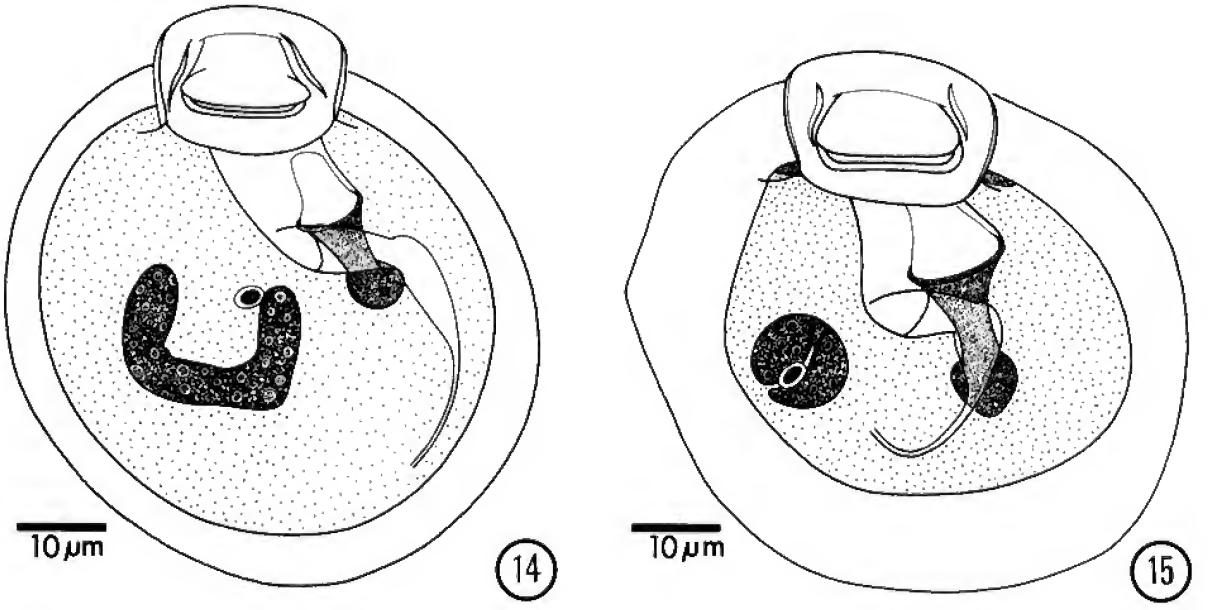

Figs. 14, 15. *Operculigera inornata* n.sp. (*14*) Dorsal view of holotype individual from type locality and host; Delafield's hematoxylin preparation, AM P62816. (*15*) Dorsal view of individual from Great Lake, Tasmania; Heidenhain's hematoxylin preparation, AM P62818.

Table 6. Comparison of species of *Operculigera* hosted by phreatoicid isopods. Information on *O. obstipa* is derived from Clamp (1991).

Operculigera species	shape of lorica	proportions of lorica	presence of curved ridge in dorsal surface of lorica	symmetry of antero-lateral part of vallum	height of anterolateral part of vallum	shape of anterolateral part of vallum	processes on antero-lateral part of vallum	host(s)
O. montanea	asymmetrical	shorter than wide	yes	uniform in height	short	posterior edges sloping abruptly; "squared-off" shape	none	*Colubotelson joyneri*, *Colubotelson* sp.
O. zeehanensis	asymmetrical	shorter than wide	no	uniform in height	moderately tall	posterior edges sloping gradually; "rounded" shape	none	*Phreatoicoides longicollis*
O. haswelli	symmetrical	shorter than wide	no	uniform in height	moderately tall	posterior edges sloping abruptly and flared outward	laterally projecting spine on left margin	*Mesacanthotelson tasmaniae*
O. inornata	asymmetrical	subcircular to longer than wide	no	uniform in height	moderately tall	posterior edges sloping abruptly; "squared-off" shape	none	*Phreatoicopsis terricola*, *Colubotelson chiltoni*
O. obstipa	asymmetrical	shorter than wide	no	sloping from right to left	short	posterior edges sloping abruptly; "squared-off" shape	none	*Metaphreatoicus australis* (Chilton, 1891)

slanting posteriad from left to right at slight angle to transverse axis. Ends of macronucleus much thicker than medial portion, curved anteriad away from medial portion.

Generic composition. The following species are currently assigned to *Setonophrys*: *S. bispinosa* (Kane, 1965); *S. communis* (Kane, 1965); *S. lingulata* (Kane, 1965); *S. nivalis* (Kane, 1969); *S. occlusa* (Kane, 1965); *S. seticola* (Kane, 1965); *S. spinosa* (Kane, 1965); *S. tricorniculata* Clamp, 1991.

Setonophrys nivalis (Kane, 1969)

Fig. 16; Table 8

Lagenophrys nivalis Kane, 1969: 369.
Circolagenophrys nivalis.–Jankowski, 1986: 87.
Setonophrys nivalis.–Clamp, 1991: 360.

Redescription. Lorica hemispheroidal, suboval in dorsal view, moderately longer than wide. Lorica symmetrical in dorsal view. Rim of lorica heavily thickened at posterior, diminishing to moderately thickened at anterior. Lips of lorica aperture tall, with vertical sides, creating almost tubular aperture. Short to moderately long spine on each side of anterior lip, originating slightly below edge of anterior lip and projecting almost directly laterad. Anterior lip thick-walled, with straight, symmetrical edge. Posterior lip thin-walled, without spines or other projections, with straight, symmetrical edge.

Macronucleus elongate, cylindroid, located in approximate centre of body. Medial portion of macronucleus slender, straight or slightly curved, usually slanting posteriad from left to right at slight angle to transverse axis of body, infrequently parallel to transverse axis of body. Ends of macronucleus thicker than medial portion; right end always curved sharply anteriad away from medial portion, left end usually curved sharply anteriad away from medial portion but sometimes extending straight out from medial portion. Micronucleus ovoid, located near right end of macronucleus.

Etymology. The specific name (Latin: snowy) refers to the montane habitat of the host.

Table 7. Distributions of values for two proportions of the lorica in *Operculigera zeehanensis* and *Operculigera inornata* n.sp. OZ, *O. zeehanensis* from the type locality; OI-V, *O. inornata* from Victoria (type locality); OI-T, *O. inornata* from Tasmania. Numerals in each column are numbers of individuals with each value. Lack of individuals expressing a particular value is indicated by a dot to enhance visibility of the distributions relative to one another. *L*, length; *W*, width.

lorica L / lorica W value	OZ	OI-V	OI-T	vallum W / lorica W value	OZ	OI-V	OI-T
1.11–1.12	·	2	·	0.41–0.42	·	1	·
1.09–1.10	·	1	·	0.39–0.40	·	·	·
1.07–1.08	·	4	1	0.37–0.38	·	8	3
1.05–1.06	·	11	4	0.35–0.36	·	6	17
1.03–1.04	1	3	3	0.33–0.34	·	3	5
1.01–1.02	·	4	5	0.31–0.32	1	·	·
0.99–1.00	·	·	3	0.29–0.30	6	1	·
0.97–0.98	·	·	2	0.27–0.28	3	·	·
0.95–0.96	3	·	·				
0.93–0.94	1	·	1				
0.91–0.92	·	·	·				
0.89–0.90	3	·	·				
0.87–0.88	2	·	·				
0.85–0.86	1	·	·				

Table 8. Measurements and proportions (expressed as ratios of attributes to one another) of *Setonophrys nivalis* from the type locality and host (n=15).

Attribute	Mean (μm)	S.D. (μm)	C.V. (%)	Range (μm)
Height of lorica	26	±3	10.8	22–30
Length of lorica	94.8	±3.3	3.5	90.3–102.5
Width of lorica	80.8	±3.0	3.8	74.9–86.0
Width of lorica aperture	23.1	±1.4	6.1	20.3–25.1
Width of lorica margin	3.2	±0.7	20.4	2.1–4.6
Width of epistomial disk	15.4	±0.9	5.7	14.1–17.2
Length of micronucleus	5.3	±0.6	11.6	4.5–6.3
Width of micronucleus	3.5	±0.3	9.3	3.0–4.1
Length/width of lorica	1.17	±0.04	3.7	1.09–1.27
Height/width of lorica	0.32	±0.03	10.4	0.27–0.36
Width of lorica aperture/width of lorica	0.29	±0.02	6.2	0.26–0.32
Width of epistomial disk/width of lorica	0.19	±0.01	4.8	0.18–0.21
Length/width of micronucleus	1.54	±0.21	13.5	1.12–1.97

Type material. LECTOTYPE, AUSTRALIA, Victoria, Mt Baw Baw (1850 m elevation); 13 Oct 1963, J.R. Kane; on *Colubotelson searlei* Nicholls, 1944, pereiopods and dorsum. Lectotype slide with lectotype organism marked by inscribed circle (Erlich's hematoxylin), AM P62819. PARALECTOTYPE slides (Erlich's hematoxylin), AM P62820, P62884, P62885, and IPTC USNM 1004292 (the latter comprises 3 slides).

Remarks. Most species of *Setonophrys* have one or more spines on the anterior lip of the lorica aperture; *S. nivalis*, however, is distinct from them in regard to the shape, position, and angle of projection of its two spines. Spines tend to be long, are always located on the anterior or anterolateral parts of the anterior lip, and project anteriad in other species of *Setonophrys* (Kane, 1965; Clamp, 1991). In addition, these spines tend to be wider at their bases, tapering gradually to a sharp tip. By contrast, the spines of *S. nivalis* are relatively short, are located on the lateral parts of the anterior lip, project directly laterad, and are quite slender from their bases to their tips (Fig. 16).

Lagenophrys Stein, 1852

Diagnosis. Solitary, loricate, with lorica aperture bounded by and closable by two opposing lips formed from folds of lorica material. Both lips of lorica aperture thin-walled, flexible, sometimes with thickened edges or processes. Spines never present on anterior lip although edges of one or both lips may be tuberculate or serrate. Lips of aperture

Table 9. Measurements and proportions (expressed as ratios of attributes to one another) of *Lagenophrys turneri* from the type locality and host (n=25). Eighteen of the individuals measured were on the holotype slide; the remainder were on one of the paratype slides.

Attribute	Mean (μm)	S.D. (μm)	C.V. (%)	Range (μm)
Height of lorica	16	±2	10.2	13–18
Length of lorica	56.1	±2.8	5	50.7–62.3
Width of lorica	61.6	±3.6	5.8	53.7–66.6
Width of anterior lip of lorica aperture	18	±0.5	2.7	16.9–18.8
Width of posterior lip of lorica aperture	16	±0.5	3.2	14.9–16.6
Thickness of anterior lip of lorica aperture	3	±0.2	7.6	2.6–3.4
Thickness of posterior lip of lorica aperture	2.1	±0.1	6.8	1.7–2.3
Width of lorica margin	3.9	±0.4	9	2.7–4.4
Width of epistomial disk	15	±0.6	4.3	13.8–15.8
Length of macronucleus	29.1	±4.9	16.9	17.3–36.1
Width of macronucleus at midpoint	5.5	±1.0	18.1	3.6–7.3
Length of micronucleus	4.3	±0.3	7.4	3.7–4.9
Width of micronucleus	3	±0.2	6.9	2.7–3.5
Length/width of lorica	0.91	±0.03	3.3	0.85–0.97
Height/width of lorica	0.26	±0.03	11.9	0.20–0.32
Width of anterior lip of lorica aperture/ width of lorica	0.3	±0.02	5.6	0.27–0.34
Width of anterior lip of lorica aperture/ width of posterior lip of lorica aperture	1.14	±0.03	2.4	1.09–1.20
Thickness of anterior lip of lorica aperture/ thickness of posterior lip of lorica aperture	1.41	±0.13	8.9	1.23–1.62
Width of epistomial disk/width of lorica	0.24	±0.02	6.6	0.22–0.28
Length/width of macronucleus	5.29	±1.51	28.6	2.10–9.84
Length/width of micronucleus	1.41	±0.12	8.8	1.14–1.59

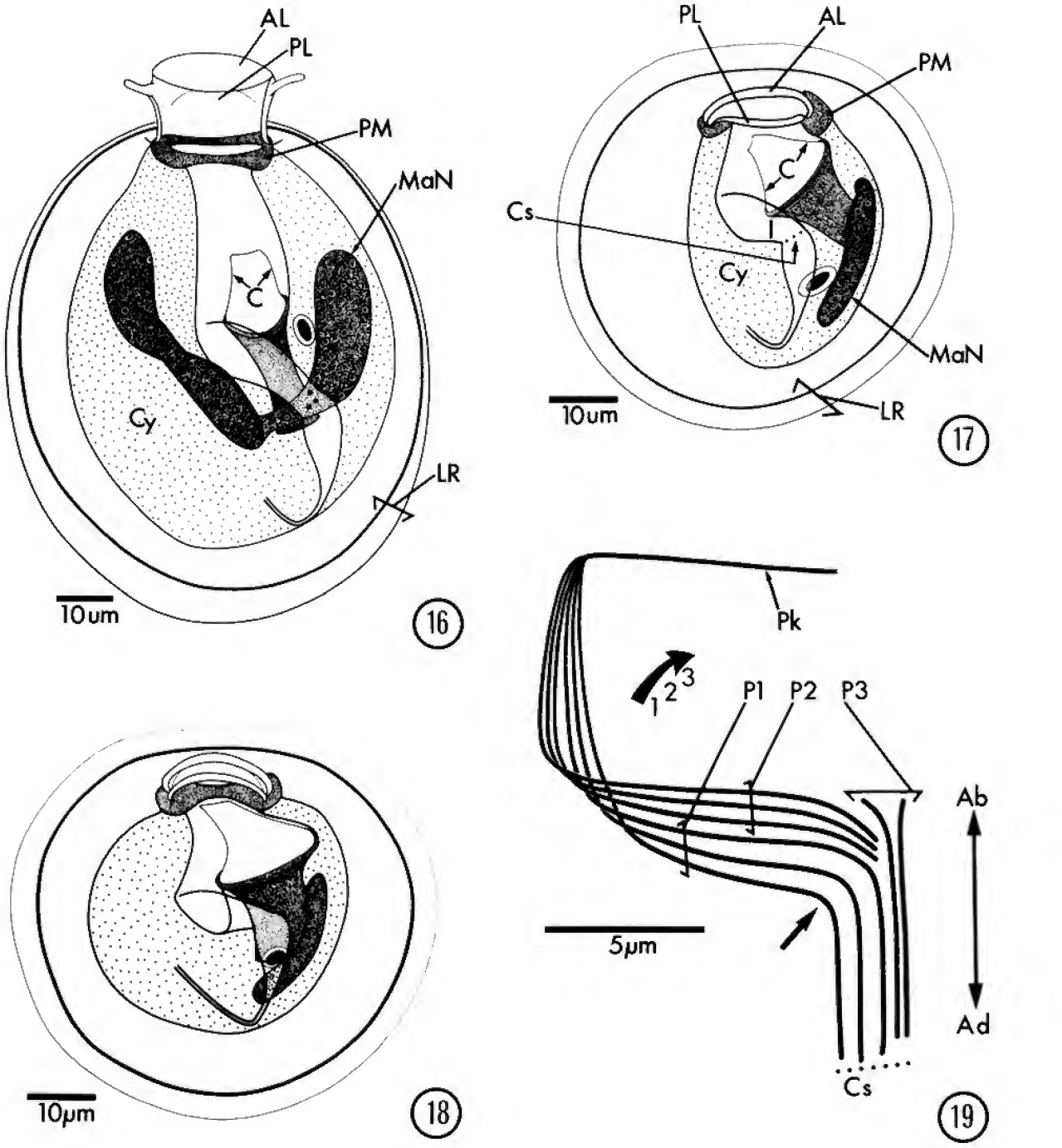

Figs. 16–19. (16) *Setonophrys nivalis*, Erlich's hematoxylin preparation. Dorsal view of lectotype individual from the type locality and host, AM P62819. (*AL*) Anterior lip of lorica aperture; (*PL*) posterior lip of lorica aperture; see Fig. 1 for explanation of other symbols. The micronucleus is the small, ovoid, darkly stained body located near the right end of the macronucleus. (17–19) *Lagenophrys turneri*. (17) Dorsal view of lectotype individual from the type locality and host; Erlich's hematoxylin preparation, AM P62821. The lorica aperture is partially open. (*Cs*) Boundary between infundibulum and cytostome (= ampulla); see Figs. 1, 16 for explanation of other symbols. The micronucleus is the small, ovoid, darkly stained body located near the posterior end of the macronucleus. (18) Dorsal view of individual from Papua New Guinea; Heidenhain's hematoxylin preparation, AM P62822. The lorica aperture is almost closed. (19) Dorsal view of infundibular polykinetids of individual from Papua New Guinea; protargol preparation, AM P62886. The polykinetids are rows of kinetosomes and associated cilia (not shown) that are located on the wall of the infundibulum (Figs. 17, 21, 22). The rows of kinetosomes that constitute the polykinetidal infraciliature normally visible under the light microscope are shown as solid lines for the sake of convenience and clarity. (*Ab*) abstomal direction (= away from the cytostomal region); (*Ad*) adstomal direction (= toward the cytostomal region); (*P1*) polykinetid 1; (*P2*) polykinetid 2; (*P3*) polykinetid 3; (*Pk*) polykinety (the part of P1 that extends out onto the peristomial lip—only the part proximal to the infundibulum is shown); *arrow with numerals* shows the convention for numbering individual rows within each polykinetid; *large arrow*, adstomal curvature of P1.

drawn together equally to effect closure of aperture, with neither one losing its shape in doing so. Vallum absent. Loricastome present; edge of peristomial lip of trophont adherent to posterior surface of loricastome. Posterior half of myonemal band within peristomial lip thickened. Shape and location of macronucleus differs among species.

Generic Composition. The following species are currently assigned to *Lagenophrys*: *L. aegleae* Mouchet-Bennati, 1932; *L. ampulla* Stein, 1852; *L. andos* (Jankowski, 1986); *Lagenophrys anisogammari* (Jankowski, 1993) **n.comb.**; *L. anticthos* Clamp, 1988c; *L. aselli* Plate, 1889; *L. awerinzewi* Abonyi, 1928; *L. bipartita* Stokes, 1890; *L. branchiarum* Nie & Ho, 1943; *L. callinectes* Couch, 1967; *L. cochinensis* Santhakumari & Gopalan, 1980; *L. commensalis* Swarczewsky, 1930; *L. crutchfieldi* Clamp, 1993; *L. darwini* Kane, 1965; *L. dennisi* Clamp, 1987; *L. deserti* Kane, 1965; *L. diogenes* (Jankowski, 1986); *L. discoidea* Kellicott, 1887; *L. dungogi* Kane, 1965; *L. engaei* Kane, 1965; *L. eupagurus* Kellicott, 1893; *L. foxi* Clamp, 1987; *Lagenophrys hokkaidos* (Jankowski, 1993) **n.comb.**; *L. inflata* Swarczewsky, 1930; *L. jacobi* (Kane, 1969); *L. johnsoni* Clamp, 1990b; *L. labiata* Stokes, 1887; *L. leniusculus* (Jankowski, 1986); *L. lenticula* (Kellicott, 1885); *L. limnoria* Clamp, 1988a; *L. machaerigera* Clamp, 1992; *L. macrostoma* Swarczewsky, 1930; *L. matthesi* Schödel, 1983; *Lagenophrys maxillaris* (Jankowski, 1993) **n.comb.**; *L. metopauliadis* Corliss & Brough, 1965; *L. missouriensis* Clamp, 1987; *L. monolistrae* Stammer, 1935; *L. nassa* Stein, 1852; *L. novazealandae* Clamp, 1994; *L. oblonga* Swarczewsky, 1930; *L. orchestiae* Abonyi, 1928; *L. ornata* Swarczewsky, 1930; *L. ovalis* Swarczewsky, 1930; *L. parva* Swarczewsky, 1930; *L. patina* Stokes, 1887; *L. petila* Clamp, 1994; *L. platei* Wallengren, 1900; *L. pontocaspica* Boshko, 1995; *L. reflexa* Kane, 1969; *L. rugosa* Kane, 1965; *L. shiftus* (Jankowski, 1986); *L. similis* Swarczewsky, 1930; *L. simplex* Swarczewsky, 1930; *L. solida* Swarczewsky, 1930; *L. stammeri* Lust, 1950; *L. stokesi* Swarczewsky, 1930; *L. stygia* Clamp, 1990a; *L. tattersalli* Willis, 1942; *L. turneri* Kane, 1969; *L. vaginicola* Stein, 1852; *L. verecunda* Felgenhauer, 1982; *L. willisi* Kane, 1965.

Note on the nomenclature of the genus *Lagenophrys*. Jankowski (1980) created the genus *Circolagenophrys* for the many species of *Lagenophrys* that have a more or less circular outline in dorsal view and reserved the genus *Lagenophrys* for its type species, *L. vaginicola* Stein, 1852, which has a narrow lorica that is adapted for attachment to setae of its host. Clamp (1991) considered this difference in shape of the lorica insufficient to justify this generic separation, citing ample evidence to support of his position, and made *Circolagenophrys* a subjective junior synonym of *Lagenophrys*. Despite this, Jankowski (1993) has continued to use *Circolagenophrys*. We find no reason to resurrect *Circolagenophrys*, in the absence of any evidence contradicting Clamp (1991), and will, therefore, continue to include *L. turneri* in *Lagenophrys* as defined originally by Stein (1852) and redefined by Clamp (1991). Three new species of *Lagenophrys* placed in *Circolagenophrys* by Jankowski (1993) have been treated as new combinations in the listing of species given above.

Lagenophrys turneri Kane, 1969

Figs. 17–22; Tables 9, 10

Lagenophrys turneri Kane, 1969: 369.–Clamp, 1991: 358.
Circolagenophrys turneri.–Jankowski, 1986: 87.

Redescription. Lorica hemispheroidal, suboval to subcircular; if suboval, slightly to moderately wider than long. Rim of lorica very broad. Inner part of lorica rim slightly to moderately thickened; rim diminishing in thickness progressively to extremely thin edge. Lips of lorica aperture short, moderately arched; anterior lip slightly wider than posterior lip. Edges of both lips heavily thickened, smooth, without projections or indentations. Edge of anterior lip usually slightly to moderately thicker than edge of posterior lip. Anterior lip without crochets.

Trochal band of kinetosomes broken on right side in trophont; ends of break separated by wide gap. Infraciliature of infundibular polykinetids as follows: kinetosome rows of infundibular polykinetid 1 (P1) approximately equal in length, ending at cytostome; kinetosome rows of P2 equal in length, ending at abstomal curvature of P1. P2 not separated from P1 by wide gap; distance between row 3 of P1 and row 1 of P2 approximately equal to distances between rows within both polykinetids. P3 consisting of two kinetosome rows of approximately equal length. Rows of P3 slightly divergent at abstomal ends, closely parallel for remainder of length. P3 extending abstomally to point slightly beyond adstomal end of P2, ending adstomally at point slightly short of adstomal end of P1 and cytostome.

Macronucleus elongate, cylindroid, slightly curved, located along right edge of body, conforming to curve of edge of body. Micronucleus ovoid, located more often near centre of macronucleus than near either end of macronucleus.

Etymology. The species is named in honour of Mr J. Turner, who provided specimens of the host from the type locality.

Type material. LECTOTYPE, AUSTRALIA, Northern Territory, Katherine, Katherine R; 13 Sep 1963, J. Turner; on *Macrobrachium rosenbergi* (de Man), gill lamellae. Lectotype slide with lectotype organism marked by inscribed circle (Erlich's hematoxylin), AM P62821. PARALECTOTYPE slide (Erlich's hematoxylin), IPTC USNM 1004293.

Other material examined. PAPUA NEW GUINEA, Gulf District, near Malalaua, Lake Kamu R.; May 1972, L.B. Holthuis; on *M. rosenbergi*, gill lamellae (NMNH-CC USNM 141316). Voucher slides, (Heidenhain's hematoxylin, protargol) AM P62822, P62886 and (Heidenhain's hematoxylin) IPTC USNM 1004294. Additional slides of this material remain in the senior author's personal collection.

Remarks. The infundibular infraciliature of *L. turneri* (Figs. 19, 22) is essentially identical to that of *L. eupagurus* Kellicott, 1893 and *L. callinectes* Couch, 1967 (Couch, 1973; Clamp, 1989). All three species also share the unusual characteristic of having the trochal band of kinetosomes broken on the right side in the trophont, leaving a wide gap (Couch, 1967, 1973; Clamp, 1989). The trochal band is a continuous ring of kinetosomes in trophonts of other species of *Lagenophrys* that have been stained with protargol (Clamp, 1987, 1988a,b, 1990a,b, 1992, 1994), as is typical in peritrichs. In addition, the shape and position of the macronucleus (Figs. 17, 18, 21) in *L. turneri* is the same as in *L. eupagurus* and *L. callinectes*.

Table 10. Measurements and proportions (expressed as ratios of attributes to one another) of *Lagenophrys turneri* from Papua New Guinea (n=25).

Attribute	Mean (μm)	S.D. (μm)	C.V. (%)	Range (μm)
Height of lorica	17	±2	12.1	13–21
Length of lorica	58.6	±1.7	2.9	55.5–62.3
Width of lorica	61.9	±2.2	3.6	56.6–66.3
Width of anterior lip of lorica aperture	16.1	±0.4	2.8	15.2–17.0
Width of posterior lip of lorica aperture	14.9	±0.5	3.4	13.6–15.6
Thickness of anterior lip of lorica aperture	1.6	±0.1	9.1	1.4–1.9
Thickness of posterior lip of lorica aperture	1.3	±0.1	11.1	1.1–1.6
Width of lorica margin	3.5	±0.5	14.3	2.4–4.7
Width of epistomial disk	15.5	±0.8	5.5	13.8–17.0
Length of macronucleus	24.8	±3.6	14.4	19.4–32.8
Width of macronucleus at midpoint	4	±0.5	12.6	3.2–4.9
Length of micronucleus	3.8	±0.4	9.7	3.1–4.5
Width of micronucleus	2.2	±0.1	6	2.0–2.5
Length/width of lorica	0.95	±0.02	1.9	0.92–0.98
Height/width of lorica	0.28	±0.03	12.3	0.21–0.34
Width of anterior lip of lorica aperture/width of lorica	0.26	±0.01	3.1	0.25–0.28
Width of anterior lip of lorica aperture/ width of posterior lip of lorica aperture	1.09	±0.02	2.2	1.04–1.14
Thickness of anterior lip of lorica aperture/ thickness of posterior lip of lorica aperture	1.23	±0.13	10.5	0.94–1.46
Width of epistomial disk/width of lorica	0.25	±0.02	6.5	0.22–0.30
Length/width of macronucleus	6.14	±0.94	15.3	3.09–7.73
Length/width of micronucleus	1.69	±0.21	112.3	1.32–2.05

The edges of both lips of the lorica aperture are heavily thickened in *L. turneri*, *L. eupagurus*, and *L. callinectes*, but the latter two species have deep clefts in each lip that are lacking in *L. turneri* (Figs. 17, 18, 21; Couch, 1967; Clamp, 1989). The lips of the lorica aperture of *L. turneri* resemble those of *L. callinectes* more than those of *L. eupagurus* in having the anterior lip significantly thicker than the posterior lip (Fig. 18; Tables 9, 10; Clamp, 1989). The differences in the morphology of the lorica aperture confirm the distinctness of *L. turneri* as a species while the several apparent synapomorphies that it shares with *L. eupagurus* and *L. callinectes* suggest that the three species may share a close phylogenetic relationship within the genus. Their restriction to decapod crustaceans as hosts reinforces this hypothesis.

Discussion

Operculigera has a far-flung distribution in the Southern Hemisphere, occurring exclusively on freshwater hosts in Australia, Chile, and Madagascar (Kane, 1969; Jankowski, 1986; Clamp, 1991, 1992). The Australian species of *Operculigera* constitute a group that is ecologically distinct from those in other areas. In Chile, all of the several known species of *Operculigera* occur on parastacid crayfishes and aeglid crabs (Jankowski, 1986; Clamp, 1991). The two species of *Operculigera* described from Madagascar also live on decapods, one on a parastacid crayfish and another on a potamoid crab (Clamp, 1992). In striking contrast to this, all species of *Operculigera* discovered in Australia so far have been found on phreatoicid isopods, with the single exception of an undescribed species on the amphipod *Austrochiltonia* (Kane, 1969; Clamp, 1991; Clamp, unpublished observations).

Observer bias cannot be the source of this disparity since, between them, the authors have examined many species of Australian parastacids and other freshwater decapods, such as shrimps and crabs, without finding a single species of *Operculigera* on any of them. Australian parastacids host a rich, diverse fauna of lagenophryid peritrichs, including many species of *Lagenophrys* and *Setonophrys* (Kane, 1964, 1965; Clamp, 1991), but *Operculigera* seems to be genuinely absent from them. By contrast, five species of *Operculigera* have been discovered on a mere handful of the many species of Australian phreatoicids, suggesting that a significant number of undescribed species of *Operculigera* may remain to be found on others.

Aside from their unusual lack of distribution on decapods, Australian species of *Operculigera* appear to form a group that is morphologically distinct from other members of the genus. Species of *Operculigera* reported from Madagascar and Chile fall into two general groups: (1) those with no vallum (*O. carcini*) or a greatly reduced vallum (*O. striata*) and (2) those with a well-developed vallum (*O. asymmetrica, O. insolita, O. madagascarensis, O. parastacis, O. seticola, O. taura, O. velata*) that usually has one or more spines or other kinds of prominent processes on the anterior part (Jankowski, 1986; Clamp, 1991, 1992). Most species in the latter group also show at least partial development of the posterior part of the vallum (see *O. parastacis* in Jankowski, 1986 and *O. insolita* in Clamp, 1991). Species of *Operculigera* on Australian phreatoicids differ from those in both of these groups by having the anterior part of their vallum well developed but, excepting the spinose morphs of *O. haswelli*, with no spines or other processes. Unlike species in the second group, all of the Australian species of *Operculigera* have the posterior half of the vallum reduced to a slight ridge of lorica material at most.

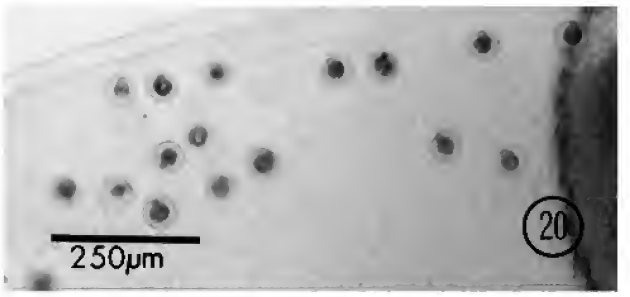

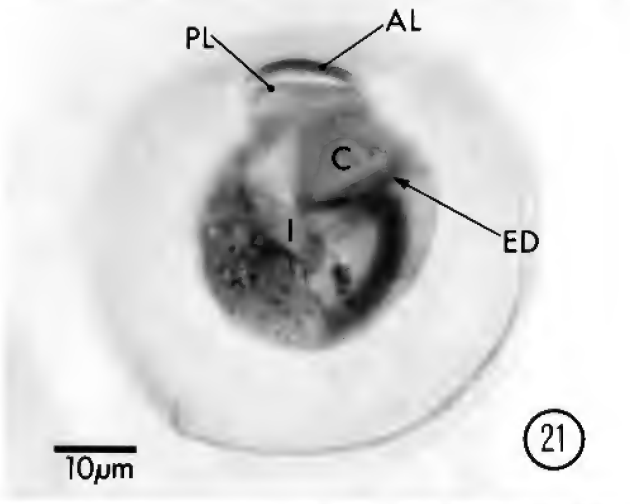

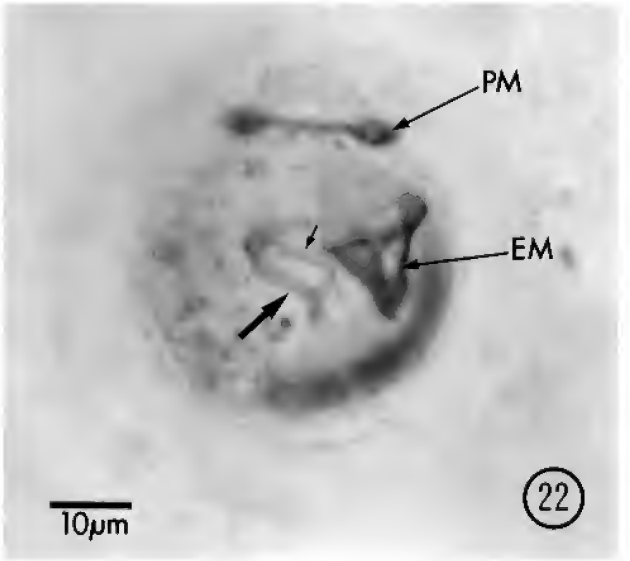

Figs. 20–22. *Lagenophrys turneri* from Papua New Guinea. (20) Infested gill lamella of host at low magnification; Heidenhain's hematoxylin preparation. (21) Dorsal view of single individual; Heidenhain's hematoxylin preparation. See Figs. 1, 16 for explanation of symbols. (22) Dorsal view of single individual; protargol preparation. Large arrow, infundibular polykinetids; small arrow, haplokinety—the haplokinety is a band of dikinetids that extends into the infundibulum from the peristome, where it is the outer band of kinetosomes. It does not vary among sessiline peritrichs and is routinely omitted from views such as Fig. 19 for that reason. See Fig. 1 for explanation of symbols.

ACKNOWLEDGMENTS. Thanks are extended to Dr George Wilson of the Australian Museum for his help in obtaining material of *Colubotelson joyneri* and for his advice concerning taxonomy of phreatoicids and nomenclatural issues. In addition, we are grateful to the Division of Crustacea, National Museum of Natural History, Smithsonian Institution for access to their collection.

References

Boshko, E.G., 1995. New species of infusoria of the genera *Sincothurnia* and *Lagenophrys* (Peritricha, Vaginicolidae, Lagenophryidae). *Zoologicheskii Zhurnal* 74: 5–9.

Bütschli, O., 1887–1889. Protozoa. Abt. III. Infusoria und System der Radiolaria. In *Klassen und Ordnung des Thiers-Reichs, Vol. 1*, ed. H.G. Bronn, pp. 1098–2035. Leipzig, Germany: C.F. Winter.

Clamp, J.C., 1973. Observations on the host-symbiont relationships of *Lagenophrys lunatus* Imamura. *Journal of Protozoology* 20: 558–561.

Clamp, J.C., 1987. Five new species of *Lagenophrys* (Ciliophora, Peritricha, Lagenophryidae) from the United States with observations on their developmental stages. *Journal of Protozoology* 34: 382–392.

Clamp, J.C., 1988a. A new species of *Lagenophrys* (Ciliophora: Peritricha: Lagenophryidae) ectocommensal on the wood-boring isopod *Limnoria* (Flabellifera: Limnoridae). *Transactions of the American Microscopical Society* 107: 12–16.

Clamp, J.C., 1988b. The occurrence of *Lagenophrys aselli* (Ciliophora: Peritricha: Lagenophryidae) in North America and a description of environmentally-induced morphological variation in the species. *Transactions of the American Microscopical Society* 107: 17–27.

Clamp, J.C., 1988c. *Lagenophrys anticthos* n.sp. and *L. aegleae* Mouchet-Bennati, 1932 (Ciliophoral, Peritricha, Lagenophryidae), ectocommensals of South American crustaceans. *Journal of Protozoology* 35: 164–169.

Clamp, J.C., 1989. Redescription of *Lagenophrys eupagurus* Kellicott (Ciliophora, Peritricha, Lagenophryidae) and a comparison of it with three similar species. *Journal of Protozoology* 36: 596–607.

Clamp, J.C., 1990a. Redescription of three species of *Lagenophrys* (Ciliophora: Peritricha: Lagenophryidae) and a new North American species of *Lagenophrys* from hypogean amphipods. *Transactions of the American Microscopical Society* 109: 1–31.

Clamp, J.C., 1990b. A new species of *Lagenophrys* (Ciliophora: Peritricha: Lagenophryidae) ectocommensal on North American species of *Gammarus* (Crustacea: Amphipoda). *Transactions of the American Microscopical Society* 109: 121–128.

Clamp, J.C., 1991. Revision of the family Lagenophryidae Bütschli, 1889 and description of the family Usconophryidae n. fam. (Ciliophora, Peritricha). *Journal of Protozoology* 38: 355–377.

Clamp, J.C., 1992. Three new species of lagenophryid peritrichs (Ciliophora) ectocommensal on freshwater decapod crustaceans from Madagascar. *Journal of Protozoology* 39: 732–740.

Clamp, J.C., 1993. A new species of *Lagenophrys* (Ciliophora: Peritricha: Lagenophryidae) from marine amphipods. *Transactions of the American Microscopical Society* 112: 62–68.

Clamp, J.C., 1994. New species of *Lagenophrys* (Ciliophora, Peritrichia) from New Zealand and Australia. *Journal of Eukaryotic Microbiology* 41: 343–349.

Couch, J.A., 1967. A new species of *Lagenophrys* (Ciliatea: Peritrichida: Lagenophryidae) from a marine crab, Callinectes sapidus. *Transactions of the American Microscopical Society* 86: 204–211.

Couch, J.A., 1973. Ultrastructural and protargol studies of *Lagenophrys callinectes* (Ciliophora: Peritrichida). *Journal of Protozoology* 20: 638–647.

Fenchel, T., 1965. On the ciliate fauna associated with the marine species of the amphipod genus *Gammarus* J.C. Fabricius. *Ophelia* 2: 281–303.

ICZN, 1999. International Code of Zoological Nomenclature, Fourth Edition. International Trust for Zoological Nomenclature, London.

Jankowski, A.W., 1980. Conspectus of a new system of the Phylum Ciliophora. In *Principles of Construction of the Macrosystem of the Unicellular Animals*, ed. M.V. Krylov & Y.I. Starobogatov, pp. 102–121. Trudy Zoologicheskogo Instituta Akademii Nauk SSSR 94.

Jankowski, A.W., 1986. New and little known genera of ciliated protozoa (Phylum Ciliophora). In *Systematics of Protozoa and Their Phylogenetic Links with Lower Eukaryotes*, ed. M.V. Krylov, pp. 72–88. Trudy Zoologicheskogo Instituta Akademii Nauk SSSR 144.

Jankowski, A.W., 1993. Taxonomy of Ciliophora. 2. New species of *Opercularia, Entziella* and *Circolagenophrys* from the Black Sea and Pacific, and taxonomic notes on other peritrichs (Peritricha). *Zoosystematica Rossica* 2: 217–222.

Kahl, A., 1935. Urtiere oder Protozoa I: Wimpertiere oder Ciliata (Infusoria). Literaturverzeichnis. In *Die Tierwelt Deutschlands*, ed. F. Dahl, pp. 843–864. Jena, Germany: Fischer.

Kane, J.R., 1964. *Australian Freshwater Malacostraca and Their Epizoic Fauna*. MSc Thesis, University of Melbourne.

Kane, J.R., 1965. The genus *Lagenophrys* Stein, 1852 (Ciliata, Peritricha) on Australasian Parastacidae. *Journal of Protozoology* 12: 109–122.

Kane, J.R., 1969. The Lagenophryidae in Australia and South Africa. In *Progress in Protozoology*, pp. 368–369. Abstracts of papers presented at the third International Congress of Protozoology, Leningrad, July, 1969.

Lynch, J.E., & A.E. Noble, 1931. Notes on the genus *Endosphaera* Engelmann and on its occasional host *Opisthonecta henneguyi* Fauré-Fremiet. *University of California Publications in Zoology* 36: 97–114.

Matthes, D., 1971. Parasitische Suktorien. *Zoologischer Anzeiger* 186: 272–291.

Nicholls, G.E., 1943. The Phreatoicoidea. Part I. The Amphisopidae. *Papers and Proceedings of the Royal Society of Tasmania* 1942: 1–145.

Nicholls, G.E., 1944. The Phreatoicoidea. Part II. The Phreatoicidae. *Papers and Proceedings of the Royal Society of Tasmania* 1943: 1–157.

Stammer, H.-J., 1935. Zwei neue troglobionte Protozoen: *Spelaeophrya troglocaridis* n.g., n.sp. von den Antennen der Höhlengarnele *Troglocaris schmidti* Dorm. und *Lagenophrys monolistrae* n.sp. von den Kiemen (Pleopoden) der Höhlenasselgattung *Monolistra*. *Archiv für Protistenkunde* 84: 518–527.

Stein, F., 1852. Neue Beitrage zur Kenntnis der Entwicklungsgeschichte und des feineren Baues der Infusionsthiere. *Zeitschrift wissenshaftliche Zoologie* 3: 475–509.

Stokes, A.C., 1890. Notices of new fresh-water infusoria. *Proceedings of the American Philosophical Society* 28: 74–80.

Wicklow, B.J., & B.F. Hill, 1992. A short procedure for protargol staining. In *Protocols in Protozoology*, ed. J.J. Lee & A.T. Soldo, pp. C-5.1–C-5.3. Lawrence, Kansas: The Society of Protozoologists.

Manuscript received 21 November 2001, revised 14 November 2002 and accepted 20 November 2002.

Associate Editor: G.D.F. Wilson.

Records of the Australian Museum (2003) Vol. 55: 169–220. ISSN 0067-1975

Early Ordovician Conodonts from Far Western New South Wales, Australia

YONG-YI ZHEN[1]*, IAN G. PERCIVAL[2] AND BARRY D. WEBBY[3]

[1] Division of Earth & Environmental Sciences,
Australian Museum, 6 College Street, Sydney NSW 2010, Australia
yongyi@austmus.gov.au

[2] Specialist Services Section, Geological Survey of New South Wales,
PO Box 76, Lidcombe NSW 2141, Australia
percivai@minerals.nsw.gov.au

[3] Centre for Ecostratigraphy & Palaeobiology,
Department of Earth & Planetary Sciences, Macquarie University NSW 2109, Australia
bwebby@laurel.ocs.mq.edu.au

ABSTRACT. Thirty species (representing 19 genera) of Early Ordovician conodonts are described and illustrated from Mount Arrowsmith and Koonenberry Gap in the northwestern part of New South Wales. One new genus, *Cooperignathus*, and the new species *Oepikodus pincallyensis*, are established. *Acodus* sp. cf. *emanuelensis* predominates in 35 samples from the Tabita Formation and upper beds of the underlying Yandaminta Quartzite at Mount Arrowsmith, associated with ramiform and pectiniform taxa including species of *Cooperignathus, Prioniodus, Oepikodus, Erraticodon, and Baltoniodus*. The Koonenberry Gap fauna is dominated by coniform species, particularly *Protopanderodus nogamii, P. gradatus*, and *Scolopodus multicostatus*. Both faunas span an age range from latest Bendigonian to Chewtonian (*evae* Zone); their compositional differences are probably related to slight variations in water depths and depositional environments. Species endemic to the shallow water Australian cratonic region, represented by *Bergstroemognathus kirki, Triangulodus larapintinensis, Acodus* sp. cf. *emanuelensis* and *Prioniodus* sp. cf. *amadeus*, support a correlation with Early Ordovician faunas of central and western Australia, particularly those from the lower Horn Valley Siltstone of the Amadeus Basin. Biogeographically significant species in the western New South Wales faunas include *Cooperignathus nyinti, C. aranda* and *Scolopodus multicostatus*, which provide linkages with counterparts in North America and South China. Cosmopolitan elements in the documented collections are represented by *Cornuodus longibasis, Drepanoistodus basiovalis*, and *Scolopodus quadratus*. Only one species, *Scalpellodus latus*, from Mount Arrowsmith appears to be otherwise confined to Baltoscandia (northern Europe).

ZHEN, YONG-YI, IAN G. PERCIVAL & BARRY D. WEBBY, 2003. Early Ordovician conodonts from far western New South Wales, Australia. *Records of the Australian Museum* 55(2): 169–220.

* author for correspondence

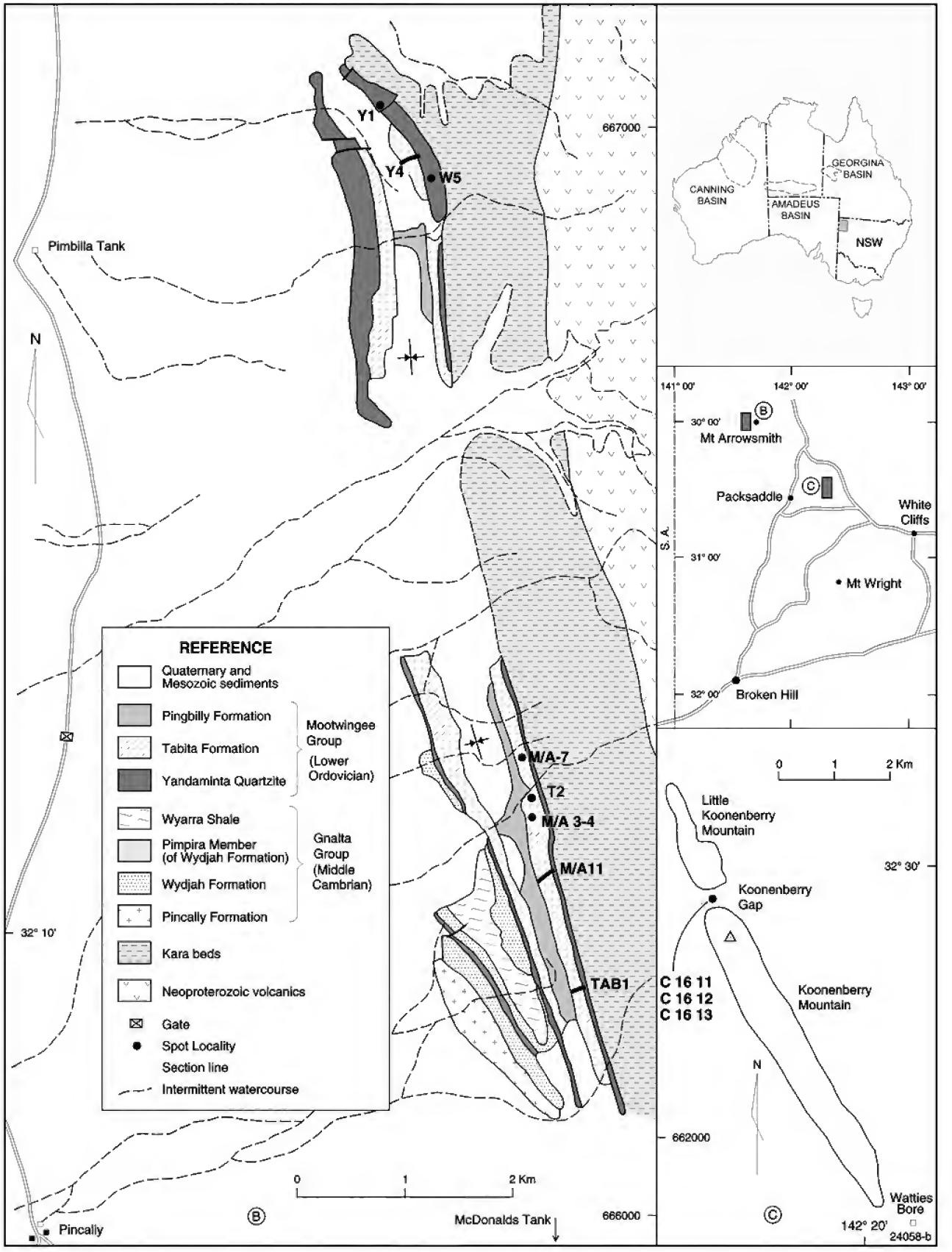

Fig. 1. Localities and geological maps of the studied areas. Maps of Australia and New South Wales, showing location of Mount Arrowsmith (*B*) and Koonenberry Range (*C*) areas to the north of Broken Hill. *B*, geological map of the Mount Arrowsmith area (modified after unpublished mapping by B. Stevens and K.J. Mills, Geological Survey of NSW Broken Hill office), showing locations of conodont samples collected from the Yandaminta Quartzite and Tabita Formation, Australian Map Grid coordinates from Mount Arrowsmith 7237 orthophotomap (first edition, 1978). *C*, map of the Koonenberry Gap area showing locations of samples collected for conodonts, Australian Map Grid coordinates from Wonnaminta 7336 orthophotomap (first edition, 1978).

Introduction

Geological setting and previous investigations

Conodont elements, the tooth-like remains of a long-extinct group of marine animals apparently with chordate affinities, are abundant microfossils in many Palaeozoic rocks (Sweet, 1988). Their global distribution and often-restricted time ranges make them ideal for biostratigraphic and biogeographic studies. During the Early Ordovician Epoch conodonts ranged widely in shallow seas across the Australian craton. Conodont faunas of this time from the edge of the craton, exposed in far western New South Wales, are here systematically described, enabling precise correlation with regional and international successions.

The cratonic rocks form part of the Upper Proterozoic–Middle Palaeozoic Koonenberry Belt (previously called the Wonominta Block, *sensu* Mills 1992), which trends southeast from near Tiboburra to between Broken Hill and White Cliffs, in the northwestern part of New South Wales (Fig. 1). In this region of mostly poor outcrop and low relief, Koonenberry Belt sediments are generally inconspicuous or largely buried beneath younger regolith. Mount Arrowsmith, situated at the northwestern extremity of this belt, is a prominent exception, being mainly composed of Proterozoic alkaline volcanic rocks—the Mount Arrowsmith Volcanics, including basaltic pillow lavas and tuffs—interposed between an eastern and western belt of metasediments (Kara Beds of Mills, 1992), also of probable late Neoproterozoic age.

Wopfner (1967) first described the Middle Cambrian and Lower Ordovician sediments on the western side of Mount Arrowsmith. Wopfner's mapping has remained the most detailed published documentation of the outcrop of these Palaeozoic units, although his informal stratigraphic nomenclature has been updated. The Middle Cambrian strata, preserved only on the southwest flank of Mount Arrowsmith, are now included within the Gnalta Group, while the Lower Ordovician sediments (which are well exposed in a syncline west of the Mount Arrowsmith summit) are correlated with the Mootwingee Group. Shergold (1971) and Webby *et al.* (1981) substituted stratigraphic names introduced in unpublished Ph.D. research by Warris (1967) to formalize the stratigraphic subdivisions introduced by Wopfner (1967). The Cambrian section is faulted against the Lower Ordovician Yandaminta Quartzite (member E of Wopfner), which is overlain by the Tabita Formation (member F) (Fig. 2) and in turn conformably succeeded by the Pingbilly Formation (Wopfner's member G). The exact nature of the boundary between the Yandaminta Quartzite and the Tabita Formation is open to interpretation; in most places the contact appears to be conformable and intergradational, but in some outcrops there is definite evidence of a subtle angular (perhaps structurally induced) relationship (K.J. Mills and R. Glen, pers. comm.). These Mootwingee Group strata unconformably overlie the western belt of the Kara Beds.

Pioneering palaeontological and biostratigraphical studies of the northwestern part of New South Wales were undertaken by Warris (1967) but much of this work remains unpublished. A brief outline of the fossil distribution at Mount Arrowsmith was given by Warris (1969), who provided an insight into the abundance and diversity of the Early Ordovician faunas, comprising mainly nautiloids, bivalves, gastropods, brachiopods, trilobites, ostracodes, and conodonts. Only a nautiloid, *Anthoceras warburtoni*, from the Tabita Formation (Crick & Teichert, 1983) and a new species of the problematical genus *Janospira, J. acuosiphon*, from the Yandaminta Quartzite (Paterson, 2001a) of this rich fauna have previously been formally described.

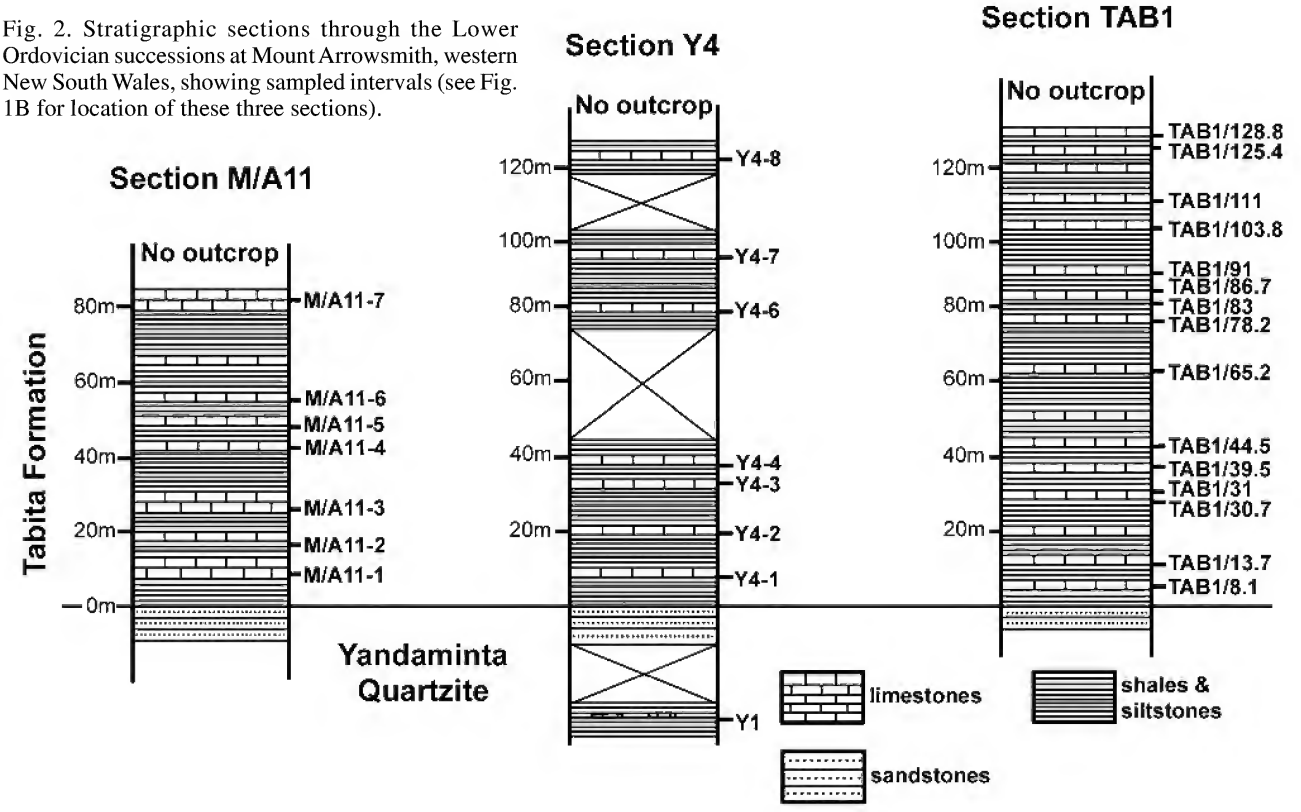

Fig. 2. Stratigraphic sections through the Lower Ordovician successions at Mount Arrowsmith, western New South Wales, showing sampled intervals (see Fig. 1B for location of these three sections).

Conodonts from a single sample (16 specimens) collected from the basal beds of the Tabita Formation were first identified by E.C. Druce (*in* Wopfner, 1967: 168, 170), who established a possible upper "Arenig" age and noted similarities with the conodonts of the Horn Valley Formation in the Amadeus Basin. Independent identifications of the same form genera determined by Druce, together with many additional form taxa, were made by Warris (1967) in a major study of the Mount Arrowsmith conodonts, based on collections of nearly 4500 identifiable specimens obtained from three measured sections in the area. In his published listing of the Mount Arrowsmith fauna, Warris (1969) emphasized forms not found in the solitary sample analysed by Druce and noted the presence of five new species of "fibrous" genera from throughout the Tabita Formation. Warris also recognized three biostratigraphically distinct conodont zones in the formation, the lower two of early "Arenig" age, and the upper one of late "Arenig" age. Jones *et al.* (1971), in a brief reference to the Mount Arrowsmith conodonts, interpreted their age as broadly mid to late "Arenig". Further studies of the Warris conodont collection were undertaken by Kennedy in the 1970s, but the revised systematics employing a combination of apparatus and form species taxonomy remains unpublished (Kennedy, 1976). Repeated requests for the return of the Warris collection to Australia have been ignored, so the original material remains unavailable for study. Accordingly, we have not relied on Kennedy's (1975) listing of 16 taxa from the area, nor have we referred to his now mainly outdated thesis research.

Our study of conodonts from Mount Arrowsmith commenced in 1999 as part of a broader program of research on the Early Ordovician biotas of western New South Wales. Conodont resampling focussed on a number of measured sections and spot localities in the Yandaminta Quartzite and the Tabita Formation (Fig. 2). Recovery of 3076 identifiable elements substantially increases knowledge of the fauna, enabling for the first time an accurate age determination and correlation of the succession with others in Australia and elsewhere in the world.

The Koonenberry Gap area, some 80km to the east of Mount Arrowsmith (Fig. 1), has received much less palaeontological attention. Packham (1969: 68) mentioned limestones at Koonenberry Mountain from which the late Brian Daily (University of Adelaide) had identified a small conodont fauna of late Early Ordovician or early Middle Ordovician age; it is not certain whether this sample was collected from the section exposed at the Gap. The prominence of Koonenberry Mountain above the surrounding flat plains is due to the northwest-southeast trending Koonenberry Fault with uplift delineating the west margin of the mountain, while a subparallel splay of this fault forms its east boundary. Webby *et al.* (1988) described a trilobite fauna of latest Cambrian-basal Ordovician (Tremadocian) age from siltstones of the Watties Bore Formation, adjacent to the faults. Well-bedded dolomitic limestones (stratigraphic unit not yet formalized) at Koonenberry Gap have previously yielded the conodont *Bergstroemognathus kirki* (Zhen *et al.*, 2001). The conodont fauna from Koonenberry Gap (determined from 446 identifiable specimens), like the Mount Arrowsmith assemblages, is of *evae* Zone age (late Bendigonian–Chewtonian), broadly equivalent to the middle "Arenig" or uppermost Ibexian (Webby, 1995, fig. 1).

Early Palaeozoic regional geography

Following the Delamerian Orogeny in Middle–Late Cambrian time (Q.Z. Wang *et al.*, 1989, fig. 3), the Lower Ordovician Mootwingee Group was deposited on the Gnalta Shelf, as part of the east-facing margin of the Australian craton, which represented also the eastern edge of the Gondwanan supercontinent. Webby (1976, 1978, 1983) interpreted quartzose clastic sedimentation, which dominates much of the Mootwingee Group to the south of Koonenberry Mountain, as derived from the Delamerian uplands to the (present) southwest, and deposited in an extensive delta. Broadly contemporaneous impure carbonates in the Tabita Formation at Mount Arrowsmith, and dolomitic limestones at Koonenberry Gap, are the only known remnants preserved of what might have been an extensive shallow shelf depositional setting extending to the northwest (Webby, 1976, fig. 6B; 1983, fig. 1). Environments probably ranged in water depth from strandline to sub wave base, in relatively sheltered situations such as protected bays or very shallow gradient shorelines, inferred from complete preservation of diverse macrofossils in the Tabita Formation. There is no convincing evidence of areas with restricted circulation or enhanced salinity, except that numerical dominance in the Tabita samples of a single species (*Acodus* sp. cf. *emanuelensis*, Fig. 4) may indicate some sort of specialized environment. Any differences in faunal content between localities of essentially the same age are therefore most plausibly related to variation in water depth.

Elsewhere on the Australian craton at this time, the Larapintine Sea provided a shallow marine connection linking the Gnalta Shelf through the Amadeus and Georgina Basins westwards to the Canning Basin (for discussion on the development of this concept refer to Webby, 1978: 55). Contemporaneous conodont faunas in the central Australian basins have been described from the Horn Valley Siltstone of the Amadeus Basin (Cooper, 1981; Nicoll & Ethington, in press; Stewart & Nicoll, in press), and the Coolibah Formation of the Georgina Basin (Stait & Druce, 1993). The known Canning Basin faunas are both slightly older (late Lancefieldian–Bendigonian: McTavish, 1973; Nicoll *et al.*, 1993) and younger (Darriwilian: Watson, 1988) than those from western New South Wales. Compositional differences in conodont faunas from these regions can be interpreted as due in part to water temperature variations, as cooler, more temperate waters entered the Larapintine Sea from the Canning Basin side to mix with warm equatorial currents flowing across the Gnalta Shelf. Local variations in faunal distribution are more likely due to water depth fluctuations, as discussed below.

Conodont ecology and biogeography

Among the 30 species recorded from the Mount Arrowsmith area, 20 (including nearly all those with relatively restricted age ranges) were also found in the Koonenberry Gap samples (Fig. 5), and hence these two assemblages are considered more or less contemporaneous in age. There are, however, some significant differences between their overall faunal composition, diversity, and relative abundance. For example, the fauna from the Tabita Formation at Mount Arrowsmith is the more diverse, including coniform, ramiform and pectiniform elements, while the Koonenberry

Fig. 3. Distribution of conodont taxa and specimens in samples from the upper Yandaminta Quartzite and the overlying Tabita Formation at Mount Arrowsmith, and from the unnamed dolomitic limestone unit at Koonenberry Gap, western New South Wales. Samples from limestone nodules in the upper Yandaminta Quartzite are labelled Y1 and W5; all other samples are from the Tabita Formation, except for C1611–C1613 which are from Koonenberry Gap.

	Y1	W5	Y4-1	Y4-2	Y4-3	Y4-4	Y4-6	Y4-7	Y4-8	M/A11-1	M/A11-2	M/A11-3	M/A11-4	M/A11-5	M/A11-6	M/A11-7	M/A3	M/A4	M/A7	TAB1/8.1	TAB1/13.7	TAB1/30.7	TAB1/31	TAB1/39.5	TAB1/44.5	TAB1/65.2	TAB1/78.2	TAB1/83	TAB1/86.7	TAB1/91	TAB1/103.8	TAB1/111	TAB1/125.4	TAB1/128.8	T2	C1611	C1612	C1613	Total
Acodus sp. cf. *emanuelensis* (total)	–	41	9	245	20	55	224	162	27	12	24	174	5	149	12	4	27	54	92	49	6	1	–	36	3	5	39	–	29	5	3	3	–	–	1	13	4	23	1556
Pa	–	7	2	31	2	8	15	16	1	2	2	18	1	12	1	1	4	10	14	8	1	–	–	6	1	1	2	–	3	–	–	–	–	–	–	2	–	–	171
Pb	–	10	–	51	3	9	52	31	5	2	6	45	1	38	2	2	6	17	12	12	1	1	–	8	1	–	10	–	5	–	–	2	–	–	–	2	–	2	336
M?	–	2	–	6	3	2	16	14	–	–	3	12	1	12	–	–	3	7	1	2	–	–	–	5	–	–	1	–	1	–	–	–	–	–	–	–	–	3	94
M	–	7	–	44	3	10	35	28	7	1	3	25	–	28	2	–	3	2	15	8	1	–	–	6	–	3	8	–	6	2	3	–	–	–	–	1	2	8	261
Sa	–	2	–	28	3	8	25	19	4	3	4	16	2	18	2	–	4	5	14	5	–	–	–	3	–	1	6	–	7	1	–	1	–	–	–	4	1	2	188
Sb	–	3	2	28	2	7	35	22	6	3	2	25	–	16	2	–	2	7	14	4	2	–	–	3	–	–	5	–	3	–	–	–	–	–	1	1	–	1	196
Sc	–	6	1	17	1	3	17	12	–	–	2	6	–	10	1	–	3	4	8	5	–	–	–	3	–	–	–	–	–	2	–	–	–	–	–	–	–	5	106
Sd	–	4	4	40	3	8	29	20	4	1	2	27	–	15	2	1	2	2	14	5	1	–	–	2	1	–	7	–	4	–	–	–	–	–	–	3	1	2	204
Acodus sp. (S elements)	–	–	–	–	–	–	2	1	1	1	–	6	1	–	–	–	–	–	–	1	1	–	–	–	–	–	2	–	–	–	–	–	–	–	–	2	–	–	18
Acodus jemtlandica (total)	–	–	–	–	–	–	–	–	–	–	–	–	–	–	–	–	–	–	4	–	–	–	–	–	–	–	–	–	–	–	–	–	–	–	–	–	1	–	5
Baltoniodus sp. A (total)	–	–	–	2	–	–	–	4	–	–	–	1	2	2	–	–	–	–	2	–	–	–	–	–	–	–	–	–	–	–	–	–	–	–	–	–	–	13
Bergstroemognathus kirki (total)	–	5	–	–	–	4	–	–	–	–	–	20	1	–	–	–	–	–	–	–	–	–	–	–	–	–	1	–	–	–	–	–	–	–	6	1	–	38
Pa	–	–	–	–	–	1	–	–	–	–	–	3	–	–	–	–	–	–	–	–	–	–	–	–	–	–	–	–	–	–	–	–	–	–	–	–	–	4
Pb	–	–	–	–	–	–	–	–	–	–	–	6	–	–	–	–	–	–	–	–	–	–	–	–	–	–	–	–	–	–	–	–	–	–	2	–	–	8
M	–	1	–	–	–	–	–	–	–	–	–	–	–	–	–	–	–	–	–	–	–	–	–	–	–	–	–	–	–	–	–	–	–	–	–	–	–	1
Sa	–	–	–	–	–	2	–	–	–	–	–	2	–	–	–	–	–	–	–	–	–	–	–	–	–	–	1	–	–	–	–	–	–	–	3	–	–	7
Sb	–	–	–	–	–	1	–	–	–	–	–	6	–	–	–	–	–	–	–	–	–	–	–	–	–	–	–	–	–	–	–	–	–	–	–	1	–	9
Sc	–	4	–	–	–	–	–	–	–	–	–	3	–	–	–	–	–	–	–	–	–	–	–	–	–	–	–	–	–	–	–	–	–	–	1	–	–	8
Sd	–	–	–	–	–	–	–	–	–	–	–	–	1	–	–	–	–	–	–	–	–	–	–	–	–	–	–	–	–	–	–	–	–	–	–	–	–	1
Cooperignathus nyinti (total)	–	6	–	2	–	–	–	1	–	1	–	1	–	–	–	–	–	–	48	1	–	–	–	2	–	5	–	–	1	–	–	–	–	–	–	1	–	69
Pa	–	–	–	–	–	–	–	–	–	–	–	–	–	–	–	–	–	–	6	–	–	–	–	–	–	–	–	–	–	–	–	–	–	–	–	–	–	6
Pb	–	–	–	1	–	–	–	–	–	–	–	–	–	–	–	–	–	–	6	–	–	–	–	–	–	–	–	–	–	–	–	–	–	–	–	–	–	7
M	–	3	–	–	–	–	–	1	–	–	–	1	–	–	–	–	–	–	15	–	–	–	–	–	–	1	–	–	1	–	–	–	–	–	–	1	–	23
Sa	–	1	–	–	–	–	–	–	–	–	–	–	–	–	–	–	–	–	5	–	–	–	–	–	–	2	–	–	–	–	–	–	–	–	–	–	–	8
Sb	–	1	–	1	–	–	–	–	–	1	–	–	–	–	–	–	–	–	6	1	–	–	–	1	–	1	–	–	–	–	–	–	–	–	–	–	–	12
Sc	–	1	–	–	–	–	–	–	–	–	–	–	–	–	–	–	–	–	10	–	–	–	–	1	–	1	–	–	–	–	–	–	–	–	–	–	–	13
Cooperignathus aranda (total)	–	2	–	1	–	2	–	–	–	–	–	8	–	–	–	–	–	–	6	–	–	–	–	6	–	2	–	–	–	–	–	–	–	–	3	1	–	31
Pa	–	–	–	–	–	1	–	–	–	–	–	2	–	–	–	–	–	–	–	–	–	–	–	2	–	–	–	–	–	–	–	–	–	–	1	–	–	6
Pb	–	–	–	–	–	–	–	–	–	–	–	2	–	–	–	–	–	–	–	–	–	–	–	–	–	–	–	–	–	–	–	–	–	–	–	–	–	2
M	–	1	–	–	–	–	–	–	–	–	–	2	–	–	–	–	–	–	3	–	–	–	–	4	–	1	–	–	–	–	–	–	–	–	1	1	–	13
Sa	–	1	–	–	–	–	–	–	–	–	–	1	–	–	–	–	–	–	1	–	–	–	–	–	–	1	–	–	–	–	–	–	–	–	–	–	–	4
Sb	–	–	–	1	–	–	–	–	–	–	–	1	–	–	–	–	–	–	2	–	–	–	–	–	–	–	–	–	–	–	–	–	–	–	–	–	–	4
Sc	–	–	–	–	–	1	–	–	–	–	–	–	–	–	–	–	–	–	–	–	–	–	–	–	–	–	–	–	–	–	–	–	–	–	1	–	–	2
Cornuodus longibasis (total)	–	5	–	28	3	12	–	1	3	–	4	32	–	–	–	–	–	1	14	2	1	–	–	5	–	–	2	–	–	–	1	–	–	–	–	1	2	117
Drepanodus sp. (total)	–	8	–	7	1	–	6	4	2	–	2	2	–	1	2	1	–	–	5	3	–	–	–	2	–	5	3	–	4	–	1	1	–	–	–	4	5	1	70
arcuatiform	–	2	–	3	1	–	3	1	1	–	1	1	–	1	2	–	–	–	2	1	–	–	–	1	–	2	2	–	1	–	–	–	–	–	–	1	3	1	30
graciliform	–	2	–	2	–	–	2	2	1	–	1	1	–	–	–	–	–	–	2	1	–	–	–	1	–	1	1	–	2	–	–	–	–	–	–	1	2	–	22
sculponeaform	–	4	–	2	–	–	1	1	–	–	–	–	–	–	–	1	–	–	1	1	–	–	–	–	–	2	–	–	1	–	1	1	–	–	–	2	–	–	18

Fig. 3. Continued.

	Y1	W5	Y4-1	Y4-2	Y4-3	Y4-4	Y4-6	Y4-7	Y4-8	M/A11-1	M/A11-2	M/A11-3	M/A11-4	M/A11-5	M/A11-6	M/A11-7	M/A3	M/A4	M/A7	TAB1/8.1	TAB1/13.7	TAB1/30.7	TAB1/31	TAB1/39.5	TAB1/44.5	TAB1/65.2	TAB1/78.2	TAB1/83	TAB1/86.7	TAB1/91	TAB1/103.8	TAB1/111	TAB1/125.4	TAB1/128.8	T2	C1611	C1612	C1613	Total
Drepanoistodus basiovalis (total)	2	11	–	22	2	9	12	7	10	–	4	14	1	6	3	–	–	4	14	2	–	–	–	4	–	–	6	–	3	–	–	–	–	–	–	4	5	12	157
P	–	4	–	6	–	2	–	1	1	–	–	–	–	–	–	–	–	–	–	–	–	–	–	–	–	–	1	–	–	–	–	–	–	–	–	–	3	18
M	–	1	–	10	1	1	5	1	–	–	–	4	1	–	–	–	–	–	3	–	–	–	–	3	–	–	1	–	1	–	–	–	–	–	–	–	–	–	32
Sa	–	1	–	–	–	2	2	2	4	–	–	5	–	1	–	–	–	1	2	–	–	–	–	–	–	–	2	–	–	–	–	–	–	–	–	–	1	3	26
Sb	–	3	–	5	1	4	3	2	4	–	2	4	–	3	2	–	–	2	5	1	–	–	–	1	–	–	1	–	1	–	–	–	–	–	–	2	1	5	52
Sc	2	2	–	1	–	–	2	1	1	–	2	1	–	2	1	–	–	1	4	1	–	–	–	–	–	–	1	–	1	–	–	–	–	–	–	2	3	1	29
Drepanoistodus costatus (total)	–	1	–	–	–	–	13	10	6	–	–	–	1	8	3	2	–	2	6	4	–	–	–	2	–	–	8	–	6	–	–	–	–	–	–	8	12	–	92
M	–	–	–	–	–	–	2	–	3	–	–	–	1	1	–	–	–	–	–	–	–	–	–	–	–	–	–	–	1	–	–	–	–	–	–	3	3	–	14
Sa	–	1	–	–	–	–	1	1	–	–	–	–	–	–	–	–	–	–	3	1	–	–	–	–	–	–	2	–	1	–	–	–	–	–	–	1	3	–	14
Sb	–	–	–	–	–	–	5	3	1	–	–	–	–	3	1	1	–	1	1	1	–	–	–	–	–	–	3	–	1	–	–	–	–	–	–	2	4	–	27
Sc	–	–	–	–	–	–	2	2	2	–	–	–	–	2	1	1	–	1	2	1	–	–	–	1	–	–	2	–	3	–	–	–	–	–	–	1	2	–	23
Sd	–	–	–	–	–	–	3	4	–	–	–	–	–	2	1	–	–	–	–	1	–	–	–	1	–	–	1	–	–	–	–	–	–	–	–	1	–	–	14
Drepanoistodus sp. (total)	–	4	–	3	–	1	–	–	–	–	–	–	–	–	–	–	–	–	–	–	–	–	–	–	–	–	–	–	–	–	–	–	–	–	–	–	1	9
Erraticodon patu (total)	–	–	–	–	–	16	73	26	24	–	–	42	1	14	15	16	3	26	8	–	–	–	–	–	–	1	27	2	16	–	3	1	–	–	–	3	5	–	322
Pa	–	–	–	–	–	3	11	7	4	–	–	11	1	2	–	1	1	2	1	–	–	–	–	–	–	–	2	–	1	–	–	1	–	–	–	–	–	–	48
Pb	–	–	–	–	–	4	5	4	1	–	–	5	–	–	1	–	–	5	2	–	–	–	–	–	–	–	1	–	1	–	–	–	–	–	–	1	–	–	30
M	–	–	–	–	–	2	11	1	5	–	–	4	–	1	1	3	1	5	2	–	–	–	–	–	–	–	3	–	3	–	2	–	–	–	–	1	–	–	45
Sa	–	–	–	–	–	2	5	1	1	–	–	2	–	3	2	3	–	3	–	–	–	–	–	–	–	–	5	–	2	–	–	–	–	–	–	–	1	–	30
Sb	–	–	–	–	–	1	8	3	3	–	–	7	–	4	3	2	–	5	2	–	–	–	–	–	–	1	7	–	4	–	–	–	–	–	–	–	1	–	51
Sc	–	–	–	–	–	2	24	4	4	–	–	9	–	2	2	3	1	2	1	–	–	–	–	–	–	–	3	1	1	–	–	–	–	–	–	–	2	–	61
Sd	–	–	–	–	–	2	9	6	6	–	–	4	–	2	6	4	–	4	–	–	–	–	–	–	–	–	6	1	4	–	1	–	–	–	–	1	1	–	57
Erraticodon sp. A (total)	–	–	–	–	–	–	–	–	–	–	–	–	–	1	–	–	–	–	4	–	–	–	–	–	–	–	–	–	–	–	–	–	–	–	–	–	–	–	5
Pa	–	–	–	–	–	–	–	–	–	–	–	–	–	–	–	–	–	–	1	–	–	–	–	–	–	–	–	–	–	–	–	–	–	–	–	–	–	–	1
Pb	–	–	–	–	–	–	–	–	–	–	–	–	–	–	–	–	–	–	1	–	–	–	–	–	–	–	–	–	–	–	–	–	–	–	–	–	–	–	1
Sa	–	–	–	–	–	–	–	–	–	–	–	–	–	1	–	–	–	–	1	–	–	–	–	–	–	–	–	–	–	–	–	–	–	–	–	–	–	–	2
Sc?	–	–	–	–	–	–	–	–	–	–	–	–	–	–	–	–	–	–	1	–	–	–	–	–	–	–	–	–	–	–	–	–	–	–	–	–	–	–	1
Jumudontus gananda (total)	–	–	–	–	–	–	–	–	–	–	–	–	–	1	–	–	–	2	–	1	–	–	–	–	–	–	2	–	–	–	–	–	–	–	3	8	–	17
Pa	–	–	–	–	–	–	–	–	–	–	–	–	–	1	–	–	–	2	–	1	–	–	–	–	–	–	2	–	–	–	–	–	–	–	2	8	–	16
Pb	–	–	–	–	–	–	–	–	–	–	–	–	–	–	–	–	–	–	–	–	–	–	–	–	–	–	–	–	–	–	–	–	–	–	1	–	–	1
Oepikodus communis (total)	–	–	–	–	–	–	–	–	–	–	1	–	–	–	–	–	–	–	–	–	–	–	–	–	–	–	–	–	–	–	–	–	–	–	–	–	–	1
Oepikodus pincallyensis (total)	–	3	–	35	–	1	2	–	1	–	–	–	–	3	–	–	–	–	18	1	–	2	–	5	–	15	5	–	–	–	–	–	2	1	1	–	–	–	95
Pa	–	–	–	6	–	–	–	–	–	–	–	–	–	–	–	–	–	–	2	1	–	1	–	–	–	1	1	–	–	–	–	–	–	1	–	–	–	–	13
Pb	–	–	–	7	–	1	–	–	–	–	–	–	–	1	–	–	–	–	1	–	–	–	–	1	–	–	–	–	–	–	–	–	–	–	–	–	–	–	11
M	–	1	–	2	–	–	2	–	–	–	–	–	–	1	–	–	–	–	7	–	–	–	–	2	–	1	1	–	–	–	–	–	–	–	–	–	–	–	17
Sa	–	1	–	4	–	–	–	–	–	–	–	–	–	–	–	–	–	–	3	–	–	1	–	1	–	5	1	–	–	–	–	–	1	–	–	–	–	–	17
Sb	–	–	–	6	–	–	–	–	–	–	–	–	–	1	–	–	–	–	3	–	–	–	–	1	–	3	1	–	–	–	–	–	1	–	1	–	–	–	17
Sc	–	1	–	7	–	–	–	–	–	–	–	–	–	–	–	–	–	–	–	–	–	–	–	–	–	2	1	–	–	–	–	–	–	–	–	–	–	–	11
Sd	–	–	–	3	–	–	–	–	1	–	–	–	–	–	–	–	–	–	2	–	–	–	–	–	–	3	–	–	–	–	–	–	–	–	–	–	–	–	9
Oneotodus sp. (total)	–	–	–	4	–	1	–	–	–	–	–	1	–	–	–	–	–	–	–	–	–	–	–	–	–	–	–	–	–	–	–	–	–	–	–	1	–	7
Prioniodus sp. cf. *amadeus* (total)	–	1	–	–	–	1	3	–	–	–	–	14	–	2	–	–	–	–	13	–	–	–	–	–	–	–	13	–	1	–	–	–	–	–	–	–	–	–	48
P	–	1	–	–	–	–	1	–	–	–	–	7	–	–	–	–	–	–	9	–	–	–	–	–	–	–	10	–	–	–	–	–	–	–	–	–	–	–	28
S	–	–	–	–	–	1	2	–	–	–	–	7	–	1	–	–	–	–	4	–	–	–	–	–	–	–	3	–	1	–	–	–	–	–	–	–	–	–	19
M	–	–	–	–	–	–	–	–	–	–	–	–	–	1	–	–	–	–	–	–	–	–	–	–	–	–	–	–	–	–	–	–	–	–	–	–	–	–	1

Fig. 3. Continued.

	Y1	W5	Y4-1	Y4-2	Y4-3	Y4-4	Y4-6	Y4-7	Y4-8	M/A11-1	M/A11-2	M/A11-3	M/A11-4	M/A11-5	M/A11-6	M/A11-7	M/A3	M/A4	M/A7	TAB1/8.1	TAB1/13.7	TAB1/30.7	TAB1/31	TAB1/39.5	TAB1/44.5	TAB1/65.2	TAB1/78.2	TAB1/83	TAB1/86.7	TAB1/91	TAB1/103.8	TAB1/111	TAB1/125.4	TAB1/128.8	T2	C1611	C1612	C1613	Total
Prioniodus sp. A (total)	–	–	–	3	–	–	–	–	–	–	–	–	–	–	–	–	–	–	1	–	–	–	–	–	–	–	–	–	–	–	–	–	–	–	–	–	–	4
Protopanderodus gradatus (total)	–	10	–	19	–	9	1	–	5	9	3	6	1	–	–	–	–	–	1	–	1	–	–	–	–	–	14	–	–	–	–	–	–	–	–	6	23	2	110
Sa	–	–	–	3	–	1	–	–	–	3	–	–	1	–	–	–	–	–	1	–	–	–	–	–	–	2	–	–	–	–	–	–	–	–	–	1	–	12
Sb	–	4	–	6	–	2	–	–	1	1	–	3	–	–	–	–	–	–	–	–	–	–	–	–	–	3	–	–	–	–	–	–	–	–	1	6	–	27
Sc	–	4	–	4	–	3	1	–	1	2	1	–	–	–	–	–	–	–	–	–	1	–	–	–	–	4	–	–	–	–	–	–	–	–	2	9	1	33
Sd	–	2	–	6	–	3	–	–	3	3	2	3	–	–	–	–	–	–	–	–	–	–	–	–	–	5	–	–	–	–	–	–	–	–	3	7	1	38
Protopanderodus leonardii (total)	–	–	–	1	1	–	–	–	1	–	–	2	–	–	–	–	–	–	–	–	–	–	–	–	1	–	–	–	–	–	–	–	–	–	–	–	–	6
Sa	–	–	–	–	–	–	–	–	–	–	–	1	–	–	–	–	–	–	–	–	–	–	–	–	–	–	–	–	–	–	–	–	–	–	–	–	–	1
Sb	–	–	–	–	–	–	–	–	1	–	–	1	–	–	–	–	–	–	–	–	–	–	–	–	1?	–	–	–	–	–	–	–	–	–	–	–	–	3
Sc	–	–	–	1	1	–	–	–	–	–	–	–	–	–	–	–	–	–	–	–	–	–	–	–	–	–	–	–	–	–	–	–	–	–	–	–	–	2
Protopanderodus nogamii (total)	–	–	–	3	–	–	–	–	–	–	–	–	–	–	–	–	–	–	–	–	–	–	–	–	–	–	–	–	–	–	–	–	–	48	80	–	131
Pa	–	–	–	–	–	–	–	–	–	–	–	–	–	–	–	–	–	–	–	–	–	–	–	–	–	–	–	–	–	–	–	–	–	8	4	–	12
Pb	–	–	–	–	–	–	–	–	–	–	–	–	–	–	–	–	–	–	–	–	–	–	–	–	–	–	–	–	–	–	–	–	–	6	12	–	18
Sa	–	–	–	–	–	–	–	–	–	–	–	–	–	–	–	–	–	–	–	–	–	–	–	–	–	–	–	–	–	–	–	–	–	13	22	–	35
Sc	–	–	–	1	–	–	–	–	–	–	–	–	–	–	–	–	–	–	–	–	–	–	–	–	–	–	–	–	–	–	–	–	–	3	2	–	6
Sb+Sd	–	–	–	2	–	–	–	–	–	–	–	–	–	–	–	–	–	–	–	–	–	–	–	–	–	–	–	–	–	–	–	–	–	18	40	–	60
Protoprioniodus yapu (total)	–	–	–	2	–	–	–	–	–	–	–	2	–	–	–	–	–	–	13	–	–	–	–	–	–	–	–	–	–	–	–	–	–	–	–	–	17
Pb	–	–	–	2	–	–	–	–	–	–	–	–	–	–	–	–	–	–	3	–	–	–	–	–	–	–	–	–	–	–	–	–	–	–	–	–	5
M	–	–	–	–	–	–	–	–	–	–	–	2	–	–	–	–	–	–	8	–	–	–	–	–	–	–	–	–	–	–	–	–	–	–	–	–	10
S?	–	–	–	–	–	–	–	–	–	–	–	–	–	–	–	–	–	–	2	–	–	–	–	–	–	–	–	–	–	–	–	–	–	–	–	–	2
Scalpellodus latus (total)	–	1	–	8	–	2	4	–	2	3	–	1	–	–	–	–	–	–	5	–	–	–	–	1	–	–	–	–	2	–	–	–	–	–	–	–	–	29
P?	–	–	–	–	–	–	–	–	–	–	–	–	–	–	–	–	–	–	–	–	–	–	–	1	–	–	–	–	–	–	–	–	–	–	–	–	–	1
Sa	–	1	–	1	–	–	–	–	–	–	–	–	–	–	–	–	–	–	1	–	–	–	–	–	–	–	–	–	–	–	–	–	–	–	–	–	–	3
Sb	–	–	–	4	–	1	2	–	1	2	–	–	–	–	–	–	–	–	2	–	–	–	–	–	–	–	–	–	–	–	–	–	–	–	–	–	–	12
Sc	–	–	–	2	–	1	1	–	–	–	–	–	–	–	–	–	–	–	1	–	–	–	–	–	–	–	–	–	–	–	–	–	–	–	–	–	–	5
Sd	–	–	–	1	–	–	1	–	1	1	–	1	–	–	–	–	–	–	1	–	–	–	–	–	–	–	–	2	–	–	–	–	–	–	–	–	–	8
Scolopodus multicostatus (total)	–	–	–	2	–	33	–	–	1	16	9	–	–	–	–	–	–	–	–	20	3	–	–	–	–	1	–	–	–	–	–	–	–	–	15	14	19	133
Pa	–	–	–	1	–	3	–	–	–	1	–	–	–	–	–	–	–	–	–	3	–	–	–	–	–	–	–	–	–	–	–	–	–	–	2	1	–	11
Pb	–	–	–	–	–	7	–	–	1	1	2	–	–	–	–	–	–	–	–	2	1	–	–	–	–	–	–	–	–	–	–	–	–	–	3	–	4	21
Sa	–	–	–	1	–	5	–	–	–	2	3	–	–	–	–	–	–	–	–	5	1	–	–	–	–	–	–	–	–	–	–	–	–	–	2	2	2	23
Sb	–	–	–	–	–	6	–	–	–	2	2	–	–	–	–	–	–	–	–	6	–	–	–	–	–	1	–	–	–	–	–	–	–	–	3	7	5	32
Sc	–	–	–	–	–	8	–	–	–	4	2	–	–	–	–	–	–	–	–	3	–	–	–	–	–	–	–	–	–	–	–	–	–	–	4	2	6	29
Sd	–	–	–	–	–	4	–	–	–	6	–	–	–	–	–	–	–	–	–	1	1	–	–	–	–	–	–	–	–	–	–	–	–	–	1	2	2	17
Scolopodus quadratus (total)	–	1	–	24	1	5	–	–	1	–	3	–	–	–	–	–	–	–	–	3	–	–	–	–	–	–	–	–	–	–	–	–	–	–	–	2	–	40
P	–	–	–	3	–	–	–	–	1	–	–	–	–	–	–	–	–	–	–	–	–	–	–	–	–	–	–	–	–	–	–	–	–	–	–	–	–	4
Sa	–	–	–	7	1	2	–	–	–	–	1	–	–	–	–	–	–	–	–	1	–	–	–	–	–	–	–	–	–	–	–	–	–	–	–	1	–	13
Sb	–	–	–	9	–	2	–	–	–	–	1	–	–	–	–	–	–	–	–	–	–	–	–	–	–	–	–	–	–	–	–	–	–	–	–	–	–	12
Sc	–	–	–	–	–	–	–	–	–	–	–	–	–	–	–	–	–	–	–	1	–	–	–	–	–	–	–	–	–	–	–	–	–	–	–	–	–	1
Sd	–	1	–	5	–	1	–	–	–	–	1	–	–	–	–	–	–	–	–	1	–	–	–	–	–	–	–	–	–	–	–	–	–	–	–	1	–	10

		Y1	W5	Y4-1	Y4-2	Y4-3	Y4-4	Y4-6	Y4-7	Y4-8	M/A11-1	M/A11-2	M/A11-3	M/A11-4	M/A11-5	M/A11-6	M/A11-7	M/A3	M/A4	M/A7	TAB1/8.1	TAB1/13.7	TAB1/30.7	TAB1/31	TAB1/39.5	TAB1/44.5	TAB1/65.2	TAB1/78.2	TAB1/83	TAB1/86.7	TAB1/91	TAB1/103.8	TAB1/111	TAB1/125.4	TAB1/128.8	T2	C1611	C1612	C1613	Total
Triangulodus larapintinensis (total)		2	–	–	19	5	9	13	24	33	9	3	16	–	3	9	–	–	5	36	27	3	1	2	–	–	4	26	–	5	6	–	–	1	–	–	17	18	8	302
	Pa	–	–	–	6	1	1	2	5	4	3	1	1	–	1	1	–	–	1	6	1	–	–	–	–	–	1	4	–	1	2	–	–	–	–	–	–	–	–	41
	Pb	–	–	–	2	3	1	2	3	2	–	–	–	–	1	1	–	–	–	4	4	–	–	–	–	–	1	6	–	–	1	–	–	–	–	–	6	–	–	37
	M	–	–	–	2	–	–	3	4	5	–	–	7	–	1	3	–	–	–	8	2	–	–	–	–	–	–	3	–	–	2	–	–	–	–	–	3	2	5	52
	Sa	–	–	–	4	–	1	3	1	7	1	1	2	–	–	2	–	–	1	4	2	–	–	–	–	–	–	2	–	–	–	–	–	–	–	–	1	1	–	33
	Sb	–	–	–	1	–	2	2	5	7	2	1	3	–	–	2	–	–	1	8	9	2	1	1	–	–	2	5	–	2	–	–	–	1	–	–	6	2	2	67
	Sc	–	–	–	2	–	3	1	4	5	3	–	2	–	–	–	–	–	2	4	7	1	–	1	–	–	1	4	–	–	1	–	–	–	–	–	7	7	1	56
	Sd	–	–	–	2	1	1	–	2	3	–	–	1	–	–	–	–	–	–	2	2	–	–	–	–	–	–	2	–	–	–	–	–	–	–	–	–	–	–	16
Triangulodus sp. A (S elements)		–	–	–	4	–	–	–	1	1	–	–	–	–	–	–	–	–	–	1	8	–	–	–	–	–	–	–	–	–	–	–	–	–	–	–	11	23	30	79
Ulrichodina simplex sp. cf. (total)		–	1	–	–	–	–	–	–	–	–	–	–	–	–	–	–	–	–	–	–	–	–	–	–	–	–	–	–	–	–	–	–	–	–	–	–	–	1
	Total	2	100	9	434	33	160	353	241	118	51	53	342	13	190	44	23	30	94	291	122	15	4	2	63	3	38	149	2	67	11	8	5	3	1	2	143	205	98	3522

Fig. 3. Continued.

Gap fauna is dominated by robust coniform elements. Particularly noticeable is the absence of *Oepikodus pincallyensis, Prioniodus* sp. cf. *amadeus, Prioniodus* sp. A and *Baltoniodus* sp. A from the Koonenberry Gap fauna. Furthermore, approximately half the total number of elements recovered from Mount Arrowsmith samples can be assigned to just one species, *Acodus* sp. cf. *emanuelensis* (Figs. 3, 4), whereas this species is much less common in the Koonenberry Gap samples. In the latter, *Protopanderodus nogamii* is the dominant species (nearly 30% of the fauna), while in the Mount Arrowsmith fauna, this species is very rare (Fig. 3). *Triangulodus* sp. A, *Scolopodus multicostatus*, and *Protopanderodus gradatus* are also relatively abundant at Koonenberry Gap compared to Mount Arrowsmith (Fig. 4).

Such compositional differences between the conodont faunas of the two localities probably reflect biofacies variations. Johnston & Barnes (1999), in a study of contemporaneous conodont faunas of western Newfoundland, recognized a *Diaphorodus* biofacies that represents a shallow-subtidal environment. *Diaphorodus* is here regarded as a junior synonym of *Acodus*—see Zhen *et al.* (in press). The domination of *A.* sp. cf. *emanuelensis* at Mount Arrowsmith suggests that the western New South Wales faunas generally inhabited a similar shallow-subtidal environment. However, the presence of *O. pincallyensis* and several species of *Prioniodus*, in association with abundant sponge spicules in some samples of the Tabita Formation, suggests interfingering of a somewhat deeper subtidal biofacies. In contrast, the absence of deeper water forms such as species of *Oepikodus* and *Prioniodus* from the Koonenberry Gap fauna, together with the abundance of robust coniform elements, probably indicates the presence of shallower, near-shore conditions in that area.

Bergstroemognathus kirki, Triangulodus larapintinensis, Acodus sp. cf. *emanuelensis* and *Prioniodus* sp. cf. *amadeus* were probably endemic to Australia. Numerically, these four species constitute slightly more than half of the western New South Wales faunas. They are widely distributed in the intracratonic basins of Australia, typically (except for *P.* sp. cf. *amadeus*) inhabiting shallow water environments (Cooper, 1981; Stait & Druce, 1993). Accompanying cosmopolitan species, including *Cornuodus longibasis, Drepanoistodus basiovalis, Scolopodus quadratus* and *Ansella jemtlandica*, together comprise only a minor component (about one-tenth) of the Mount Arrowsmith and Koonenberry Gap faunas.

Domination of endemic taxa in the cratonic shelf of western New South Wales is in striking contrast to the composition of deeper water faunas inhabiting offshore parts of the Gondwanan margin; for example, the conodonts of the Hensleigh Siltstone (*elegans* Zone) in central New South Wales where cosmopolitan and widespread species are overwhelmingly dominant (Zhen *et al.*, 2001, in press). In correlating faunas from the cratonic platform and margins, those non-endemic species which are not long-ranging cosmopolitan forms, assume critical importance. These comprise the remaining third of the western New South Wales shelf margin fauna, with many exhibiting particularly important biogeographic relationships (discussed below).

Cooperignathus nyinti and *C. aranda* are widely distributed in Australian cratonic successions, as well as being represented in South China (An, 1987), North American Midcontinent successions (Ethington & Clark,

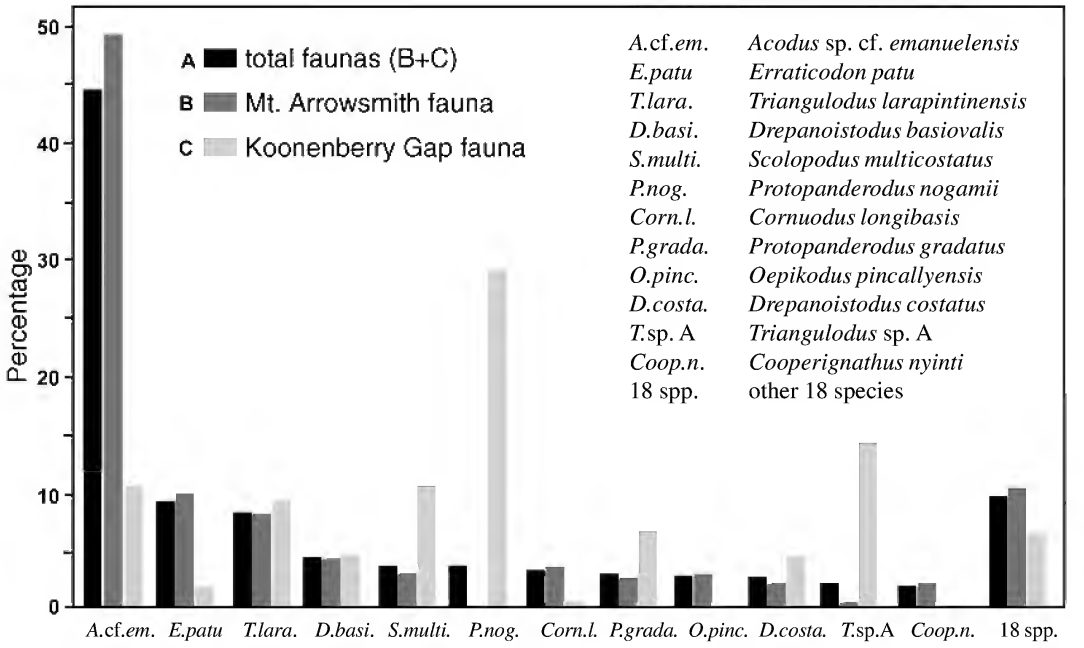

Fig. 4. Bar charts illustrating relative species abundances in the Lower Ordovician conodont faunas of western New South Wales.

1982; Repetski, 1982) and in peri-Laurentian offshore deeper water successions (Pohler, 1994; Johnston & Barnes, 2000). They are not only biostratigraphically significant due to their short stratigraphic range, but are also valuable biogeographically in establishing links between eastern Gondwana and Laurentia. *Erraticodon patu* has been reported from North America (Nowlan, 1976; Bauer, 1990), the Argentine Precordillera (Lehnert, 1995) and western Argentina (Albanesi & Vaccari, 1994), although some of these assignments have doubtful validity (see later discussion). *Scolopodus multicostatus* is also widely distributed in Australian cratonic successions, and in North American Midcontinent successions such as the St. George Group, Newfoundland (Barnes & Tuke, 1970) and the Fillmore Formation (zone G2) of the Ibex area, Utah (Ethington & Clark, 1982).

Jumudontus gananda, Drepanoistodus costatus, Protopanderodus gradatus, P. leonardii and *Protoprioniodus yapu* were widespread species, occurring in Australia, peri-Gondwanan blocks (including South and North China), the Argentine Precordillera, and in Laurentia. However, these species have not been recorded in typical North European (Baltoscandian) successions, except for doubtful occurrences of *P. gradatus* from a higher stratigraphical interval (*variabilis* Zone to *E. lindstroemi* Subzone) of the Mójcza Limestone in the Holy Cross Mountains, Poland (Dzik, 1994), and from a lower stratigraphical level (middle *P. proteus* Zone) in central Sweden (Löfgren, 1994).

Protopanderodus nogamii, the dominant species in the Koonenberry Gap fauna (Figs. 3, 4), is widely distributed in North China, South China, Korea, southeast Asia, Australia, and the Argentine Precordillera. In North China, this species had a relatively long range (An *et al.*, 1983; Chen *et al.*, 1995) with its earliest appearance in the Beianzhuang Formation (Chewtonian to Castlemainian equivalents, *evae* to *originalis* zones), extending up into the early Late Ordovician Fengfeng Formation. The species is known from the basal Setul Limestone of possibly Early Ordovician age in the Langkawi Islands, Malaya (Igo & Koike, 1967). Also, in the Argentine Precordillera, Serpagli (1974) recorded *P. nogamii* in a post-*evae* zone occurrence.

Elements of typical Baltoscandian faunas are represented only by *Scalpellodus latus*, which is a minor component of the Mount Arrowsmith fauna. This species was also recorded from the Horn Valley Siltstone of the Amadeus Basin (Cooper, 1981).

Biostratigraphy and regional correlation

Given that the most abundant species in the faunas under discussion are confined to Australia (Figs. 4, 5), it is not surprising that their precise age determination and international correlation are difficult. Zonal index species of neither the North Atlantic nor North American Midcontinent biostratigraphic successions are recognizable in the western New South Wales conodont faunas. However, co-occurrence of *Oepikodus communis, Cooperignathus nyinti, C. aranda*, and *Jumudontus gananda* in the Tabita Formation suggests a latest Bendigonian to Chewtonian age, corresponding to the *evae* Zone of the North Atlantic faunal scheme, or the *andinus* to *aranda* zones (top Ibexian) of the North American Midcontinent succession. No evidence exists in these Tabita Formation faunas to support the earlier contention of Warris (1969) that the formation spanned three conodont zones.

Within the Australian craton, the Mount Arrowsmith and Koonenberry Gap conodont faunas correlate well with the Horn Valley Siltstone fauna of the Amadeus Basin, central Australia, for which Cooper (1981) suggested an age ranging from the *Oepikodus evae* Zone to *Baltoniodus navis/triangularis* Zone. While this age assignment remains acceptable, presence of the index species *O. evae* and *B. navis* cannot be confirmed in the Horn Valley Siltstone, based on Cooper's illustrated specimens. Re-examination of a large topotype collection of the Horn Valley specimens, provided courtesy of Dr Barry Cooper, has also failed to reveal these

Fig. 5. Comparative distribution of the Early Ordovician conodont faunas from western New South Wales (reference sources: central New South Wales, Hensleigh Siltstone, Zhen *et al.*, in press; Amadeus Basin, Horn Valley Siltstone, Cooper, 1981; Georgina Basin, Coolibah Formation, Stait & Druce, 1993; Canning Basin, Emanuel Formation, McTavish, 1973, Goldwyer & Nita formations, Watson, 1988; Argentine Precordillera, San Juan Formation, Serpagli, 1974, Lehnert, 1995, Albanesi, *in* Albanesi *et al.*, 1998; San Rafael, western Argentina, Ponon Trehue Formation, Lehnert *et al.*, 1998; Newfoundland, Cow Head Group, Pohler, 1994, Johnston & Barnes, 1999, 2000; eastern New York, Landing, 1976; Ibex area, Utah, Ethington & Clark, 1982; Franklin Mountains, southern New Mexico, El Paso Group, Repetski, 1982; Hebei Province, North China, Beianzhuang Formation (Lower Majiagou Formation), An *et al.*, 1983; Ordos Basin, North China, An & Zheng, 1990; South China, Dawan formation and equivalents, An, 1987, Wang, 1993; east and north Greenland, Smith, 1991; Sweden, van Wamel, 1974, Löfgren, 1978, 1999).

	AUSTRALIA					ARGENTINA			N. AMERICA				CHINA				
	Mount Arrowsmith	Koonenberry Gap	central NSW	Amadeus Basin	Georgina Basin	Canning Basin	Precordillera	San Rafael	Newfoundland	E. New York	S. Franklin Mt.	Ibex area, Utah	Hebei, N. China	Ordos Basin	South China	GREENLAND	SWEDEN
Acodus sp. cf. *emanuelensis*	●	●	–	●	–	–	–	–	–	–	–	–	–	–	–	–	–
Acodus sp.	●	●	–	–	–	–	–	–	–	–	–	–	–	–	–	–	–
Ansella jemtlandica	●	●	–	●	–	–	●	–	●	–	–	–	–	–	–	–	●
Baltoniodus sp. A	●	–	–	?●	–	–	–	–	–	–	–	–	–	–	–	–	–
Bergstroemognathus kirki	●	●	–	●	●	–	–	–	–	–	–	–	–	–	–	–	–
Cooperignathus nyinti	●	●	–	●	●	–	–	–	●	–	●	●	–	–	–	–	–
Cooperignathus aranda	●	●	–	●	–	–	–	–	●	–	●	●	–	–	●	–	–
Cornuodus longibasis	●	●	●	●	–	–	●	–	●	●	–	–	●	●	●	–	●
Drepanodus sp.	●	●	–	–	–	–	–	–	–	–	–	–	–	–	–	–	–
Drepanoistodus basiovalis	●	●	–	●	–	●	●	●	●	–	–	●	–	–	●	–	●
Drepanoistodus costatus	●	●	–	●	●	●	●	–	?	–	–	–	●	●	–	●	–
Drepanoistodus sp.	●	●	–	–	–	–	–	–	–	–	–	–	–	–	–	–	–
Erraticodon patu	●	●	–	●	–	–	–	–	–	–	–	–	–	–	–	–	–
Erraticodon sp. A	●	–	–	–	–	–	–	–	–	–	–	–	–	–	–	–	–
Jumudontus gananda	●	●	●	●	–	–	●	–	●	●	–	●	–	●	–	●	–
Oepikodus communis	●	–	?	?	–	●	●	–	●	–	●	●	–	–	–	●	–
Oepikodus pincallyensis n.sp.	●	–	–	–	–	–	–	–	–	–	–	–	–	–	–	–	–
Oneotodus sp.	●	●	–	●	–	–	–	–	–	–	–	–	–	–	–	–	–
Prioniodus sp. cf. *amadeus*	●	–	–	–	–	–	–	–	–	–	–	–	–	–	–	–	–
Prioniodus sp. A	●	–	–	–	–	–	–	–	–	–	–	–	–	–	–	–	–
Protopanderodus gradatus	●	●	●	●	–	●	●	●	●	●	●	●	–	●	●	●	–
Protopanderodus leonardii	●	–	●	–	–	–	●	–	●	–	●	●	–	–	–	●	–
Protopanderodus nogamii	●	●	–	●	●	●	●	–	–	–	–	–	●	●	●	–	–
Protoprioniodus yapu	●	–	–	●	–	–	–	–	●	–	–	–	–	–	●	–	–
Scalpellodus latus	●	–	–	●	–	–	–	–	–	–	–	–	–	–	–	–	●
Scolopodus multicostatus	●	●	–	–	●	–	–	–	–	–	–	●	–	–	–	●	–
Scolopodus quadratus	●	●	●	–	–	●	●	●	●	●	●	●	●	●	●	●	●
Triangulodus larapintinensis	●	●	–	●	●	–	–	–	–	–	–	–	–	–	–	–	–
Triangulodus sp. A	●	●	–	–	–	–	–	–	–	–	–	–	–	–	–	–	–
Ulrichodina sp. cf. *simplex*	●	–	–	–	–	–	●	–	–	–	?	?	–	–	–	?	–
total species in common with Mount Arrowsmith		20	5	17	6	6	11	3	11	4	6	9	4	6	7	7	5

two species. Nicoll & Ethington (in press) recognized a new species of *Oepikodus*, apparently closely related to *O. communis*, occurring in the Horn Valley Siltstone. In the Tabita Formation, *O. communis* is extremely rare, whereas *O. pincallyensis* (a transitional form morphologically between *O. evae* and *O. communis*) is relatively abundant. The stratigraphic range of *O. communis* extends upwards at least to the base of the *flabellum/laevis* Zone (Sweet, 1988), and indeed, Cooper (1981) recorded *Microzarkodina flabellum* from the upper part of the Horn Valley Siltstone. However, *M. flabellum* has not been recognized in the western New South Wales conodont faunas, suggesting that strict equivalence of the Tabita Formation is with the lower part of the Horn Valley Siltstone (Fig. 6).

Correlation of the Mount Arrowsmith and Koonenberry Gap faunas with those of the Coolibah Formation of the Georgina Basin (Stait & Druce, 1993) is based on co-occurrence in both regions of *Bergstroemognathus kirki, Cooperignathus nyinti, C. aranda, Drepanoistodus costatus, Protopanderodus nogamii, Scolopodus multicostatus* and *Triangulodus larapintinensis* (Fig. 5). Of the three biostratigraphic associations recognized by Stait & Druce (1993), the western New South Wales faunas are most closely aligned with those of the middle Coolibah Formation, where the first appearances of *C. nyinti, C. aranda* and *T. larapintinensis* occur. These species also range into the upper biostratigraphic association in the Coolibah Formation. Although Stait & Druce (1993)

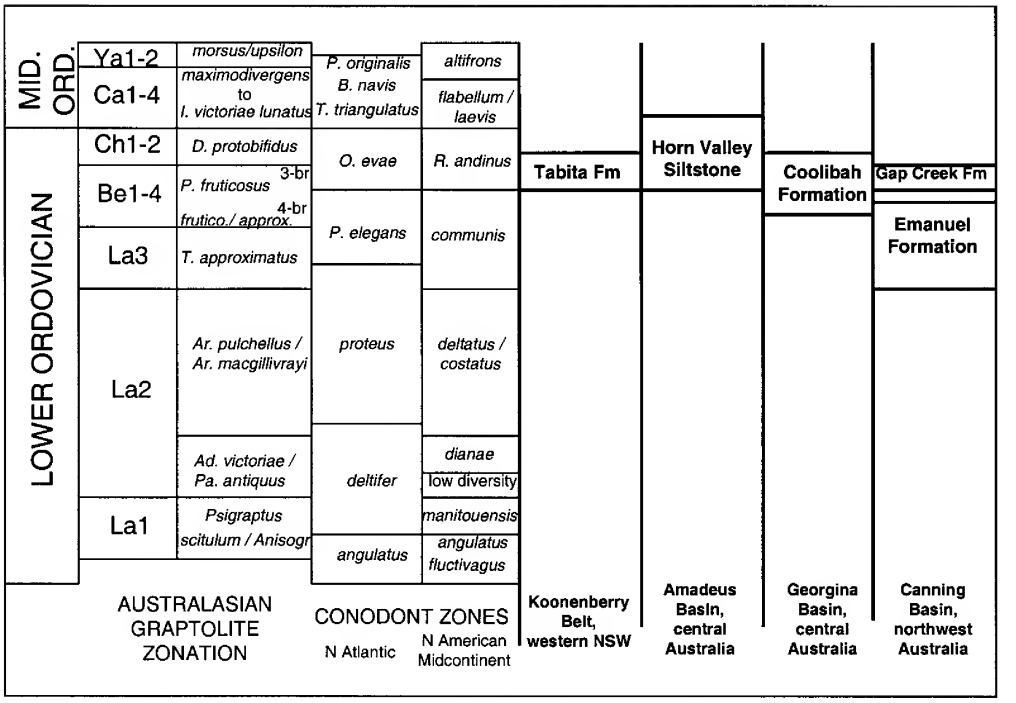

Fig. 6. Correlation of Lower to Middle Ordovician (pre Darriwilian) successions in the Amadeus, Georgina and Canning basins of Australia with the Tabita Formation (including at its base the Yandaminta Quartzite) at Mount Arrowsmith, based on global graptolite and conodont zonations.

correlated the uppermost Coolibah Formation with the lower Horn Valley Siltstone, our study (Fig. 6) concludes that the Mount Arrowsmith and Koonenberry Gap conodont faunas were contemporaneous with the assemblages of the middle to upper Coolibah Formation and the lower Horn Valley Siltstone.

Many of the Lower and Middle Ordovician conodonts from the Canning Basin remain undescribed, so hindering precise correlation with western New South Wales faunas. The conodont fauna from the Emanuel Formation (McTavish, 1973; Nicoll, 1992; Zhen *et al.*, 2001) spans from late Lancefieldian (La3) to middle Bendigonian (Be2) according to Nicoll (*in* Shergold *et al.*, 1995), with at least the middle part of the formation corresponding to the interval from the *A. deltatus–O. costatus* to lower *O. communis* conodont zones of the North American Midcontinental faunal succession (Ethington *et al.*, 2000). A late Bendigonian (*O. communis* Zone) age was assigned to the overlying Gap Creek Formation by Nicoll (*in* Shergold *et al.*, 1995). The conodont faunas described by Watson (1988) are mainly from stratigraphically younger, Darriwilian, units including the Nita and Goldwyer formations.

As previously discussed, the western New South Wales faunas of the shallow cratonic shelf margin exhibit significant differences from the slightly older (*elegans* Zone) fauna of the Hensleigh Siltstone in central New South Wales, which inhabited deeper water, lower slope environments of an offshore island arc setting (Zhen *et al.*, in press). At species level, the only forms common to these two regions are *Cornuodus longibasis, Protopanderodus gradatus, P. leonardii* and *Scolopodus quadratus*, which are all long-ranging or cosmopolitan in extent (Fig. 5).

Globally, the Lower Ordovician conodont faunas of far western New South Wales are most closely correlated with those from the San Juan Formation (upper part of assemblage B to lower part of assemblage C) of the Argentine Precordillera (Serpagli, 1974), the Cow Head Group (Bed 11) of Newfoundland (Johnston & Barnes, 1999), and the Ibex area of Utah through the *Jumudontus gananda–Reutterodus andinus* interval (Ethington & Clark, 1982) (Fig. 5). These assemblages occupy either the interval from the *andinus* Zone to basal *flabellum/laevis* Zone of a shallow, warm water "North American mid continent" type setting, or the correlative *evae* Zone of the cooler and/or deeper water "North Atlantic" type setting.

Material and methods

Nineteen samples (average weight 5kg) collected at Mount Arrowsmith yielded well preserved, moderately abundant conodonts. Locations of all samples from this area (Fig. 1) refer to grid references (GR) on the Mount Arrowsmith 7237 1:100 000 orthophotomap (first edition, 1978). Samples Y1 (GR 556150mE 6670200mN) and W5 (GR 556720mE 6669500mN) were collected from limestone nodules within shales and mudstones exposed below the topmost beds of the Yandaminta Quartzite, which forms distinctive linear topographic ridges in the area. Due to deep weathering of the shales, their direct contact with the overlying quartzite beds cannot be established. According to the stratigraphic definition given by Warris (1967), these two samples should lie within the upper Yandaminta Quartzite. Seven samples (Y4–1 to Y4–4 and Y4–6 to Y4–8) were collected from the gully section Y4 (centred on GR 558100mE 66632 00mN) through the overlying Tabita Formation on the northwest flank of Mount Arrowsmith. In the southern part of the area, seven samples (M/A11-1 to M/A11-7) were collected from a hill slope section (centred on GR 557000mE 6663000mN) on the southwestern flank of Mount Arrowsmith. In both

the Y4 and M/A11 sections (Fig. 2), the contact between the predominantly calcareous Tabita Formation and the underlying Yandaminta Quartzite is shown, but the boundary with shales of the overlying Pingbilly Formation is not exposed due to deep weathering and alluvium cover. Spot sample M/A7 (GR 557700mE 6664250mN) is from a laminated thinly bedded limestone near the middle part of the Tabita Formation, on the northeast side of the synclinal axis (Fig. 1). Two other spot samples (M/A3 and M/A4), which are five metres apart stratigraphically, were collected from thinly bedded limestones within green shale exposed in a creek near the axis of the syncline (GR 557800mE 6663700mN) about 600 m south of sample M/A7. All these samples were completely dissolved in 10% acetic acid, with residues separated and concentrated using sodium polytungstate.

Fifteen additional samples were collected at Mount Arrowsmith from a measured section TAB1 which crosses the site of Department of Mineral Resources borehole DMR Koonenberry RDH/DDH7 at GPS GR 558300mE 6662200mN (Figs. 1, 2). One sample (T2, GR 557850mE 6663750mN) was taken from the top of the Tabita Formation close to the boundary with the overlying Pingbilly Formation. These 16 samples, collected and processed by J. Paterson (Paterson, 2001b), were only partially dissolved in 10% acetic acid.

At Koonenberry Gap (GR 624950mE 6624500mN, Wonnaminta 7336 1:100 000 orthophotomap, first edition 1978) approximately 800 m northwest of Koonenberry Mountain trig station, three samples (C1611, C1612, C1613) were collected from a continuous section (Fig. 1) of as yet unnamed thickly bedded dolomitic limestones. These samples were dissolved in a solution of 10% acetic acid buffered with 5% formic acid to break down the dolomitic matrix.

A total of 3522 identifiable conodont specimens were obtained from the 35 samples collected in the Mount Arrowsmith and Koonenberry Gap areas (Fig. 3).

All photographic illustrations shown in Figs. 7–29 are SEM photomicrographs captured digitally. Figured specimens bear the prefix AMF and are deposited in the collections of the Palaeontology Section at the Australian Museum in Sydney. Yong-yi Zhen is the sole author of the new genus *Cooperignathus*, and new species *Oepikodus pincallyensis*.

Purnell *et al.* (2000) recently proposed a new scheme of anatomical notation and a set of new terms for orientation of conodont elements. However, since the anatomical nature and even the apparatus composition of most of the conodont taxa described herein remains poorly understood, the conventional orientation and notation scheme (Clark *et al.*, 1981; Sweet, 1988) is maintained in order to avoid confusion.

Systematic palaeontology

Class Conodonta Pander, 1856

Acodus Pander, 1856

Type species. *Acodus erectus* Pander, 1856.

Remarks. Zhen *et al.* (in press) provided an extensive discussion of *Acodus* and its junior synonyms, adopting a slightly broader generic concept than that of some other authors such as Johnston & Barnes (2000).

Acodus sp. cf. *emanuelensis* McTavish, 1973

Fig. 7A–Y

Acodus emanuelensis.–Cooper, 1981: 158, pl. 28, figs. 1, 5, 6, 9, 10, 12.

Material. Forty-one specimens (7 Pa, 10 Pb, 9 M, 2 Sa, 3 Sb, 6 Sc, 4 Sd) from limestone nodules within shales of the upper Yandaminta Quartzite, and 1475 specimens (162 Pa, 322 Pb, 332 M, 179 Sa, 191 Sb, 95 Sc, 194 Sd) from the overlying Tabita Formation at Mount Arrowsmith; 40 specimens (2 Pa, 4 Pb, 14 M, 7 Sa, 2 Sb, 5 Sc, 6 Sd) from unnamed dolomitic limestone unit at Koonenberry Gap.

Diagnosis. A septimembrate species of *Acodus*, consisting of acodiform Pa and Pb, makellate M, and costate S elements bearing two (Sc), three (Sa and Sb), and four (Sd) strong, blade-like costae.

Description. *Pa element* with robust, laterally compressed, erect or slightly proclined cusp, anteroposteriorly extended base and moderately open basal cavity; cusp slightly curved inwards with straight, sharp anterior margin and nearly straight and sharp posterior margin; base triangular in outline in lateral view, formed by adenticulate posterior process and triangular anticusp; posterior process with straight or gently arched upper margin meeting straight posterior margin of the cusp at an angle of 90–115°; basal margin straight, forming an angle of about 50° with anterior margin; inner lateral face typically with a prominent, rounded-faced mid costa; outer lateral face smooth or with weak mid carina (Fig. 7A–F). *Pb element* similar to the Pa, but with its cusp slightly reclined, and also more curved inwards (Fig. 7G); in lateral view, curvature of anterior margin variable; posterior margin also curved, forming an angle of 50–90° with upper margin of the posterior process; anticusp less pointed, with an angle of 60–65° between basal and anterior margins (Fig. 7I–L). *M element* makellate,

Fig. 7 (opposite). *Acodus* sp. cf. *emanuelensis* McTavish, 1973: *A–C*, Pa element, AMF120282, M/A3, A, inner lateral view, B, basal view, C, outer lateral view; *D–F*, Pa element, AMF120283, M/A3, D, inner lateral view, E, basal inner lateral view, F, outer lateral view; *G*, Pb element, AMF120290, M/A3, upper view; *H*, M element, AMF120288, M/A7, posterior view; *I–K*, Pb element, AMF120292, M/A4, I, outer lateral view, J, basal view, K, inner lateral view; *L*, Pb element, AMF120291, M/A11-3, outer lateral view; *M*, ?M element, AMF120293, TAB1/39.5, posterior view; *N*, M element, AMF120289, Y4–8, anterior view; *O*, M element, AMF120295, M/A3, anterior view; *P*, Sa element, AMF120298, C1613, posterolateral view; *Q*, Sa element, AMF120299, M/A3, anterolateral view; *R*, Sa element, AMF120297, M/A3, posterior view; *S*, Sb element, AMF120300, M/A4, lateral view; *T*, Sb element, AMF120301, M/A3, anterolateral view; *U*, Sc element, AMF120286, M/A7, outer lateral view; *V*, Sc element, AMF120287, M/A7, inner lateral view; *W*, Sd element, AMF120294, M/A11-3, upper view; *X*, Sd element, AMF120302, M/A7, upper view; *Y*, Sd element, AMF120303, TAB1/8.1, outer lateral view. Scale bars 100 μm.


A
B
C
D
E
F
G
H
I
J
K
L
M
N
O
P
Q
R
S
T
U
V
W
X
Y

anteroposteriorly compressed, with broad, smooth anterior face (Fig. 7N,O), and a weak basal buttress on the posterior face (Fig. 7H,M); anticusp triangular in outline; outer lateral process low, adenticulate with straight or slightly arched upper margin. *Sa element* symmetrical, triconodelliform, with broad anterior face, a blade-like costa on each lateral face and a third costa along the posterior margin; the three costae extended basally as short adenticulate processes (Fig. 7P–R). *Sb element* like the Sa, but asymmetrical (Fig. 7S,T). *Sc element* laterally compressed with a sharp costa along anterior and posterior margins, which extend basally merging into the upper margin of a low posterior process and an anticusp-like shorter anterior process; cusp slightly inner laterally curved, with smooth lateral faces (Fig. 7U,V). *Sd element* asymmetrical with four blade-like costae, which extend basally into short adenticulate processes (Fig. 7W–Y); costa along the posterior margin stronger than others; one costa on each lateral face, and the fourth costa along the anterior margin, but inner laterally curved (Fig. 7W).

Remarks. Specimens from western New South Wales are identical with those described as *A. emanuelensis* from the Horn Valley Siltstone of central Australia (Cooper, 1981). Although generally comparable with the type material from the Emanuel Formation of the Canning Basin, the New South Wales specimens do not develop the prominent thin blade-like arched upper margin of the posterior process displayed by the figured specimens from the Canning Basin. The Horn Valley material will be described as a new species by R.S. Nicoll (in prep.), to which the western New South Wales specimens would be assigned. Pending completion of that study, the present material is left in open nomenclature. *Acodus* sp. cf. *emanuelensis*, the most common species in the Mount Arrowsmith fauna, exhibits a wide range of variation. Specimens from samples with associated sponge spicules, such as M/A7 (inferred to represent relatively deeper water environments) are smaller, with costae extended basally into adenticulate processes in the S elements (Fig. 7Y). Specimens from other, presumably shallower water, samples are larger with more weakly developed processes (Fig. 7W).

Acodus sp.

Fig. 8M–Q

Material. 16 specimens (S elements) from the Tabita Formation at Mount Arrowsmith; two from unnamed dolomitic limestone unit at Koonenberry Gap.

Remarks. Multicostate coniform elements referred to herein as *Acodus* sp. are symmetrical or nearly so. At least two types can be distinguished: a quadricostate element (Fig. 8Q) with an anterior costa, posterior costa, and one median costa on each lateral side; and a septicostae element (Fig. 8M–P) with rounded anterior face, a costa along the posterior margin, and three costa on each lateral side. An additional pentacostate element was also recovered. It has a broad anterior face, two costae on each side and a posterior costa along the posterior margin, and cusp star-shaped in cross section. These specimens show some resemblance to the S elements of *Acodus comptus* (Branson & Mehl), but with less strongly developed costae in comparison to that species. They might represent a separate species, but the material available now precludes a complete description.

Ansella Fåhraeus & Hunter, 1985

Type species. *Belodella jemtlandica* Löfgren, 1978.

Ansella jemtlandica (Löfgren, 1978)

Fig. 8K,L

"*Belodella*" sp. A Serpagli, 1974: 38,39, pl. 8, fig. 7, pl. 20, fig. 10.
Belodella jemtlandica Löfgren, 1978: 46–49, pl. 15, figs. 1–8, fig. 24A–D (*cum syn.*).
Belodella jemtlandica.–Cooper, 1981, pl. 26, fig. 14.
Ansella jemtlandica Fåhraeus & Hunter, 1985: 1173–1175, pl. 1, figs. 1–5, 9, pl. 2, fig. 12a,b, text-fig. 1 (*cum syn.*).
Ansella jemtlandica.–Albanesi, *in* Albanesi *et al.*, 1998: 160, pl. 1, figs. 18–23, text-fig. 27 (*cum syn.*).

Material. Four specimens (Sa elements) from the Tabita Formation at Mount Arrowsmith, and an additional specimen (Sa) from the unnamed dolomitic limestone unit at Koonenberry Gap.

Remarks. This species is rare in our collections, only the symmetrical Sa element being recovered. It has a proclined cusp, an anterolateral costa on each lateral side, and a thin posterior margin basally bearing a row of small, closely spaced denticles. The specimen illustrated from the Horn Valley Siltstone (Cooper, 1981) is a weakly asymmetrical, acostate Sc element of the same species.

Baltoniodus Lindström, 1971

Type species. *Prioniodus navis* Lindström, 1955.

Baltoniodus sp. A

Fig. 11P–X

?*Baltoniodus navis*.–Cooper, 1981: 168, pl. 30, fig. 2.

Material. Thirteen specimens (11 P, 2 M) from the Tabita Formation at Mount Arrowsmith.

Description. Only P and M elements recovered; the P element is pastinate with denticulate anterior and posterior processes, and adenticulate outer lateral process; cusp more or less triangular in cross section (Fig. 11T,U), with sharp anterior and posterior margins, and smooth inner lateral side; the outer lateral face with a broad costa which extends basally into a short adenticulate process; anterior process extending downward with three or four stout denticles; posterior process longer, bearing five to seven stout denticles; basal cavity open, rather deep. *M element* strongly geniculate, bearing a long anticusp with fine saw tooth-like denticles on its upper margin (Fig. 11Q,R); base of denticles with distinctive surface sculpture (Fig. 11P).

Remarks. The species is assigned to *Baltoniodus* based on its wide basal cavity and orientation of the anterior and posterior processes essentially in a single plane. The P element of this species differs from those of *Oepikodus pincallyensis* in having a much smaller cusp, an adenticulate outer lateral process, and a more open basal cavity. The anterior and posterior processes are more or less straight within a single plane, whereas in the P elements of *Oepikodus pincallyensis* the anterior process is strongly curved inward. The P element described herein is close to the specimen referred to *Baltoniodus navis* illustrated by

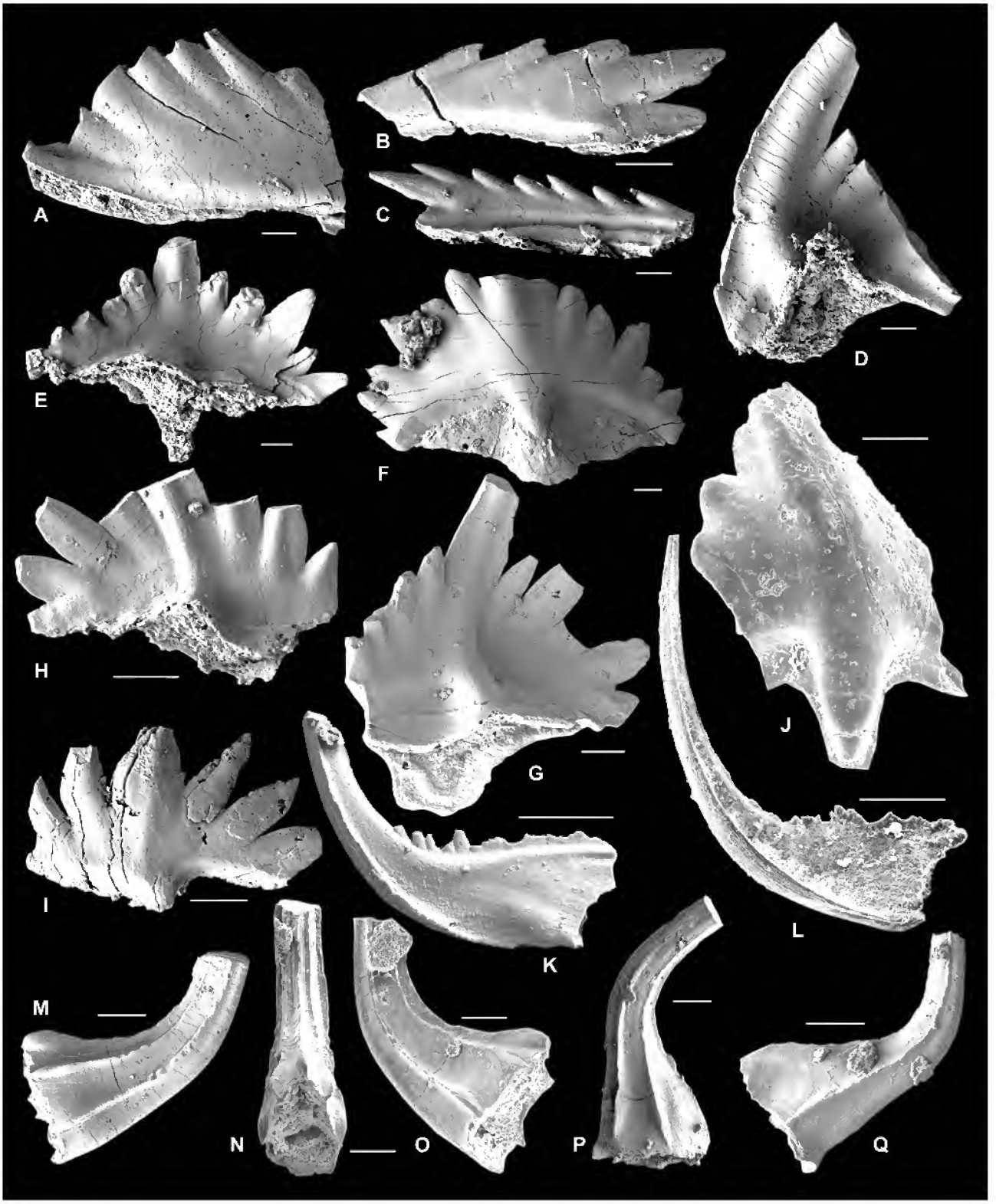

Fig. 8. *A–J*, *Bergstroemognathus kirki* Stait & Druce, 1993: *A*, Pa element, AMF120307, M/A11-3, outer lateral view; *B*, Pb element, AMF120308, M/A11-3, outer lateral view; *C*, Pb element, AMF120309, M/A11-3, inner lateral view; *D*, M element, AMF120310, M/A11-3, posterior view; *E*, Sa element, AMF120311, Y4–4, posterior view; *F*, Sa element, AMF120212, Y4–4, anterior view; *G*, Sb element, AMF120313, Y4–4, posterior view; *H*, Sc element, AMF120314, M/A11-3, posterior view; *I*, Sc element, AMF120315, M/A11-3, anterior view; *J*, Sd element, AMF120316, M/A11-4, anterior view. *K,L*, *Ansella jemtlandica* (Löfgren, 1978): *K*, Sa element, AMF120317, M/A7, lateral view; *L*, Sa element, AMF120318, C1612, lateral view. *M–Q*, *Acodus* sp.: *M–O*, septicostae element, AMF120305, M/A11-3, lateral view; *P*, septicostae element, AMF120304, M/A11-3, lateral view; *Q*, quadricostae element, AMF120306, M/A11-3, lateral view. Scale bars 100 μm.

Cooper (1981, pl. 30, fig. 2) from the Horn Valley Siltstone. However, that element has a longer posterior process bearing up to nine denticles, which are more widely spaced than in the Mount Arrowsmith material. The originally described P elements of *Baltoniodus navis* Lindström, 1955 possess long denticulate outer lateral processes which meet the anterior process at an angle of about 30°, whereas the Tabita Formation species has an adenticulate, short outer lateral process, which is almost normal to the anterior and posterior processes; the anterior process is in the same plane with the posterior process (Fig. 11T,V), or only very slightly curved inner laterally (Fig. 11X).

Bergstroemognathus Serpagli, 1974

Type species. *Oistodus extensus* Graves & Ellison, 1941.

Bergstroemognathus kirki Stait & Druce, 1993

Fig. 8A–J

Bergstroemognathus extensus (Graves & Ellison).–Cooper, 1981: 161, pl. 31, fig. 12, pl. 32, figs. 9–11, *non* fig. 7.

Bergstroemognathus kirki Stait & Druce, 1993: 302–303, figs. 12H, 16D,F–H,J.

Bergstroemognathus kirki.–Zhen *et al.*, 2001: 201–204, figs. 4.14–4.20, 8.1?, 8.2–8.22.

Material. Five specimens (1 M, 4 Sc) from limestone nodules within shales of the upper Yandaminta Quartzite, and 26 specimens (4 Pa, 6 Pb, 4 Sa, 8 Sb, 3 Sc, 1 Sd) from the overlying Tabita Formation at Mount Arrowsmith; seven specimens (2 Pb, 3 Sa, 1 Sb, 1 Sc) from unnamed dolomitic limestone unit at Koonenberry Gap.

Remarks. A septimembrate apparatus of *B. kirki* has been recognized, based on material from the Horn Valley Siltstone of the Amadeus Basin (Zhen *et al.*, 2001). The western New South Wales material has the same apparatus composition.

Cooperignathus Zhen n.gen.

Type species. *Protoprioniodus nyinti* Cooper, 1981.

Etymology. For Dr Barry J. Cooper who described the type species from central Australia.

Diagnosis. Conodonts of ramiform-pectiniform configuration consisting of a seximembrate apparatus; all elements albid, with adenticulate processes, and a prominent basal surface defined by a ledge-like costa parallel to and slightly above the basal margin; P elements pectiniform with a variably developed platform, and adenticulate anterior, posterior, and outer lateral processes; cusp lacking, with the upper surface of the unit occupied by thin blade-like crest(s); basal cavity shallow, represented by a small basal pit and narrow basal grooves extending to tips of the processes; M element makellate, with adenticulate outer lateral and inner lateral processes, basal buttress variably developed; S elements tertiopedate, consisting of nearly symmetrical Sa, slightly asymmetrical Sb, and asymmetrical Sc element.

Remarks. *Cooperignathus* appears closely related to *Protoprioniodus* McTavish, as indicated by the general similarity of their S and M elements. The two genera are distinguished by their P elements, those of *Cooperignathus* being planate, lacking a cusp, but exhibiting a variably developed platform. Species of *Protoprioniodus* have pastinate P elements with a prominent cusp, and a more open basal cavity.

One of the most distinctive characters of *Cooperignathus* is the development of a ledge-like costa to define the basal surface. A comparable structure is also developed in the elements of *Protoprioniodus yapu*, and some specimens referable to *Acodus* sp. cf. *emanuelensis* (Fig. 9A) from western New South Wales. Evolution of *Cooperignathus* from *Protoprioniodus* may have proceeded firstly by reduction and subsequent total loss of the cusp, accompanied by an increase in the area of the basal surface, and secondly by the displacement of this area from the basal lateral side to the underside of the P elements (Fig. 9). The *Cooperignathus* apparatus appears to be the earliest form with planate elements, and phylogenetically might represent an early stage of evolutionary development of the Polyplacognathidae clade.

Two species, *C. aranda* and *C. nyinti*, are included in *Cooperignathus*. They are widely distributed in the Early Ordovician (*O. evae* Zone) of Australia, South China and North America. Because the diagnostic P elements are relatively rare, both species were previously ascribed to *Protoprioniodus* based on the M and S elements.

Occurrence. Horn Valley Siltstone, Amadeus Basin (Cooper, 1981), Coolibah Formation, Georgina Basin (Stait & Druce, 1993) in central Australia; Tabita Formation at Mount Arrowsmith, and unnamed dolomitic limestone unit at Koonenberry Gap, western New South Wales (herein); Dawan Formation, Hubei Province, South China (An, 1987); Wah Wah Limestone, Ibex area of western Utah (Ethington & Clark, 1982), Juab Limestone, Utah (Sweet *et al.*, 1971; Ethington & Clark, 1982); El Paso Group, western Texas and southern New Mexico (Repetski, 1982); Broken Skull and Sunblood formations, southern District of Franklin, Canada (Tipnis *et al.*, 1978); upper part of the Eleanor River and Ship Point formations, Arctic Canada (Barnes, 1974); Cow Head Group (Pohler, 1994; Johnston & Barnes, 2000), and St. George Group (Stouge, 1982; Ji & Barnes, 1994), western Newfoundland, Canada.

Cooperignathus nyinti (Cooper, 1981)

Figs. 10A–N, 11A–O

New genus A Sweet *et al.*, 1971: *partim* only pl. 1, fig. 19.

New genus A Sweet *et al.*, 1971.–Repetski, 1982: 56, *partim* only pl. 27, figs. 3, 4.

Protoprioniodus nyinti Cooper, 1981: 176, pl. 29, figs. 1–8, 11, 12.

Protoprioniodus nyinti.–Stait & Druce, 1993: *partim* only fig. 19N,O.

Protoprioniodus aranda.–Ethington & Clark, 1982: 87, *partim* only pl. 9, figs. 24–26, 30.

Protoprioniodus aranda.–Johnston & Barnes, 2000: *partim* only pl. 6, figs. 23, 24.

Material. Six specimens (3 M, 1 Sa, 1 Sb, 1 Sc) from limestone nodules within shales of the upper Yandaminta Quartzite, and 62 specimens (6 Pa, 7 Pb, 19 M, 7 Sa, 11 Sb, 12 Sc) from the overlying Tabita Formation at Mount Arrowsmith; one additional specimen (M) from unnamed dolomitic limestone unit at Koonenberry Gap.

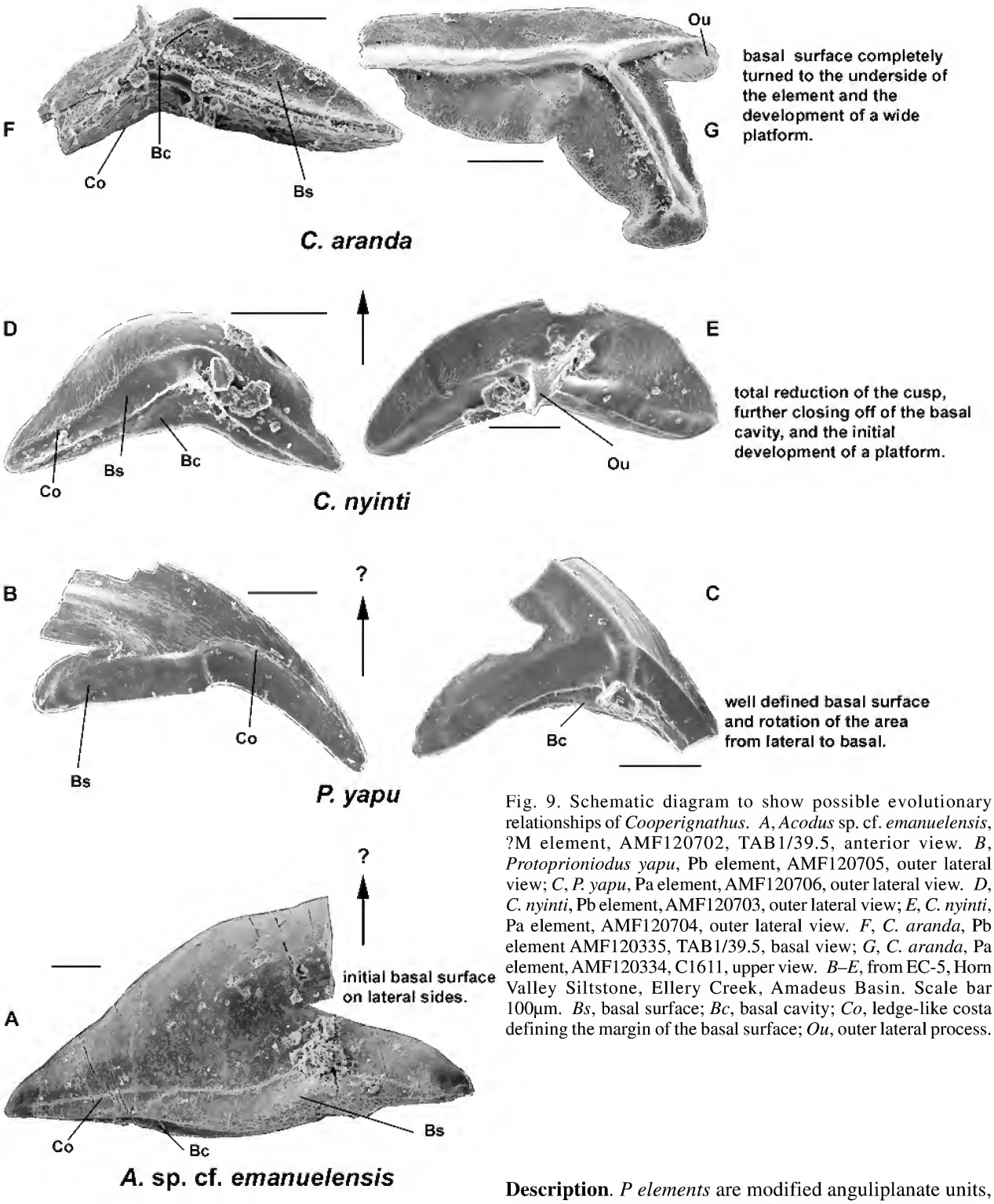

Fig. 9. Schematic diagram to show possible evolutionary relationships of *Cooperignathus*. *A*, *Acodus* sp. cf. *emanuelensis*, ?M element, AMF120702, TAB1/39.5, anterior view. *B*, *Protoprioniodus yapu*, Pb element, AMF120705, outer lateral view; *C*, *P. yapu*, Pa element, AMF120706, outer lateral view. *D*, *C. nyinti*, Pb element, AMF120703, outer lateral view; *E*, *C. nyinti*, Pa element, AMF120704, outer lateral view. *F*, *C. aranda*, Pb element AMF120335, TAB1/39.5, basal view; *G*, *C. aranda*, Pa element, AMF120334, C1611, upper view. *B–E*, from EC-5, Horn Valley Siltstone, Ellery Creek, Amadeus Basin. Scale bar 100μm. *Bs*, basal surface; *Bc*, basal cavity; *Co*, ledge-like costa defining the margin of the basal surface; *Ou*, outer lateral process.

Diagnosis. A ramiform-pectiniform species consisting of a seximembrate apparatus including modified anguliplanate P elements, makellate M element, alate Sa, and modified tertiopedate Sb and Sc elements; all elements albid, with adenticulate processes, and a ledge-like costa lying parallel to and slightly above the basal margin to define the basal surface, which is represented by a shallow groove between this costa and the basal margin.

Description. *P elements* are modified anguliplanate units, arched and crescentic in outline in lateral view, with convex outer lateral face and concave inner lateral face; upper surface with a thin anteroposteriorly extended blade-like crest which lacks recognizable cusp and denticles and curves inwards, and also with its upper margin gently bowed inward; ledge-like costa on each side extending throughout the whole unit, more or less parallel to the basal margin, to define a groove-like basal surface on each side between costa and the basal margin in lateral view, and a narrow platform in the upper view; on the concave side, the groove-like basal surface is more strongly developed and extends

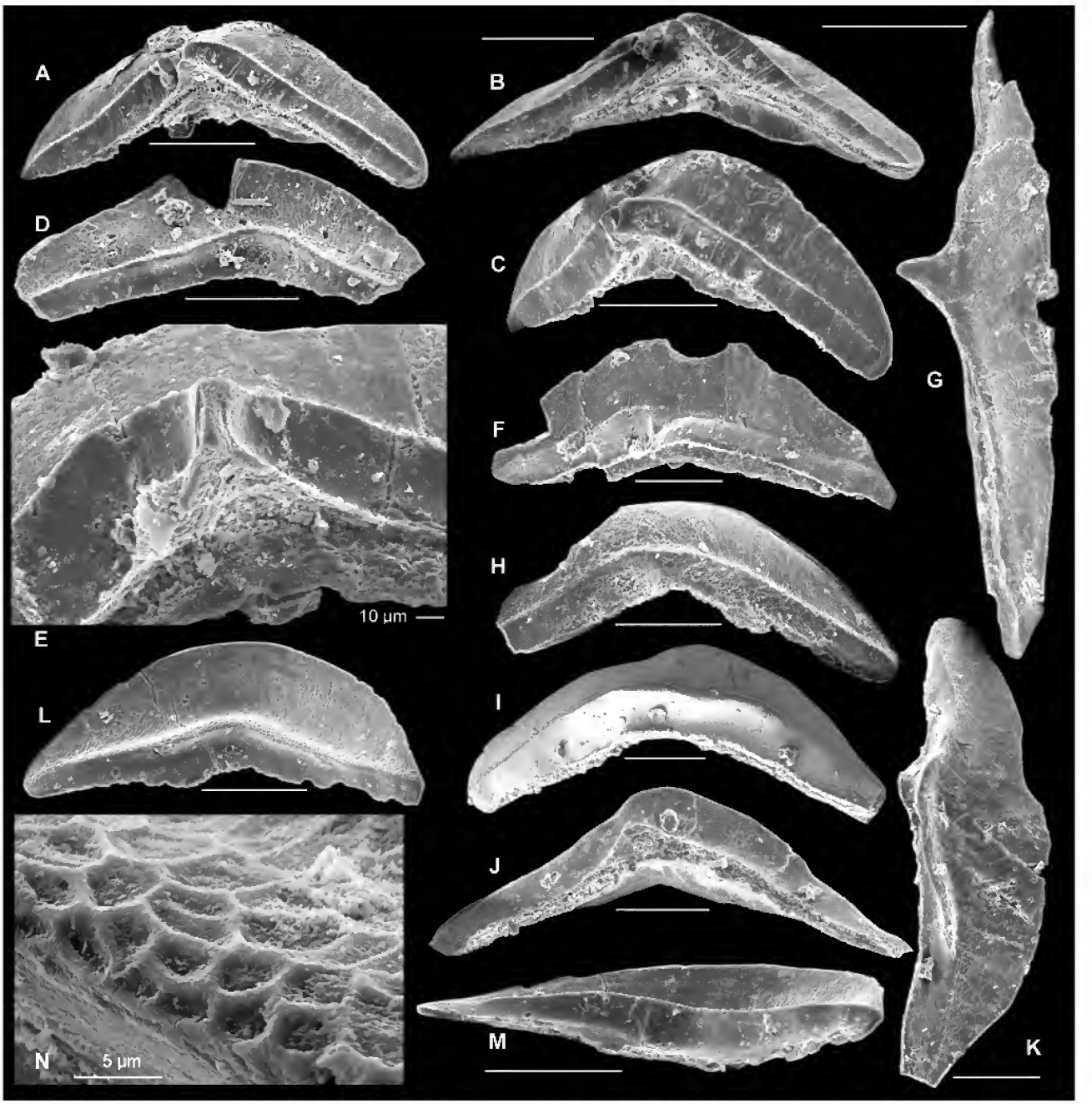

Fig. 10. *Cooperignathus nyinti* (Cooper, 1981): *A–C*, Pa element, AMF120319, M/A7, *A*, basal, outer lateral view, *B*, basal view, *C*, antero-outer lateral view; *D*, Pa element, AMF120320, M/A7, inner lateral view; *E–G*, Pa element, AMF120321, M/A7, *E*, close up showing the basal cavity and outer lateral process, *F*, outer lateral view, *G*, upper, outer lateral view; *H*, Pb element, AMF120322, M/A7, outer lateral view; *I–K*, Pb element, AMF120323, Y4–2, *I*, outer lateral view, *J*, basal view, *K*, upper, outer lateral view; *L–N*, Pb element, AMF120324, M/A7, *L*, inner lateral view, *M*, inner lateral-basal view, *N*, showing reticulate surface structure. Scale bars 100 µm, unless otherwise indicated.

continuously from anterior to posterior extremities; underneath the element, the basal margins on both sides narrow to define a small, shallow basal pit at mid curvature and a narrow groove extending towards the distal ends of the anterior and posterior processes; on the convex side, the Pa element displays a short ridge-like outer lateral process (Fig. 10G) developed between the horizontal, ledge-like costa and the basal margin to divide this groove-like area into a slightly shorter anterior part and a longer posterior part, and basally this short process forms a prominent basal buttress (Fig. 10A–C,E); in the Pb element this outer lateral process is much weaker or even absent (Fig. 10I); surface of the P elements ornamented by reticulation which is best developed near the ledge-like costa (Fig. 10L,N). *M element* anteroposteriorly compressed, with a robust outer laterally strongly recurved cusp, an adenticulate outer lateral process and an adenticulate, anticusp-like inner lateral process; cusp also slightly curved posteriorly, and inner- and outer-lateral processes curved slightly anteriorly; anterior and posterior faces bearing a round-faced costa; basally, the costa on the posterior face is truncated by a strong, ledge-like horizontal costa

Fig. 11. *A–O*, *Cooperignathus nyinti* (Cooper, 1981): *A*, M element, AMF120325, M/A7, anterior view; *B*, M element, AMF120326, TAB1/86.7, basal view; *C*, Sa element, AMF120327, M/A7, lateral view; *D*, Sb element, AMF120328, TAB1/39.5, outer lateral view; *E–J*, Sb element, AMF120329, TAB1/8.1, *E*, upper view, *F*, close up of the cusp, upper view, *G*, outer lateral view, *H*, inner lateral view, *I*, anterior view, *J*, close up showing striation and basal surface, anterior view; *K–M*, Sc element, AMF120330, M/A7, *K*, outer lateral view, *L*, upper inner-lateral view, *M*, upper view; *N*, Sc element, AMF120331, TAB1/39.5, outer lateral view; *O*, Sc element, AMF120332, M/A7, inner lateral view. *P–X*, *Baltoniodus* sp. A; *P,Q*, M element, AMF120425, Y4–2, *P*, close up showing the surface sculpture, *Q*, anterior view; *R*, M element, AMF120426, Y4–2, anterior view; *S*, P element, AMF120423, Y4–7, inner lateral view; *T,U*, P element, AMF120424, M/A7, *T*, upper view, *U*, upper, outer lateral view; *V*, P element, AMF120284, M/A11-5, basal view; *W,X*, P element, AMF120285, M/A11-5, *W*, outer lateral view, *X*, upper view. Scale bars 100 µm, unless otherwise indicated.

extending from the outer lateral process to the inner lateral process, with an acute angle (about 30°) between them; posteriorly, the broad basal buttress defining a more or less triangular opening of the basal cavity (Fig. 11B). *S elements* bearing a tricostate cusp, a sharp costa along the posterior margin, and a costa along the anterolateral corner on each lateral face, and with a broad anterior face; three costae extending basally into three adenticulate processes, which are tripod-like in lateral view; posterior process long, straight or inner laterally curved; lateral processes extending

basally and laterally, ornamented with fine striae which are vertically arranged more or less parallel to the axis of the cusp in anterior view (Fig. 11J); in upper view, the three processes meet the cusp in a T- or Y-shaped junction; three processes with a prominent costa on each side more or less parallel the basal margin to define the basal surface. Three morphotypes are recognized, based mainly on curvature of the posterior process; Sa element symmetrical with straight posterior process; Sb element slightly asymmetrical, with posterior process slightly curved inward and a more strongly downwardly extended inner lateral process; Sc like the Sb, but asymmetrical with a more strongly inwardly curved posterior process.

Remarks. In the Horn Valley Siltstone, *C. nyinti* is very common while *C. aranda* is less so, but always occurs with *C. nyinti* except in the lowest stratigraphic horizons (Cooper, 1981). Morphologically, *C. nyinti* and *C. aranda* are very similar. The latter was originally defined only on S and M elements. No P elements were formally recognized previously for this species, although Cooper (1981: 175) stated that the P element of *C. aranda* might be very similar to its counterpart in *C. nyinti* with differences "solely in size, degree of thickening, and robustness". The S elements of *C. nyinti* and *C. aranda* are similar, except that those of *C. aranda* have an indentation at the junction between the posterior margin of the cusp and the upper margin of the posterior process. The M elements of these two species are also very similar. Both have a strong posterior costa, a basal buttress, and a strong costa paralleling the basal margin to define a basal groove on the posterior face. However, the M element of *C. nyinti* has a more strongly outer-laterally reclined cusp, and a straight or slightly arched basal margin, whereas that of *C. aranda* has a longer inner lateral process with the lowest point of the basal margin underneath the basal buttress, and with a more strongly arched upper margin to the outer lateral process.

The P elements illustrated from the Horn Valley Siltstone (Cooper, 1981) show a distinctive short outer lateral process on the convex outer lateral side that links the horizontal ledge-like costa and the basal margin to divide the groove into two parts. These specimens are referred herein to the Pa position. Re-examination of a large topotype collection of this species confirms that Pa and Pb elements of *C. nyinti* are also represented at the type locality. Like the Horn Valley Siltstone samples, P elements are relatively rare in the Mount Arrowsmith samples, with a similar situation noted in the Wah Wah and Juab formations of the Ibex area, Utah (Ethington & Clark, 1982). These latter authors recorded a ratio of about 8(S):11(M):1(P) for the species (*C. nyinti*+*C. aranda*), and argued that the P elements must have been very minor constituents of the apparatus. Hence they regarded *P. nyinti* as a probable junior synonym of *P. aranda*, and suggested that the differences on which Cooper (1981) distinguished these two species might merely represent a broad spectrum of morphologic variation within the one species apparatus. Repetski (1982), and Johnston & Barnes (2000) expressed similar views. However, recovery of two additional types of pectiniform elements from the Mount Arrowsmith samples, which are now referred to as the Pa and Pb elements of *C. aranda*, strongly suggests the coexistence of the two species of *Cooperignathus*.

Cooperignathus aranda (Cooper, 1981)

Fig. 12A–P

New genus A Sweet *et al.*, 1971: 168, 170, *partim* only pl. 1, fig. 22.
New genus A Sweet *et al.*, 1971.–Repetski, 1982: 56, *partim* only pl. 27, figs. 1, 2, 5, 6.
Protoprioniodus aranda Cooper, 1981: 175, pl. 29, figs. 1, 6, 7, 10, 12.
Protoprioniodus aranda.–Ethington & Clark, 1982: 86, *partim* only pl. 9, figs. 27–29.
Protoprioniodus aranda.–Fåhraeus & Roy, 1993: 30, text-figs. 5.21–5.23.
Protoprioniodus aranda.–Pohler, 1994: 27, *partim* only pl. 6, figs. 10–11, ?12.
Protoprioniodus aranda.–Johnston & Barnes, 2000: 42, *partim* only pl. 6, figs. 17, ?26, 30.
Protoprioniodus costatus.–An, 1987: 174, *partim* only pl. 14, fig. 5.
Protoprioniodus aff. *simplicissimus*.–An, 1987: 175, *partim* only pl. 16, fig. 18.
Protoprioniodus nyinti.–Stait & Druce, 1993: 317, *partim* only fig. 19M.
Protoprioniodus simplicissimus.–Ji & Barnes, 1994: 54, *partim* only pl. 16, figs. 10, 11.

Material. Two specimens (1 M, 1 Sa) from limestone nodules within shales of the upper Yandaminta Quartzite, and 25 specimens (5 Pa, 2 Pb, 10 M, 3 Sa, 4 Sb, 1 Sc) from the overlying Tabita Formation at Mount Arrowsmith; four specimens (1 Pa, 2 M, 1 Sc) from unnamed dolomitic limestone unit at Koonenberry Gap.

Diagnosis. A ramiform-pectiniform species with a seximembrate apparatus, including albid, pastiniplanate P elements, makellate M element, alate Sa, and modified tertiopedate Sb and Sc elements; S elements with a distinctive indentation at the conjunction of the posterior margin of the cusp with the upper margin of the posterior process.

Description. *P elements* bearing a longer anterior process, a posterior process and a shorter posterolaterally extended outer lateral process; each process with a wide platform and an adenticulate blade-like crest, which join at the centre, but without a recognizable cusp; basal cavity small, represented by a weak keel with a narrow groove underneath each process to join a shallow basal pit (Fig. 12E); zone of recessive basal margin not recognized on the basal surface; the Pa element has a wider platform, with anterior and posterior processes strongly curved inwards meeting at an angle of 90–120°; distal end of the posterior process bent sharply downwards; the inner lateral margin of the platform forming a discernible niche at the curvature (Fig. 12B,D). *Pb element* has a narrower platform, and with anterior and posterior processes much less inner laterally curved, meeting at an angle of about 150–160° (Fig. 12F). *M element* anteroposteriorly compressed, with a robust cusp and adenticulate inner and outer lateral processes; in posterior view, the outer lateral process bears a blade-like crest with strongly arched upper margin (Fig. 12I,J), and sharply pointed, inner lateral process (Fig. 12I,K); basal costa extends more or less parallel to the basal margin from distal end of the outer lateral process to the tip of inner lateral process on both anterior and posterior faces (Fig. 12I–K); cusp reclined outer laterally and also slightly curved posteriorly, with a ridge-like costa along the anterior and posterior faces; the costa on the anterior face extends basally to join the basal costa and then merges into a weakly

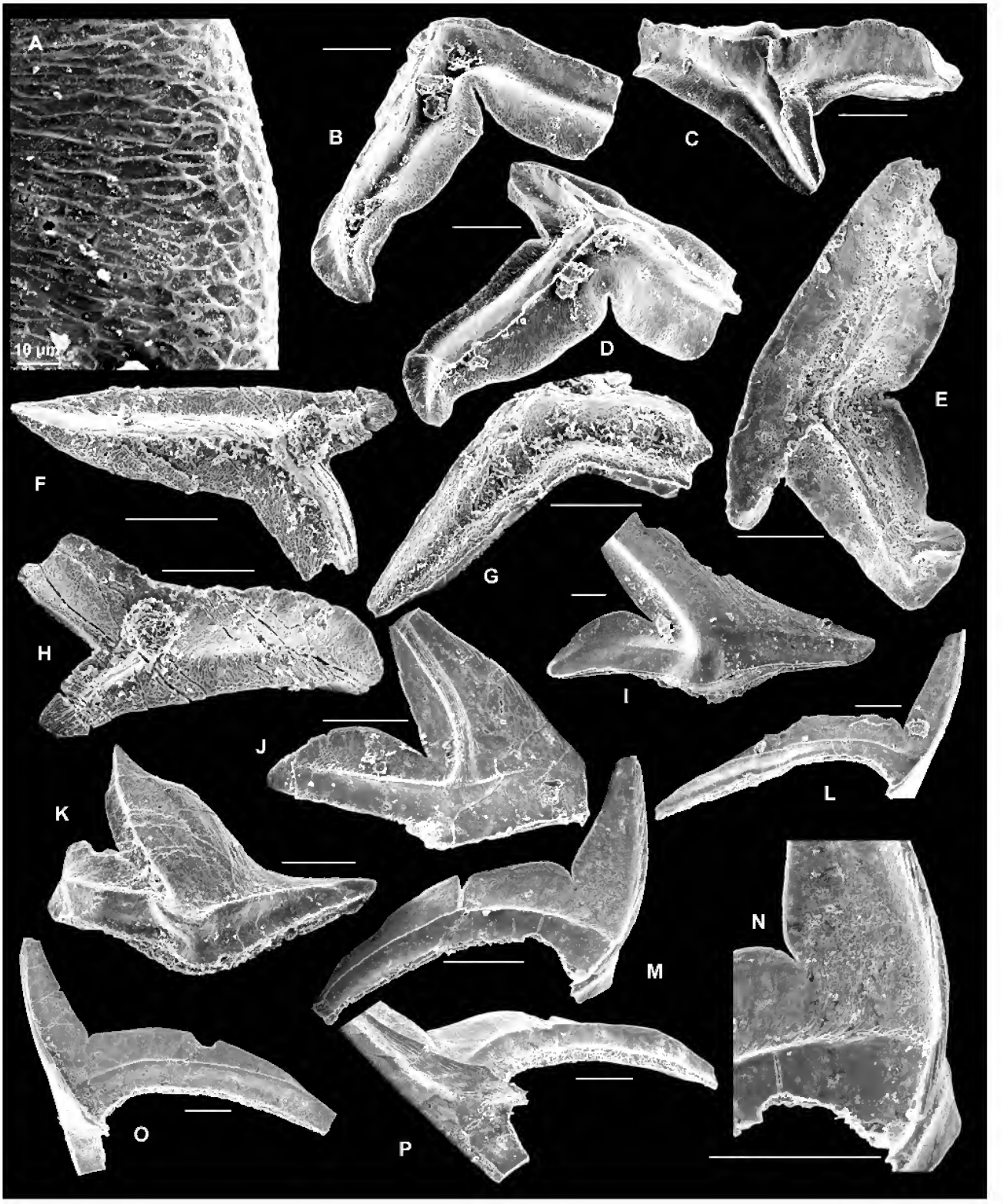

Fig. 12. *Cooperignathus aranda* (Cooper, 1981): *A–D*, Pa element, AMF120333, Y4–4, *A*, close up showing reticulate surface structure, *B*, inner lateral view, *C*, outer lateral view, *D*, inner lateral, upper view; *E*, Pa element, AMF120334, C1611, basal view; *F–H*, Pb element, AMF120335, TAB1/39.5, *F*, upper view, *G*, inner lateral view, *H*, outer lateral, upper view; *I*, M element, AMF120336, W5, anterior view; *J*, M element, AMF120337, M/A7, posterior view; *K*, M element, AMF120338, C1612, basal posterior view; *L*, Sa element, AMF120339, TAB1/65.2, lateral view; *M,N*, Sb element, AMF120340, M/A7, *M*, lateral view, *N*, close up, lateral view; *O,P*, Sc element, AMF120341, Y4–4, *O*, lateral view, *P*, basal lateral view. Scale bars 100 µm, unless otherwise indicated.

developed basal buttress; the costa on the posterior face generally much stronger, truncated by the basal costa and merging with a more strongly developed basal buttress, with an angle of 50–65° between the posterior costa and the basal costa on the outer lateral process; in posterior view, the basal margin curves upwards distally, with the buttress at the lowest point. *S elements* ramiform, but adenticulate, with a prominent suberect or proclined cusp, a long posterior process, and a lateral process on each side along the anterolateral corner; a basal costa developed on each side of both processes, more or less parallel to the basal margin, so defining a shallow groove on each side just above the basal margin; posterior process gently curved downwards distally, bearing a blade-like crest, with gently arched upper margin forming a distinct cleft at its junction with the posterior margin of the cusp (Fig. 12M,N); lateral processes shorter, extending from tip of the cusp as a blade-like costa on each side and produced basally into a short adenticulate process (Fig. 12 O,P); in upper view, the three processes join the cusp to form a T- or Y-shaped junction; Sa element symmetrical (or nearly so) with straight posterior process and equally developed lateral processes; Sb element slightly asymmetrical with posterior process gently curved inner laterally; Sc element asymmetrical with more strongly inner laterally curved posterior and inner lateral processes.

Remarks. Cooper (1981), who described and illustrated only the M and S elements of this species, suggested the possible P element might be similar to its counterpart in the *C. nyinti* apparatus. Two types of pectiniform (pastiniplanate) elements recovered from the Tabita Formation are now designated as the Pa and Pb elements to complete the seximembrate apparatus of *C. aranda*. However, these pectiniform elements were not recorded from the Horn Valley Siltstone (Cooper, 1981; Nicoll, pers. comm. 2002). Similar Pa elements were previously recorded from the El Paso Group of southern New Mexico (Repetski, 1982) in association with S and M elements of *C. aranda* and *C. nyinti*, but one specimen (Repetski, 1982, pl. 27, fig. 5) shows weak development of a secondary process on the distal end of the posterior process. A possible P element of *C. aranda* reported from Ibex area, Utah (Ethington & Clark, 1982: 87), was interpreted as a pathogenic development of the *C. nyinti* P element.

Johnston & Barnes (2000) regarded *Protoprioniodus yapu* Cooper, 1981 as a junior synonym of *C. aranda*. They suggested that *P. yapu* might represent variants of *C. aranda* M elements. However, based on Cooper's definition (1981) of *P. yapu*, distinctive differences exist between the P elements of these two species, as well as in their M and S elements, which allow these two taxa to be readily differentiated.

Cornuodus Fåhraeus, 1966

Type species. *Cornuodus erectus* Fåhraeus, 1966 (= *Drepanodus longibasis* Lindström, 1955).

Remarks. *Cornuodus* was comprehensively revised recently (Löfgren, 1999), with the only known species *C. longibasis* (Lindström, 1955) shown to range from the late Tremadocian to Ashgill. This species had a widespread biogeographic distribution within various biofacies as a minor component of faunas, but is apparently absent from typical North American Midcontinent faunas. Löfgren (1999) suggested that *Cornuodus* was most closely related to *Protopanderodus* and *Drepanodus*, assigning it to the Family Protopanderodontidae, Lindström, 1970.

Cornuodus longibasis (Lindström, 1955)

Fig. 13A–D

"Cornuodus" longibasis Serpagli, 1974: 43, pl.7, fig. 2a,b, pl. 20, fig. 21.
Cornuodus longibasis.–Cooper, 1981: 161, pl. 26, figs. 10–11.
Cornuodus longibasis.–Löfgren, 1999: 175–184, pls. 1–3 (*cum syn.*).
Cornuodus longibasis.–Johnston & Barnes, 2000: 15, pl. 7, figs. 3, 4, 8, 9 (*cum syn.*).
Cornuodus longibasis.–Zhen *et al.*, in press: pl. 2, fig. 19 (*cum syn.*).

Material. Five specimens from limestone nodules within shales of the upper Yandaminta Quartzite, and 109 specimens from the overlying Tabita Formation at Mount Arrowsmith; three specimens from unnamed dolomitic limestone unit at Koonenberry Gap.

Remarks. Löfgren (1999) recently defined a septimembrate apparatus for the species. However, we experienced great difficulties in differentiating our specimens, which all seem to be S elements. No P elements have been confirmed in the western New South Wales collections.

Drepanodus Pander, 1856

Type species. *Drepanodus arcuatus* Pander, 1856.

Drepanodus sp.

Fig. 13E–I

Material. Eight specimens (2 arcuatiform, 2 graciliform, 4 sculponeaform) from limestone nodules within shales of the upper Yandaminta Quartzite, and 52 specimens (23 arcuatiform, 17 graciliform, 12 sculponeaform) from the overlying Tabita Formation at Mount Arrowsmith; ten specimens (5 arcuatiform, 3 graciliform, 2 sculponeaform) from unnamed dolomitic limestone unit at Koonenberry Gap.

Remarks. This species of *Drepanodus* comprises small, albid, laterally compressed, conical units with sharp anterior and posterior margins and smooth lateral sides. The basal cavity is relatively deep, extending to near the maximum curvature of the cusp. Three morphotypes have been recovered. The arcuatiform element is nearly symmetrical with a proclined cusp. The graciliform element is asymmetrical with a slightly reclined cusp, and the sculponeaform element is nearly symmetrical and has a recurved cusp. Elements resemble those of the type species of the genus, but lack a prominent mid-carina on the lateral faces (van Wamel, 1974). Arcuatiform elements referred to *D. arcuatus*, illustrated from the Ninguo Formation of southeast China (Z.H. Wang & Bergström, 1999, pl. 2, figs. 4, 5), also have smooth lateral faces, but the Chinese specimens exhibit a posteriorly reclined cusp.

Drepanoistodus Lindström, 1971

Type species. *Oistodus forceps* Lindström, 1955.

Remarks. Nicoll (1994) suggested that most euconodonts in the Order Protopanderodontida comprised seximembrate coniform-coniform apparatuses including S (Sa, Sb, Sc, Sd) and P (Pa, Pb) elements. However, this configuration for

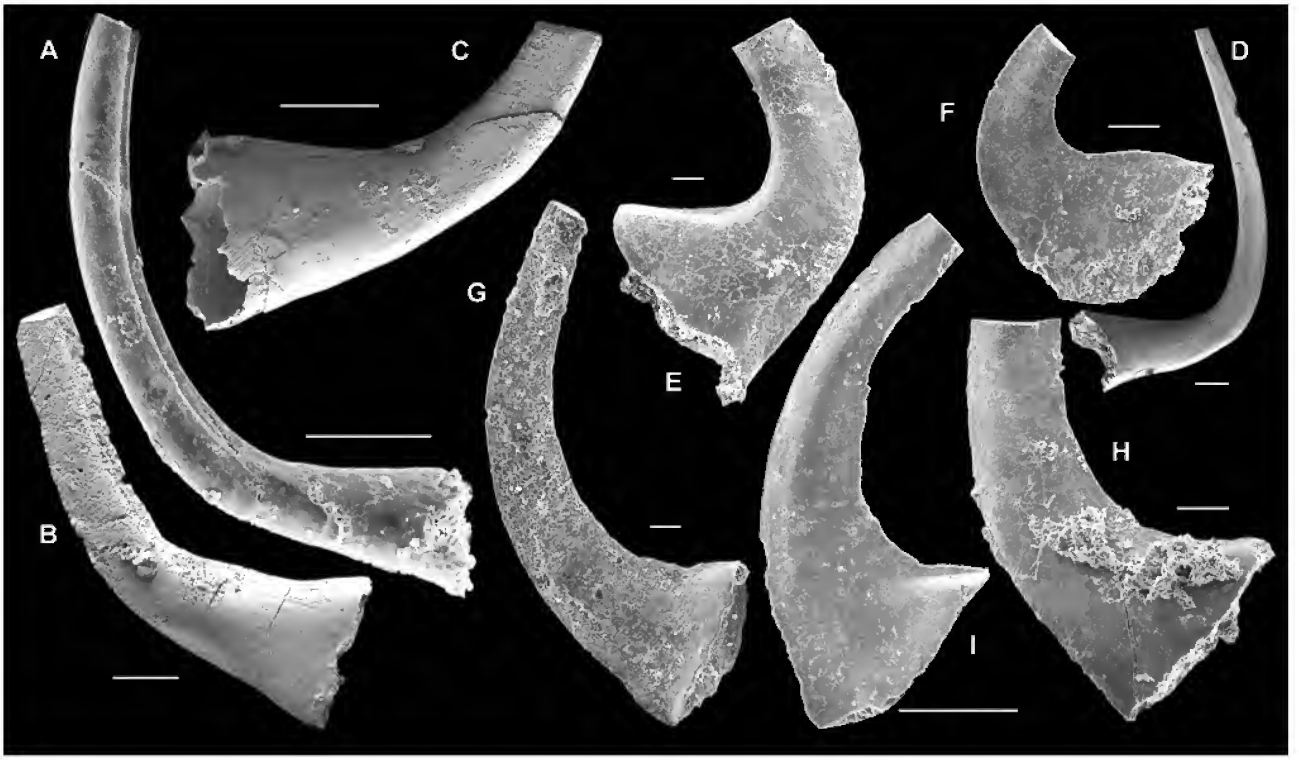

Fig. 13. *A–D*, *Cornuodus longibasis* (Lindström, 1955): *A*, Sa element, AMF120342, Y4–2, lateral view; *B*, Sa element, AMF120343, M/A11-3, lateral view; *C*, Sd2 element, AMF120344, M/A11-3, lateral view; *D*, Sb element, AMF120345, M/A11-2, inner lateral view. *E–I*, *Drepanodus* sp.: *E*, sculponeaform element, AMF120346, C1613, outer lateral view; *F*, sculponeaform element, AMF120347, W5, inner lateral view; G. arcuatiform element, AMF120348, C1612, inner lateral view; *H*, arcuatiform element, AMF120349, C1613, outer lateral view; *I*, graciliform element, AMF120350, Y4–8, outer lateral view. Scale bars 100 μm.

coniform species has not subsequently been widely accepted. Hence the commonly used notation schemes are followed for the two species of *Drepanoistodus* documented herein.

Drepanoistodus basiovalis (Sergeeva, 1963)

Fig. 14A–K

Oistodus basiovalis Sergeeva, 1963: 96, pl. 7, figs. 6, 7, text-fig. 3.
Drepanoistodus basiovalis Löfgren, 1978: 55, pl. 1, figs. 11–17, fig. 26B,C (*cum syn.*).
Drepanoistodus suberectus Cooper, 1981: 164, pl. 26, figs. 1, 2, 6.
Drepanoistodus basiovalis.–Johnston & Barnes, 2000: 18, pl. 11, figs. 10, 11, 15, 16 (*cum syn.*).

Material. Thirteen specimens (4 P, 1 M, 1 Sa, 3 Sb, 4 Sc) from limestone nodules within shales of the upper Yandaminta Quartzite, and 123 specimens (11 P, 31 M, 21 Sa, 41 Sb, 19 Sc) from the overlying Tabita Formation at Mount Arrowsmith; 21 specimens (3 P, 4 Sa, 8 Sb, 6 Sc) from unnamed dolomitic limestone unit at Koonenberry Gap.

Description. Apparatus quinquimembrate, all elements are hyaline, laterally compressed with sharp anterior and posterior margins, non-costate lateral faces, and have an open basal cavity. The *P element* (Fig. 14A,B,D–F,H) is asymmetrical with a reclined cusp and an extended anterobasal corner, triangular in outline. The M element is geniculate with a short outer lateral process, and a rounded inner lateral corner; a mid-carina may develop on the anterior and posterior faces (Fig. 14J,K). The *S elements* consist of a symmetrical (or nearly so) Sa element with an erect cusp (Fig. 14G), an asymmetrical Sb element with a reclined cusp and an oval-shaped opening of the basal cavity (Fig. 14C), and an asymmetrical Sc element with a strongly recurved, more laterally compressed cusp, having a narrower opening of the basal cavity (Fig. 14I).

Remarks. The definition of this widely distributed species given by Löfgren (1978) is followed here. However, the element with an outer lateral costa (Löfgren, 1978, pl. 1, fig. 12) is not recognized in our collections. The P element corresponds to the scandodiform element of many previous authors (e.g., Stouge & Bagnoli, 1990, pl. 5, fig. 19). Compared with their material from Sweden, M elements from western New South Wales are characterized by a shorter outer lateral process.

Drepanoistodus costatus (Abaimova, 1971)

Fig. 15A–R

Drepanodus costatus Abaimova, 1971: 490, pl. 10, fig. 6, text-fig. 3.
Scolopodus cornutiformis Lee, 1976: 172, pl. 2, fig. 18.
Drepanodus pitjanti Cooper, 1981: 162, pl. 26, figs. 3–5, 7, 8.
Scolopodus flexilis An, 1981: 216, pl. 3, figs. 1, 2.
Scolopodus flexilis.–An *et al.*, 1983: 142, pl. 14, figs. 13–18, pl. 33, fig. 4.
Scolopodus ordosensis Z.H. Wang & Luo, 1984: 284, pl. 4, figs. 22, 23.
Drepanodus pitjanti.–Watson, 1988: 111, pl. 3, figs. 14, 16, 17, pl. 5, fig. 15.
Scolopodus flexilis.–An & Zheng, 1990: 173, pl. 5, figs. 1–6 (*cum syn.*).
Drepanodus? costatus.–Smith, 1991: 30, fig. 17k.
Drepanoistodus costatus Stait & Druce, 1993: 303, figs. 12L,M, 17J,K,M,N,?L (*cum syn.*).
Drepanodus pitjanti.–Albanesi, *in* Albanesi *et al.*, 1998: 136, pl. 4, figs. 1–7, text-fig. 16.

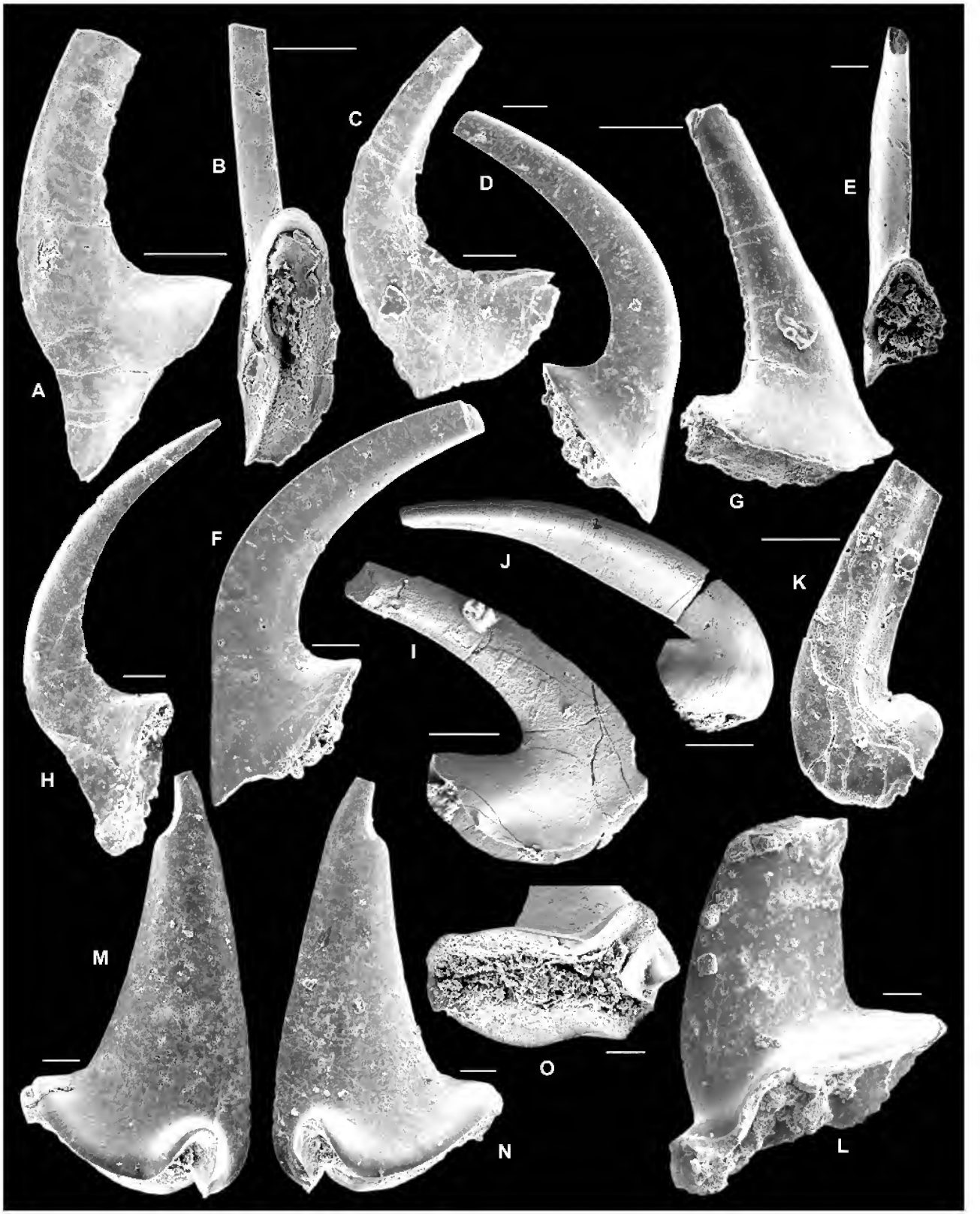

Fig. 14. *A–K*, *Drepanoistodus basiovalis* (Sergeeva, 1963): *A,B*, P element, AMF120351, Y4–2, *A*, outer lateral view, *B*, basal view; *C*, Sb element, AMF120352, M/A7, outer lateral view; *D–F*, P element, AMF120354, W5, *D*, outer lateral view, *E*, posterior view, *F*, inner lateral view; *G*, Sa element, AMF120356, M/A11-3, lateral view; *H*, P element, AMF120355, Y4–2, outer lateral view; *I*, Sc element, AMF120358, M/A11-2, inner lateral view; *J*, M element, AMF120357, Y4–2, anterior view; *K*, M element, AMF120353, A/M11–3, posterior view. *L*, *Drepanoistodus* sp., AMF120360, W5, outer lateral view. *M–O*, *Ulrichodina* sp. cf. *simplex* Ethington & Clark, 1982, AMF120359, W5, *M,N*, lateral views, *O*, basal view. Scale bars 100 μm.

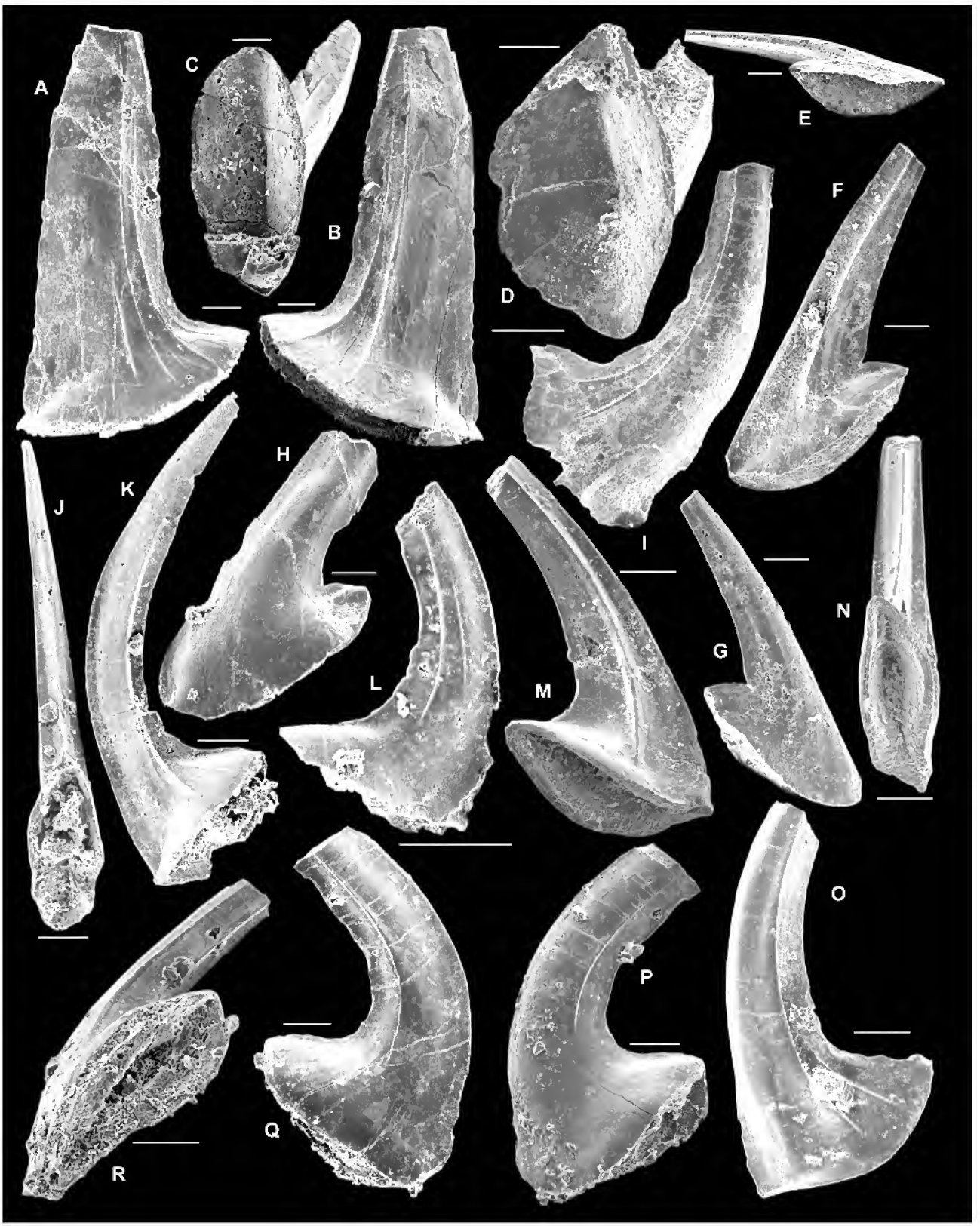

Fig. 15. *Drepanoistodus costatus* (Abaimova, 1971): *A–C*, Sa element, AMF120361, TAB1/78.2, *A*, anterolateral view, *B*, lateral view, *C*, basal view; *D*, Sa element, AMF120362, C1612, basal view; *E–G*, M element, AMF120369, C1611, *E*, basal view, *F*, posterior view, *G*, anterior view; *H*, M element, AMF120368, TAB1/86.7, anterior view; *I*, Sb element, AMF120363, C1612, outer lateral view; *J,K*, Sb element, AMF120364, M/A11-5, *J*, basal view, *K*, inner lateral view; *L*, Sc element, AMF120365, M/A7, inner lateral view; *M–O*, Sc element, AMF120366, Y4–8, *M*, inner lateral view, *N*, basal view, *O*, outer lateral view; *P–R*, Sd element, AMF120367, Y4–7, *P,Q*, lateral views, *R*, basal view. Scale bars 100 μm.

Material. One specimen (Sa) from limestone nodules within shales of the upper Yandaminta Quartzite, and 71 specimens (8 M, 9 Sa, 21 Sb, 20 Sc, 13 Sd) from the overlying Tabita Formation at Mount Arrowsmith; 20 specimens (6 M, 4 Sa, 6 Sb, 3 Sc, 1 Sd) from unnamed dolomitic limestone unit at Koonenberry Gap.

Remarks. Specimens from western New South Wales appear identical to the type material of *D. pitjanti*, from the Horn Valley Siltstone, for which Cooper (1981) recognized a quinquimembrate apparatus consisting of an M and four S elements. Albanesi (*in* Albanesi *et al.*, 1998) reinterpreted the Sb element originally defined by Cooper (1981), as occupying the P position of the apparatus.

Cooper (1981) suggested that *D. pitjanti* and *Drepanodus costatus* are closely related, but that the latter lacks a geniculate M element. In material from the Coolibah Formation of the Georgina Basin, central Australia, Stait & Druce (1993) also recognized a quinquimembrate (M, Sa to Sd) apparatus for *Drepanodus costatus*, and referred this species to *Drepanoistodus*. They suggested that *D. costatus* could be differentiated from *D. pitjanti* mainly by its more strongly costate cusp. Stait & Druce (1993) correctly regarded *Scolopodus flexilis* An—widely distributed in the Liangjiashan Formation and the Beianzhuang Formation (Lower Majiagou Formation) of North China—as a junior synonym of *D. costatus*. With its less strongly developed costa, *S. flexilis* is very similar morphologically to the type material of *D. pitjanti*. The M element of the Chinese species (An & Zheng, 1990, pl. 5, fig. 2; referred to as a graciliform element) is almost identical with the M element of *D. costatus* illustrated from the Coolibah Formation (Stait & Druce, 1993), except that only one strong costa and an additional much weaker costa are developed on the posterior face, whereas the illustrated Coolibah specimen (Stait & Druce, 1993, fig. 17J) shows three much less strongly developed costae. The M element (Fig. 15E–H) of the Mount Arrowsmith and Koonenberry Gap material is identical to that of *D. pitjanti* from the Horn Valley Siltstone, both forms being characterized by a single strong costa on the posterior face. They also have a cusp more strongly outer laterally curved than do corresponding elements illustrated from the Georgina Basin and North China. The complex variations in the number of costae and other morphological details of M elements in the taxa discussed above suggest that such characters are of little or no use in differentiating these species.

Drepanoistodus sp.

Fig. 14L

Material. Four specimens from limestone nodules within shales of the upper Yandaminta Quartzite, and four specimens from the Tabita Formation, at Mount Arrowsmith; an additional specimen from unnamed dolomitic limestone unit at Koonenberry Gap.

Remarks. Specimens of a large suberect element, here identified as *Drepanoistodus* sp. (Fig. 14L), are asymmetrical with the basal cavity inflated inner-laterally and with an undulose basal margin at the inner side. Löfgren (1978) noticed some variations among Swedish specimens assigned to the P element of *D. basiovalis*. Some forms showing a flaring anterobasal corner (Löfgren, 1978, pl. 1, fig. 13), are comparable with the elements here referred to *D.* sp. This element might occupy the Pa position to complete a seximembrate apparatus for *D. basiovalis*.

Erraticodon Dzik, 1978

Type species. *Erraticodon balticus* Dzik, 1978.

Diagnosis. Septimembrate apparatus with a ramiform-ramiform structure including digyrate (or modified) P, makellate M, alate Sa, bipennate Sb and Sc, and tertiopedate Sd, hyaline elements with a prominent cusp, discrete peg-like denticles on the processes, and a shallow basal cavity.

Remarks. The type material of *E. balticus* was recovered from an erratic boulder found near Kartuzy, Pomerania, Poland, but believed to be transported from the Baltic region. Dzik (1978) originally recognized a seximembrate apparatus for the species, consisting of a makellate M, which has a denticulate outer lateral process but apparently lacks an anticusp (Dzik, 1978, pl. 15, fig. 5, text-fig. 6d), bipennate Sb and Sc with a denticulate posterior process and an anterolateral process, tertiopedate Sa and Sd with a denticulate posterior process and a lateral process on each side, and digyrate Pb elements (Dzik, 1978, text-fig. 2, spathognathiform element). Subsequently, Dzik (1991) indicated that the species had a septimembrate composition, but unfortunately provided neither description nor further details of the revised apparatus. Based on his schematic illustration (Dzik, 1991, p. 299, text-fig. 12A), both Pa and Pb elements are digyrate; the Pb (Dzik, 1991, text-fig. 12 A-sp) has a straight basal margin, and an anterior costa which extends to the anticusp, while the Pa (Dzik, 1991, text-fig. 12A-oz) has a rather strongly arched basal margin and lacks an anticusp. The other elements he illustrated are reinterpreted here as ne=M, tr=Sa, pl=Sd, ke-hi=Sb, and lo=Sc.

Watson (1988, pl. 8, fig. 13) recovered a very rare bipennate element with a long, curved posterior process from the Goldwyer Formation of the Canning Basin which he attributed to *E. balticus*. This may represent a variant of the Sb element.

Erraticodon balticus is characterized by having an accentuated denticle on the posterior process of the Sa, Sb and Sc elements. The species is widely distributed in the Baltic region and the Siberian Platform (Dzik, 1978), the Canning Basin of Western Australia (Watson, 1988), South China (Ding *et al.*, *in* Wang, 1993), Argentine Precordillera (Lehnert, 1995; Albanesi, *in* Albanesi *et al.*, 1998), Utah (Ethington & Clark, 1982), and western Newfoundland (Stouge, 1984; Pohler, 1994; Johnston & Barnes, 2000).

Three additional named species are ascribed to *Erraticodon*. Locally these include *E. patu* Cooper, of *O. evae* Zone age, from the Horn Valley Siltstone (Cooper, 1981), the Tabita Formation at Mount Arrowsmith and an unnamed unit at Koonenberry Gap. Records of this species outside Australia are in need of reassessment. The stratigraphically younger *E. balticus* supposedly co-occurs with *E. patu* at the top of the San Juan Formation in the Argentine Precordillera, but of the four illustrated specimens, only an Sa element (Lehnert, 1995, pl. 10, fig. 11) can be assigned doubtfully to *E. patu*. Illustrated P elements from the Suri Formation (*navis* Zone) in the

Famatina Range of western Argentina (Albanesi & Vaccari, 1994) seem comparable with those of *E. patu* from western New South Wales, but associated S and M elements from western Argentina do not conclusively belong to *E. patu*. Bauer (1990) reported *E. patu* from the McLish Formation of the Arbuckle Mountains, Oklahoma. A mid-late Darriwilian age was suggested for this unit, based on the occurrence of *Eoplacognathus* and other typical Middle Ordovician taxa (Bauer, 1987). Of the two figured specimens referred to *E. patu*, even the generic assignment is doubtful for one (Bauer, 1990, pl. 2, fig. 17). The other figured specimen is a Pb element, resembling *E. patu* but probably more closely related to an unpublished new species of *Erraticodon* from the Oakdale Formation (mid-late Darriwilian) of central New South Wales (Zhen & Percival, in prep.). Cooper (1981) indicated that *E. patu* also occurred in the Whiterockian Bay Fiord Formation of Arctic Canada (Nowlan, 1976). The description and illustration of the Canadian specimens (Nowlan, 1976: 442–445, pl. 11, figs. 1–11) indicate that they too are closely related to the unpublished species from the Oakdale Formation. The Pa and Pb elements of this Canadian species are comparable with those of *E. patu*, but S and M elements of these two species are readily distinguishable.

Erraticodon tangshanensis Yang & Xu, *in* An *et al.*, 1983, first described from the Beianzhuang Formation (*evae* to *originalis* zones) and the Majiagou Formation (Middle Ordovician) of North China, consists of a septimembrate apparatus, which differs from that of *E. balticus* in having a modified digyrate Pa element, and in possessing stout denticles on the Sa element. It has also been reported from Korea (Lee, 1975, 1976, 1979), and from the Coolibah Formation of the Georgina Basin (Stait & Druce, 1993), but this latter occurrence in central Australia is questionable, given that it is based on four poorly preserved specimens. The two figured specimens (Stait & Druce, 1993, fig. 21B,C) do not appear to be conspecific with *E. tangshanensis*.

The other species, *E. hexianensis* An & Ding, 1985, consists of a quinquimembrate apparatus. The type material was from the Lower Ordovician Xiaotan Formation of Anhui Province (An & Ding, 1985), but the full stratigraphic range extends from the upper Lower Ordovician (Dawan Formation and equivalents) to the Middle Ordovician (Kuniutan Formation and equivalents) of South China (Ding *et al.*, *in* Wang, 1993). S elements (Sa, Sb, Sc, Sd) of *E. hexianensis* resemble those of *E. patu*, except that the Sc element of *E. hexianensis* has a shorter anterior process. The M element of the Chinese species has an erect cusp with rounded inner lateral corner, and apparently has neither anticusp nor denticles on the inner lateral corner. P elements of *E. hexianensis* were not adequately illustrated or documented; the only figured Pb element (An & Ding, 1985, pl. 1, fig. 15) seems digyrate with a robust cusp, a sharp anterior costa, and a lateral process on each side with three denticles. However, in a later publication, An (1987, pl. 22, fig. 12) illustrated this same specimen but referred it to *Phragmodus* sp. Further confusion arises because although this and the immediately preceding figure are stated in the caption to plate 22 of An (1987) to be different views of the one specimen, this does not seem to be the case. Nicoll (pers. comm. 2002) suggested that this and another specimen (figured by An, 1987, pl. 22, fig. 15 as *Oulodus* sp.) might represent the Pb and Pa elements of *E. hexianensis* respectively.

A potential fifth species of the genus, referred to herein as *E.* sp. A, is a rare component in the Tabita Formation fauna, but due to limited material is not formally named. Features distinguishing it from *E. patu* are discussed below.

Erraticodon patu Cooper, 1981

Figs. 16A–K, 17A–O

Erraticodon patu Cooper, 1981: 166, pl. 32, figs. 1–6, 8.
Erraticodon patu.–Nicoll, 1990, fig. 2.1.
?*Erraticodon patu*.–Albanesi & Vaccari, 1994: 137, pl. 1, figs. 11–16.
?*Erraticodon patu*.–Lehnert, 1995: 88, pl. 10, *partim* only fig. 11.

Material. 314 specimens (48 Pa, 29 Pb, 44 M, 29 Sa, 50 Sb, 59 Sc, 55 Sd) from the Tabita Formation at Mount Arrowsmith, and eight specimens (1 Pb, 1 M, 1 Sa, 1 Sb, 2 Sc, 2 Sd) from unnamed dolomitic limestone unit at Koonenberry Gap.

Diagnosis. A species of *Erraticodon* with a septimembrate ramiform-ramiform apparatus, consisting of digyrate Pa and Pb elements, makellate M, alate Sa, bipennate Sb and Sc, and tertiopedate Sd elements; all hyaline with a prominent cusp, and two or three denticulate processes bearing discrete peg-like denticles; cusp bearing two or three thin, flange-like costae which extend basally to form the upper margin of the processes; basal cavity shallow, extending as shallow grooves towards the tips of the processes.

Description. *Pa element* digyrate with a less prominent cusp than the Pb element; the inner lateral process extending horizontally, with a straight basal margin which is normal to the axis of the cusp; the outer lateral process extending downwards at an angle of about 130° to the cusp, with a gently arched basal margin. The cusp varies from straight and erect (Fig. 16A,B) to prominently curved posteriorly (Fig. 16C); in the latter variation, denticles on the lateral processes also curve posteriorly; cusp and denticles have broad anterior and posterior faces and a flange-like costa on each lateral face; in cross section, cusp and denticles vary from rounded near the base to anteroposteriorly compressed towards the tips; shallow basal cavity represented by a small pit beneath the cusp, extending as a faint basal groove underneath each of the lateral processes. *Pb element* is a modified digyrate element with a lateral process on each side, bearing up to five denticles, and a shorter anterior process generally bearing three denticles; cusp erect (Fig. 16E), rounded or water drop-like in cross section near the base (Fig. 16G), with a sharp anterior margin, broadly rounded posterior face (Fig. 16D,G,H), and a thin flange-like lateral costa on each side which extend downwards to form the upper margin of the lateral process; the anterior process inner laterally curved, in the same plane as the outer lateral process, and forming an angle of 60–70° with the inner lateral process in upper view (Fig. 16G,H); denticles on the lateral processes more or less rounded in cross section near the base, but towards tips they become anteroposteriorly compressed with sharp lateral margins marked by a flange-like costa, and broad anterior and posterior faces; denticles on the anterior process compressed laterally with sharp anterior and posterior margins, marked by a flange-like costa extending from the tip of the cusp, along its anterior margin and the upper

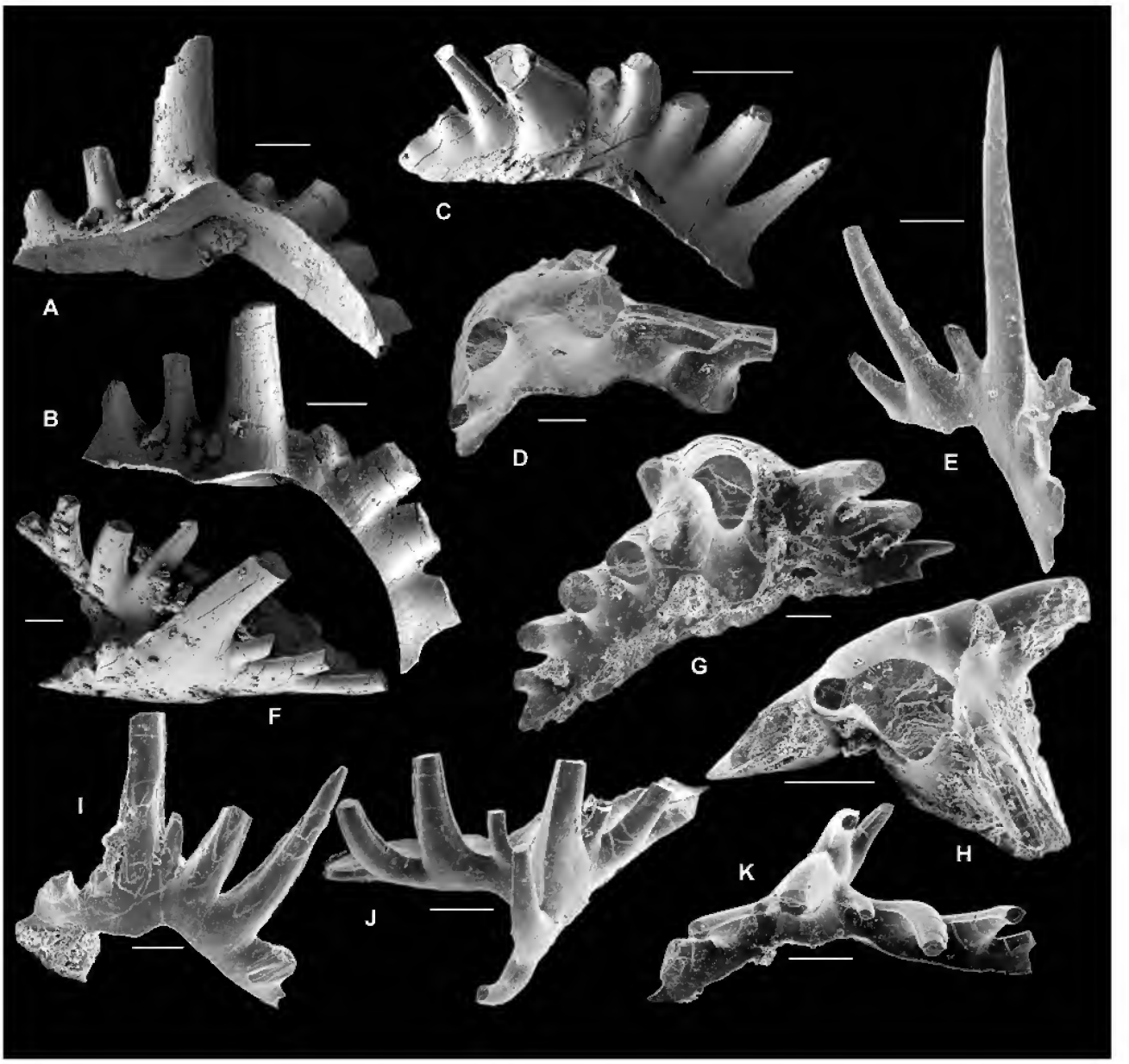

Fig. 16. *Erraticodon patu* Cooper, 1981: *A,B*, Pa element, AMF120370, M/A11-3, *A*, posterobasal view, *B*, posterior view; *C*, Pa element, AMF120371, Y4–6, posterior view; *D*, Pb element, AMF120372, M/A4, postero-upper view; *E*, Pb element, AMF120373, Y4–5, antero-outer lateral view; *F*, Pb element, AMF120374, Y4–7, upper, anterior view; *G*, Pb element, AMF120375, Y4–7, upper, posterior view; *H*, Pb element, AMF120376, M/A4, upper, posterior view; *I*, Pa element, AMF120296, Y4–6, anterior view; *J,K*, Pb element, AMF124209, M/A7, *J*, antero-upper view, *K*, postero-upper view. Scale bars 100 μm.

margin of the anterior process, to the distal end of the process (Fig. 16J,K). *M element* makellate with a shorter inner lateral process bearing one or two denticles, and an outer lateral process bearing three to five denticles (Fig. 17A,B); cusp robust, anteroposteriorly compressed, and slightly curved posteriorly, with broad anterior and posterior faces, and sharp lateral margins; basal margin straight; basal buttress weakly developed. *Sa element* alate, symmetrical (or nearly so) bearing a posterior process and a lateral process on each side (Fig. 17F,G); cusp more or less rounded in cross section with broad anterior margin, a sharp posterior costa and a median costa on each lateral face; costae extending downwards to form the upper margins of the processes; lateral processes bearing two or three antero-posteriorly compressed denticles; posterior process bearing three or more, smaller, laterally compressed denticles; the posterior process of all Sa elements studied from western New South Wales is broken. *Sb element* bipennate, with a posterior process bearing three to five denticles and a downward extending and strongly inner laterally curved anterior process (Fig. 17K–O); cusp robust, posteriorly inclined, with posterior and anterior costa; anterior costa and anterior process strongly curved inner-laterally so that in lateral view, they appear to be more inner lateral than anterior in position (Fig. 17K). *Sc element* bipennate with a strongly downwardly extended anterior process bearing three or more denticles and a posterior process bearing three or more denticles (Fig. 17C–E); cusp suberect, laterally compressed with sharp anterior and posterior margins; thin anterior margin sharply curved inner-laterally; basal margin

Fig. 17. *Erraticodon patu* Cooper, 1981: *A*, M element, AMF120378, Y4–6, anterior view; *B*, M element, AMF120379, Y4–6, posterior view; *C*, Sc element, AMF120380, Y4–6, inner lateral view; *D*, Sc element, AMF120381, M/A11-6, outer lateral view; *E*, Sc element, AMF120382, Y4–6, outer lateral view; *F*, Sa element, AMF120383, M/A11-5, anterior view; *G*, Sa element, AMF120384, Y4–4, posterior view; *H*, Sd element, AMF120385, Y4–8, anterior view; *I*, Sd element, AMF120386, M/A11-3, posterior view; *J*, Sd element, AMF120387, Y4–7, posterior view; *K*, Sb element, AMF120388, Y4–7, inner lateral view; *L*, Sb element, AMF120389, Y4–7, outer lateral view; *M*, Sb element, AMF120377, Y4–6, posterobasal view; *N,O*, Sb element, AMF120390, M/A11-5, *N*, postero-inner lateral view, *O*, antero-inner lateral view. Scale bars 100 μm.

strongly arched with the two processes nearly normal to each other. *Sd element* tertiopedate, asymmetrical, with a short inner lateral process bearing two or three denticles, and a longer outer lateral process bearing three to six denticles (Fig. 17H–J); two lateral processes extending downwards forming an angle of about 60 to 70°; posterior process bearing two or more denticles; cusp erect, oval in cross section with broad anterior margin, a posterior costa, and a mid-lateral costa on each side; costae extending downwards to mark the upper margins of the processes.

Remarks. Specimens from the Tabita Formation are identical with the type material from the Horn Valley Siltstone. The majority of the Mount Arrowsmith elements bear a basal attachment, and similarly, many of the Horn Valley specimens also have well preserved attachment cones (Nicoll, 2002, pers. comm.). Cooper (1981) originally described the Pb element as having three processes—anterior, posterior and a lateral. However, Sweet (1988) correctly indicated that the Pb element is actually a modified digyrate element, with a lateral process on each side and a strongly curved anterior process. This morphology is also clearly illustrated in the holotype of the species (Cooper, 1981, pl. 32, fig. 6). Close examination of specimens of the Pb element from Mount Arrowsmith has confirmed that these lack a posterior process.

Cooper (1981) described the M element as neoprioniodiform. Subsequently, Nicoll (1990) introduced the term makellate for the element occupying the M position, and suggested that the M element of *E. patu* was a typical makellate element. In the Mount Arrowsmith specimens, however, the anticusp is actually an antero-inner lateral process bearing one or two denticles. The basal buttress on the posterior face is generally weak (Fig. 17B).

The stratigraphically older *E. patu* is readily distinguished from the type species, *E. balticus*, from the Middle Ordovician by having a distinct Pb element with a denticulate anterior process, M element with a denticulate inner lateral process, and by absence of an accentuated denticle on the posterior process in the Sa, Sb and Sc elements.

The Pb element of *E. tangshanensis* Yang & Xu, *in* An *et al.*, 1983 is a modified digyrate form (originally termed plectospathognathiform, but including both Pb and Sd elements) which resembles the same element in *E. patu*, but the elements of *E. tangshanensis* have much more robust denticles and some S elements bear an accentuated denticle on the posterior process. The alate Sa element of this Chinese species has a short lateral process, represented by a single stout denticle, on each side, while the M element is more comparable with that of *E. balticus* in lacking an inner lateral process.

Erraticodon sp. A

Fig. 18A–G

Material. Five specimens (1 Pa, 1 Pb, 2 Sa, 1 Sc?) from the Tabita Formation at Mount Arrowsmith.

Description. Pa element digyrate, with a long posterior process bearing three or more peg-like widely spaced and posteriorly inclined denticles (Fig. 18C,D); cusp oval in cross section, slightly twisted inward, with a sharp anterior margin, which extends basally into a short anticusp; inner lateral side bearing a long process with three or more peg-like, widely spaced denticles which are anteroposteriorly compressed and distally rather sharply curved inward. Pb element modified digyrate, with a longer inner lateral process bearing three or more widely spaced, peg-like denticles, and a short outer lateral process with a single denticle; anterior process also short and represented by a single denticle (Fig. 18A,B); cusp and denticles curved posteriorly. Sa element alate, symmetrical, with a robust cusp, a denticulate posterior process, and lateral processes on each side bearing a small denticle (Fig. 18F,G). Sc element possibly represented by a poorly preserved specimen with a short anterior process bearing a single denticle, and a posterior process with three or more, long, posteriorly reclined denticles (Fig. 18E).

Remarks. This species is rare in the Tabita fauna, with only Pa, Pb, Sa and a doubtful Sc element recovered. It can be easily differentiated from the co-occurring *E. patu* by having widely spaced denticles, a short anterior process in the Pb element, and a laterally compressed cusp with a prominent anticusp in the Pa element. Although possibly a new species, formal designation is deferred pending recovery of all element types.

Jumudontus Cooper, 1981

Type species. *Jumudontus gananda* Cooper, 1981.

Jumudontus gananda Cooper, 1981

Fig. 18H–J

Jumudontus gananda Cooper, 1981: 170, pl. 31, fig. 13.
Jumudontus gananda.–Nicoll, 1992: 216–223, figs. 4–8 (*cum syn.*).
Jumudontus gananda.–Pohler, 1994, pl. 3, figs. 15, 16.
New genus A n. sp. 1 s.f. Pohler, 1994: 42, pl. 7, fig. 29, text-fig. 15T,U (= S elements).
New genus A n. sp. 2 s.f. Pohler, 1994: 42, pl. 7, figs. 27, 28, text-fig. 15R,S (= Pb element).
New genus C n. sp. 1 s.f. Pohler, 1994: 43, pl. 7, fig. 26, text-fig. 15X (= Pb element).
Jumudontus gananda.–Johnston & Barnes, 2000, pl. 4, fig. 22.
Jumudontus gananda?.–Zhen *et al.*, in press: pl. 3, fig. 19 (*cum syn.*).

Material. Six specimens (all Pa) from the Tabita Formation at Mount Arrowsmith, and eleven specimens (10 Pa, 1 Pb) from unnamed dolomitic limestone unit at Koonenberry Gap.

Remarks. *Jumudontus gananda* was originally described (Cooper, 1981) as a form species with only the Pa element recognized from the Horn Valley Siltstone of the Amadeus Basin. Nicoll (1992) revised the species as consisting of a septimembrate coniform-pectiniform apparatus, also based on a collection from the Horn Valley Siltstone, with a recovered element ratio of 60(Pa):21(Pb):2(M):1(Sa): 5(Sb): 3(Sc):8(Sd). In samples from western New South Wales, the species is comparatively rare, and only the more common Pa and Pb elements were recovered. Pohler (1994) briefly documented some Pb and S elements of this species, assigning them to three informal form species without knowledge of Nicoll's (1992) revision.

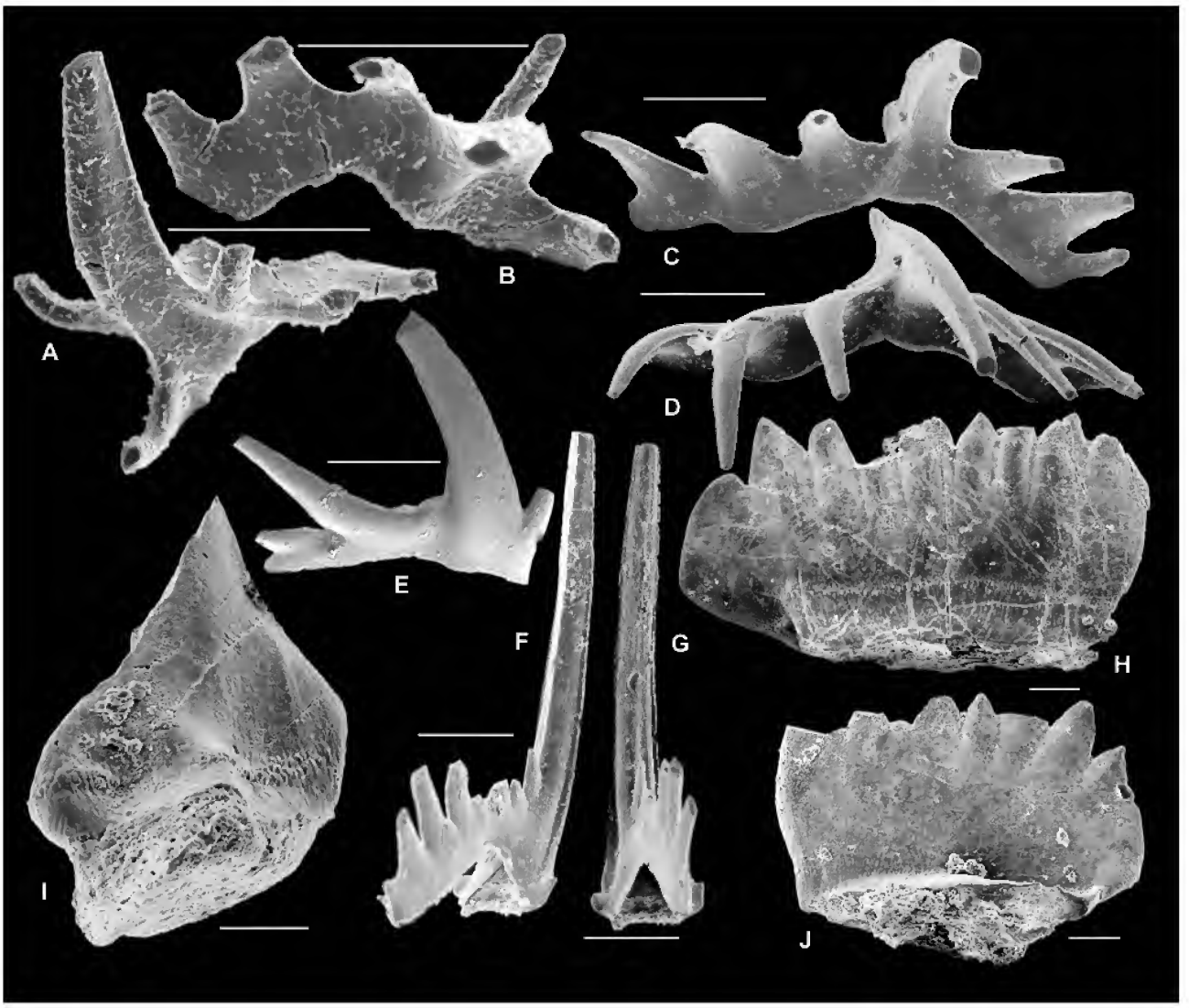

Fig. 18. *A–G*, *Erraticodon* sp. A: *A,B*, Pb element, AMF120391, M/A7, *A*, anterior view, *B*, posterior view; *C,D*, Pa element, AMF120392, M/A7, *C*, posterior view, *D*, upper view; *E*, Sc? element, AMF120393, M/A7, outer lateral view; *F,G*, Sa element, AMF120394, M/A7, posterolateral views. *H–J*, *Jumudontus gananda* Cooper, 1981: *H*, Pa element, AMF120395, M/A4, lateral view; *I*, Pb element, AMF120397, C1611, basal lateral view; *J*, Pa element, AMF120396, C1611, lateral view. Scale bars 100 μm.

Oepikodus Lindström, 1955

Type species. *Oepikodus smithensis* Lindström, 1955.

Remarks. Revision of the original form species concept (Lindström, 1955) led to recognition of a trimembrate apparatus consisting of prioniodiform, oepikodiform, and oistodiform elements (Lindström, 1971; Lindström, *in* Ziegler, 1975; Lindström, *in* Ziegler, 1977; Bergström & Cooper, 1973; van Wamel, 1974). Subsequently, Sweet (1988) and Johnston & Barnes (2000) interpreted the genus as consisting of a quinquimembrate apparatus incorporating three morphotypes of ramiform S elements. Further recognition of two pastinate (Pa and Pb) elements (Stouge & Bagnoli, 1988; Albanesi, *in* Albanesi *et al.*, 1998) and four morphotypes of ramiform S (Sb1, Sb2, Sc, and Sd) elements (Repetski, 1982) imply a seximembrate or septimembrate apparatus for the genus, including pastinate Pa and Pb, makellate M, and ramiform S elements. In a more recent revision (Stewart & Nicoll, in press; Nicoll & Ethington, in press), *Oepikodus* was defined as consisting of a septimembrate apparatus, including pastinate Pa and Pb, makellate M, and quadriramate or modified quadriramate S elements. Nicoll & Ethington (in press) suggested that *Oepikodus* can be distinguished from *Prioniodus* (and *Baltoniodus*) mainly on the basis of the morphology of their Sa elements, those of *Oepikodus* being quadriform alate, while Sa elements in the other two genera are triform alate.

Oepikodus communis (Ethington & Clark, 1964)

Fig. 19 O

Gothodus communis Ethington & Clark, 1964: 690–692, pl. 114, figs. 6, 14, text-fig. 2F.

Oepikodus equidentatus Ethington & Clark, 1964: 692–693, pl. 113, figs. 6, 8, 10, 11, 14.

Subcordylodus sp. aff. *S. delicatus* (Branson & Mehl) Ethington & Clark, 1964: 701–702, pl. 115, figs. 1, 5, 7, 10.

Oepikodus communis.–Ethington & Clark, 1982: 61–62, pl. 6, figs. 18, 22, 25 (*cum syn.*).

Oepikodus communis.–Smith, 1991: 42, figs. 24a–f,i,j, 25, 26 (*cum syn.*).

Fig. 19. *A–N*, *Oepikodus pincallyensis* Zhen sp. nov.: *A*, M element, paratype, AMF120399, M/A7, anterior view; *B,C*, Pa element, paratype, AMF120401, Y4–2, *B*, outer lateral view, *C*, anterior view; *D,E*, Pa element, paratype, AMF120402, Y4–2, *D*, outer lateral view, *E*, upper view; *F*, Pa element, paratype, AMF124210, M/A7, basal view; *G,H*, paratype, Pb element, AMF124211, Y4–2, *G*, outer lateral view, *H*, anterior view; *I–L*, Pb element, Holotype, AMF120398, Y4–2, *I*, antero-outer lateral view, *J*, inner lateral view, *K*, upper view, *L*, outer lateral view; *M,N*, M element, paratype, AMF120400, M/A/7, *M*, posterior view, *N*, postero-inner lateral view, showing basal buttress. *O*, *Oepikodus communis* (Ethington & Clark, 1964): Pb element, AMF120403, M/A11-2, outer lateral view. Scale bars 100 µm.

Material. One Pb element, from the Tabita Formation, at Mount Arrowsmith.

Remarks. *Oepikodus communis* is extremely rare at Mount Arrowsmith; the single Pb element recovered (sample M/A11-2) has a denticulate posterior process, and adenticulate outer lateral and anterior processes (Fig. 19O). Morphological differentiation and apparatus composition of *O. evae, O. communis* and *O. intermedius* have been widely discussed in Ordovician conodont literature. Serpagli (1974) considered *O. intermedius* to be transitional between *O. evae* and *O. communis*, showing *O. intermedius* first appearing in the San Juan Formation directly above the last appearance of *O. evae*. He further correlated the range of *O. intermedius* in the San Juan Formation with the *O. communis* Zone of the North American Midcontinent faunal succession, and suggested an evolutionary trend from *O. evae–O. intermedius–O. communis*. More recently, however, the *O. communis* Zone has been correlated in part with the *P. elegans* Zone, *below* the *O. evae* Zone (Webby, 1995), implying that *O. intermedius* might be the youngest species of the three. Although Serpagli (1974) distinguished *O. intermedius* from *O. communis* on curvature of processes on the P elements and curvature of the basal margin of the M elements, we agree with most subsequent authors (Ethington & Clark, 1982; Repetski, 1982; Smith, 1991) that these details are within the variation of *O. communis*. However, merging of these two species has the effect of extending the range of *O. communis* upwards into the *flabellum/laevis* Zone.

Oepikodus pincallyensis Zhen n.sp.

Figs. 19A–N, 20A–R

Etymology. After Pincally Homestead (Fig. 1), which is located southwest of the type locality (Y4).

Material. Three specimens (1 M, 1 Sa, 1 Sc) from limestone nodules within shales of the upper Yandaminta Quartzite, and 92 specimens (13 Pa, 11 Pb, 16 M, 16 Sa, 10 Sc, 17 Sb, 9 Sd) from the overlying Tabita Formation at Mount Arrowsmith, western New South Wales, including the HOLOTYPE AMF120398 (Pb element), from sample Y4–2 (C1822), and 15 paratypes AMF120399–120402, AMF120404–120411, AMF124210–124212.

Diagnosis. A species of *Oepikodus* consisting of a septimembrate apparatus with a ramiform-pectiniform structure; all elements albid; both Pa and Pb elements pastinate with a longer denticulate posterior process, a shorter denticulate outer lateral process, and an inner-laterally curved anterior process which is adenticulate (Pa) or denticulate (Pb); S elements typical (Sa and Sd) or modified (Sb and Sc) quadriramate.

Description. *Pa element* has a prominent, slightly procline, laterally compressed cusp which is triangular in cross section, with sharp posterior and anterior margins; an inwardly curved blade-like costa extends along the anterior margin, merging downward into the upper margin of an adenticulate, inwardly curved, anterior process (Fig. 19E); outer lateral face has a rounded distinctive costa that extends downwards to merge into the upper margin of the outer lateral process (Fig. 19B); the outer lateral process extends anterolaterally forming an obtuse angle with the posterior process (Fig. 19E); small, closely spaced denticles developed on the posterior and outer lateral processes (Fig. 19B–E); in upper view, these processes meet at a Y-shaped junction; basal cavity triangular in outline (Fig. 19F); none of the specimens recovered have processes preserved for their full length. *Pb element* similar to the Pa, with denticulate outer lateral and posterior processes, but with the cusp more or less erect or slightly reclined, also with a blade-like anterior costa that extends basally to merge into a shorter, denticulate, anterior process (Fig. 19G–L); outer lateral process extending more or less normal to the posterior process (Fig. 19K). *M element* geniculate, makellate, with a long adenticulate outer lateral process and a shorter, triangular adenticulate inner lateral process (anticusp) (Fig. 19A,M,N); cusp robust, inclined outer laterally, and also slightly curved posteriorly, anteroposteriorly compressed with sharp lateral margins, and a strong rounded costa on the anterior and posterior faces; surface ornament of fine striae; anterior costa extending to the basal margin, becoming stronger and wider on the base; posterior costa extending into a moderately developed basal buttress; outer lateral process with a sharp, gently arched upper margin and costa extending from cusp to distal end of the process on each of its sides, and more or less parallel to the basal margin; inner lateral process with a sharp upper margin which is a continuously straight extension of the inner lateral margin of the cusp; basal cavity shallow, extending as narrow grooves underneath the lateral processes, with only slightly arched basal margin. *Sa element* symmetrical or nearly so, and quadriramate; cusp slightly proclined, more or less diamond-shaped in cross section with sharp anterior and posterior margins and a sharp costa on each lateral side; anterior margin extended basally into a long downwardly directed anticusp; sharp lateral process extending basally into a weakly developed rudimentary adenticulate lateral process on each side; posterior process long, denticulate, bearing closely spaced and erect denticles of different sizes, larger denticles about two or three times as wide as the smaller denticles in the lateral view, typically with three to five smaller denticles between two larger denticles; basal margin of the posterior process nearly straight, forming an angle of about 40 to 50° with the basal margin of the anticusp (Fig. 20A–D). *Sb element* asymmetrical, with a weak carina on the inner lateral face, an inner laterally curved posterior process, and a proclined cusp; on the outer lateral face a prominent costa is developed which extends basally into a short adenticulate outer lateral process (Fig. 20I–M). *Sc element* similar to Sb, modified quadriramate, asymmetrical with cusp and anticusp slightly curved inwards; cusp erect or slightly proclined with sharp anterior and posterior margins, smooth outer lateral face and a weak carina on the inner lateral face; posterior process long, extending posteriorly as well as downwards, with a slightly arched upper margin, bearing numerous small, laterally compressed, and closely spaced denticles; none of the specimens examined have the full length of the posterior process preserved; anticusp long, triangular in shape, extending anteriorly and downwards, forming an angle of about 70–80° with the posterior process (Fig. 20E–H). *Sd element* quadriramate, like the Sa but asymmetrical, with cusp and the anterior process (anticusp) prominently curved inward, and with a long denticulated posterior process, a sharp anterior margin extended basally into a strongly downwardly directed anticusp; cusp


A
B
C
D
E
F
G
H
I
J
K
L
M
N
O
P
Q
R

proclined, more or less diamond-shaped in cross section, with sharp posterior and anterior margins, and a strong costa on each lateral face, which extends basally into a rudimentary adenticulate lateral process on each side (Fig. 20N–R).

Remarks. S and M elements of *O. evae, O. communis* and the new species *O. pincallyensis* closely resemble each other. *Oepikodus evae* was revised recently in detail (Stewart & Nicoll, in press) based on material from Australia and Sweden including well preserved bedding-plane assemblages. Compared with the revised concept of *O. evae*, the new species has a short anticusp in the M and S elements, and the Sb and Sc elements exhibit only rudimentary development of the lateral processes, which are reduced to a weakly developed carina on the inner lateral face of the Sb and Sc elements. Denticles on the posterior process in the S elements of *O. communis* are regular in size, whereas Sa elements of *O. pincallyensis* display variably sized denticles. Instead of a rather arched basal margin in the M elements of both *O. evae* and *O. communis, O. pincallyensis* shows a more or less straight basal margin. However, differentiation of these three species is mainly reliant on the P elements, specifically the absence of denticles on both the anterior and outer lateral processes on the P element of *O. communis*. The new species differs from *O. evae* in having smaller, rudimentary denticles on the anterior and outer lateral processes of the P elements. Furthermore, the anterior and outer lateral processes in the P element of *O. evae*, as shown by the type material from the Lower Ordovician of south-central Sweden (Lindström, 1955) and newly documented specimens from Australia (Stewart & Nicoll, in press), extend strongly downwards. In possessing smaller denticles and much less downwardly extended anterior and outer lateral processes on the P elements, the new species more closely resembles *Oepikodus communis* (Ethington & Clark, 1964), and *Oepikodus intermedius* Serpagli, 1974, but both of these latter species (which are probably conspecific) have adenticulate anterior and outer lateral processes.

In a recent study of the conodonts from the Horn Valley Siltstone of central Australia, Nicoll & Ethington (in press) recognized another new species of *Oepikodus*, previously recorded by Cooper (1981) as *O. evae*. It differs from *O. pincallyensis* and other *Oepikodus* species in having a pronounced v-shaped cleft separating the posterior margin of the cusp and the first denticle of the posterior process in the S and P elements. Rudimentary denticles are also developed on the anterior process of some Sc, Sb and M elements of this species from Horn Valley Siltstone.

Oneotodus Lindström, 1955

Type species. *Distacodus? simplex* Furnish, 1938.

Oneotodus sp.

Fig. 24E,F

Oneotodus sp. Cooper, 1981: 172, pl. 27, figs. 1, 2.

Material. Six specimens from the Tabita Formation at Mount Arrowsmith, and one specimen from unnamed dolomitic limestone unit at Koonenberry Gap.

Remarks. The generic concept of *Oneotodus* adopted here follows that given by Ethington & Brand (1981) and Sweet (1988: 52). The western New South Wales species is comparable with specimens illustrated from the Horn Valley Siltstone (Cooper, 1981). It is a simple cone unit, with shallow but flaring basal cavity, which is rounded in basal view (Fig. 24E); in cross section, the cusp is rounded near the base and laterally compressed distally. Some elements display weak costae on the lateral faces (Fig. 24F).

Prioniodus Pander, 1856

Type species. *Prioniodus elegans* Pander, 1856.

Remarks. Generic concepts and the apparatus compositions of *Prioniodus* and *Baltoniodus* Lindström, 1971 have long been debated. Fåhraeus & Nowlan (1978), and Cooper (1981) regarded the two as separate genera, based mainly on differentiation of the P elements, and also on the nature of the basal cavity. This definition has been more or less accepted by Löfgren (1978), Clark *et al.* (1981), Sweet (1988), and Stouge & Bagnoli (1988). However, Serpagli (1974) considered *Baltoniodus* to be a subgenus of *Prioniodus*, while van Wamel (1974) regarded *Baltoniodus* as a junior synonym of *Prioniodus*. Many authors (Cooper, 1981; Sweet, 1988; Dzik, 1994; Nicoll & Ethington, in press) considered that both genera might have been derived independently from species of *Acodus*, while *Oepikodus* may have evolved from *Prioniodus* (Dzik, 1983; Sweet, 1988) or also from *Acodus* (Stouge & Bagnoli, 1999). In a recent revision of *Oepikodus*, Nicoll & Ethington (in press) suggested the triform alate Sa elements, and relatively larger basal cavity distinguish both *Prioniodus* and *Baltoniodus* from *Oepikodus*. Sa elements of *Prioniodus* and *Baltoniodus* have a lateral process on each side and a long posterior process, but lack an anterior process.

Fig. 20 (opposite). *Oepikodus pincallyensis* Zhen sp. nov.: *A,B*, Sa element, paratype, AMF120409, Y4–2, lateral views; *C,D*, Sa element, paratype, AMF120410, Y4–2, lateral views; *E,F*, Sc element, paratype, AMF120407, Y4–2, *E*, outer lateral view, *F*, inner lateral view; *G,H*, Sc element, paratype, AMF120405, Y4–2, *G*, inner lateral view, *H*, outer lateral view; *I*, Sb element, paratype, AMF120406, Y4–2, inner lateral view; *J,K*, Sb element, paratype, AMF120408, Y4–2, *J*, inner lateral view, *K*, outer lateral view; *L,M*, Sb element, paratype, AMF120404, Y4–2, *L*, inner lateral view, *M*, outer lateral view; *N,O*, Sd element, paratype, AMF120411, Y4–2, *N*, inner lateral view, *O*, outer lateral view; *P–R*, Sd element, paratype, AMF124212, TAB1/65.2, *P*, outer lateral view, *Q*, upper view, *R*, postero-inner lateral view. Scale bars 100 μm.

Prioniodus sp. cf. *P. amadeus* Cooper, 1981

Fig. 21A–L

Material. One specimen (P) from limestone nodules within shales of the upper Yandaminta Quartzite and 47 specimens (27 P, 1 M, 19 S) from the overlying Tabita Formation at Mount Arrowsmith.

Description. The pastinate *P elements* are not differentiated into Pa and Pb due to limited material. They have a prominent, strongly laterally compressed, blade-like cusp with sharp anterior and posterior margins, and a sharp costa on the outer lateral face. The anterior and posterior margins, and the outer lateral costa extend basally into three processes (Fig. 21A–D). The posterior and outer lateral processes are longer and have several (up to seven) small denticles; anterior process shorter with a few small rudimentary denticles; cusp triangular in cross section with sharp anterior and posterior margins, and a sharp-edged costa on the outer lateral face; anterior process slightly curved inward, and outer lateral process extending anterolaterally, forming a more or less Y-shaped outline in upper view. *M element* makellate, with a long adenticulate outer lateral process, which has a straight basal margin and an arched upper margin, and a short inner lateral process, which is triangular in outline in anterior view (Fig. 21L); cusp anteroposteriorly compressed, with a broad costa on the anterior and posterior faces, and a straight inner lateral margin forming an acute angle (about 40–45°) with the basal margin of the outer lateral process. *Sa element* triform alate, symmetrical, with a long denticulate posterior process, a broad anterior face, and a sharp ridge-like costa on each lateral face, which extends basally into a short adenticulate process (Fig. 21J,K). *Sb element* modified bipennate, strongly asymmetrical with a slightly proclined cusp, inner laterally curved anterior margin, a straight denticulate posterior process and a short adenticulate anticusp-like anterior process (Fig. 21E,F). *Sc element* modified bipennate, similar to Sb but slightly asymmetrical with a long denticulate posterior process and a short, anticusp-like adenticulate anterior process; cusp erect, laterally compressed, with sharp anterior and posterior margins; anterior process slightly curved inward, and posterior process slightly arched with denticles of uniform size pointed posteriorly (Fig. 21G). *Sd element* tertiopedate, asymmetrical with a denticulate posterior process; cusp proclined, and inner laterally curved, with broad anterior margin and a blade-like costa on each lateral side, which extends basally into a lateral process; inner lateral process more prominent, with a few rudimentary denticles distally (Fig. 21H,I).

Remarks. This species, consisting possibly of a septimembrate apparatus, is relatively uncommon in the Mount Arrowsmith collections. Although the modified bipennate Sb and Sc elements resemble those of *P. amadeus* Cooper, 1981 from the Horn Valley Siltstone of the Amadeus Basin (see especially Cooper, 1981, pl. 31, fig. 6), that species differs in inclusion of quadriramate elements in the apparatus, and its P elements have a less laterally compressed cusp and an adenticulate anterior process.

Some broad similarities are apparent between *P.* sp. cf. *amadeus* and *Oepikodus pincallyensis*. However, S elements of the former (differentiated into a triform alate Sa, modified bipennate Sb and Sc, and tertiopedate Sd) are generally larger, with more robust posterior processes bearing posteriorly pointed denticles of uniform size. S elements of *O. pincallyensis* are quadriramate, or modified quadriramate. The P elements of *P.* sp. cf. *amadeus* have a more laterally compressed blade-like cusp compared to *O. pincallyensis*, and exhibit a shorter and less inner laterally curved anterior process, and a relatively larger and deeper triangular basal cavity.

Prioniodus sp. A

Fig. 21M–Q

Material. Four specimens (3 Pa, 1 Pb) from the Tabita Formation at Mount Arrowsmith.

Description. Both Pa and Pb elements have a robust, erect cusp with sharp anterior and posterior margins; *Pb element* with a more laterally compressed blade-like cusp, and short posterior and outer lateral processes, with four denticles on the former and a single denticle on the latter; the anterior process long, inner laterally curved, bearing more than ten denticles (Fig. 21M,N). Cusp of *Pa element* more or less triangular in cross section, with a sharp mid-costa along the outer lateral face, which extends basally into a long denticulate outer lateral process (Fig. 21P,Q); long denticulate posterior process bearing closely spaced denticles which are erect and laterally compressed; outer lateral process normal to the posterior process (Fig. 21 O), bearing over ten closely spaced denticles which are anteroposteriorly compressed, with tips slightly curved posteriorly; neither anticusp nor denticles developed at the anterobasal corner.

Remarks. The Pa element is well defined and is distinguished from those of other species of the genus by its long denticulate posterior and outer lateral processes. The Pb element of this species is characterized by a prominent cusp, and long denticulate anterior process. It shows some resemblance to the P element of *Prioniodus* sp. A McTavish, 1973 from the Emanuel Formation of the Canning Basin (McTavish, 1973, pl. 2, fig. 4), but has an even longer anterior process with prominent denticles, and a much shorter outer lateral process.

Protopanderodus Lindström, 1971

Type species. *Acontiodus rectus* Lindström, 1955.

Protopanderodus gradatus Serpagli, 1974

Fig. 22A–K

Protopanderodus gradatus Serpagli, 1974: 75, pl. 15, figs. 5a–8b, pl. 26, figs. 11–15, pl. 30, fig. 1a,b; text-fig. 17.
Protopanderodus gradatus.–Zhen *et al.*, in press: pl. 5, figs. 1–10 (*cum syn.*).

Material. Ten specimens (4 Sb, 4 Sc, 2 Sd) from limestone nodules within shales of the upper Yandaminta Quartzite, and 69 specimens (11 Sa, 16 Sb, 17 Sc, 25 Sd) from the overlying Tabita Formation at Mount Arrowsmith; 31 specimens (1 Sa, 7 Sb, 12 Sc, 11 Sd) from unnamed dolomitic limestone unit at Koonenberry Gap.

Fig. 21. *A–L*, *Prioniodus* sp. cf. *P. amadeus* Cooper, 1981: *A,B*, P element, AMF120412, TAB1/78.2, *A*, outer lateral view, *B*, upper, inner lateral view; *C,D*, P element, AMF120413, TAB1/78.2, *C*, upper, antero-inner lateral view, *D*, postero-outer lateral view; *E*, Sb element, AMF120415, M/A7, inner lateral view; *F*, Sb element, AMF120416, M/A7, outer lateral view; *G*, Sc element, AMF120414, TAB1/78.2, lateral view; *H,I*, Sd element, AMF120417, TAB1/78.2, *H*, inner lateral view, *I*, posterior view; *J,K*, Sa element, AMF120418, M/A11-3, lateral views; *L*, M element, AMF124213, W/A11-5, anterior view. *M–Q*, *Prioniodus* sp. A: *M,N*, Pb element, AMF120420, M/A7, *M*, inner lateral view, *N*, anterior view; *O*, Pa element, AMF120419, Y4–2, outer lateral view; *P*, Pa element, AMF120422, Y4–2, postero-outer lateral view; *Q*, Pa element, AMF120421, Y4–2, upper view. Scale bars 100 μm.

Remarks. This species was recently reported from the slightly older (upper *P. elegans* Zone) Hensleigh Siltstone of central New South Wales, where five morphotypes were recognized (Zhen *et al.*, in press). Four elements have been recovered from the western New South Wales samples, and are regarded as occupying S positions in the species apparatus. The Sa element (termed element "d" by Zhen *et al.*, in press) is symmetrical or nearly so with a posterolateral

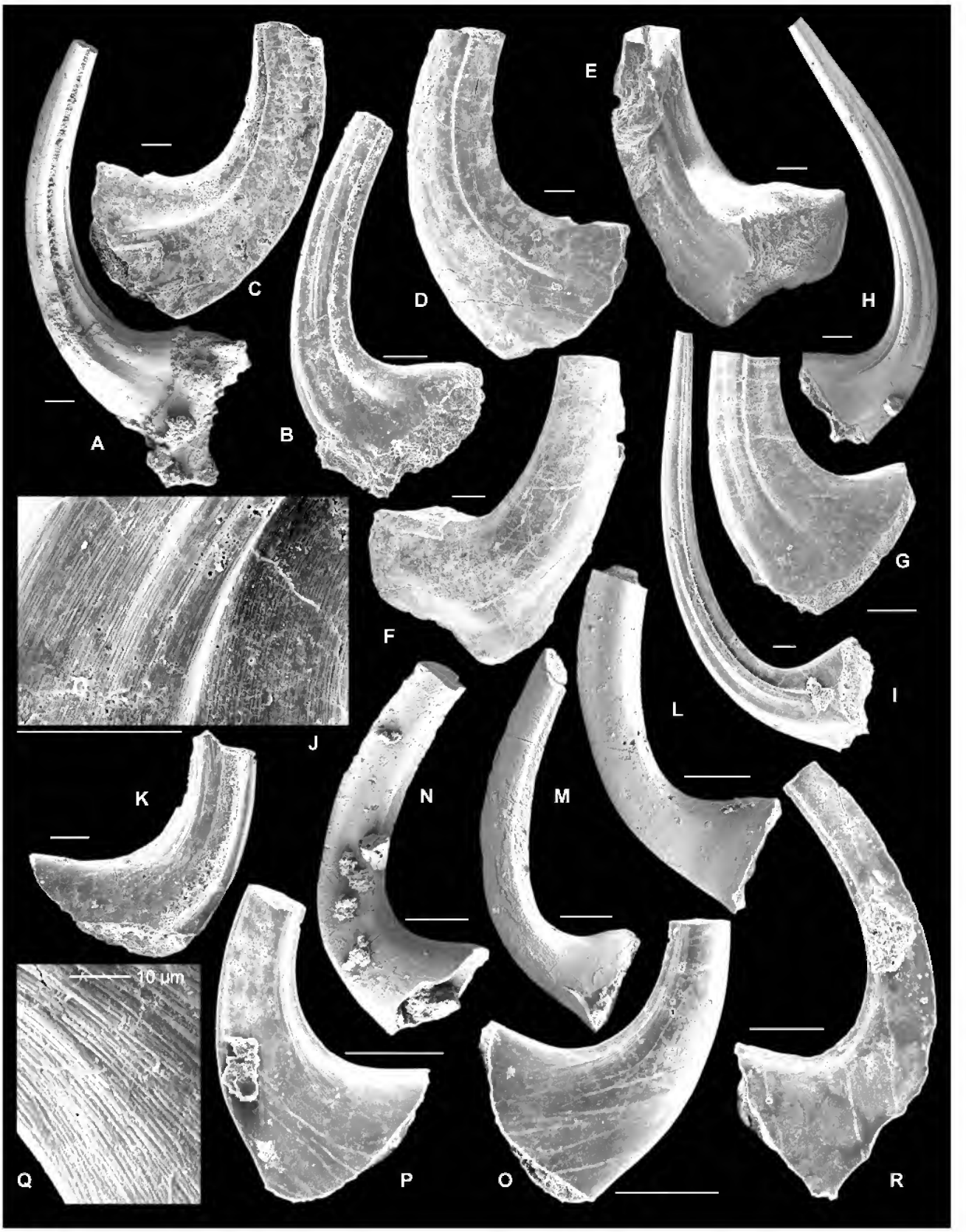

Fig. 22. *A–K*, *Protopanderodus gradatus* Serpagli, 1974: *A*, Sa element, AMF120436, M/A11-1, posterolateral view; *B*, Sd element, AMF120437, C1612, outer lateral view; *C,D*, Sb element, AMF120438, C1612, *C*, inner lateral view, *D*, outer lateral view; *E,F*, Sc element, AMF120439, C1612, *E*, inner lateral view, *F*, outer lateral view; *G*, Sd element, AMF120440, C1612, outer lateral view; *H–J*, Sa element, AMF120441, Y4–2, *H,I*, lateral views, *J*, close up showing the fine striae; *K*, Sd element, AMF120442, C1612, inner lateral view. *L–R*, *Protopanderodus leonardii* Serpagli, 1974: *L*, Sa element, AMF120443, M/A11-3, lateral view; *M*, Sb element, AMF120444,

costa and an anterolateral costa on each side (Fig. 22A,H–J). The Sb element (element "c" of Zhen *et al.*, in press) is weakly asymmetrical, with a lateral costa on each side and slightly inner laterally curved cusp (Fig. 22C,D). Specimens referred to as element "b" by Zhen *et al.* (in press) may represent a variant of the Sb element; they are not recognized here. The Sc element is strongly asymmetrical with a smooth outer face and a costate inner face (Fig. 22E,F). It is similar to element "a" from the Hensleigh Siltstone, but the latter is more strongly twisted with a smooth inner face and a costate outer face. The Sd element (element "e" of Zhen *et al.*, in press) is similar to the Sa with a posterolateral costa and an additional anterolateral costa on each side, but apparently asymmetrical (Fig. 22B,G,K).

Our specimens are identical with the type material from the San Juan Formation of Argentina (Serpagli, 1974). In lateral view, elements of *P. gradatus* from the Hensleigh Siltstone are less laterally compressed with the basal margins more or less straight, rather than gently curved as shown by the types from the Argentine Precordillera.

Protopanderodus leonardii Serpagli, 1974

Fig. 22L–R

Protopanderodus leonardii Serpagli, 1974: 77, pl. 16, figs. 1a–4c, pl. 27, figs. 12–16, text-fig. 6.
Protopanderodus leonardii.–Zhen *et al.*, in press: pl. 4, figs. 23, 24 (*cum syn.*).

Material. Six specimens (1 Sa, 3 Sb, 2 Sc) from the Tabita Formation at Mount Arrowsmith.

Remarks. This species differs from *P. gradatus* mainly in having sharp anterior margins. Serpagli (1974) initially recognized a trimembrate apparatus consisting of a symmetrical bicostate Sa, asymmetrical bicostate Sb, and asymmetrical acostate Sc elements. However, his illustrations depict two distinct forms of elements. The holotype (Serpagli, 1974, pl. 27, fig. 15) and a paratype (Serpagli, 1974, pl. 27, fig. 14) have an extremely short base, and are interpreted as P elements. The other three figured paratypes have a relatively longer base supporting a more or less erect cusp, and represent a symmetry transition series of S elements.

This species is uncommon at Mount Arrowsmith. Three types of S elements were recovered, but no P elements have been recognized. The Sa element is symmetrical or nearly so with a posterolateral costa on each side (Fig. 22L). The Sb element is similar to the Sa, but asymmetrical, with cusp curved inwards and slightly twisted (Fig. 22M,N). The Sc element is asymmetrical with sharp anterior and posterior margins, and a more expanded base; it has a posterolateral costa on each side, and a thin inner-laterally curved anterior edge (Fig. 22 O–R).

Protopanderodus nogamii (Lee, 1975)

Fig. 23A–P, ?Q

Scolopodus cf. *bassleri* Igo & Koike, 1967: 23, pl. 3, figs. 7, 8, text-fig. 6B.
Scolopodus sp. A Hill *et al.*, 1969: O.14, pl. O VII, fig. 13.
Scolopodus sp. C Hill *et al.*, 1969: O.14, pl. O VII, fig. 15.
"*Panderodus*" sp. Serpagli, 1974: 59, pl. 24, figs. 12, 13, pl. 30, figs. 12, 13.
Scolopodus nogamii Lee, 1975: 179, pl. 2, fig. 13.
Protopanderodus primitus Druce (MS), *in* Cooper, 1981 (*nomen nudum*): 174, pl. 27, figs. 3, 4 (*cum syn.*).
Scolopodus euspinus Jiang & Zhang, *in* An *et al.*, 1983: 140, pl. 13, fig. 27, pl. 14, figs. 1–8 (*cum syn.*).
Protopanderodus nogamii.–Watson, 1988: 124, pl. 3, figs. 1, 6.
Scolopodus euspinus.–An & Zheng, 1990: 173, pl. 2, figs. 7–11, 13, 14, 16.
Protopanderodus primitus.–Stait & Druce, 1993: 307, figs. 13A–C, 18D,E,G–K (*cum syn.*).
Parapanderodus paracornuformis.–Albanesi, *in* Albanesi *et al.*, 1998: 116, *partim* pl. 12, fig. 13, 8?–10?, *non* 11, 12.

Material. Three specimens (2 Sb, 1 Sc) from the Tabita Formation at Mount Arrowsmith, and 128 specimens (12 Pa, 18 Pb, 35 Sa, 55 Sb, 5 Sc, 3 Sd) from unnamed dolomitic limestone unit at Koonenberry Gap.

Description. A species of *Protopanderodus* consisting of a seximembrate apparatus; all elements with a distinctive deep and narrow furrow on one lateral side (Sc) or both sides (other elements); surface coarsely striated, with striae more prominent on the base. *P elements* slightly asymmetrical, more laterally compressed, with a median furrow on each side and a shorter base; cusp with a broad anterior face, and a sharp blade-like posterior margin; basal cavity peanut-like in outline (Fig. 23I,N); some specimens (Fig. 23J) with a prominent rounded costa situated posterior to the furrow on the inner lateral face. The Pa element (Fig. 23I–N) has a suberect cusp and shorter base, the curvature between the posterior margin of the cusp and the base is about 90° or slightly less; the Pb element (Fig. 23 O,P) has a more or less proclined cusp with a longer base, and a more gradational curvature between the posterior margin of the cusp and the base. *S elements* are less laterally compressed, with a longer base, and a more or less rounded posterior margin. Sa element (Fig. 23A,B) symmetrical with a furrow on each side; Sb element similar to Sa, but with a more laterally compressed base (Fig. 23C,D); Sc element (Fig. 23E,F) asymmetrical, with a furrow only on inner lateral face; Sd element similar to Sb but asymmetrical, with cusp slightly twisted and curved inward (Fig. 23G,H).

Remarks. This species is characterized by having a distinctive deep furrow on one or two lateral faces, and by its coarsely striate surface. The furrow is not a true panderodontid furrow, and disappears just before reaching the basal margin, as do also the coarse striae.

[continuation of Fig. 22 caption]... M/A11-3, outer lateral view; *N*, Sb element, AMF120445, M/A11-3, inner lateral view; *O–Q*, Sc element, AMF120446, Y4–2, *O*, outer lateral view, *P*, inner lateral view, *Q*, inner lateral view, close up showing the fine striae; *R*, Sc element, AMF120447, Y4–3, inner lateral view. Scale bars 100 μm, unless otherwise indicated.

Fig. 23. *A–P*, *Protopanderodus nogamii* (Lee, 1975): *A*, Sa element, AMF120430, C1611, basal view showing the basal cavity; *B*, Sa element, AMF120428, C1612, lateral view; *C,D*, Sb element, AMF120427, C1612, *C*, lateral view of the basal part showing furrow and striation, *D*, lateral view; *E,F*, Sc element, AMF120431, Y4–2, *E*, inner lateral view, *F*, outer lateral view; *G,H*, Sd element, AMF120429,

Although Cooper (1981) figured two S elements of *Protopanderodus primitus* Druce (MS), he provided neither adequate description nor designation of the types in the expectation that the species would be fully described by Druce in a subsequent publication. However, the species was not formally introduced until Stait & Druce (1993) designated the specimen figured by Cooper (1981, pl. 27, fig. 4) as the lectotype and the other figured specimen (Cooper, 1981, pl. 27, fig. 3) as the paralectotype for *P. primitus*. They also cited Cooper as the original author of the species, rather than Druce. Jiang & Zhang (*in* An *et al.*, 1983) in the meantime had erected *Scolopodus euspinus*, based on material from the Beianzhuang Formation (approximately Chewtonian to Castlemainian age) of Hebei Province, North China, without knowledge of Cooper's work. Jiang & Zhang (*in* An *et al.*, 1983) described *S. euspinus* as a form species characterized by a furrow on each side and a low costa immediately anterior to it. Among their figured specimens, two morphotypes can be recognized—one, represented by the holotype (An *et al.*, 1983, pl. 14, fig. 3) and two other illustrated specimens (pl. 14, figs. 1, 2), is more laterally compressed with a wider base (referred to herein as the P elements), while the other morphotype (assigned here to the S elements) is less laterally compressed with a longer base (see An *et al.*, 1983, pl. 14, figs. 4, 5).

Stait & Druce (1993) correctly considered *S. euspinus* conspecific with *P. primitus*, but the Chinese species has priority over *P. primitus* which in 1983 was a nomen nudum. They revised this species in terms of multielement terminology, referring the laterally compressed symmetrical form to the Pa element, and also recognized an asymmetrical Pb element. The less laterally compressed symmetrical form was assigned to the Sa element. Two additional asymmetrical elements, one uni-furrowed (here referred to Sc) and a tri-furrowed form were also recovered from the Coolibah Formation to form the first symmetry transition series (Stait & Druce, 1993). The Sc element is comparatively rare in the western New South Wales faunas. The Sb element defined by Stait & Druce (1993) is similar to the Sa, but slightly asymmetrical with the furrow on the outer lateral face situated more towards the posterior margin and with the cusp slightly curved inward—it is recognized here as the Sd element. Their figured tri-furrowed Sd element (Stait & Druce, 1993, fig. 18K) is regarded as representing the Pb position, being laterally compressed with a proclined cusp and a shorter base. The rounded second costa posterior to the furrow on the inner side is not considered a distinctive feature. It may occur in either Pa (Fig. 23J herein) or Pb (Stait & Druce, 1993, fig. 18K) elements, and in our material is relatively weak in comparison with the specimen illustrated by Stait & Druce (1993).

Watson (1988) interpreted *Protopanderodus euspinus* as a junior synonym of *Protopanderodus nogamii* (Lee, 1975). Jiang & Zhang (*in* An *et al.*, 1983) differentiated *P. nogamii* from *P. euspinus* mainly on its shorter base and reclined cusp. They stated that whereas both species generally co-occur over an extended stratigraphic range in North China, from the Liangjiashan Formation (Bendigonian) to the Fengfeng Formation (Gisbornian) of North China, only *P. nogamii* was recorded from South China (An, 1987), and therefore, the species were treated as separate.

Protopanderodus nogamii was originally described from the Nandal Formation, of suggested Middle Ordovician age, in North Korea. Based on the illustration of the holotype and only figured specimen (Lee, 1975, pl. 2, fig. 13), the following differences in comparison with the type material of *P. euspinus* are noticed. The holotype of *P. nogamii* is a larger specimen (width of the base 570 μm), with a reclined cusp, and coarser striae (8/100 μm) which are developed only on a shorter, posteriorly more extended base. In contrast, the holotype of *P. euspinus* is smaller (width of the base 150 μm) with a proclined or suberect cusp, and bears finer striae (20–25/100 μm). Otherwise, the two species are closely comparable, with *P. nogamii* representing one extreme morphotype in the species apparatus (Albanesi pers. comm., 2002). Therefore, despite being defined on a solitary element, *P. nogamii*—according to strict application of nomenclatural priority—takes precedence over *P. euspinus* and all other synonyms mentioned in this discussion.

An & Zheng (1990: 173) included two specimens designated as ?*Panderodus* sp. by Ethington & Clark (1982) from the Lehman Formation of the Ibex area, Utah, with *Protopanderodus euspinus*. Since both specimens appear to have a true panderodontid furrow situated on the posterior face, it seems that this reassignment is unjustified.

One specimen (Fig. 23Q) from Koonenberry Gap (C1612) is a symmetrical element resembling *P. nogamii*, but is doubtfully assigned due to its much shorter proclined cusp, and a curved lateral costa and furrow on each side. These variations might reflect some kind of pathological deformation.

Protoprioniodus McTavish, 1973

Type species. *Protoprioniodus simplicissimus* McTavish, 1973.

Remarks. As pointed out by Smith (1991), interpretations of the apparatus composition of the genus and its phylogenetic relationships vary considerably. It is clear that at least three distinct species groups have been previously assigned to *Protoprioniodus*. The first group, represented by the type species, *P. simplicissimus* McTavish, 1973, and *P. yapu* Cooper, 1981, have a pastinate P element with a robust cusp, similar to the P elements of *Prioniodus* but with adenticulate processes in this and all other elements. Based on this interpretation, which was followed by Cooper (1981), Ethington & Clark (1982), and Smith (1991), the apparatus has a ramiform-pectiniform configuration. Material from the western New South Wales collections supports the interpretation of Sweet (1988: 61) who

[continuation of Fig. 23 caption]... C1612, *G*, inner lateral view, *H*, basal inner lateral view at the base; *I–K*, Pa element, AMF120432, C1611, *I*, basal view, *J*, inner lateral view, *K*, outer lateral view; *L–N*, Pa element, AMF120433, C1611, *L*, inner lateral view, *M*, outer lateral view, *N*, basal view; *O,P*, Pb element, AMF120434, C1611, *O*, inner lateral view, *P*, outer lateral view. *Q*, *Protopanderodus nogamii*? (Lee, 1975): Sa element, AMF120435, C1612, lateral view. Scale bars 100 μm.

envisaged the apparatus as consisting of pectiniform P elements, makellate M element and adenticulate ramiform S elements.

The second group, including *P. nyinti* and *P. aranda* from the Amadeus Basin previously referred to the genus by Cooper (1981), have the P positions occupied by pectiniform elements, but in lacking a recognizable cusp they do not conform to the concept of *Protoprioniodus*. These species are now distinguished as the new genus *Cooperignathus*, in which the anterior, posterior and outer lateral processes are characterized by having blade-like crests on upper surfaces, rather than rows of nodes in more derived forms like *Eoplacognathus*.

The third species group is represented by *P. papiliosus* (van Wamel, 1974) and *P. cowheadensis* Stouge & Bagnoli, 1988. These latter authors, as well as Johnston & Barnes (2000), regarded the genus as including oistodiform elements in both the P and M positions, implying a ramiform-ramiform configuration.

Some authors (McTavish, 1973; Cooper, 1981) have suggested that *Protoprioniodus* might have evolved from *Acodus* based on general similarity of their P elements, although in *Protoprioniodus* these have a more strongly developed adenticulate outer-lateral process. An alternate proposal (Sweet, 1988: 61) related *Protoprioniodus* more closely to *Oistodus*, citing the geniculate nature of their skeletal elements.

Protoprioniodus yapu Cooper, 1981

Fig. 24A–D

Protoprioniodus yapu Cooper, 1981: 178, pl. 30, figs. 3–5, 8, 9, 11, 13.

Protoprioniodus costatus An, 1987: 174, *partim* only, pl. 14, figs. 1, 4, pl. 16, fig. 25.

?*Protoprioniodus yapu*.–An, 1987, pl. 16, fig. 27.

Protoprioniodus costatus.–Ding *et al.*, *in* Wang, 1993: 197, pl. 14, fig. 27.

Protoprioniodus yapu.–Ding *et al.*, *in* Wang, 1993, pl. 15, figs. 10, 12.

Protoprioniodus aranda.–Johnston & Barnes, 2000: 42, *partim* only pl. 6, fig. 22.

Material. Seventeen specimens (5 Pb, 10 M, 2 doubtful S) from the Tabita Formation at Mount Arrowsmith.

Remarks. Nicoll (2002, pers. comm.) indicated that *Protoprioniodus yapu* may belong to part of the species apparatus of either *P. nyinti* or *P. aranda* (both transferred to the new genus *Cooperignathus* herein). As *P. yapu* is relatively rare in the Tabita Formation, Cooper's (1981) definition is retained herein pending further study of the type material from the Horn Valley Siltstone.

In erecting *P. yapu*, Cooper (1981) illustrated two morphotypes of the P elements, both of which are highly modified pastinate units with a prominent cusp. The paratype (Cooper, 1981, pl. 30, fig. 11) with rudimentary denticulate outer lateral processes is here designated as the Pa element. The holotype (Cooper, 1981, pl. 30, fig. 9) lacks an outer lateral process, and is assigned to the Pb position (Fig. 24B–D). The M element is characterized by having a strongly inner laterally recurved cusp and an adenticulate, long outer lateral process, and apparently lacks an anticusp or inner lateral process (Fig. 24A). The strongly laterally compressed S elements (not identified with certainty at Mount Arrowsmith) have a strong mid-costa on the inner-lateral face.

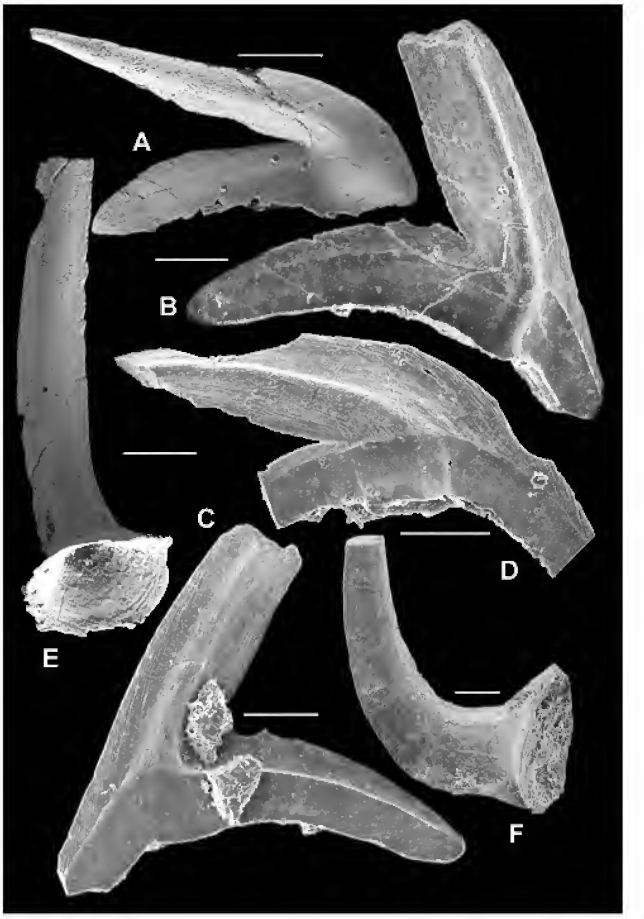

Fig. 24. *A–D*, *Protoprioniodus yapu* Cooper, 1981: *A*, M element, AMF120448, M/A7, posterior view; *B,C*, Pb element, AMF 120449, Y4–2, *B*, outer lateral view, *C*, inner lateral view; *D*, Pb element, AMF120450, M/A7, outer lateral view. *E,F*, *Oneotodus* sp.: *E*, AMF120451, M/A11-3, posterolateral view; *F*, AMF 124226, C1612, inner lateral view. Scale bars 100 µm.

Protoprioniodus was distinguished by An (1987) from *Oelandodus* van Wamel, 1974 by having a prominent ridge-like costa above the basal margin. Comparison of the two species originally ascribed to *Oelandodus* shows that the type species, *O. elongatus* (Lindström, 1955), apparently lacks this feature, while its presence in *O. costatus* van Wamel, 1974 justifies An's (1987) reassignment of this species to *Protoprioniodus*. The P elements of *P. costatus* and *P. yapu* are similar in morphology, but their S and M elements are easily distinguished. The S element of *P. costatus* shows some resemblance to the S elements of *C. nyinti*; both have a tricostate cusp, costae extending basally to a lateral process on each side, and a long posterior process. The M element has a long pointed anticusp, straight basal margin and a strongly outer laterally recurved cusp. On this basis, the P, S and M elements referred to *P. costatus* by An (1987) from China are identical with those of *P. yapu*, rather than conspecific with the Swedish type material of *P. costatus*.

Scalpellodus Dzik, 1976

Type species. *Protopanderodus latus* van Wamel, 1974.

Scalpellodus latus (van Wamel, 1974)

Fig. 25A–J

Protopanderodus latus van Wamel, 1974: 91, pl. 4, figs. 1–3.
Scalpellodus latus.–Löfgren, 1978: 99, pl. 5, figs. 10, 14, pl. 6, figs. 1–4, 7, 21 (*cum syn.*).
Scalpellodus latus.–Cooper, 1981: 179, pl. 27, figs. 7–10, 13–15.

Material. One specimen (Sa) from limestone nodules within shales of the upper Yandaminta Quartzite and 28 specimens (1 P?, 2 Sa, 12 Sb, 5 Sc, 6 Sd) from the overlying Tabita Formation at Mount Arrowsmith.

Remarks. This coniform species is similar to *Cornuodus longibasis*, but is more laterally compressed, and ornamented with fine striae (Fig. 25A,H), which is a critical character in recognition of this species. Of the three morphotypes distinguished by Cooper (1981), we also recognize a symmetrical Sa element with a broad anterior face, a sharp costa on each lateral face, and a costa along the posterior margin (Fig. 25A,B). All three costae on the Mount Arrowsmith specimens are relatively weakly developed in comparison with the Sa element illustrated from the Horn Valley Siltstone (Cooper, 1981, pl. 27, figs. 7, 9). Asymmetrical forms (defined as the Sb element by Cooper), with a sharp posterior margin and an anterolateral costa only on the inner lateral side, can be segregated into an Sb element (Fig. 25C,D) with a proclined cusp, and another type with an erect cusp and a more laterally compressed base—here referred to the Sd element (Fig. 25E,F,H,I). The nearly symmetrical element with sharp anterior and posterior margins, which Cooper (1981) identified as the Sc element, is also recognized (Fig. 25J). A small, nearly symmetrical specimen with a recurved cusp (Fig. 25G) possibly occupied the P position of this species.

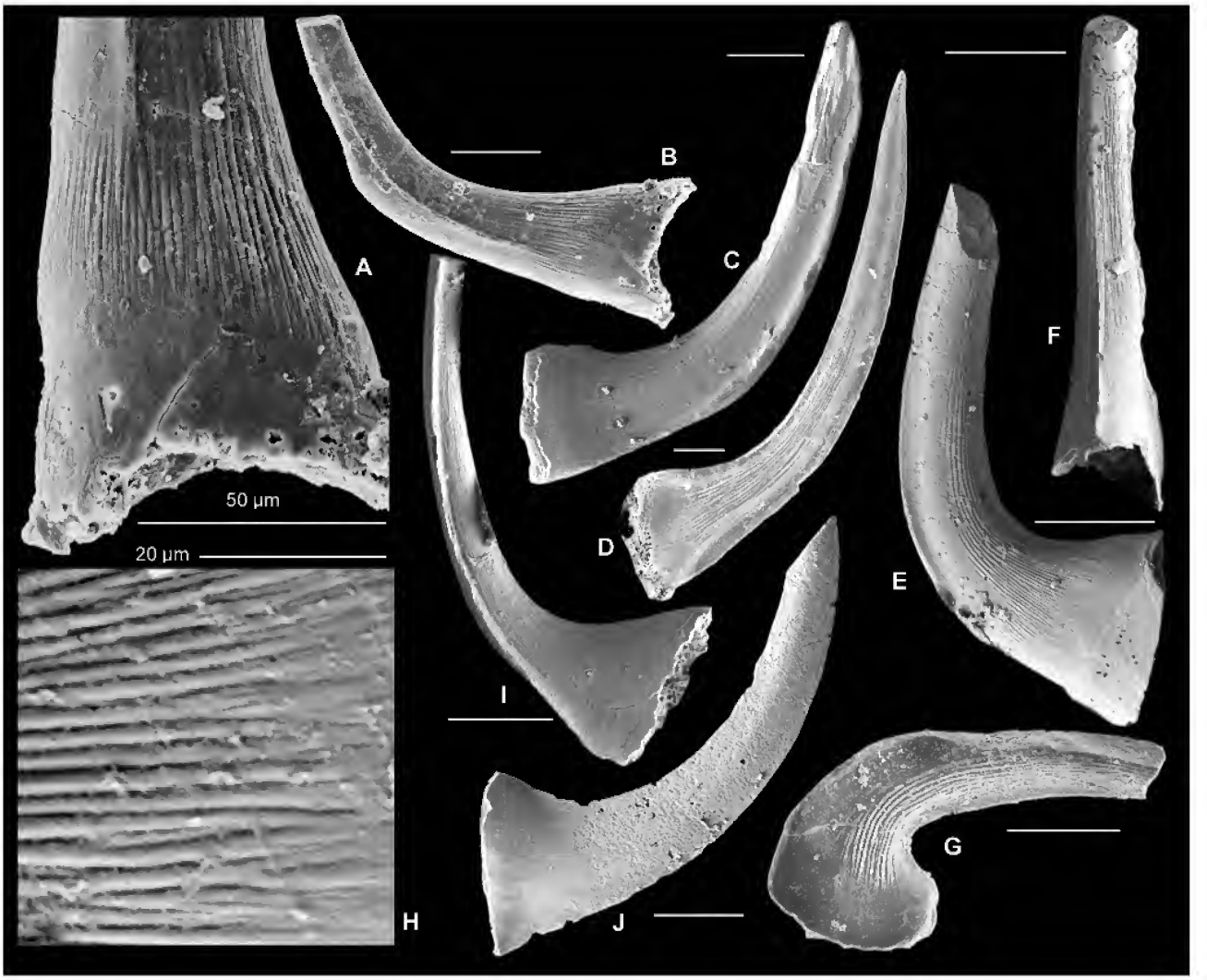

Fig. 25. *Scalpellodus latus* (van Wamel, 1974): *A,B*, Sa element, AMF120452, Y4–2, *A*, inner lateral view of the basal part showing the fine striae, *B*, lateral view; *C*, Sb element, AMF120453, Y4–2, inner lateral view; *D*, Sb element, AMF120454, M/A11-1, inner lateral view; *E,H*, Sd element, AMF120455, M/A7, *E*, inner lateral view, *H*, close up showing fine striae; *F*, Sd element, AMF120456, M/A7, posterior view; *G*, P element, AMF120457, TAB1/39.5, inner lateral view; *I*, Sd element, AMF120458, M/A7, inner lateral view; *J*, Sc element, AMF120459, Y4–2, lateral view. Scale bars 100 µm, unless otherwise indicated.

Scolopodus Pander, 1856

Type species. *Scolopodus sublaevis* Pander, 1856.

Scolopodus multicostatus Barnes & Tuke, 1970

Fig. 26A–R

Scolopodus multicostatus Barnes & Tuke, 1970: 92, pl. 18, figs. 5, 9, 15, 16, text-fig. 6D.
Scolopodus multicostatus.–Ethington & Clark, 1982: 101, pl. 11, figs. 19, 20.
Scolopodus multicostatus.–Stait & Druce, 1993: 310, figs. 13H–I, 19F–J,L.

Material. 85 specimens (8 Pa, 14 Pb, 17 Sa, 17 Sb, 17 Sc, 12 Sd) from the Tabita Formation at Mount Arrowsmith, and 48 specimens (3 Pa, 7 Pb, 6 Sa, 15 Sb, 12 Sc, 5 Sd) from the unnamed dolomitic limestone unit at Koonenberry Gap.

Diagnosis. A species of *Scolopodus* consisting of a seximembrate apparatus including two laterally compressed scandodiform P elements with a short base, and multicostate S elements with a longer base and a broad anterior margin; symmetrical Sa and Sd elements more or less rounded in cross section, asymmetrical Sb and Sc elements laterally more compressed.

Description. P elements scandodiform with erect cusp; *Pa element* with a smooth outer lateral face; inner face multicostate with a median costa, an anterolateral costa, a posterior costa and a number of interposed weaker costae (Fig. 26A,B). *Pb element* has a stronger, more or less blade-like antero-inner lateral costa, and a costa along the posterior margin (Fig. 26C–E); outer lateral face smooth or with a few weak, short costae near the base. *Sa element* symmetrical, with a reclined cusp which is more or less rounded in cross section, a broad smooth anterior face, and bearing three or more costae on each posterolateral face (Fig. 26F–I). *Sb element* slightly asymmetrical, laterally compressed; cusp proclined with a broad anterior face and sharp posterior margin; the inner lateral face with two to four stronger costa and several finer ones in between; outer lateral face with a stronger anterolateral costa and several finer ones posterior to it (Fig. 26J,K,M,N). *Sc element* asymmetrical, laterally compressed; cusp suberect with a sharp posterior costa along the posterior margin and a sharp anterolateral costa on the inner side (Fig. 26L), as well as a number of weaker costae (typically three or four) on each lateral face; costae on the outer lateral face weaker than those on the inner lateral face (Fig. 26 O). *Sd element* nearly symmetrical, less laterally compressed in comparison with the Sb and Sc elements; basal cavity opening rounded (often flared); broad anterior face, a costa along the posterior margin, with several costae on each of the lateral faces; the anterolateral costa on each side stronger than others (Fig. 26Q,R).

Remarks. Two species of *Scolopodus* are present in western New South Wales; *S. multicostatus* is distinguished in generally having fewer costae, which are also much weaker and not as sharp-edged as in the co-occurring *S. quadratus*. The Newfoundland type specimens of *S. multicostatus* figured by Barnes & Tuke (1970), which are all slightly asymmetrical with a short base and erect cusp, are identical to the New South Wales Sb elements. Stait & Druce (1993) recognized a seximembrate apparatus for *S. multicostatus* from the Coolibah Formation of the Georgina Basin, including scandodiform (Pa), posteriorly keeled scandodiform (Pb), acontiodiform (Sa), planoconvex (Sb), laterally compressed paltodiform (Sc) and equidimensional paltodiform (Sd) elements. The Coolibah Formation material generally exhibits more numerous, strongly developed costae than do the specimens in western New South Wales; however, Pa elements from both areas are identical. Specimens referred to the symmetrical Sa element in our collections have weakly developed costae, a broader anterior face, and a more strongly reclined cusp in comparison with the Sa element illustrated from the Coolibah Formation (Stait & Druce, 1993, fig. 19L).

Scolopodus quadratus Pander, 1856

Fig. 27A–O

Scolopodus quadratus Pander, 1856: 26, pl. 2, fig. 6a–d, pl. A, fig. 5d.
Scolopodus costatus Pander, 1856: 26, pl. 2, fig. 7a–d, pl. A, fig. 5e.
Scolopodus striatus Pander, 1856: 26, pl. 2, fig. 8a–d, pl. A, fig. 5f.
Scolopodus rex Lindström, 1955: 595, 596, pl. 3, fig. 32.
Scolopodus rex var. *paltodiformis* Lindström, 1955: 596, pl. 3, figs. 33, 34.
Scolopodus quadratus.–Fåhraeus, 1982: 21, pl. 2, figs. 1–14, pl. 3, figs. 1–8, 15.
Scolopodus rex.–Seo *et al*., 1994, fig. 10.10–10.12.
Scolopodus rex.–Albanesi, *in* Albanesi *et al*., 1998: 133, pl. 12, figs. 14–17 (*cum syn*.).
Scolopodus quadratus.–Zhen *et al*., in press: pl. 5, figs. 15–21 (*cum syn*.).

Material. One specimen (Sd) from limestone nodules within shales of the upper Yandaminta Quartzite and 37 specimens (4 Pb, 12 Sa, 12 Sb, 1 Sc, 8 Sd) from the overlying Tabita Formation at Mount Arrowsmith; two specimens (1 Sa, 1 Sd) from the unnamed dolomitic limestone unit at Koonenberry Gap.

Remarks. Five element types have been recovered from the Tabita Formation, including a scandodiform Pb element with a proclined cusp, four costae on the inner lateral face and a smooth outer lateral face (Fig. 27A–C), and four scolopodiform elements: the symmetrical Sa (Fig. 27D–F), nearly symmetrical Sb (Fig. 27G–I), laterally compressed nearly symmetrical Sc element (Fig. 27M–O), and asymmetrical Sd element with slightly twisted cusp (Fig. 27J–L). However, the species is highly variable, and there are intermediate morphotypes varying in the number of costae, symmetry, curvature of the cusp, and degree of lateral compression. *Scolopodus quadratus* also occurs in the slightly older Hensleigh Siltstone of the Lachlan Fold Belt (Zhen *et al*., in press).

Triangulodus van Wamel, 1974

Type species. *Paltodus volchovensis* Sergeeva, 1963.

Triangulodus larapintinensis (Crespin, 1943)

Fig. 28A–V

Oistodus larapintinensis Crespin, 1943: 231, *partim* only pl. 31, figs. 1–6, 9, 12, 13.
Trigonodus triangularius Nieper, *in* Hill *et al*., 1969: O.14, pl. O 7, fig. 22.
Trigonodus larapintinensis.–Cooper, 1981: 180, pl. 27, figs. 5, 6, 11, 12, 16, 17 (emend.).
?*Trigonodus larapintinensis*.–Watson, 1988: 129, pl. 2, figs. 12–14, 18–20, 22, 23.
Triangulodus larapintinensis.–Stait & Druce, 1993: 315, figs. 14A–C, 21D–F,H–J.

Fig. 26. *Scolopodus multicostatus* Barnes & Tuke, 1970: *A,B*, Pa element, AMF120460, Y4–2, *A*, inner lateral view, *B*, outer lateral view; *C,D*, Pb element, AMF120461, M/A11-2, *C*, outer lateral view, *D*, postero-inner lateral view; *E*, Pb element, AMF120462, M/A11-2, posterior view; *F*, ?Sa element, AMF120463, TAB1/8.1, basal view; *G–I*, ?Sa element, AMF120464, C1613, *G,H*, anterolateral views, *I*, anterior view; *J,K*, Sb element, AMF120465, C1613, *J*, inner lateral view, *K*, outer lateral view; *L*, Sc element, AMF120468, M/A11-1, inner lateral view; *M,N*, Sb element, AMF120466, C1613, *M*, inner lateral view, *N*, outer lateral view; *O,P*, Sc element, AMF120467, C1613, *O*, outer lateral view, *P*, inner lateral view; *Q,R*, Sd element, AMF120469, C1613, lateral views. Scale bars 100 μm.

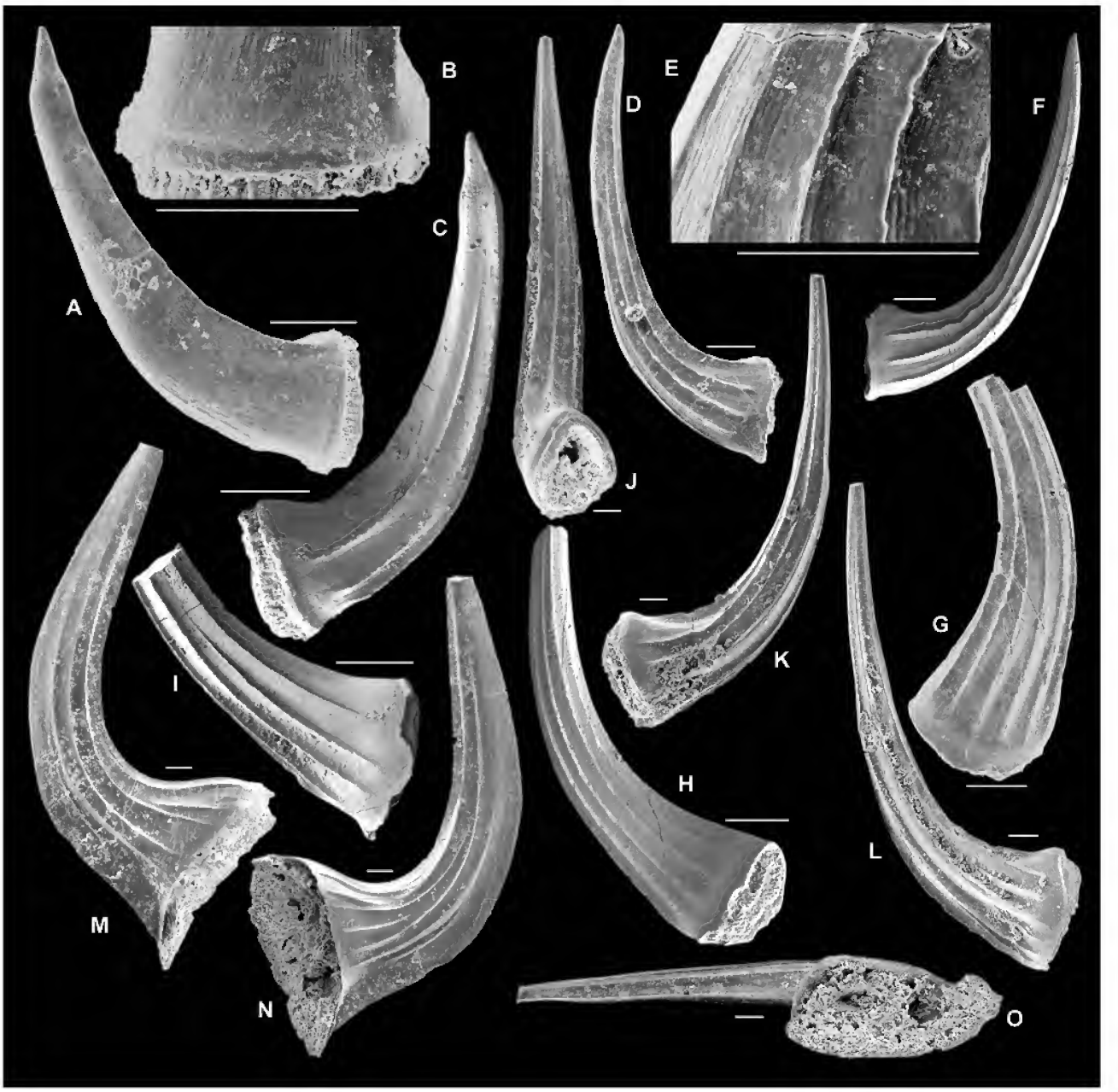

Fig. 27. *Scolopodus quadratus* Pander, 1856: *A–C*, Pb element, AMF120472, Y4–2, *A*, outer lateral view, *B*, outer lateral view of the basal part, showing fine striae, *C*, inner lateral view; *D–F*, Sa element, AMF120475, Y4–2, *D,F*, lateral views, *E*, close up showing sharp costae and fine striae; *G,H*, Sb element, AMF120473, Y4–2, *G*, outer lateral view, *H*, inner lateral view; *I*, Sb element, AMF120471, Y4–2, inner lateral view; *J–L*, Sd element, AMF120474, W5, *J*, posterior view, *K*, inner lateral view, *L*, outer lateral view; *M–O*, Sc element, AMF120470, TAB1/8.1, *M*, outer lateral view, *N*, inner lateral view, *O*, basal view. Scale bars 100 µm.

Material. 259 specimens (41 Pa, 31 Pb, 42 M, 31 Sa, 57 Sb, 41 Sc, 16 Sd) from the Tabita Formation at Mount Arrowsmith, and 43 specimens (6 Pb, 10 M, 2 Sa, 10 Sb, 15 Sc) from unnamed dolomitic limestone unit at Koonenberry Gap.

Description. Apparatus septimembrate; the Pa element scandodiform with erect cusp, and sharp anterior and posterior margins (Fig. 28A,B). Pb element similar to the Pa, but with cusp curved inward and inner laterally twisted and the posterior margin showing a rounded gradational curvature towards the base (proclined near the base, Fig. 28C,D). M element geniculate with a short adenticulate outer lateral process (Fig. 28E,F). Sa element symmetrical, with a broad anterior face, a posterior costa, and a lateral costa on each side (Fig. 28G–K). Sb element asymmetrical with a broad anterior face, a weak costa along the posterior margin and a sharp costa on the inner lateral face near the anterior margin, and with a smooth outer lateral face (Fig. 28L–O). Sc element asymmetrical with a suberect cusp, having a sharp costa along the posterior and anterior margins; base more inflated on the outer side with anterior margin inner laterally curved (Fig. 28P–S). Sd element similar to Sc, but strongly asymmetrical and less laterally compressed with a twisted cusp (Fig. 28T–V).

Remarks. The type material from the Waterhouse Range, central Australia, which was poorly illustrated by Crespin

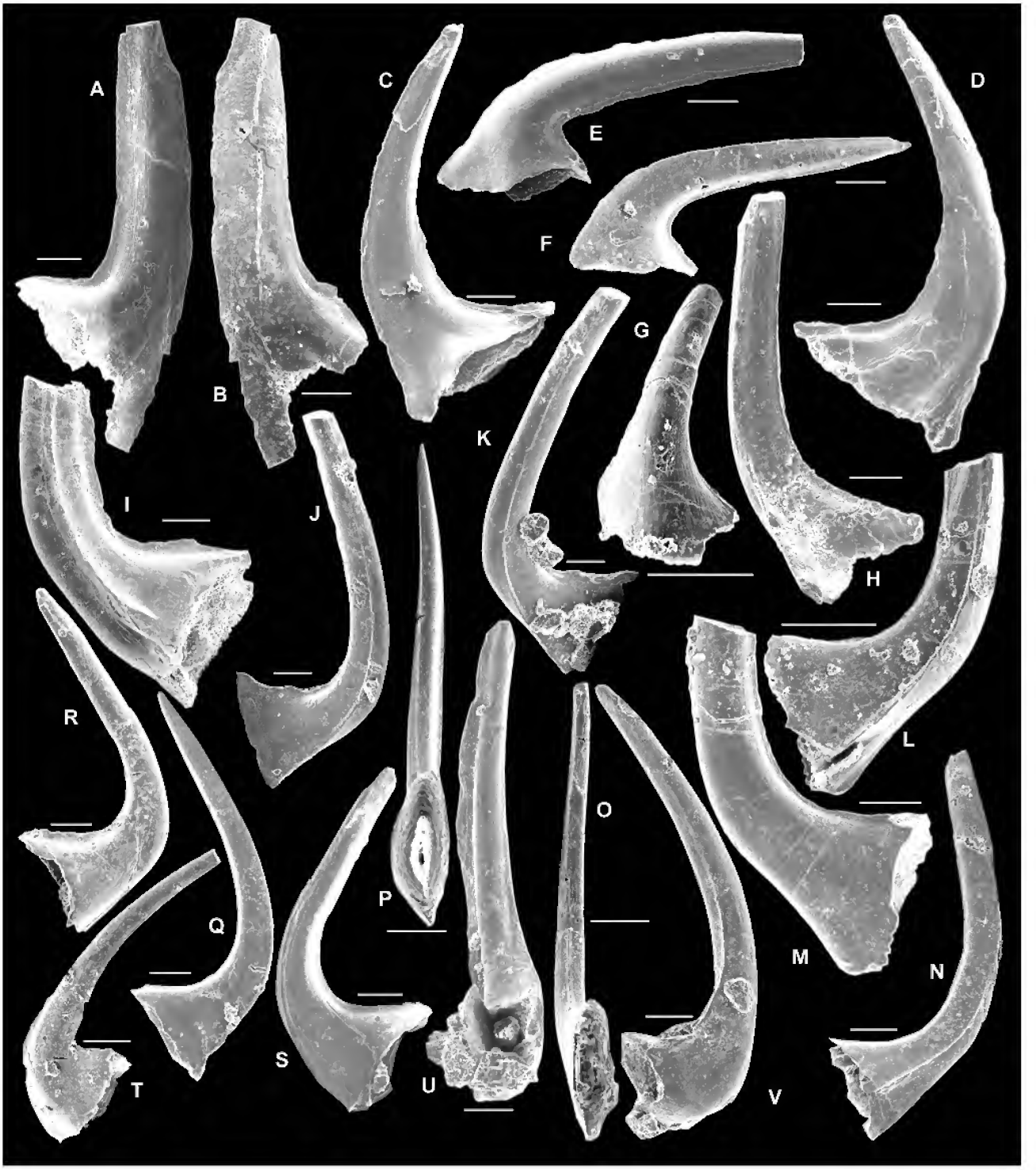

Fig. 28. *Triangulodus larapintinensis* (Crespin, 1943): *A,B*, Pa element, AMF120476, TAB1/85.7, *A*, inner lateral view, *B*, outer lateral view; *C,D*, Pb element, AMF120477, Y4–6, *C*, inner lateral view, *D*, outer lateral view; *E*, M element, AMF120478, Y4–6, anterior view; *F*, M element, AMF120479, M/A7, posterior view; *G*, Sa element, AMF120480, M/A7, anterior view; *H*, Sa element, AMF120481, Y4–6, posterolateral view; *I*, Sa element, AMF120482, M/A4, lateral view; *J,K*, Sa element, AMF124214, Y4–8, lateral views; *L,M*, Sb element, AMF120484, Y4–7, *L*, inner lateral view, *M*, outer lateral view; *N,O*, Sb element, AMF124215, Y4–8, *N*, inner lateral view, *O*, basal view; *P,Q*, Sc element, AMF124216, Y4–8, *P*, basal view, *Q*, inner lateral view; *R,S*, Sc element, AMF124217, Y4–7, *R*, outer lateral view, *S*, inner lateral view; *T*, Sd element, AMF124218, M/A11-3, outer lateral view; *U,V*, Sd element, AMF124219, Y4–8, *U*, posterior view, *V*, outer lateral view. Scale bars 100 μm.

(1943), was re-examined by Cooper (1981) who assigned the species to *Trigonodus* Nieper, *in* Hill *et al.*, 1969. However, as C.Y. Wang (1992) pointed out, that name is pre-occupied by the Triassic bivalve *Trigonodus* Sandberger, *in* Alberti, 1864, leaving *Triangulodus* as the valid genus. A brief discussion of the complex nomenclatural history of Crespin's species, provided by Strusz (1994: 132, 252), suggests further study (probably involving recollec-

tion at the type locality) is needed to fully resolve the species concept. As this is beyond the scope of the present work, we are reliant on Cooper's concept of the species, together with comments kindly provided by R.S. Nicoll who is in the process of reviewing Crespin's and Cooper's types.

The material from western New South Wales is identical with that of the species illustrated from the Horn Valley Siltstone, except that the Pb element from central Australia has a much more strongly twisted cusp (Cooper, 1981, pl. 27, fig. 11). Cooper (1981) recognized a quadricostate asymmetrical Sb element, which he did not illustrate. The asymmetrical Sc element (Cooper, 1981, pl. 27, fig. 5), described as tricostate (anterior, posterior, and one lateral), is here regarded as the Sb element. Cooper's Sd element (1981, pl. 27, fig. 12) is the most laterally compressed specimen, with a sharp costa along the posterior margin, and an inner laterally curved costa along the anterior margin. It is now reassigned to the Sc position. A asymmetrical element like Sc but with a twisted cusp from the western New South Wales fauna is interpreted as the Sd element (Fig. 28T–V); it is also distinguished by its less laterally compressed base.

Triangulodus sp. A

Fig. 29A–P

Material. 15 specimens (4 Sa, 5 Sb, 5 Sc, 1 Sd) from the Tabita Formation at Mount Arrowsmith, 64 specimens (11 Sa, 30 Sb, 21 Sc, 2 Sd) from unnamed dolomitic limestone unit at Koonenberry Gap.

Description. Only S elements are recognized for this species, characterized by having an open, slightly inflated basal cavity. Sa element symmetrical, tricostate, with a costa along the posterior margin, a broad anterior face, and a costa on each lateral side (Fig. 29A–E); cusp suberect, triangular in cross section. Sb element asymmetrical, bicostate, with an anterolateral costa on the inner lateral side, a posterolateral costa on the outer lateral side, and with broad anterior and posterior surfaces (Fig. 29F–I). Sc element asymmetrical, with a sharp costa along the anterior and posterior margins, and with the most laterally compressed base of all elements recognized; anterior costa inner laterally curved; a broad carina also developed on the inner lateral face (Fig. 29J–M). Sd element nearly symmetrical, with broad anterior and posterior margins, and with a sharp costa on each lateral face (Fig. 29N–P).

Remarks. This species, especially the Sa and Sc elements, somewhat resembles *T. larapintinensis*, but generally all elements are less laterally compressed with an open, slightly inflated basal cavity.

Ulrichodina Furnish, 1938

Type species. *Acontiodus abnormalis* Branson & Mehl, 1933.

Ulrichodina sp. cf. *simplex* Ethington & Clark, 1982

Fig. 14M–O

"*Drepanodus*" sp. 3 Serpagli, 1974: 45, pl. 10, fig. 7a–b, pl. 21, fig. 15.
?*Ulrichodina* ?*simplex* Ethington & Clark, 1982: 113, pl. 13, figs. 3–4, 9.
?*Ulrichodina* ?*simplex*.–Smith, 1991: 71, fig. 40d.
?*Ulrichodina* n.sp. 3 Repetski, 1982: 56, pl. 26, fig. 7a–c, fig. 8H.

Material. A single specimen from limestone nodules within shales of the upper Yandaminta Quartzite at Mount Arrowsmith.

Remarks. Due to limited material, neither generic nor specific identification is certain. This specimen may well correspond to the Sa element of a *Drepanoistodus* species. However, based on its distinctive basal cavity shape and the notch on each side, it is tentatively ascribed to *Ulrichodina*. The specimen is a symmetrical, hyaline coniform unit with a laterally compressed, stout, erect cusp, having a distinctive, short, strongly posteriorly curved anticusp-like projection, which has a narrow but rounded anterior corner, and a distinct notch on the basal margin of both sides. It is nearly identical to a specimen referred to as "*Drepanodus*" sp. 3 from the San Juan Formation of the Argentine Precordillera (Serpagli, 1974). However, it is about twice the size of the San Juan specimen, and has the anticusp-like projection at the anterobasal corner more strongly curved posteriorly.

Ethington & Clark (1982) doubtfully assigned Serpagli's San Juan specimen to their new species, ?*Ulrichodina simplex*, which was based on four elements from the Fillmore Formation of the Ibex area, Utah. The three figured type specimens are rather poorly preserved. The holotype is a very large element (about three times as large as the San Juan specimen), has a much weaker development of the notch on each side of the basal margin, and a more laterally compressed cusp with sharp anterior and posterior margins. *Ulrichodina simplex* was also reported from the El Paso Group (Repetski, 1982), and from the Wandel Valley Formation of Greenland (Smith, 1991). In all these occurrences, it is represented by just a few specimens. The figured Greenland specimen, even more doubtfully assigned to *U. simplex*, is an albid element, with a laterally flared buttress on each side, rather than exhibiting a notch deeply carved into the base, as in the Mount Arrowsmith specimen.

Fig. 29. *Triangulodus* sp. A: *A,B*, Sa element, AMF124220, TAB1/8.1, *A*, basal view, *B*, posterolateral view; *C–E*, Sa element, AMF124221, Y4–8, *C,D*, posterolateral view, *E*, basal view; *F*, Sb element, AMF120483, Y4–2, inner lateral view; *G,H*, Sb element, AMF120485, C1613, *G*, upper, inner lateral view, *H*, upper, outer lateral view; *I*, Sb element, AMF120486, C1613, postero-inner lateral view; *J,K*, Sc element, AMF124222, C1613, *J*, basal view, *K*, inner lateral view; *L,M*, Sc element, AMF124223, C1613, *L*, inner lateral view, *M*, postero-inner lateral view; *N–P*, Sd element, AMF120487, M/A7, *N*, anterolateral view, *O*, posterolateral view, *P*, close up showing the fine striae. Scale bars 100 µm, unless otherwise indicated.

ACKNOWLEDGMENTS. Fieldwork by YYZ & BDW at Mount Arrowsmith was undertaken with the support of the Australian Research Council (grant A39600788 to BDW). The study was also supported by a Research Fellowship to YYZ kindly provided by the Sydney Grammar School. John Paterson (Macquarie University) is thanked for providing some additional conodont material from a measured section in the Mount Arrowsmith area. IGP sampled the Koonenberry Gap section under the guidance of Kingsley Mills (Geological Survey of New South Wales). Barry Cooper (Primary Industry & Resources Department of South Australia) kindly made available additional Horn Valley Siltstone collections for comparative study. Gary Dargan (Geological Survey of New South Wales) assisted with acid leaching, residue separation and other laboratory work. Scanning electron microscope photographs were prepared in the Electron Microscope Unit of the Australian Museum; Sue Lindsay is thanked for providing helpful assistance with the SEM work. Helen Beare is thanked for kindly carrying loan material to and from Adelaide. We are grateful for detailed reviews provided by Bob Nicoll (Australian National University) and Guillermo Albanesi (CONICET, Cordoba, Argentina) which markedly contributed to our understanding of several species. IGP publishes with permission of the Director General, NSW Department of Mineral Resources. This is a contribution to IGCP Project no. 410: the Great Ordovician Biodiversification Event.

References

Abaimova, G.P., 1971. New Early Ordovician conodonts from the southeastern part of the Siberian Platform. *Paleontological Journal*, 1971(4): 486–493.

Albanesi, G.L., M.A. Hünicken & C.R. Barnes, 1998. Bioestratigrafía, biofacies y taxonomia de conodontes de las secuencias ordovícicas del Cerro Porterillo, Precordillera central de San Juan, R. Argentina. *Actas de la Academia Nacional de Ciencias* 12: 1–249.

Albanesi, G.L., & N.E. Vaccari, 1994. Conodontos del Arenig en la Formacion Suri, Sistema del Famatina, Argentina. *Revista Española de Micropaleontología* 26: 125–146.

Alberti, F.V., 1864. Überblick über die Trias. Stuttgart.

An, T.X., 1981. Recent progress in Cambrian and Ordovician conodont biostratigraphy of China. *Geological Society of America Special Paper* 187: 209–226.

An, T.X., 1987. *Early Paleozoic conodonts from South China*. Beijing: Peking University Publishing House. [In Chinese with English abstract]

An, T.X., & L.S. Ding, 1985. Ordovician conodont biostratigraphy in Hexian, Anhui Province. *Geological Review* 31(1): 11–20. [In Chinese]

An, T.X., F. Zhang, W.D. Xiang, Y.Q. Zhang, W.H. Xu, H.J. Zhang, D.B. Jiang, C.S. Yang, L.D. Lin, Z.T. Cui & X.C. Yang, 1983. *The conodonts in North China and adjacent regions*. Beijing: Science Press. [In Chinese with English abstract]

An, T.X., & S.C. Zheng, 1990. *The conodonts of the marginal areas around the Ordos Basin, north China*. Beijing: Science Press. [In Chinese with English abstract]

Barnes, C.R., 1974. Ordovician conodont biostratigraphy of the Canadian Arctic. In *Canadian Arctic geology, Proceedings of the symposium on the geology of the Canadian Arctic, Saskatoon, May 1973*, ed. J.D. Aitken & D.J. Glass, pp. 221–240. Geological Association of Canada, and Canadian Society of Petroleum Geologists.

Barnes, C.R., & M.F. Tuke, 1970. Conodonts from the St. George Formation (Ordovician), northern Newfoundland. *Geological Survey of Canada Bulletin* 187: 79–97.

Bauer, J.A., 1987. Conodonts and conodont biostratigraphy of the McLish and Tulip Creek formations (Middle Ordovician) of south-central Oklahoma. *Oklahoma Geological Survey, Bulletin* 141: 1–55.

Bauer, J.A., 1990. Stratigraphy and conodont biostratigraphy of the upper Simpson Group, Arbuckle Mountains, Oklahoma. In *Early to Middle Paleozoic Conodont Biostratigraphy of the Arbuckle Mountains, Southern Oklahoma*, ed. S.M. Ritter. *Oklahoma Geological Survey Guidebook* 27: 39–46.

Bergström, S.M., & R.A. Cooper, 1973. *Didymograptus bifidus* and the trans-Atlantic correlation of the Lower Ordovician. *Lethaia* 6: 313–340.

Branson, E.R., & M.G. Mehl, 1933. Conodont studies. *University of Missouri Studies* 8: 1–349.

Chen, X., J.Y. Rong, X.F. Wang, Z.H. Wang, Y.D. Zhang & R.B. Zhan, 1995. Correlation of the Ordovician rocks of China: charts and explanatory notes. *International Union of Geological Sciences, Publication* 31: 1–104.

Clark, D.L., W.C. Sweet, S.M. Bergström, G. Klapper, R.L. Austin, F.H.T. Rhodes, K.J. Müller, W. Ziegler, M. Lindström, J.F. Miller & A.G. Harris, 1981. Conodonta. In *Treatise on Invertebrate Paleontology, part W, Miscellanea, supplement 2*, ed. R.A. Robison. Boulder: Geological Society of America, and Lawrence: University of Kansas.

Cooper, B.J., 1981. Early Ordovician conodonts from the Horn Valley Siltstone, central Australia. *Palaeontology* 24: 147–183.

Crespin, I., 1943. Conodonts from the Waterhouse Range, Central Australia. *Transactions of the Royal Society of South Australia* 67: 231–233.

Crick, R.E., & C. Teichert, 1983. Ordovician endocerid genus *Anthoceras*: its occurrence and morphology. *Alcheringa* 7: 155–162.

Dzik, J., 1976. Remarks on the evolution of Ordovician conodonts. *Acta Palaeontologica Polonica* 21: 395–455.

Dzik, J., 1978. Conodont biostratigraphy and paleogeographical relations of the Ordovician Mójcza Limestone (Holy Cross Mts, Poland). *Acta Palaeontologica Polonica* 23: 51–72.

Dzik, J., 1983. Relationships between Ordovician Baltic and North American Midcontinent conodont faunas. *Fossils and Strata* 15: 59–85.

Dzik, J., 1991. Evolution of oral apparatuses in the conodont chordates. *Acta Palaeontologica Polonica* 36: 265–323.

Dzik, J., 1994. Conodonts of the Mójcza Limestone. In *Ordovician carbonate platform ecosystem of the Holy Cross Mountains*, ed. J. Dzik, E. Olempska & A. Pisera, *Palaeontologica Polonica* 53: 43–128.

Ethington, R.L., & U. Brand, 1981. *Oneotodus simplex* (Furnish) and the genus *Oneotodus* (Conodonta). *Journal of Paleontology* 55: 239–247.

Ethington, R.L., & D.L. Clark, 1964. Conodonts from the El Paso Formation (Ordovician) of Texas and Arizona. *Journal of Paleontology* 38: 685–704.

Ethington, R.L., & D.L. Clark, 1982. Lower and Middle Ordovician conodonts from the Ibex area, western Millard County, Utah. *Brigham Young University, Geological Studies* 28(2): 1–160.

Ethington, R.L., O. Lehnert & J.E. Repetski, 2000. *Stiptognathus* new genus (Conodonta: Ibexian, Lower Ordovician), and the apparatus of *Stiptognathus borealis* (Repetski, 1982). *Journal of Palaeontology* 74: 92–100.

Fåhraeus, L.E., 1966. Lower Viruan (Middle Ordovician) conodonts from the Güllhögen Quarry, southern central Sweden. *Sveriges Geologiska Undersökning, Ser. C* 610: 1–40.

Fåhraeus, L.E., 1982. Recognition and redescription of Pander's (1856) *Scolopodus* (form) species—constituents of multi-element taxa (Conodontophorida, Ordovician). *Geologica et Palaeontologica* 16: 19–28.

Fåhraeus, L.E., & D.R. Hunter, 1985. Simple-cone conodont taxa from the Cobbs Arm Limestone (Middle Ordovician), New World Island, Newfoundland. *Canadian Journal of Earth Sciences* 22: 1171–1182.

Fåhraeus, L.E., & G.S. Nowlan, 1978. Franconian (Late Cambrian) to early Champlainian (Middle Ordovician) conodonts from the Cow Head Group, western Newfoundland. *Journal of Paleontology* 52(2): 444–471.

Fåhraeus, L.E., & K. Roy, 1993. Conodonts from the Cambro-Ordovician Cooks Brook and Middle Arm Point Formations, Bay of Islands, western Newfoundland. *Geologica et Palaeontologica* 27: 1–53.

Furnish, W.M., 1938. Conodonts from the Prairie du Chien (Lower Ordovician) beds of the upper Mississippi Valley. *Journal of Paleontology* 12: 318–340.

Graves, R.W., & S. Ellison, 1941. Ordovician conodonts of the Marathon Basin, Texas. *Missouri University School of Mines & Metallurgy Bulletin, Technical Series* 14: 1–26.

Hill, D., G. Playford & J.T. Woods, eds., 1969. *Ordovician and Silurian fossils of Queensland*. O.2–O.15 and S.2–S.18. Brisbane: Queensland Palaeontographical Society.

Igo, H., & T. Koike, 1967. Ordovician and Silurian conodonts from the Langkawi Islands, Malaya, Part I. *Geology and Palaeontology of Southeast Asia* 3: 1–29.

Ji, Z.L., & C.R. Barnes, 1994. Lower Ordovician conodonts of the St. George Group, Port au Port Peninsula, western Newfoundland, Canada. *Palaeontographica Canadiana* 11: 1–149.

Johnston, D.I., & C.R. Barnes, 1999. Early and Middle Ordovician (Arenig) conodonts from St. Pauls Inlet and Martin Point, Cow Head Group, western Newfoundland, Canada. 1. Biostratigraphy and paleoecology. *Geologica et Palaeontologica* 33: 21–70.

Johnston, D.I., & C.R. Barnes, 2000. Early and Middle Ordovician (Arenig) conodonts from St. Pauls Inlet and Martin Point, Cow Head Group, western Newfoundland, Canada. 2. Systematic paleontology. *Geologica et Palaeontologica* 34: 11–87.

Jones, P.J., J.H. Shergold & E.C. Druce, 1971. Late Cambrian and Early Ordovician stages in western Queensland. *Journal of the Geological Society of Australia* 18: 1–32.

Kennedy, D.J., 1975. Conodonts from a Lower-Middle Ordovician formation, Mt. Arrowsmith, northwest New South Wales. *Abstracts with Programs, Geological Society of America, North-Central section* 7(6): 796.

Kennedy, D.J., 1976. *Conodonts from Lower Ordovician Rocks at Mount Arrowsmith, Northwest New South Wales, Australia*. Ph.D. thesis, University of Missouri, Columbia, 110 pp., 4 pls. (unpublished).

Landing, E., 1976. Early Ordovician (Arenigian) conodont and graptolite biostratigraphy of the Taconic allochthon, eastern New York. *Journal of Paleontology* 50: 614–646.

Lee, H.Y., 1975. Conodonten aus dem unteren und mittleren Ordovizium von Nordkorea. *Palaeontographica Abteilung* A 150: 161–186, Stuttgart.

Lee, H.Y., 1976. Conodonts from the Maggol and Jeongseon Formation (Ordovician), Kangweon-Do, South Korea. *Journal of the Geological Society of Korea* 12: 151–181.

Lee, H.Y., 1979. A study on biostratigraphy and bioprovince of the Middle Ordovician conodonts from South Korea. *Journal of the Geological Society of Korea* 15: 37–60.

Lehnert, O., 1995. Ordovizische Conodonten aus der Präkordillere Westargentiniens: Ihre Bedeutung für Stratigraphie und Paläogeographie. *Erlanger Geologische Abhandlungen* 125: 1–193.

Lehnert, O., M. Keller & O. Bordonaro, 1998. Early Ordovician conodonts from the southern Cuyania Terrane (Mendoza Province, Argentina). *Palaeontologica Polonica* 58: 47–65.

Lindström, M., 1955. Conodonts from the lowermost Ordovician strata of south-central Sweden. *Geologiska Föreningens i Stockholm Förhandlingar* 76: 517–604.

Lindström, M., 1970. A suprageneric taxonomy of the conodonts. *Lethaia* 3: 427–445.

Lindström, M., 1971. Lower Ordovician conodonts of Europe. In *Symposium on conodont biostratigraphy*, ed. W.C. Sweet & S.M. Bergström. *Geological Society of America, Memoir* 127: 21–61.

Löfgren, A., 1978. Arenigian and Llanvirnian conodonts from Jämtland, northern Sweden. *Fossils and Strata* 13: 1–129.

Löfgren, A., 1994. Arenig (Lower Ordovician) conodonts and biozonation in the eastern Siljan District, central Sweden. *Journal of Paleontology* 68: 1350–1368.

Löfgren, A., 1999. A septimembrate apparatus model for the Ordovician conodont genus *Cornuodus* Fåhraeus, 1966. In *Studies on Conodonts—Proceedings of the Seventh European Conodont Symposium, Bologna-Modena, 1998*, ed. E. Serpagli. *Bollettino della Società Paleontologica Italiana* 37: 175–186.

McTavish, R.A., 1973. Prioniodontacean conodonts from the Emanuel Formation (Lower Ordovician) of Western Australia. *Geologica et Palaeontologica* 7: 27–58.

Mills, K.J., 1992. Geological evolution of the Wonominta Block. *Tectonophysics* 214: 57–68.

Nicoll, R.S., 1990. The genus *Cordylodus* and a latest Cambrian-earliest Ordovician conodont biostratigraphy. *BMR Journal of Australian Geology & Geophysics* 11: 529–558.

Nicoll, R.S., 1992. Analysis of conodont apparatus organisation and the genus *Jumudontus* (Conodonta), a coniform-pectiniform apparatus structure from the Early Ordovician. *BMR Journal of Australian Geology & Geophysics* 13: 213–228.

Nicoll, R.S., 1994. Seximembrate apparatus structure of the Late Cambrian coniform conodont *Teridontus nakamurai* from the Chatsworth Limestone, Georgina Basin, Queensland. *AGSO Journal of Australian Geology & Geophysics* 15: 367–379.

Nicoll, R.S., & R.L. Ethington, in press. *Lissoepikodus nudus* gen. et sp. nov. and *Oepikodus cleftus* sp. nov., new septimembrate conodont taxa from the Early Ordovician of Australia and Nevada. *Courier Forschungsinstitut Senckenberg*.

Nicoll, R.S., J.R. Laurie & M.T. Roche, 1993. Revised stratigraphy of the Ordovician (Late Tremadoc-Arenig) Prices Creek Group and Devonian Poulton formation, Lennard Shelf, Canning Basin, Western Australia. *AGSO Journal of Australian Geology & Geophysics* 14: 65–76.

Nowlan, G.S., 1976. *Late Cambrian to Late Ordovician Conodont Evolution and Biostratigraphy of the Franklinian Miogeosyncline, Eastern Canadian Arctic Islands*. Ph.D. thesis, University of Waterloo, Ontario (unpublished).

Packham, G.H., 1969. Northwestern Region IV. Palaeozoic sequences. In *The Geology of New South Wales*, ed. G.H. Packham. *Journal of the Geological Society of Australia* 16(1): 67–70.

Pander, C.H., 1856. *Monographie der fossilen Fische des Silurischen Systems der Russisch-Baltischen Gouvernements*. St. Petersburg: Akademie der Wissenschaften.

Paterson, J., 2001a. First occurrence of *Janospira* from the Early Ordovician of Australia. *Alcheringa* 25(1–2): 129–130.

Paterson, J., 2001b. *Early Ordovician Geology & Palaeontology of Mount Arrowsmith, Northwestern New South Wales*. B.Sc. (Hons.) thesis, Macquarie University, Sydney (unpublished).

Pohler, S.M.L., 1994. Conodont biofacies of Lower to lower Middle Ordovician megaconglomerates, Cow Head Group, Western Newfoundland. *Geological Survey of Canada, Bulletin* 459: 1–71.

Purnell, M.A., P.C.J. Donoghue & R.J. Aldridge, 2000. Orientation and anatomical notation in conodonts. *Journal of Paleontology* 74(1): 113–122.

Repetski, J.E., 1982. Conodonts from El Paso Group (Lower Ordovician) of westernmost Texas and southern New Mexico. *New Mexico Bureau of Mines & Mineral Resources, Memoir* 40: 1–121.

Seo, K.S., H.Y. Lee & R.L. Ethington, 1994. Early Ordovician conodonts from the Dumugol Formation in the Baegunsan Syncline, eastern Yeongweol and Samcheog areas, Kangweon-Do, Korea. *Journal of Paleontology* 68(3): 599–616.

Sergeeva, S.P., 1963. Conodonts from the Lower Ordovician of the Leningrad region. *Akademia Nauk SSSR Paleontologicheskiy Zhurnal* 1963(2): 93–108.

Serpagli, E., 1974. Lower Ordovician conodonts from Precordilleran Argentina (Province of San Juan). *Bollettino della Società Paleontologica Italiana* 13: 17–98.

Shergold, J.H., 1971. Resume of data on the base of the Ordovician in northern and central Australia. In *Colloque Ordovicien-Silurien*, ed. C. Babin, *Mémoires du Bureau de Recherches géologiques et minières* 73: 391–402.

Shergold, J.H., J.R. Laurie & R.S. Nicoll, 1995. Biostratigraphy of the Prices Creek Group (Early Ordovician, late Lancefieldian-Bendigonian), on the Lennard Shelf, Canning Basin, Western Australia. In *Ordovician Odyssey: short papers for the Seventh International Symposium on the Ordovician System*, ed. J.D. Cooper, M.L. Droser & S.C. Finney, pp. 93–96. Fullerton: Pacific Section, Society for Sedimentary Geology (SEPM).

Smith, M.P., 1991. Early Ordovician conodonts of East and North Greenland. *Meddelelser om Grønland, Geoscience* 26: 1–81.

Stait, K., & E.C. Druce, 1993. Conodonts from the Lower Ordovician Coolibah Formation, Georgina Basin, central Australia. *BMR Journal of Australian Geology & Geophysics* 13: 293–322.

Stewart, I., & R.S. Nicoll, in press. The 15 element, septimembrate, apparatus structure of the Early Ordovician conodont *Oepikodus evae* Lindström from Australia and Sweden. *Courier Forschungsinstitut Senckenberg*.

Stouge, S., 1982. Preliminary conodont biostratigraphy and correlation of Lower to Middle Ordovician carbonates of the St. George Group, Great Northern Peninsula, Newfoundland. *Newfoundland Department of Mines & Energy Report* 82–3: 1–59.

Stouge, S., 1984. Conodonts of the Middle Ordovician Table Head Formation, western Newfoundland. *Fossils and Strata* 16: 1–145.

Stouge, S., & G. Bagnoli, 1988. Early Ordovician conodonts from Cow Head Peninsula, western Newfoundland. *Palaeontographica Italica* 75: 89–179.

Stouge, S., & G. Bagnoli, 1990. Lower Ordovician (Volkhovian-Kundan) conodonts from Hagudden, northern Öland, Sweden. *Palaeontographia Italica* 77: 1–54.

Stouge, S., & G. Bagnoli, 1999. The suprageneric classification of some Ordovician prioniodontid conodonts. In *Studies on Conodonts—Proceedings of the Seventh European Conodont Symposium, Bologna-Modena, 1998*, ed. E. Serpagli. *Bollettino della Società Paleontologica Italiana* 37: 145–158.

Strusz, D.L., 1994. Catalogue of Type, Figured and Cited specimens in the Commonwealth Palaeontological Collection. CPC Catalogues: 5. Conodonta. Australian Geological Survey Organisation, Record 1994/35.

Sweet, W.C., 1988. *The Conodonta: Morphology, Taxonomy, Paleoecology, and Evolutionary History of a Long-Extinct Animal Phylum*. Oxford: Clarendon Press.

Sweet, W.C., R.L. Ethington & C.R. Barnes, 1971. North American Middle and Upper Ordovician conodont faunas. In *Symposium on conodont biostratigraphy*, ed. W.C. Sweet & S.M. Bergström. *Geological Society of America, Memoir* 127: 163–193.

Tipnis, R.S., B.D.E. Chatterton & R. Ludvigsen, 1978. Ordovician conodont biostratigraphy of the southern District of Mackenzie, Canada. In *Western and Arctic Canadian biostratigraphy*, ed. C.R. Stelck & B.D.E. Chatterton. *Geological Association of Canada, Special Paper* 18: 39–91.

van Wamel, W.A., 1974. Conodont biostratigraphy of the Upper Cambrian and Lower Ordovician of north-western Öland, south-eastern Sweden. *Utrecht Micropalaeontological Bulletins* 10: 1–125.

Wang, C.Y., 1992. *Trigonodus* Nieper, an invalid name for Lower Ordovician conodonts. *Acta Palaeontologica Sinica* 31(5): 621–622.

Wang, C.Y., ed., 1993. *Conodonts of the Lower Yangtze Valley—an index to biostratigraphy and organic metamorphic maturity*. Beijing: Science Press. [In Chinese with English summary]

Wang, Q.Z., K.J. Mills, B.D. Webby & J.H. Shergold, 1989. Upper Cambrian (Mindyallan) trilobites and stratigraphy of the Kayrunnera Group, western New South Wales. *BMR Journal of Australian Geology & Geophysics* 11: 107–118.

Wang, Z.H., & S.M. Bergström, 1999. Conodonts across the base of the Darriwilian Stage in South China. *Acta Micropalaeontologica Sinica* 16(4): 325–350.

Wang, Z.H., & K.Q. Luo, 1984. Late Cambrian and Ordovician conodonts from the marginal areas of the Ordos Platform, China. *Bulletin of Nanjing Institute of Geology and Palaeontology, Academia Sinica* 8: 237–304; Nanjing.

Warris, B.J., 1967. *The Palaeozoic Stratigraphy and Palaeontology of North-western New South Wales*. Ph.D. thesis, University of Sydney, 470 pp., 20 pls. (unpublished).

Warris, B.J., 1969. The Mt Arrowsmith area. In *The Geology of New South Wales*, ed. G.H. Packham. *Journal of the Geological Society of Australia* 16(1): 69–70.

Watson, S.T., 1988. Ordovician conodonts from the Canning Basin (W. Australia). *Palaeontographica Abteilung* A. 203(4–6): 91–147.

Webby, B.D., 1976. The Ordovician System in south-eastern Australia. In *The Ordovician System: proceedings of a Palaeontological Association symposium, Birmingham, September 1974*, ed. M.G. Bassett, pp. 417–446. Cardiff: University of Wales Press and National Museum of Wales.

Webby, B.D., 1978. History of the Ordovician continental platform shelf margin of Australia. *Journal of the Geological Society of Australia* 25: 41–63.

Webby, B.D., 1983. Lower Ordovician arthropod trace fossils from western New South Wales. *Proceedings of the Linnean Society of New South Wales* 107: 61–76.

Webby, B.D., 1995. Towards an Ordovician time scale. In *Ordovician Odyssey: Short Papers for the Seventh International Symposium on the Ordovician System*, ed. J.D. Cooper, M.L. Droser & S.C. Finney, pp. 5–9. Fullerton: Pacific Section, Society for Sedimentary Geology (SEPM).

Webby, B.D., Q.Z. Wang & K.J. Mills, 1988. Upper Cambrian and basal Ordovician trilobites from western New South Wales. *Palaeontology* 31: 905–938.

Webby, B.D., *et al.*, 1981. The Ordovician System in Australia, New Zealand, and Antarctica. Correlation chart and explanatory notes. *International Union of Geological Sciences, Publication* No. 6.

Wopfner, H., 1967. Cambro-Ordovician sediments from the north-eastern margin of the Frome Embayment (Mt. Arrowsmith, N.S.W.). *Journal and Proceedings, Royal Society of New South Wales* 100: 163–177.

Zhen, Y.Y., R.S. Nicoll, I.G. Percival, M.A. Hamedi & I. Stewart, 2001. Ordovician rhipidognathid conodonts from Australia and Iran. *Journal of Paleontology* 75: 186–207.

Zhen, Y.Y., I.G. Percival & B.D. Webby, in press. Early Ordovician (Bendigonian) conodonts from central New South Wales, Australia. *Courier Forschungsinstitut Senckenberg* 243.

Ziegler, W., ed., 1975. *Catalogue of Conodonts*. II: 1–403. Stuttgart: E. Schweizerbart'sche.

Ziegler, W., ed., 1977. *Catalogue of Conodonts*. III: 1–574. Stuttgart: E. Schweizerbart'sche.

Manuscript received 29 May 2002, revised 11 October 2002 and accepted 11 October 2002.

Associate Editor: G.D. Edgecombe.

Records of the Australian Museum (2003) Vol. 55: 221–230. ISSN 0067-1975

Early Ordovician Orthide Brachiopods from Mount Arrowsmith, Northwestern New South Wales, Australia

JOHN R. PATERSON* AND GLENN A. BROCK

Centre for Ecostratigraphy and Palaeobiology,
Department of Earth and Planetary Sciences, Macquarie University NSW 2109, Australia
agnostid@hotmail.com · Glenn.Brock@mq.edu.au

ABSTRACT. Two new late Early Ordovician orthide brachiopods, *Celsiorthis bulancis* n.gen. and n.sp. and *Alocorthis psygmatelos* n.gen. and n.sp., are described from the Tabita and Pingbilly formations at Mount Arrowsmith, northwestern New South Wales. The associated conodont assemblage from the succession at Mount Arrowsmith indicates a late Bendigonian to Chewtonian age for the brachiopod bearing horizons.

PATERSON, JOHN R., & GLENN A. BROCK, 2003. Early Ordovician orthide brachiopods from Mount Arrowsmith, northwestern New South Wales, Australia. *Records of the Australian Museum* 55(2): 221–230.

In a global review of Ordovician brachiopod distribution, Jaanusson (1973) was so frustrated by the lack of data from Australia that he used the term "terra incognita" to describe the major lacuna in knowledge concerning the occurrence of taxa from austral waters. Whilst Percival (in Webby *et al.*, 2000) indicated this situation has improved significantly, especially for Late Ordovician faunas from Tasmania (Laurie, 1991a,b) and New South Wales (Percival, 1979a,b, 1991; Percival *et al.*, 2001), knowledge of Early and Middle Ordovician brachiopod faunas from Australia remains deficient.

The oldest known formally described Ordovician brachiopod fauna from Australia was recorded by Laurie (1987) from the Lancefieldian Digger Island Formation in Victoria. The fauna consists of two orthid species, *Finkelnburgia lindneri* Laurie and *Archaeorthis waratahensis* Laurie.

Prendergast (1935) described eleven brachiopod species, including the orthid *Spanodonta hoskingiae*, from the Gap Creek Formation of the Canning Basin, Western Australia, and indicated a Late Palaeozoic (Permo-Carboniferous) age for the fauna. The Gap Creek Formation is now known to be late Bendigonian (Be3–Be4) in age (Laurie, 1997). Laurie (1997) also described the orthids ?*Pseudomimella* sp., ?*Oligorthis* sp., *Tritoechia* sp., and *Tinopena shergoldi* from the Gap Creek Formation.

Brown (1948) described two clitambonitoid and one porambonitoid species from the Lower Ordovician (Lancefieldian-Castlemanian—see Laurie, 1991a,b) Florentine Valley Formation of southern Tasmania. Laurie (1980) later redescribed *Tritoechia lewisi* and recorded several new orthoid and clitambonitoid species from the Florentine Valley Formation and overlying Karmberg Limestone. The species Brown (1948) described as ?*T. careyi* was tentatively referred to *Nanorthis carinata* by Laurie (1987). The taxon documented as *Orthis lenticularis* Wahlenberg by Etheridge (1904, pl. 10, figs. 5–9) was also placed in synonymy with *N. carinata* by Laurie (1987). Laurie (1991a) developed a detailed biostratigraphic scheme for the Ordovician of Tasmania based on twenty brachiopod assemblages. In his comprehensive study of the Ordovician and Early Silurian articulate brachiopods of Tasmania, Laurie (1991b) recorded six Early Ordovician brachiopod assemblages, ranging in age from the Lancefieldian to Chewtonian. These six brachiopod assemblages extend from the Pontoon Hill Siltstone Member of the Florentine Valley Formation through to the lower parts of the Karmberg Limestone.

* author for correspondence

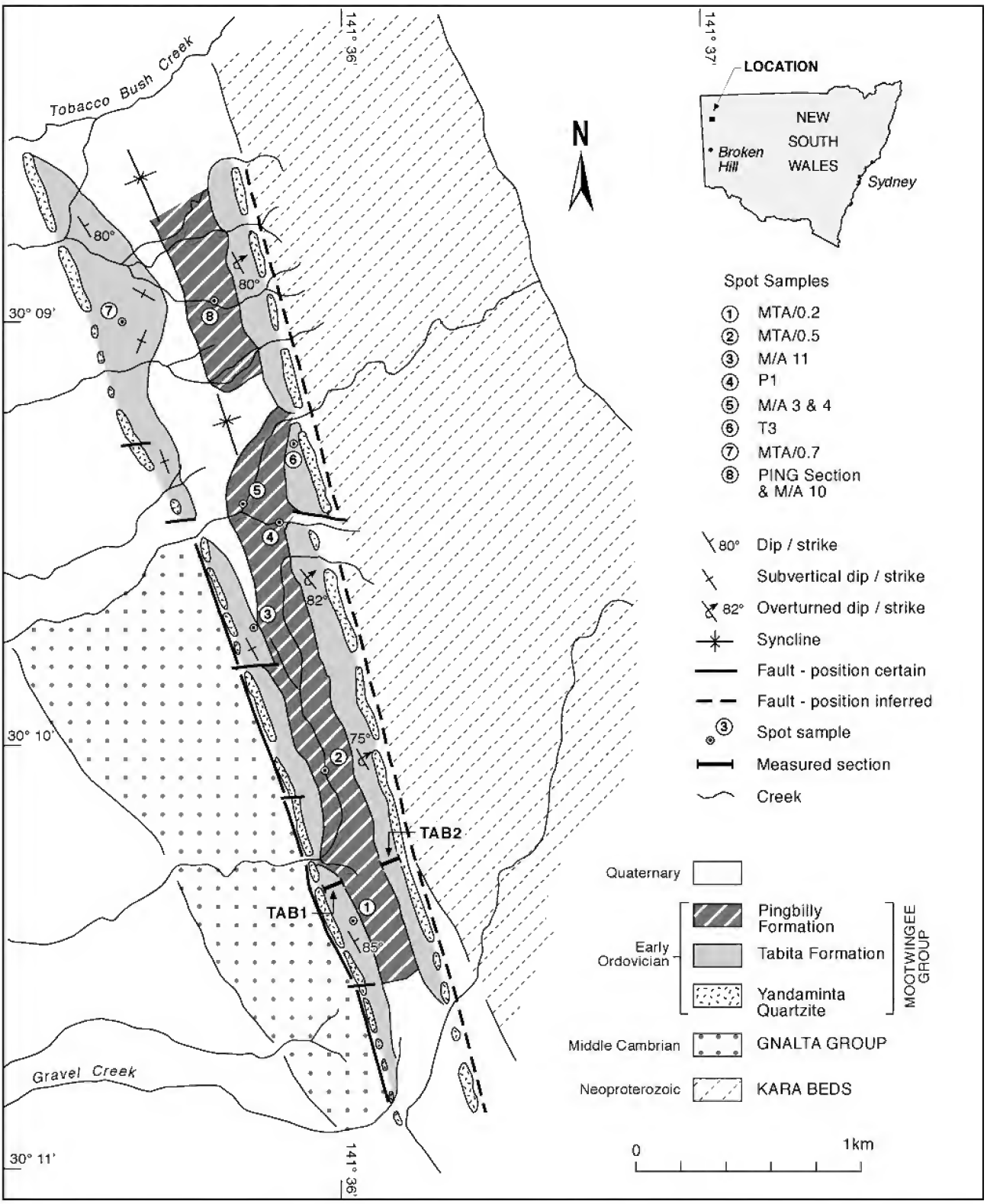

Fig. 1. Geological map of the southwest portion of the Mount Arrowsmith Inlier, northwestern New South Wales. All measured stratigraphic sections and spot localities are shown.

The focus of this paper is to describe two new Early Ordovician orthide brachiopods, apparently endemic to the Mount Arrowsmith region (Gnalta Shelf) of northwestern New South Wales (Fig. 1), and thereby add significant new data on the early evolution and distribution of the Orthida in Australia.

Locality, stratigraphy and age

Mount Arrowsmith is situated in the northwestern corner of New South Wales (Fig. 1), approximately 80 km SSW of Tibooburra and 200 km north of Broken Hill. The Proterozoic-Palaeozoic inlier at Mount Arrowsmith is one of several protruding through the Mesozoic sediment

blanket in far northwest New South Wales, forming part of the Wonominta Block (Mills, 1992). Sediments of the Mount Arrowsmith inlier consist of the Neoproterozoic Kara Beds and Mount Arrowsmith Volcanics, Middle Cambrian Gnalta Group, and the Lower Ordovician Mootwingee Group (Fig. 1). The metasediments of the Kara Beds and the intercalated basic-intermediate Mount Arrowsmith Volcanics are latest Neoproterozoic (586±7 Ma), determined from Zircon U-Pb SHRIMP data from the Mount Arrowsmith Volcanics in the Mount Wright area (Crawford *et al.*, 1997). Sediments of the Middle Cambrian Gnalta Group unconformably overlie the Neoproterozoic Kara Beds, and are subdivided into three units: the Pincally Formation (lowest), Wydjah Formation, and the Wyarra Shale (highest). Brock & Percival (2000) suggested an early Middle Cambrian (Ordian–Early Templetonian) age for the succession based on lingulate brachiopods, molluscs and other small shelly fossils.

The Lower Ordovician Mootwingee Group sediments unconformably overlie the Middle Cambrian Gnalta Group. This unconformity probably corresponds to the Delamerian Orogeny, which began during the latest Middle Cambrian and continued into the Early Ordovician (Webby, 1978; Mills, 1992). In terms of palaeogeographic setting, the sediments of the Mootwingee Group were deposited on the Gnalta Shelf near the palaeocontinental margin at the eastern extremity of the Larapintine Sea, a major epicratonic seaway linking cratonic basins such as the Canning, Amadeus, Georgina and Warburton basins with the palaeo-oceans to the east and west of Australia (see Webby *et al.*, 2000, fig. 6).

The Mootwingee Group is subdivided into three distinct units: the Yandaminta Quartzite (lowest), Tabita Formation, and Pingbilly Formation (highest). The Lower Ordovician succession is exposed within a tight overturned syncline 11 km in length, plunging in a SSE direction. The syncline is separated into northern and southern outcrop tracts by flat-lying Mesozoic and Quaternary sediments that cover its central portion. This study focussed mainly on the southern portion of the syncline (Fig. 1) where material was recovered from measured stratigraphic sections through the Tabita Formation (TAB 1: 30°10'20"S 141°35'56"E) and the Pingbilly Formation (PING: 30°08'57"S 141°35'38"E), as well as isolated spot samples (including some from the northern part of the syncline).

Specimens of both *Celsiorthis bulancis* n.gen. and n.sp. and *Alocorthis psygmatelos* n.gen. and n.sp. are preserved as internal and external moulds within the siltstones and coquinites of the Tabita Formation. Associated biota include dasyclad algae, gastropods, bivalves, cephalopods, trilobites, echinoderms, conodonts, trace fossils and numerous problematic forms (Paterson, 2001a,b, 2002, in press). *Alocorthis psygmatelos* has a relatively narrow stratigraphic range in the Tabita Formation with the first recorded occurrence of the taxon at 40 m above the base of the TAB 1 section and the last recorded occurrence at 60 m above the base of the section (Fig. 2). *Celsiorthis bulancis* is the dominant brachiopod taxon in the section and has a long stratigraphic range extending through most of the Tabita and Pingbilly formations (Fig. 2). The shells in the quartz siltstones and coquinites of the Tabita Formation are often disarticulated but unbroken and tend to be oriented parallel to bedding. The brachiopod and bivalve shells are often preserved in a hydrodynamically stable convex-up position. The orientation of fossil allochems and the occasional presence of imbrication structures in quartz grains within the siltstones suggest the presence of traction currents. These palaeontological and sedimentological data indicate that the Tabita Formation was deposited in a relatively low energy, well oxygenated, shallow marine, inner shelf environment.

The Pingbilly Formation, of approximately 70 m maximum thickness, is generally poorly outcropping, but where exposed is dominated by mudstones composed of well sorted, fine, subangular quartz grains with minor grains of muscovite and biotite. The mudstone hosts subangular to rounded lithic clasts ranging in diameter from 0.5–40 mm. The Pingbilly Formation was also probably deposited in a shallow marine environment, possibly in slightly deeper water than the underlying sediments of the Tabita Formation, but the presence of lithic clasts indicates sporadic terrestrial influence.

Conodonts from the Mount Arrowsmith area are largely endemic and lack zonal index taxa making precise age determination and correlation difficult (Zhen *et al.*, 2003). The conodont assemblage described by Zhen *et al.* (2003), is indicative of the *Oepikodus evae* conodont Zone from the North Atlantic zonal scheme, or the *andinus-aranda* zones of the North American Midcontinent succession. This is equivalent to a late Bendigonian to Chewtonian age for the Tabita Formation, based on the Australian Stage scale (Webby, 1998).

Systematic palaeontology

Type specimens are held in the Australian Museum Palaeontology type collection (AM); museum numbers are given in figure captions and are prefixed F. Higher level systematics follows Williams *et al.* (1996).

Phylum Brachiopoda Duméril, 1806

Subphylum Rhynchonelliformea Williams, Carlson, Brunton, Holmer & Popov, 1996

Class Rhynchonellata Williams, Carlson, Brunton, Holmer & Popov, 1996

Order Orthida Schuchert & Cooper, 1932

Suborder Orthidina Schuchert & Cooper, 1932

Superfamily Orthoidea Woodward, 1852

Family Orthidae Woodward, 1852

Celsiorthis n.gen.

Type species. *Celsiorthis bulancis* n.gen. and n.sp.

Etymology. Latin, m., *celsus*, high, upright; referring to the high, steeply apsacline to catacline ventral valve interarea.

Diagnosis. Shell ventribiconvex. Ventral valve interarea wide, high, steeply apsacline to catacline. Finely costellate becoming ramicostellate anteriorly, with costellae arising mainly by bifurcation (number of costellae ranges from 80–90 at anterior margin). Ventral valve with large dental plates and bilobed muscle field. Dorsal valve with broad, well-developed notothyrial platform occupied by ridge-like cardinal process. Brachiophores tusk-like with thick bases, weakly divergent (40–60°). Dental sockets large. Fulcral plates absent.

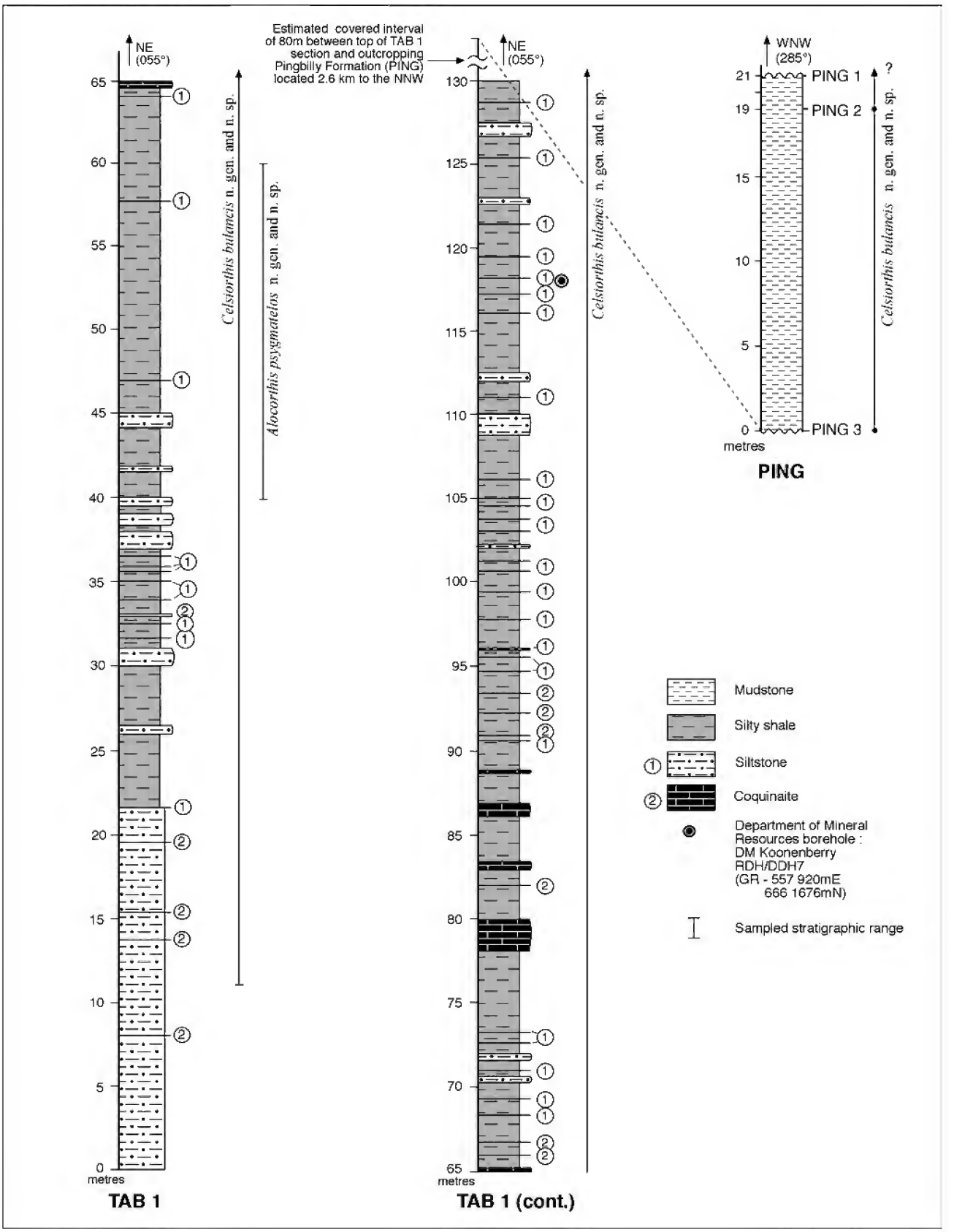

Fig. 2. Stratigraphic ranges of *Celsiorthis bulancis* n.gen. and n.sp. and *Alocorthis psygmatelos* n.gen. and n.sp. in the Tabita Formation (TAB 1 section) and Pingbilly Formation (PING section). First outcrop of the PING section is located 2.6 km NNW from the top of the TAB 1 section (see Fig. 1). The base and top of the Pingbilly Formation are undefined due to poor outcrop caused by alluvial cover.

Celsiorthis bulancis n.gen. and n.sp.

Fig. 3A–N, Table 1

Type material. HOLOTYPE: AM F120718, ventral valve (Fig. 3L–N). PARATYPES: AM F120710, dorsal valve (Fig. 3A,B); AM F120711, dorsal valve (Fig. 3C); AM F120712, complete shell (Fig. 3D–F); AM F120713, ventral valve (Fig. 3G); AM F120714, ventral valve (Fig. 3H); AM F120715, ventral valve (Fig. 3I); AM F120716, ventral valve (Fig. 3J); AM F120717, ventral valve (Fig. 3K).

Type locality. Tabita Formation, TAB1 section, 30 m above base of section (Figs. 1, 2).

Etymology. Latin *bu*, prefix meaning large, and *lancis*, plate; referring to the large dental plates in the ventral valve.

Diagnosis. As for genus by monotypy.

Description. Exterior: ventribiconvex, subquadrate in outline. Ventral valve moderately and uniformly convex with slightly swollen umbo; hinge width approximately 90–95% maximum valve width. Ventral interarea wide, high, flat, steeply apsacline to catacline. Delthyrium open. Dorsal valve moderately convex with shallow sulcus occupying median part of valve; maximum length about 60% of maximum width. Dorsal interarea low, anacline, with open notothyrium; hinge line mainly straight, but slightly deflected posteriorly in the posteromedian region. Commissure rectimarginate.

Shell finely costellate, becoming ramicostellate anteriorly; ribs low and rounded, becoming wider at anterior margin. Costae in umbonal area range between 25 and 35. Costellae arise principally by bifurcation and number 80–90 along the anterior margin in adult shells. Fine, closely spaced concentric filae occur between costellae in larger specimens.

Ventral valve interior: dental plates large, divergent (approximately 20–30°), extending forward as raised lateral muscle bounding ridges. Muscle field large, well impressed, bilobed, about one-third valve length. Diductor scars large, elongate, subparallel; adductors slender, enclosed by diductors, and unbounded anteriorly. Costellae variably impressed around inner margin of shell.

Table 1. Measurements for *Celsiorthis bulancis* n.gen. and n.sp. Abbreviations: Mw = maximum width of valve (mm); Ml = maximum length of valve (mm); Hti = maximum of height of interarea (mm); Mrc = maximum number of ribs at commissure; NA = dimension not available.

museum no.	valve		Mw	Ml	Hti	Mrc
AM F120710	dorsal	paratype	6	3	NA	NA
AM F120711	dorsal	paratype	5.5	4.5	NA	NA
AM F120712	dorsal	paratype	18.5	14	5.5	NA
AM F120713	ventral	paratype	9.5	7.5	NA	NA
AM F120714	ventral	paratype	5.5	5	NA	NA
AM F120715	ventral	paratype	7	4.5	NA	NA
AM F120716	ventral	paratype	7	8.5	NA	NA
AM F120717	ventral	paratype	9.5	8	NA	88
AM F120718	ventral	holotype	8.5	6	3	86

Dorsal valve interior: cardinalia with broad, well-developed notothyrial platform which merges anteriorly with a short, low, broad median ridge. Cardinal process thick, ridge-like, with anterior portion merging with notothyrial platform. Brachiophores short, thick, tusk-like, anterolaterally divergent at 40–60°, grooved along inner faces, with narrow tops, rounded anterior ends, and thick bases joined to the notothyrial platform. Sockets very large with well rounded floors. Fulcral plates absent. Muscle field large, quadripartite, occupying about one-third valve length, bisected longitudinally by low median ridge. Posterior pair of adductors ovate, impressed below notothyrial platform, separated from smaller anterior pair by short transverse extension of the median ridge. Costellae impressed on anterior margin of shell.

Discussion. *Celsiorthis bulancis* can be distinguished from most other Ordovician members of the Orthidae (see Williams & Harper, 2000, p. 724–728), such as *Orthis* Dalman, *Orthambonites* Pander, *Paralenorthis* Havlíček, *Sulcatorthis* Zeng, *Sulevorthis* Jaanusson & Bassett, and *Trondorthis* Neuman in Neuman & Bruton by its finely costellate to ramicostellate external ornament and steeply anacline to catacline interarea in the ventral valve.

Celsiorthis bulancis is similar to *Sivorthis* Jaanusson & Bassett, in particular the type species *S. filistera* Jaanusson & Bassett (1993, pl. 7, figs. 1–7), from the Ordovician (Caradoc) of Sweden. Both taxa possess a ventribiconvex shell, a high, wide ventral valve interarea, and have a similar costellate ornament. However, *C. bulancis* can be distinguished by its nearly flat, steeply apsacline to catacline ventral interarea (Figs. 3D,F,M,N), whereas *S. filistera* has a weakly apsacline ventral valve interarea. *Celsiorthis bulancis* is also more finely costellate (80–90 costellae along the anterior margin; Figs. 3L,K) than *S. filistera* (40–50 costellae at anterior margin). The internal morphology of the ventral valve is very similar in both species; both have a large bilobed or subcordate muscle field bounded by relatively large dental plates (Figs. 3G–J). The interior of the dorsal valve of *C. bulancis* is also similar to *S. filistera* in having a well-developed notothyrial platform supported by a broad median ridge, and a large, quadripartite muscle field in which the posterior muscle scars are larger than the anterior pair (Figs. 3A–C). However, *C. bulancis* has considerably larger dental sockets, and tusk-like brachiophores with thick bases (Figs. 3A–C), unlike *S. filistera* which has simple, tabular brachiophores. Other species assigned to *Sivorthis* by Jaanusson & Bassett (1993, p. 46) differ greatly from *C. bulancis*, primarily in their coarser ornamentation and cardinalia, and thus do not warrant close comparison.

The genus *Sinorthis*, based on *S. typica*, described by Wang (1955) from the Lower Ordovician (Arenig) of south China is also finely costellate, but can be distinguished from *C. bulancis* by its widely divergent brachiophores and weakly apsacline, relatively small ventral valve interarea. *Orthostrophia* Hall, is a significantly younger genus and can be distinguished from *C. bulancis* by its coarser ramicostellate ornament, dorsibiconvex to resupinate shell and subtriangular ventral valve muscle scar.

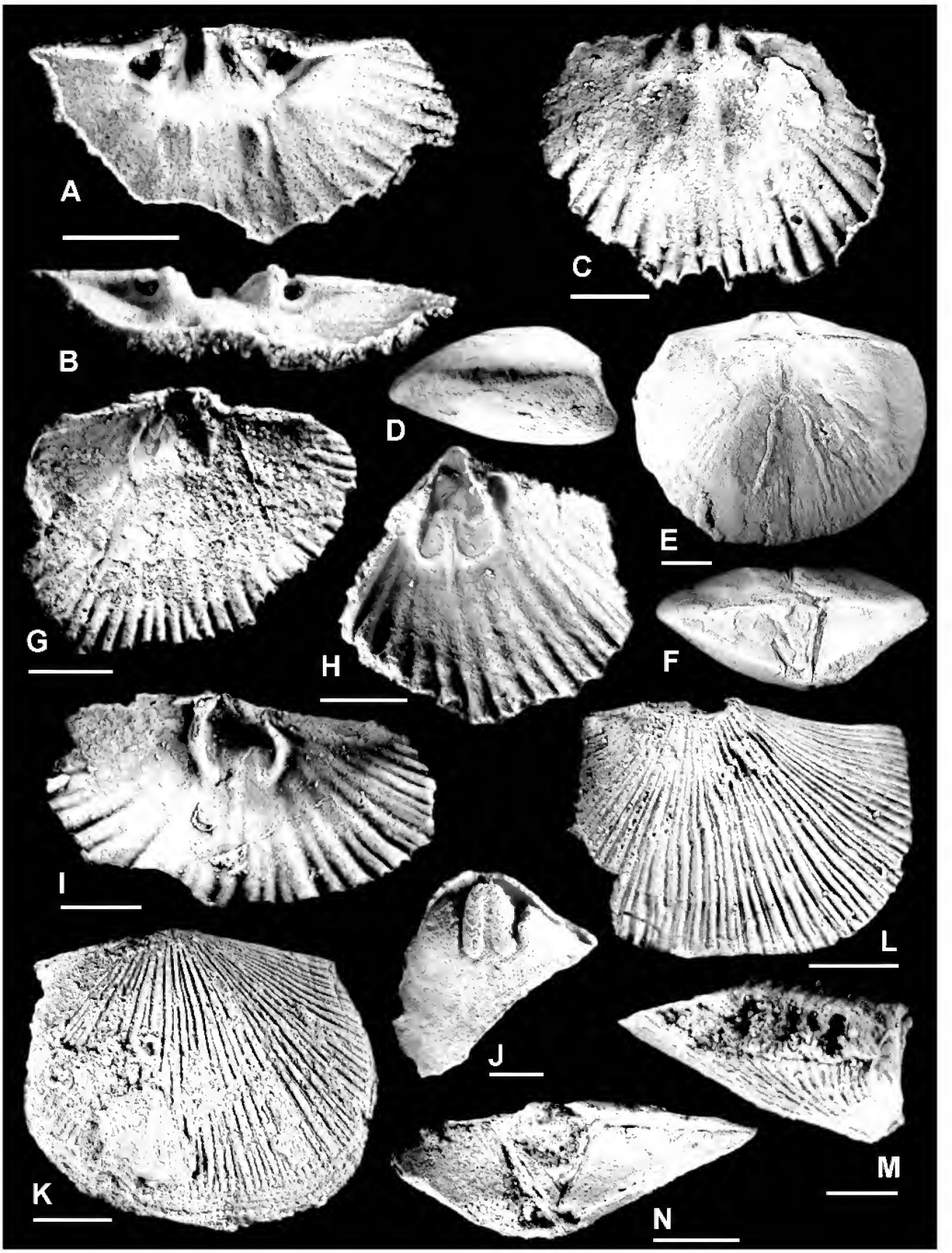

Fig. 3. *Celsiorthis bulancis* n.gen. and n.sp. (*A,B*) dorsal valve interior and anterior, locality T3, AM F120710, scale bar = 1.5 mm; (*C*) latex of dorsal valve interior, PING1, AM F120711, scale bar = 1 mm; (*D–F*) lateral, dorsal and posterior views of complete abraded shell, TAB1/20 m, AM F120712, scale bar = 3 mm; (*G*) latex of ventral valve interior, PING1, AM F120713, scale bar = 2.5 mm; (*H*) latex of ventral valve interior, PING1, AM F120714, scale bar = 2 mm; (*I*) latex of ventral valve interior, PING1, AM F120715, …

Family Nanorthidae Havlíček, 1977

Alocorthis n.gen.

Type species. *Alocorthis psygmatelos* n.gen. and n.sp.

Etymology. Greek, f., *alokos*, meaning furrow; referring to the furrows extending along the dorsal surfaces of the brachiophores.

Diagnosis. Shell transverse, weakly ventribiconvex. Ventral muscle field subtriangular, raised above valve floor and restricted to delthyrial cavity, bounded by short receding dental plates. Notothyrial platform short and very wide, anteriorly elevated above valve floor, supported by broad median ridge. Cardinal process absent. Brachiophores short, widely divergent (100–110°), with furrows extending along dorsal surfaces and with fan-like terminations. Dental sockets simple, subcircular. Fulcral plates absent.

Alocorthis psygmatelos n.gen. and n.sp.

Fig. 4A–J, Table 2

Type material. HOLOTYPE: AM F120719, dorsal valve (Fig. 4A,B). PARATYPES: AM F120720, dorsal valve (Fig. 4C,D); AM F120721, dorsal valve (Fig. 4E); AM F120722, ventral valve (Fig. 4F,G); AM F120723, ventral valve (Fig. 4H,I); AM F120724, ventral valve (Fig. 4J).

Type locality. Tabita Formation (spot locality MTA/IV/4, northern section of the syncline at 30°06'36"S 141°35'05"E).

Etymology. Greek *psygma*, fan, and *telos*, end; referring to the fan-like anterior extremities of the brachiophores.

Diagnosis. As for genus by monotypy.

Description. Exterior: poorly preserved in available material, but apparently weakly ventribiconvex, transverse, subquadrate in outline. Ventral valve interarea low and weakly apsacline; delthyrium open; maximum length of ventral valve approximately 70% maximum width. Dorsal valve interarea anacline; notothyrium open; maximum length of dorsal valve approximately 55% maximum width. Fine ramicostellate ornament, with ribs arising by bifurcation.

Ventral valve interior: muscle field subtriangular with curved anterior margin, restricted to delthyrial cavity, bounded laterally by short receding dental plates; muscle field slightly raised above valve floor, about one-fifth valve length in larger specimens. Teeth relatively large, simple, deltidiodont. Strap-like *vascula media* weakly impressed, proximal portions well separated and divergent (Fig. 4I). Ribs impressed on periphery of valve.

Dorsal valve interior: notothyrial platform short and very wide, anteriorly elevated above valve floor, supported by short, wide, very low median ridge. Cardinal process absent. Brachiophores short, robust, with narrow furrows (≤0.25 mm in width) situated along dorsal surfaces and fan-like anterior extremities, widely divergent anterolaterally at about 100–110°. Dental sockets simple, subcircular and deep. Fulcral plates absent. Musculature poorly defined; posterior pair large and subcircular, situated on either side of a relatively wide, low median ridge, below the notothyrial platform. Internal ribbing as in ventral valve.

Table 2. Measurements for *Alocorthis psygmatelos* n.gen. and n.sp. Abbreviations: Mw = maximum width of valve (mm); Ml = maximum length of valve (mm); Hti = maximum of height of interarea (mm); Mrc = maximum number of ribs at commissure; NA = dimension not available.

museum no.	valve		Mw	Ml	Hti	Mrc
AM F120719	dorsal	holotype	12	6	NA	NA
AM F120720	dorsal	paratype	10	5	NA	74
AM F120721	dorsal	paratype	6	5.5	NA	NA
AM F120722	ventral	paratype	7.5	5.5	NA	NA
AM F120723	ventral	paratype	6.5	5.5	1.5	NA
AM F120724	ventral	paratype	5.5	6.5	2	NA

Discussion. The relatively small (Table 2) subquadrate, weakly ventribiconvex, transverse shell, subtriangular ventral valve muscle scar (Figs. 4F–J), presence of a wide notothyrial platform, short, robust, widely divergent brachiophores, and absence of a cardinal process in the dorsal valve (Figs. 4A–E) indicate that *Alocorthis psygmatelos* could be placed in either the Nanorthidae (Superfamily Orthoidea) or the Eoorthidae (Superfamily Plectorthoidea). As noted by Williams & Harper (2000, p. 766) the eoorthids differ significantly from other typical plectorthoids in lacking brachiophore supporting structures and fulcral plates. Williams & Harper (2000) indicate that the eoorthids should be viewed as the link group between the plectorthoids and the orthoids. On balance, *Alocorthis* probably has more features in common with the Nanorthidae than with the Eoorthidae and we refer this genus, with some hesitation, to the Nanorthidae Havlíček.

Of the genera lacking a cardinal process that are currently assigned to the Nanorthidae (see Williams & Harper, 2000, p. 742–745), *Alocorthis* is similar to both *Nanorthis* Ulrich & Cooper and *Archaeorthis* Schuchert & Cooper. *Nanorthis* has a similar ornament, shell shape and size range to *Alocorthis*, but *Nanorthis* can be discriminated from *Alocorthis* by its short, blade-like brachiophores and rudimentary notothyrial platform (Laurie, 1980; Williams & Harper, 2000). The species *N. brachymyaria* recently described from the Late Tremadoc of Argentina (Benedetto & Carrasco, 2002, fig. 4) is very similar to *Alocorthis* in size and external ornament. However, *N. brachymyaria* can be distinguished from *A. psygmatelos* by its more acute brachiophore angle, lack of a raised muscle field in the ventral valve and more arched vascula media. It is interesting to note that Benedetto & Carrasco (2002, fig. 4.11) figure one specimen of *N. brachymyaria* that appears to show brachiophores with narrow furrows along the dorsal surfaces and fan-like terminations which indicate this species may be referable to *Alocorthis*.

[Fig. 3, caption continued] ... scale bar = 1.5 mm; (*J*) ventral valve internal mould, TAB1/25 m, AM F120716, scale bar = 2.5 mm; (*K*) latex of ventral valve exterior, MTA/0.2, AM F120717, scale bar = 2.5 mm; (*L–N*) Holotype, latex of ventral valve exterior (scale bar = 2.5 mm), lateral view (scale bar = 1.5 mm) and interarea (scale bar = 2 mm), TAB1/30 m, AM F120718.

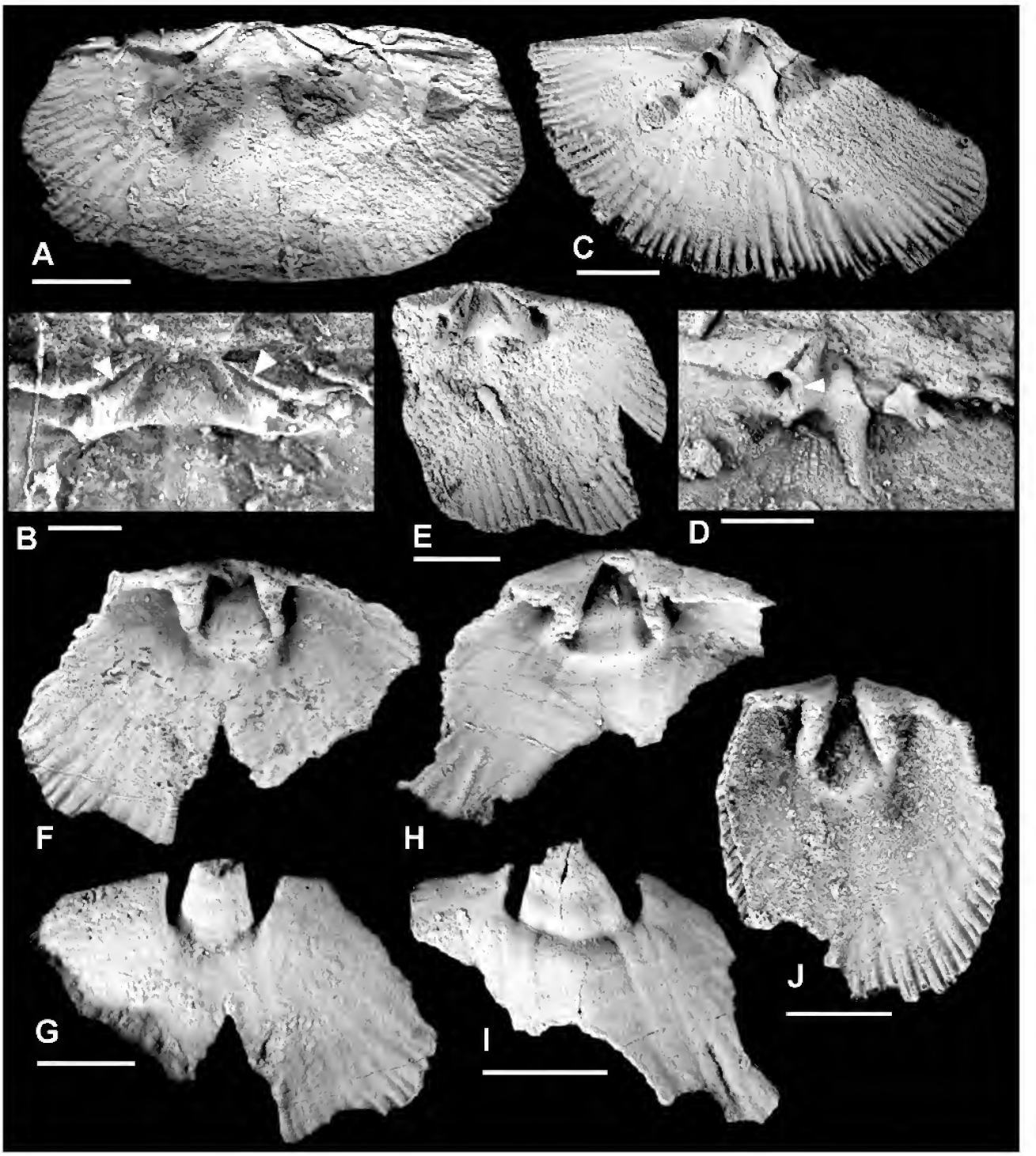

Fig. 4. *Alocorthis psygmatelos* n.gen. and n.sp. Scale bars = 2 mm, unless otherwise stated; (*A,B*) holotype, latex of dorsal valve interior, and detail of cardinalia (*B*, scale bar = 1 mm); furrows extending along dorsal surface of brachiophores are arrowed in *B*; Note wide notothyrial platform lacking cardinal process, MTA/IV/4, AM F120719; (*C,D*) latex of dorsal valve interior, and detail of cardinalia (*D*, scale bar = 1.5 mm); fan-like termination of left brachiophore is arrowed in *D*, TAB1/55 m, AM F120720; (*E*) latex of dorsal valve interior, TAB1/45 m, AM F120721; (*F,G*) latex cast and original mould of ventral valve interior, MTA/0.2, AM F120722; (*H,I*) latex cast and original mould of ventral valve interior, MTA/0.2, AM F120723; (*J*) latex cast of ventral valve interior, TAB1/45 m, AM F120724.

Archaeorthis is also similar to *Alocorthis* in basic dimensions, but most species of this genus have the ventral muscle scar impressed on a well-developed callosity which extends forward as a wide median ridge (Ulrich & Cooper, 1938, p. 92). *Alocorthis psygmatelos* does not possess this feature (Figs. 4F–J). Laurie (1987) described the species *Archaeorthis waratahensis* from the Early Ordovician Digger Island Formation in south Gippsland, Victoria, that is characterized by the presence of a weakly developed callosity in the ventral valve (at least in early growth stages). This species can be discriminated from *Alocorthis psygmatelos* by its fascicostellate ornament, deep notothyrial

cavity and well-developed dorsal sulcus in the dorsal valve. The brachiophores are also much simpler than those in *Alocorthis psygmatelos* (Figs. 4A–E).

Other nanorthid genera such as *Cyrtonotella* Schuchert & Cooper, *Diplonorthis* Mitchell, *Nicoloidea* Zeng, *Nothorthis* Ulrich & Cooper, *Pleurorthis* Cooper, *Riograndella* Kobayashi, *Shoshonorthis* Jaanusson & Bassett and *Xinanorthis* Xu, Rong & Liu can be distinguished from *Alocorthis* by a combination of features such as planoconvex to concavoconvex shape, presence of a well-developed cardinal process, weakly developed notothyrial platform or bilobed muscle field in the ventral valve (see Williams & Harper, 2000, pp. 742–745).

Of the genera within the Eoorthidae that lack a cardinal process, *Alocorthis* is most similar to the type species of *Robertorthis, R. holoubkovensis* Havlíček (1977, pl. V, figs. 8–10, 17), from the Early Ordovician (Tremadoc) of Bohemia. The internal morphology of the dorsal valve is almost identical in both species. The major differences are that the notothyrial platform of *R. holoubkovensis* is not supported by a median ridge, and the anterior extremities of the brachiophores in *R. holoubkovensis* bear fine ridges running parallel with the hinge line to define slit-like dental sockets. The ventral valve interiors of both taxa are also very similar, in that they possess a subtriangular muscle field which is raised above the valve floor and restricted to the delthyrial cavity.

Brahimorthis Havlíček from the Middle Cambrian of north Africa and Europe is also somewhat similar to *Alocorthis* in that it has ramicostellate ornament and lacks a cardinal process (see Havlíček, 1977, pl. II, figs. 15–19). *Brahimorthis* can be distinguished from *Alocorthis* by its lack of dental plates, and the presence of a raised transverse ridge in the delthyrial cavity (Williams & Harper, 2000).

ACKNOWLEDGMENTS. The authors thank Ms Annie O'Connor for access to "Mount Arrowsmith" Station and for providing accommodation during fieldwork in February 2001. Dr Yong-Yi Zhen kindly identified the conodonts collected from the TAB 1 section and, in conjunction with Dr Ian Percival and Prof Barry Webby, provided access to an in press manuscript on the conodonts from Mount Arrowsmith. James Valentine kindly read an earlier draft of this manuscript. Drs Ian Percival and Des Strusz provided helpful reviews of the manuscript. Partial funding for this work was provided by a Betty Mayne Grant from the Linnean Society of New South Wales to JRP, and a Macquarie University Research Grant to GAB. Dean Oliver drafted Figs. 1–2 with characteristic accuracy and efficiency.

References

Benedetto, J.L., & P.A. Carrasco, 2002. Tremadoc (earliest Ordovician) brachiopods from Purmamarca and the Sierra de Mojotoro, Cordillera Oriental of northwestern Argentina. *Geobios* 35: 647–661.

Brock, G.A., & I.G. Percival, 2000. Cambrian faunas from Mount Arrowsmith, north-western New South Wales, Australia. *Palaeontology Down Under 2000, Geological Society of Australia, Abstracts* 61: 13.

Brown, I.A., 1948. Lower Ordovician brachiopods from Junee district, Tasmania. *Journal of Paleontology* 22: 35–39.

Crawford, A.J., B.P.J. Stevens & M. Fanning, 1997. Geochemistry and tectonic setting of some Neoproterozoic and Early Cambrian volcanics in western New South Wales. *Australian Journal of Earth Sciences* 44: 831–852.

Etheridge, R. Jr., 1904. Trilobite remains collected in the Florentine Valley, west Tasmania. *Records of the Australian Museum* 5: 98–101.

Havlíček, V., 1977. Brachiopods of the order Orthida in Czechoslovakia. *Rozpravy Ústředního Ústavu Geologického* 44: 1–293.

Jaanusson, V., 1973. Ordovician articulate brachiopods. In *Atlas of Palaeobiogeography*, ed. A. Hallam, pp. 19–25. Amsterdam: Elsevier.

Jaanusson, V., & M.G. Bassett, 1993. *Orthambonites* and related Ordovician brachiopod genera. *Palaeontology* 36: 21–63.

Laurie, J.R., 1980. Early Ordovician orthide brachiopods from southern Tasmania. *Alcheringa* 4: 11–23.

Laurie, J.R., 1987. Early Ordovician orthide brachiopods from the Digger Island Formation, Waratah Bay, Victoria. *Memoirs of the Museum of Victoria* 48: 101–106.

Laurie, J.R., 1991a. Ordovician brachiopod biostratigraphy of Tasmania. In *Brachiopods through time*, ed. D.I. MacKinnon, D.E. Lee & J.D. Campbell, pp. 303–310. Rotterdam: A.A. Balkema.

Laurie, J.R., 1991b. Articulate brachiopods from the Ordovician and Lower Silurian of Tasmania. *Memoir of the Association of Australasian Palaeontologists* 11: 1–106.

Laurie, J.R., 1997. Early Ordovician fauna from the Gap Creek Formation, Canning Basin, Western Australia. *AGSO Journal of Australian Geology & Geophysics* 16: 701–716.

Mills, K.J., 1992. Geological evolution of the Wonominta Block. In *The Palaeozoic Eastern Margin of Gondwanaland: Tectonics of the Lachlan Fold Belt, southeastern Australia and Related Orogens*, ed. C.L. Fergusson & R.A. Glen, *Tectonophysics* 214: 57–68.

Paterson, J.R., 2001a. Early Ordovician Geology and Palaeontology of Mount Arrowsmith, northwestern New South Wales. *Unpublished Hons thesis, Macquarie University*, 123 pp.

Paterson, J.R., 2001b. First occurrence of *Janospira* from the Early Ordovician of Australia. *Alcheringa* 25: 129–130.

Paterson, J.R., 2002. Early Ordovician trilobites from Mt. Arrowsmith, northwestern N.S.W., Australia: Biostratigraphic and biogeographic implications. IPC2002, *Geological Society of Australia, Abstracts* 68: 128.

Paterson, J.R., in press. Palaeobiogeography of the Ordovician trilobite *Prosopiscus*, with a new species from western New South Wales, Australia. *Alcheringa* 27.

Percival, I.G., 1979a. Ordovician plectambonitacean brachiopods from New South Wales. *Alcheringa* 3: 91–116.

Percival, I.G., 1979b. Late Ordovician articulate brachiopods from Gunningbland, central western New South Wales. *Proceedings of the Linnean Society of New South Wales* 103: 175–187.

Percival, I.G., 1991. Late Ordovician articulate brachiopods from central New South Wales. *Memoir of the Association of Australasian Palaeontologists* 11: 107–177.

Percival, I.G., B.D. Webby & J. Pickett, 2001. Ordovician (Bendigonian, Darriwilian to Gisbornian) faunas from the northern Molong Volcanic Belt of central New South Wales. *Alcheringa* 25: 211–250.

Prendergast, K.L., 1935. Some Western Australian Upper Palaeozoic fossils. *Journal of the Royal Society of Western Australia* 21: 9–35.

Ulrich, E.O., & G.A. Cooper, 1938. Ozarkian and Canadian Brachiopoda. *Geological Society of America, Special Papers* 13: 1–323.

Wang Yu, 1955. New genera of brachiopods. *Scientia Sinica* 4(2): 327–357. [In Chinese].

Webby, B.D., 1978. History of the Ordovician continental platform shelf margin of Australia. *Journal of the Geological Society of Australia* 25: 41–63.

Webby, B.D., 1998. Steps towards a global standard for Ordovician stratigraphy. *Newsletters on Stratigraphy* 36(1): 1–33.

Webby, B.D., I.G. Percival, G.D. Edgecombe, R.A. Cooper, A.H.M. Vandenberg, J.W. Pickett, J. Pojeta Jr, G. Playford, T. Winchester-Seeto, G.C. Young, Y.Y. Zhen, R.S. Nicoll, J.R.P. Ross & R. Schallreuter, 2000. Ordovician palaeobiogeography of Australasia. *Memoir of the Association of Australasian Palaeontologists* 23: 63–126.

Williams, A., S.J. Carlson, C.H.C. Bruton, L.E. Holmer & L. Popov, 1996. A supra-ordinal classification of the Brachiopoda. *Philosophical Transactions of the Royal Society, London B* 351: 1171–1193.

Williams, A., & D.A.T. Harper, 2000, Orthida. In *Treatise on Invertebrate Palaeontology, Part H (revised)*, ed. R.L. Kaesler, vol. 3, pp. 714–782. Geological Society of America and University of Kansas Press.

Zhen, Y.-Y., I.G. Percival & B.D. Webby, 2003. Early Ordovician conodonts from far western New South Wales, Australia. *Records of the Australian Museum* 55(2): 169–220.
http://www.amonline.net.au/pdf/publications/1383_complete.pdf · [from Nov 2003]

Manuscript received 29 November 2002, revised 15 March 2003 and accepted 2 April 2003.

Associate Editor: G.D. Edgecombe.

Records of the Australian Museum (2003) Vol. 55: 231–244. ISSN 0067-1975

A New Siphonotretid Brachiopod from the Silurian of Central-Western New South Wales, Australia

JAMES L. VALENTINE* AND GLENN A. BROCK

Centre for Ecostratigraphy and Palaeobiology, Department of Earth and Planetary Sciences, Macquarie University NSW 2109, Australia
jvale002@student.mq.edu.au · gbrock@els.mq.edu.au

ABSTRACT. A new genus and species of Silurian siphonotretid brachiopod, *Orbaspina gelasinus* n.gen. and n.sp., is described from the late Llandovery (*amorphognathoides* Zone) to early Wenlock (*ranuliformis* Zone) Boree Creek Formation of central-western New South Wales, Australia. This represents the first confirmed report of a post-Ordovician siphonotretid from east Gondwana. Other supposed post-Ordovician siphonotretid occurrences are reviewed. Higher-level taxonomic relationships between the Siphonotretida and other linguliformean groups are discussed; based on present knowledge, the siphonotretids appear closest to the lingulellotretids or dysoristids.

VALENTINE, JAMES L., & GLENN A. BROCK, 2003. A new siphonotretid brachiopod from the Silurian of central-western New South Wales, Australia. *Records of the Australian Museum* 55(2): 231–244.

Siphonotretid brachiopods first appeared during the late Middle Cambrian with the oldest species, *Schizambon reticulatus* MacKinnon (in Shergold *et al.*, 1976), occurring in the Mayaian stage of the Saian-Altai region in southwest Siberia (Aksarina & Pel'man, 1978). The siphonotretids slowly diversified throughout the Late Cambrian and Early Ordovician, reaching a peak diversity of 13 genera during the late Arenig as part of the great Ordovician diversification event (Bassett *et al.*, 1999). Throughout the Middle and Late Ordovician, siphonotretid diversity steadily decreased and they were believed to have disappeared along with most of the Cambrian Evolutionary Fauna during the end-Ordovician extinction event; an event which saw a significant turnover in brachiopod communities worldwide (Harper & Rong, 1995; Rong & Harper, 1999; Bassett *et al.*, 1999; Sheehan, 2001).

Until recently, the youngest accepted siphonotretid species was *Multispinula drummuckensis* Harper, from the upper Ashgill (upper Rawtheyan) South Threave Formation of southwest Scotland (Harper, 1984). Mergl (2000, 2001a,b) has recently documented fragmentary material from the Early Silurian to Early Devonian of the Barrandian of central Bohemia that he identified as belonging to four indeterminate siphonotretid species.

This paper describes a new genus of Silurian siphonotretid brachiopod, *Orbaspina* n.gen., with type species *Orbaspina gelasinus* n.gen. and n.sp., from the late Llandovery (*amorphognathoides* Zone) to early Wenlock (*ranuliformis* Zone) carbonate sequence of the Boree Creek Formation in central-western New South Wales, Australia (Valentine *et al.*, 2003). *Orbaspina* n.gen. represents the first post-Ordovician siphonotretid brachiopod to be documented from east Gondwana.

Geology and stratigraphy of the Boree Creek Formation

The Boree Creek Formation, a sequence of impure limestones and sandstones, crops out extensively in central-western New South Wales. Sherwin (1971) divided the Boree Creek Formation in the type area at Cheesemans Creek into three lithological members (oldest to youngest):

* author for correspondence

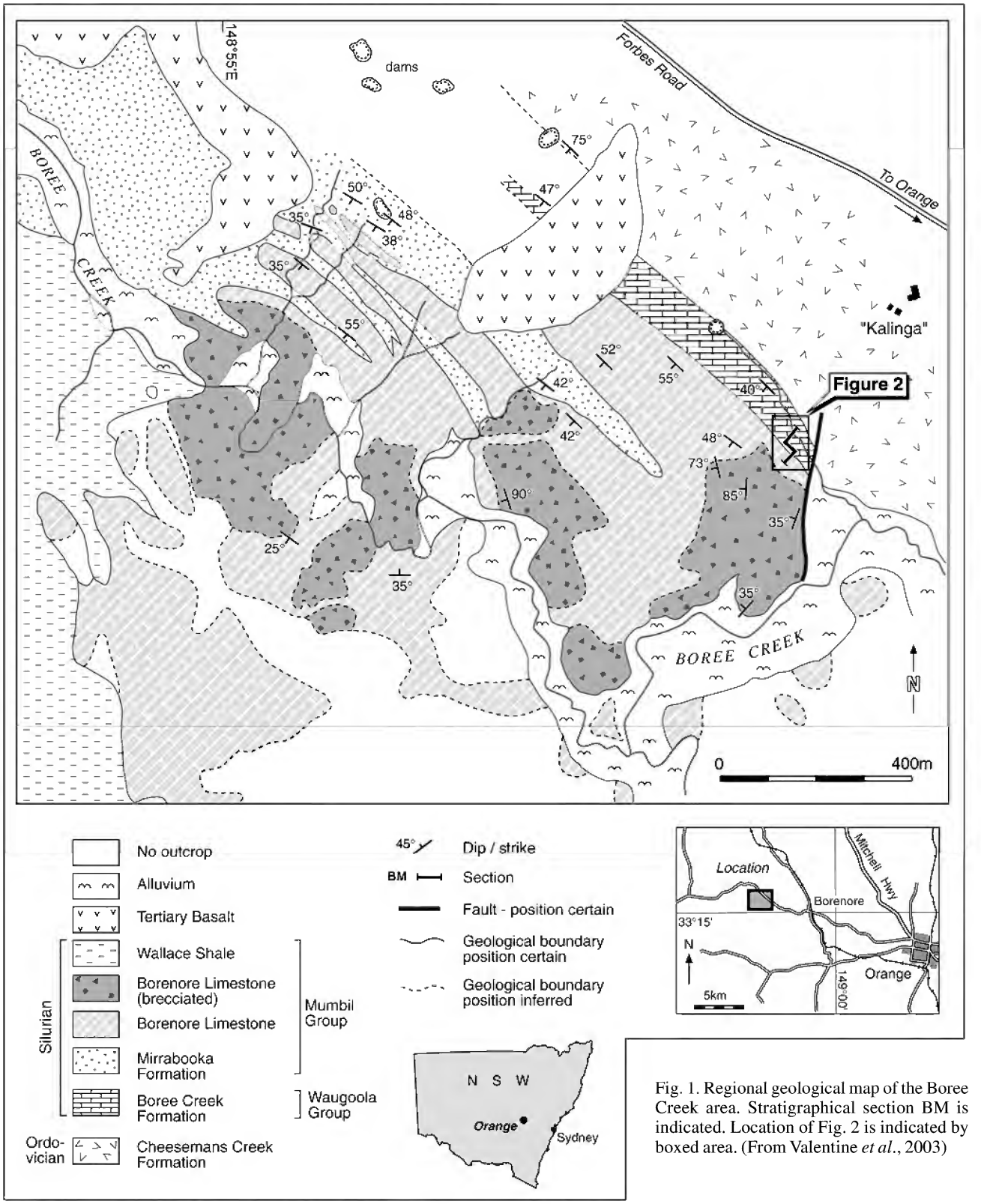

Fig. 1. Regional geological map of the Boree Creek area. Stratigraphical section BM is indicated. Location of Fig. 2 is indicated by boxed area. (From Valentine *et al.*, 2003)

Limestone A, the tuffaceous trilobite beds and Limestone B. However, rapid lateral facies changes and lithological interfingering mean these units are only readily discernible in the type area (Pickett, 1982; Holloway & Lane, 1998). At the easternmost exposure of the Boree Creek Formation, where the BM section is located (Fig. 1), five distinct lithological units can been identified (Fig. 2). These include (from oldest to youngest): argillaceous and red limestones (equivalent to Sherwin's [1971] Limestone A), grey lensoidal limestone and sandstone (equivalent to Sherwin's [1971] tuffaceous trilobite beds), and Limestone B (Fig. 2). The lithology and faunal composition of each of these units has recently been described in detail by Valentine *et al.* (2003).

Conodont faunas documented by Bischoff (1986) and Cockle (1999) suggest the Boree Creek Formation ranges in age from late Llandovery (*amorphognathoides* Zone) to early Wenlock (*ranuliformis* Zone). Simpson (1995) speculated that the argillaceous limestone might fall within the late Llandovery *celloni* conodont Zone, based on Männik & Aldridge's (1989) phylogeny of *Pterospathodus amorphognathoides* Walliser, and interpretation of the conodont distribution charts presented by Bischoff (1986, table 8). Through detailed sampling of the argillaceous limestone, Molloy & Simpson (2002) and Molloy (unpub. data), have recovered *P. amorphognathoides*-type Pa elements from samples BM-19.80, -19.70 and -14.70 and a Pb element from sample BM-19.80, suggesting the *amorphognathoides* zone extends down to at least sample BM-19.80 (Fig. 3). No evidence of *celloni* Zone conodont assemblages have been recovered (Molloy, unpub. data).

Talent *et al.* (1993) used isotopic data to document the likely presence of the Ireviken Extinction Event in the Boree Creek Formation, which Jeppsson (1997) confirmed using Bischoff's (1986, tables 7–9) conodont distribution charts. *Orbaspina gelasinus* n.gen. and n.sp. occurs as part of a moderately diverse linguliformean brachiopod assemblage documented through the Ireviken Event by Valentine *et al.* (2003); elements of which have been recovered from each unit of the Boree Creek Formation, except the sandstone unit. *Orbaspina gelasinus* n.gen. and n.sp. occurs only in the massive red and grey lensoidal limestones, from which 55 and 231 specimens have been recovered, respectively (Fig. 3). Specimens from the red limestone tend to be rather small and fragmentary, whereas those from the grey lensoidal limestone, most which occur in a 0.47 m thick sequence from sample BM13.80 to BM14.85, are larger and better preserved (Tables 1, 2).

Post-Ordovician siphonotretid brachiopods

A number of supposed post-Ordovician siphonotretids have been documented from Europe, North America and Australia, particularly during the mid 1800s to early 1900s (e.g., Morris, 1849; Davidson, 1866; Hall & Clarke, 1892; Chapman, 1903, 1913). Following the introduction of the Ordovician System by Lapworth (1879), and its subsequent acceptance, most of these supposed post-Ordovician siphonotretids were reassigned to strata of Ordovician age. Taxa such as "*Siphonotreta*" *anglica* Morris, "*Siphonotreta*" *australis* Chapman, and "*Siphonotreta*" *plicatella* Chapman, recovered from genuine Silurian strata, have generally been dismissed or ignored.

"*Siphonotreta*" *anglica*, described by Morris (1849) from the Wenlock Limestone of Dudley, England, has been dated as Wenlock by Dorning (1983) based on acritarchs, chitinozoans and miospores. This species is unusual for a siphonotretid in that it has spines with regularly developed transverse grooves (giving them a beaded appearance) and a pitted post-larval shell (Morris, 1849; Davidson, 1866). The taxonomic assignment of this species was strongly refuted by Rowell (1962: 150) who noted "apart from the fact that the shell is spinose there is no evidence to support that the species is a *Siphonotreta*, or indeed that it is a member of the Siphonotretacea." Both Cocks (1978) and Holmer & Popov (2000) have also questioned the taxonomic assignment of this species. Only three specimens

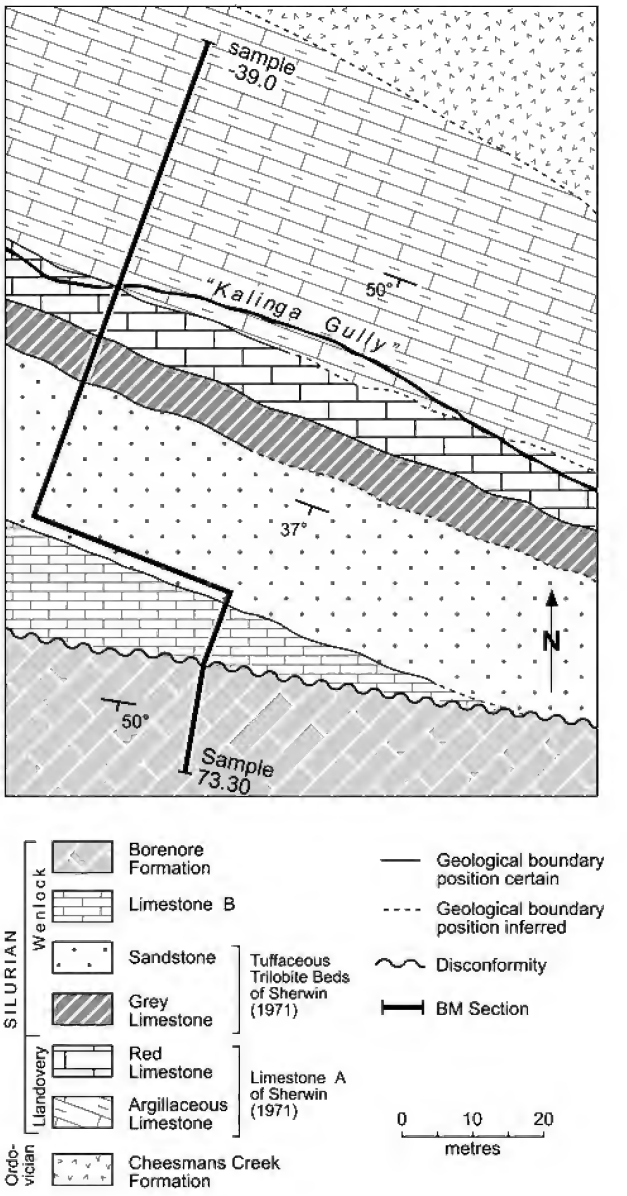

Fig. 2. Detailed geological map of the study area, showing location of the BM section. Note that section starts at sample BM-39.0 and ends at sample BM 73.30. (Modified after Valentine *et al.*, 2003)

of "*Siphonotreta*" *anglica* are known to exist and a definitive assessment of this taxon must await detailed examination of the type material. However, it is worth noting the presence of a few weakly developed transverse grooves on the spines and a pitted post larval shell also occurs in *O. gelasinus* n.gen. and n.sp. (Figs. 5h–k, 6i, 7h).

Chapman (1903, 1910, 1914) also documented a possible post-Ordovician siphonotretid, "*Siphonotreta*" *australis*, from the Melbourne Formation cropping out in the Sewerage works in Domain Road, South Yarra, Melbourne, Australia. Rickards & Sandford (1998) have dated the Melbourne Formation at South Yarra as lower Ludlow in age based on graptolites. Syntype material of "*Siphonotreta*" *australis* examined by the authors (National Museum of Victoria Numbers 604 and 605) (Fig. 4), consist of internal moulds. No trace of spine bases or post-larval shell pitting, as described by Chapman (1903: 65), is evident on the

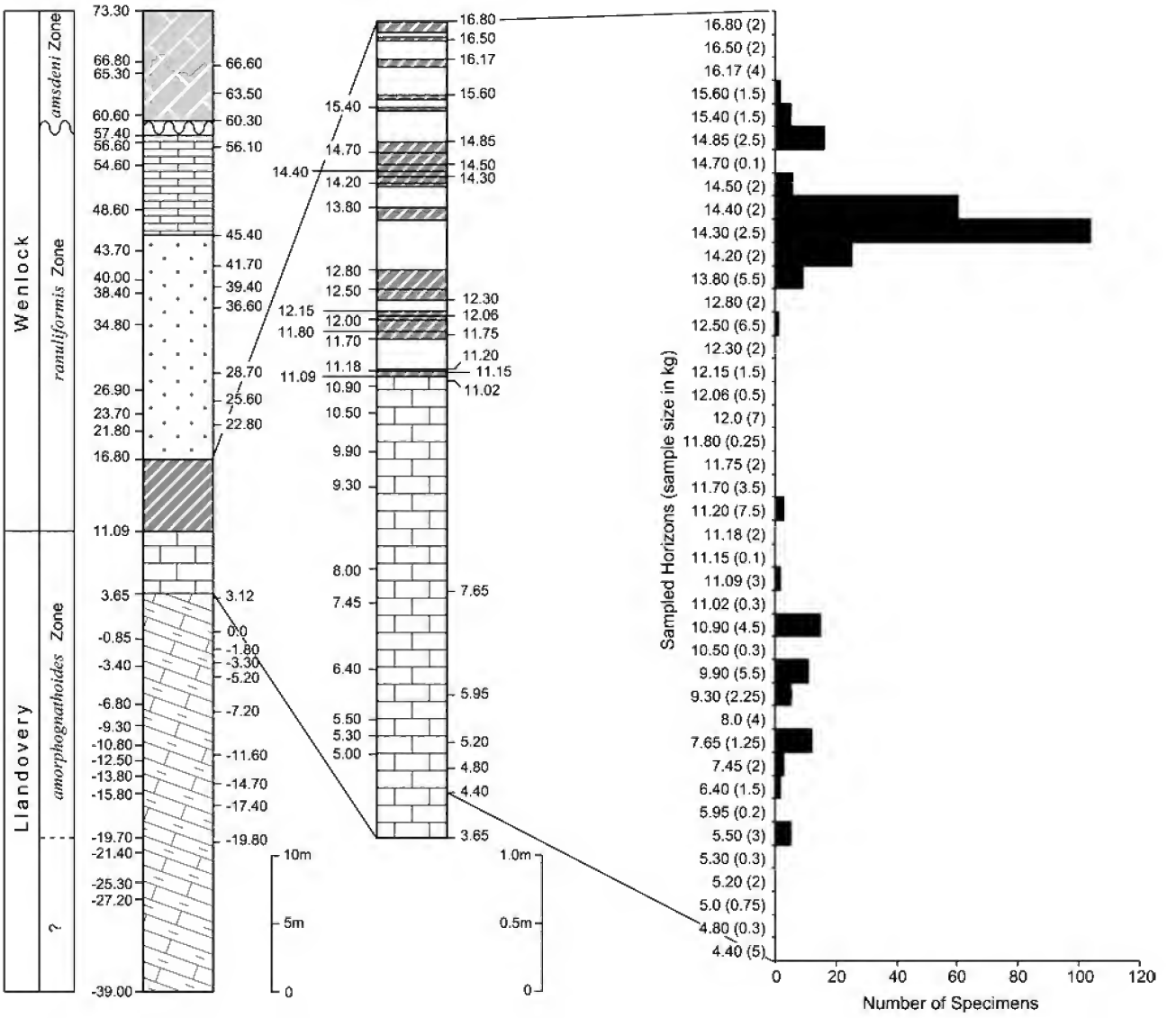

Fig. 3. Stratigraphic column of the BM section showing lithology and all sampled horizons. Lithological details of massive red and grey lensoidal limestones and sampled horizons for the 5.87 metres of section around the Llandovery-Wenlock boundary, from sample BM 3.65 to BM 16.80, is enlarged in the middle. Key to lithology as for Fig. 2; blank areas indicate no exposure. Modified after Valentine *et al.* (2003). Distribution and abundance of *Orbaspina gelasinus* n.gen. and n.sp. recovered from each sampled horizon in the massive red and grey lensoidal limestones is shown to the right. Sample size in kilograms for each horizon is given in brackets after each sample number.

specimens (Fig. 4). The lack of spines, large size of the specimens (specimen 604: width = 14 mm, length = 15 mm; specimen 605: width = 12 mm, length = 14 mm), well-developed, broad concentric rugae and apparent lack of a larval shell (Fig. 4) indicate the specimens are not siphonotretids. The material may well represent an indeterminate bivalve taxon. "*Siphonotreta*" *australis* can therefore be confidently rejected from the Siphonotretida.

Chapman (1913) described a second possible post-Ordovician siphonotretid, "*Siphonotreta*" *plicatella*, based on a single specimen recovered from the Yea Yean Formation of Victoria, Australia. Based on graptolite data, the Yea Yean Formation has been dated as middle to late Ludlow in age (Strusz *et al.*, 1972). At the time of writing the holotype was unavailable for study. Chapman (1913: 100) described the exterior ornament as "consisting of concentric laminar folds and vertical striae; the latter probably representing remnants of short, spinose processes". There is no evidence of tubular hollow spines on the pedicle valve figured by Chapman (1913, pl. 10, figs. 1a–c). The fact that hollow spines are not actually preserved, and that a larval shell is not apparent, leads us to strongly question the siphonotretid affinity of this taxon.

More recently, Mergl (2000, 2001a,b) documented four indeterminate siphonotretids from the Barrandian of central Bohemia: Siphonotretine sp. from the Ludfordian Kopanina Formation of Řeporyje; Schizambonine sp. A from the Pragian Dvorce-Prokop Limestone of Klukovice; Schizambonine sp. B from the upper Dalejan Daleje-Třebotov Formation of Holyně; and Acanthambonine sp. from the Wenlock of the Motol Formation of Loděnice. These ages are based primarily on graptolite data presented

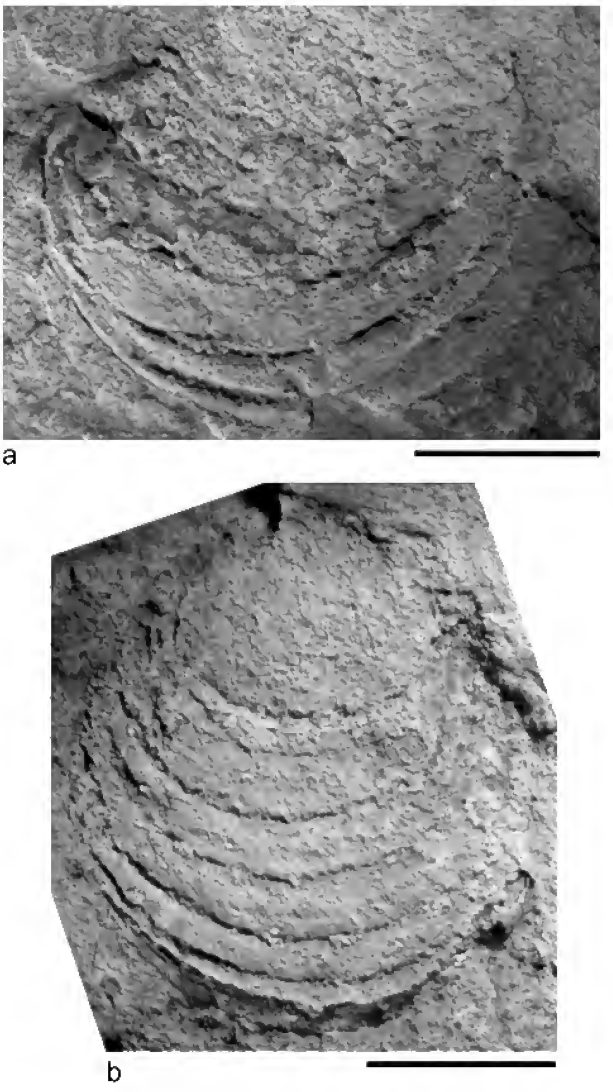

Fig. 4. "*Siphonotreta*" *australis*: *a*, syntype National Museum of Victoria Number 604, internal mould; *b*, syntype National Museum of Victoria Number 605, internal mould. Note the lack of spine bases and post-larval shell pitting contrary to the opinion of Chapman (1903). Scale bars = 5 mm.

in Mergl (2001b). Although rare, and based on fragmentary remains, the presence of tubular hollow spines (*sensu* Alvarez & Brunton, 2001), on each of these species is unmistakable, confirming siphonotretid affinities (Mergl, 2001a, fig. 35.3c–g; 2001b, pl. 36, figs. 6–16). Siphonotretine sp. and Schizambonine sp. A are both unusual in possessing a pitted post-larval shell, indicating both species may be related to *O. gelasinus* n.gen. and n.sp.

Systematic palaeontology

Type and figured paratypic material is lodged in the palaeontological collections of the Australian Museum (AMF).

Phylum Brachiopoda Duméril, 1806

Discussion. The higher level classification used herein follows that of Holmer & Popov (2000).

Subphylum Linguliformea Williams, Carlson, Brunton, Holmer & Popov, 1996

Class Lingulata Goryanskij & Popov, 1985

Order Siphonotretida Kuhn, 1949

Discussion. Under Beecher's (1891) brachiopod classification scheme, the siphonotretids were placed in the order Neotremata, erected for the so-called "more advanced" inarticulates which had the pedicle opening confined to the ventral valve (Beecher, 1891; Carlson, 2001). Prior to this, higher-level brachiopod taxonomy had followed a wide variety of classification schemes that saw the siphonotretids associated with a number groups including the obolids (e.g., Morris, 1849; Gagel, 1890) and the discinids (e.g., Davidson, 1866). Beecher's (1891) classification scheme, or variations thereof, remained in vogue for over a century before being supplanted by Rowell (1965) for the first edition of the *Treatise on Invertebrate Paleontology* and Goryanskij (in Sarytcheva, 1960) in the *Osnovy Paleontologii*.

Following Rowell (1962), Williams (1962) and Wright (1963), Rowell (1965: H287-H288) classified the siphonotretids as a superfamily of the Acrotretida, stating that the "structure of the dorsal posterior margin, particularly that of early genera, suggests that the acrotretaceans may have provided the ancestral stock." This "traditional" view of siphonotretid classification was maintained by numerous workers (e.g., Krause & Rowell, 1975; Aksarina & Pel'man, 1978; Havlíček, 1982; Williams & Curry, 1985; Mergl, 1995). Phylogenetic analysis of the relationships between higher-level brachiopod taxa undertaken by Rowell (1981), Carlson (1991) and Popov *et al.* (1993) supported this view.

Under Goryanskij's (in Sarytcheva, 1960) classification scheme, the siphonotretids were placed in their own order, the Siphonotretida, a scheme also followed by numerous workers (Goryanskij, 1969; Popov & Nõlvak, 1987; Holmer, 1989; Popov & Holmer, 1994; Robson & Pratt, 2001). The cladistic analyses of higher level brachiopod relationships undertaken by Holmer & Popov (1994), Holmer *et al.* (1995), Williams *et al.* (1996), Holmer & Popov (2000), revising the earlier work of Rowell (1981), Carlson (1991) and Popov *et al.* (1993), supported Goryanskij's (in Sarytcheva, 1960) view that the siphonotretids were a distinct, monophyletic group united by the presence of tubular hollow spines.

Acrotretid affinities can also be rejected on several additional counts. Siphonotretids lack the small pitted larval shell characteristic of all acrotretids (Biernat & Williams, 1970; Williams & Curry, 1991; Holmer & Popov, 2000), instead having a larger and smooth larval shell (Holmer & Popov, 2000).

Acrotretid shells are composed of 1 μm thick horizontal laminae connected by numerous round columellae, about 3 μm in diameter, aligned perpendicular to the laminae. The laminae and columellae are composed of needle-shaped apatite crystallites about 170 nm wide and 1 μm long (Poulsen, 1971; Ushatinskaya *et al.*, 1988; Holmer, 1989; Ushatinskaya, 1990). In contrast, the shell structure of siphonotretids consists of up to 15, 1 μm thick horizontal laminae composed of microgranular apatite measuring up to 500 nm across. Biernat & Williams (1970) and Ushatinskaya *et al.* (1988) considered each of the narrow spaces between the lamina to have been filled with organic material during life. Ushatinskaya *et al.* (1988: 45) remark that "this structure most closely resembles the lingulid shell structure, but an important difference is the development, at the surface of the siphonotretid valves, of hollow spines..."

Both the acrotretids and siphonotretids possess a foramen located wholly within the ventral valve, a possible uniting feature. However, a similar type of foramen has also been described in the lingulid family Lingulellotretidae (Koneva & Popov, 1983). The foramen of most siphonotretids becomes enlarged through resorption forming an elongate, triangular pedicle track. While such a feature is known in members of the acrotretid family Curticiidae (Rowell & Bell, 1961), it has also been documented from the lingulid family Dysoristidae (Popov & Ushatinskaya, 1992).

Muscle scars and mantle canal systems are poorly defined in most siphonotretid genera, and this is generally attributed to poor mineralization of the innermost shell layer (Holmer & Popov, 1994, 2000). Features of the muscle system have been described to varying degrees for *Schizambon* (Rowell, 1962, 1977; Chuang, 1971), *Siphonotreta, Siphonobolus* and *Celdobolus* (Havlíček, 1982). Chuang (1971) and Rowell (1977) both attempted (through very different interpretations) to reconstruct the muscle system of *Schizambon* on the assumption that it resembled the muscle system of a discinid. However, Havlíček (1982) has shown that the siphonotretid muscle system is also comparable with many early Palaeozoic lingulids, an arrangement accepted by Holmer & Popov (2000). The siphonotretid mantle canal system has been best described by Havlíček (1982) for *Celdobolus* and *Siphonobolus*, and by Rowell (1962) for *Schizambon*. Despite still being poorly known, the mantle canal systems of these genera appear most like those of early Palaeozoic lingulids (Holmer & Popov, 2000).

Unfortunately, the earliest history of the siphonotretids is poorly represented in the fossil record. The oldest known species, *Schizambon reticulatus* from the Mayaian of the Saian-Altai region of southwest Siberia (Aksarina & Pel'man, 1978) and the late Idamean of the Bowers Group of Northern Victoria Land, Antarctica (MacKinnon in Shergold *et al.*, 1976) already possesses an ornament of hollow spines and an elongate pedicle track formed through resorption. The other known Cambrian siphonotretid genera, *Gorchakovia* and *Helmersenia*, also possess these features.

Based on the evidence presented above, Rowell's (1962, 1965) assessment that the siphonotretids were most closely related to the acrotretids cannot be sustained. Despite many features of the siphonotretids still being poorly understood, they appear most similar to the lingulellotretids or dysoristids from which they are most likely to be descended (Holmer & Popov, 2000).

Superfamily Siphonotretoidea Kutorga, 1848

Family Siphonotretidae Kutorga, 1848

Genera included. *Siphonotreta* de Verneuil, 1845; *Acanthambonia* Cooper, 1956; *Alichovia* Goryanskij, 1969; *Celdobolus* Havlíček, 1982; *Cyrbasiotreta* Williams & Curry, 1985; *Eosiphonotreta* Havlíček, 1982; *Gorchakovia* Popov & Khazanovitch (in Popov *et al.*, 1989); *Helmersenia* Pander (in von Helmersen, 1861); *Karnotreta* Williams & Curry, 1985; *Mesotreta* Kutorga, 1848; *Multispinula* Rowell, 1962; *Nushbiella* Popov (in Kolobova & Popov, 1986); ?*Quasithambonia* Bednarczyk & Biernat, 1978; *Schizambon* Walcott, 1884; *Siphonobolus* Havlíček, 1982; *Siphonotretella* Popov & Holmer, 1994; *Orbaspina* n.gen., described herein.

Discussion. Walcott (1912) included the Obolellidae, comprising the genera *Obolella, Botsfordia, Schizopholis* and *Quebecia*, in the superfamily Siphonotretacea regarding these taxa as "primitive" siphonotretids. Despite comprising a mixed assemblage of calcareous and phosphatic taxa this group remained essentially unchallenged until the reviews of Goryanskij (in Sarytcheva, 1960) and Rowell (1962, 1965). Each of these genera lack hollow spines, except for *Schizopholis*, which belongs to the Acrothelidae, a group characterized by the presence of hollow spines developed on the larval shell of both valves. Schindewolf (1955) rejected Walcott's (1912) taxonomic assignment for *Schizopholis*, reassigning the genus to a new family and superfamily, Schizopholididae and Schizopholidacea, respectively. Holmer & Popov (2000) have since synonymized Schizopholidacea with Acrothelidae. Rowell (1962: 146) synonymized *Quebecia* with *Yorkia*, believing it to show "all the essential characters of *Yorkia*." Goryanskij (in Sarytcheva, 1960) also included the calcareous obolids within the Siphonotretida, but these were regarded by Rowell (1962) to constitute a separate superfamily on the basis of their calcitic shell structure. *Botsfordia* was reassigned by Schindewolf (1955) to a new family, Botsfordiidae.

In addition to *Siphonotreta* and *Schizambon*, Walcott (1908, 1912) assigned a second group of calcareous and phosphatic taxa consisting of *Dearbornia, Trematobolus* and *Keyserlingia*, to the Siphonotretidae. Walcott (1912: 80) described *Dearbornia clarki* Walcott as "one of the simple or rudimentary forms of the Siphonotretidae". Bell (1941: 219) reassigned *D. clarki* to *Acrothele* on the basis of its organophosphatic shell composition and "a morphology congeneric with *Acrothele*." *Trematobolus*, while superficially resembling *Schizambon*, lacks hollow spines and has a calcareous composition that led Rowell (1962) to reassign this genus to the Obolellidae. *Keyserlingia* now resides within the acrotretid family Ceratretidae (Holmer & Popov, 2000).

As discussed by Brock (1998), Walcott (1897, 1912) also assigned the yorkiids to the Siphonotretidae. However, the calcareous shell composition, rudimentary articulation structures and lack of hollow spines in the yorkiids led Rowell (1962) to relocate them into a new family, the Yorkiidae, within the Obolelloidea. As their placement here was also uncomfortable, Rowell (1965) relocated them a second time to the Kutorginoidea, a classification that has since been accepted by most other workers (see Brock, 1998: 611).

Cooper (1956) assigned *Acanthambonia*, residing within a new subfamily, Acanthamboniinae, to the obolids. Despite

being a somewhat uncomfortable placement, it was followed by Wright (1963), Rowell (1965), Cocks (1978) and Williams & Curry (1985). Goryanskij (1969), while maintaining Cooper's (1956) taxonomic placement of *Acanthambonia*, questioned this assignment and highlighted a number of common features shared between *Acanthambonia* and *Helmersenia* (including tubular hollow spines). This led Havlíček (1982) and subsequent workers (e.g., Popov & Nõlvak, 1987; Holmer, 1989; Schallreuter, 1999) to reassign Acanthamboniinae to the siphonotretids.

Rowell (1962, 1965), Havlíček (1982) and Harper *et al.* (1993) placed *Dysoristus* and *Ferrobolus* within the Siphonotretidae. However, the lack of hollow spines, baculate shell structure and pitted larval shell microornament in both genera (Popov & Ushatinskaya, 1992; Popov & Holmer, 1994), indicates their affinities lie more closely with the Lingulida (Holmer & Popov, 2000), particularly the zhanatellids (Popov & Holmer, 1994).

The poorly known genus *Craniotreta*, from the Middle Cambrian west Taurus Mountains of Turkey, was described by Termier & Monod (1978) as a siphonotretid. However, the acrotretid-like shell structure, apical process, muscle scars and lack of hollow spines indicate the affinities of *Craniotreta* do not lie with the siphonotretids. Holmer & Popov (2000) have speculated that *Craniotreta* may be synonymous with the acrotretid *Linnarssonia*.

Orbaspina n.gen.

Type species. *Orbaspina gelasinus* n.gen. and n.sp., Llandovery to Wenlock, central-western New South Wales, Australia.

Diagnosis. A siphonotretid with large, keyhole-shaped pedicle foramen extending forward through resorption to form an elongate, broadly triangular, pedicle track; pedicle track covered posteriorly by a concave plate and anteriorly by short "listrum-like" plate; tubular hollow spines of uniform size arranged in concentric rows close to valve margin; post larval shell bearing numerous subcircular dimples loosely arranged in concentric rows.

Etymology. *Orba* L., orphan, refers to the occurrence of this taxon after the supposed demise of the siphonotretids during the end-Ordovician extinction event; *spina* L., thorny, in reference to the post-larval shell ornament of tubular hollow spines.

Remarks. Features considered to be of generic significance among the siphonotretids include the nature of the pedicle foramen and tube, the pseudointerarea of both valves and the presence of tubular hollow spines (Holmer & Popov, 2000). Based on these features, *Orbaspina* n.gen. appears closest morphologically to those genera grouped together by Havlíček (1982) and Popov & Holmer (1994) in the subfamily Schizamboninae. The most characteristic feature of these siphonotretids is the large pedicle foramen that extends forward through resorption, forming an elongate triangular pedicle track that may be covered posteriorly by a plate. However, the dimpled post-larval shell of *Orbaspina* n.gen. is unknown in any previously described Cambrian or Ordovician siphonotretid. This feature is present on a number of post-Ordovician siphonotretids including, "*Siphonotreta*" *anglica* Morris (1849), and Siphonotretine sp. and Schizambonine sp. A Mergl (2001a,b). The short "listrum-like" plate anteriorly covering the pedicle track of *O. gelasinus* n.gen. and n.sp. (Fig. 6g) has not been previously documented among the siphonotretids.

Orbaspina gelasinus n.sp.

Figs. 5–7

"New genus A" Valentine, Brock & Molloy (2003): pl. 3, figs. 18–29.

Type material. HOLOTYPE: AMF120610 (Fig. 5a–g): dorsal valve from sample BM 14.85, *ranuliformis* Zone, Boree Creek Formation (Fig. 3). Figured PARATYPES: AMF122212 (Fig. 5h–k): dorsal valve from sample BM 14.85, *ranuliformis* Zone, Boree Creek Formation (Fig. 3); AMF120612 (Fig. 6a–d): ventral valve from sample BM 14.30, *ranuliformis* Zone, Boree Creek Formation (Fig. 3); AMF120613 (Fig. 6e, f): ventral valve from sample BM 14.30, *ranuliformis* Zone (Fig. 3); AMF122213 (Fig. 6g): ventral valve from sample BM 13.80, *ranuliformis* Zone (Fig. 3); AMF122214 (Fig. 6h): ventral valve from sample BM 9.90, *amorphognathoides* Zone (Fig. 3); AMF122215 (Fig. 6i): fragment from sample BM 9.30, *amorphognathoides* Zone (Fig. 3); AMF122216 (Fig. 7a–d): fragment from sample BM 13.80, *ranuliformis* Zone (Fig. 3); AMF122217 (Fig. 7e, f): fragment from sample BM 14.30, *ranuliformis* Zone (Fig. 3); AMF122218 (Fig. 7g): dorsal valve fragment from sample BM 11.20, *ranuliformis* Zone (Fig. 3); AMF122220 (Fig. 7i,j): dorsal valve fragment from sample BM 14.40, *ranuliformis* Zone (Fig. 3). Unfigured PARATYPES: 34 ventral valves, 101 dorsal valves and 140 fragments (Fig. 3).

Type locality and horizon. Massive red and grey lensoidal limestones at "Kalinga", along the BM section (samples BM 5.50 to BM 15.60) (Fig. 3) through the Boree Creek Formation, central-western New South Wales, Australia (Fig. 1).

Age. Early Silurian: late Llandovery (*amorphognathoides* Zone) to early Wenlock (*ranuliformis* Zone) (Bischoff, 1986; Cockle, 1999; Molloy, unpub. data).

Etymology. *Gelasinus* L., dimpled, in reference to the dimpled post-larval shell ornament.

Diagnosis. As for genus by monotypy.

Description. Ventral valve incompletely known, planar to weakly convex, ?subcircular in outline. Lateral margins evenly curved; posterior margin weakly angular. Maximum width at, or slightly anterior of, valve midlength. In lateral profile, valve highest around midlength. Larval shell subrectangular, smooth, averaging 65 μm in width and 30 μm in length, separated from post-larval shell by distinct change in elevation. Foramen keyhole-shaped, ?centrally located at anterior end of elongate triangular to subtriangular pedicle track. Pedicle track covered posteriorly by concave plate bearing numerous, closely spaced growth lamellae and anteriorly by very short, flat "listrum-like" plate. Post-larval shell ornament with low rounded concentric ridges, becoming stronger towards margins, spaced at intervals averaging 25 μm. Tubular hollow spines sparsely developed along tops of concentric ridges, projecting at low angle from valve surface, becoming more numerous towards valve margins.

Ventral valve interior with long, posteriorly convex, ridge-like pseudointerarea following line of posterior margin. Pseudointerarea extending up to 88% valve width. Propareas long, narrowly triangular, separated from central portion of pseudointerarea by long, anteriorly divergent,

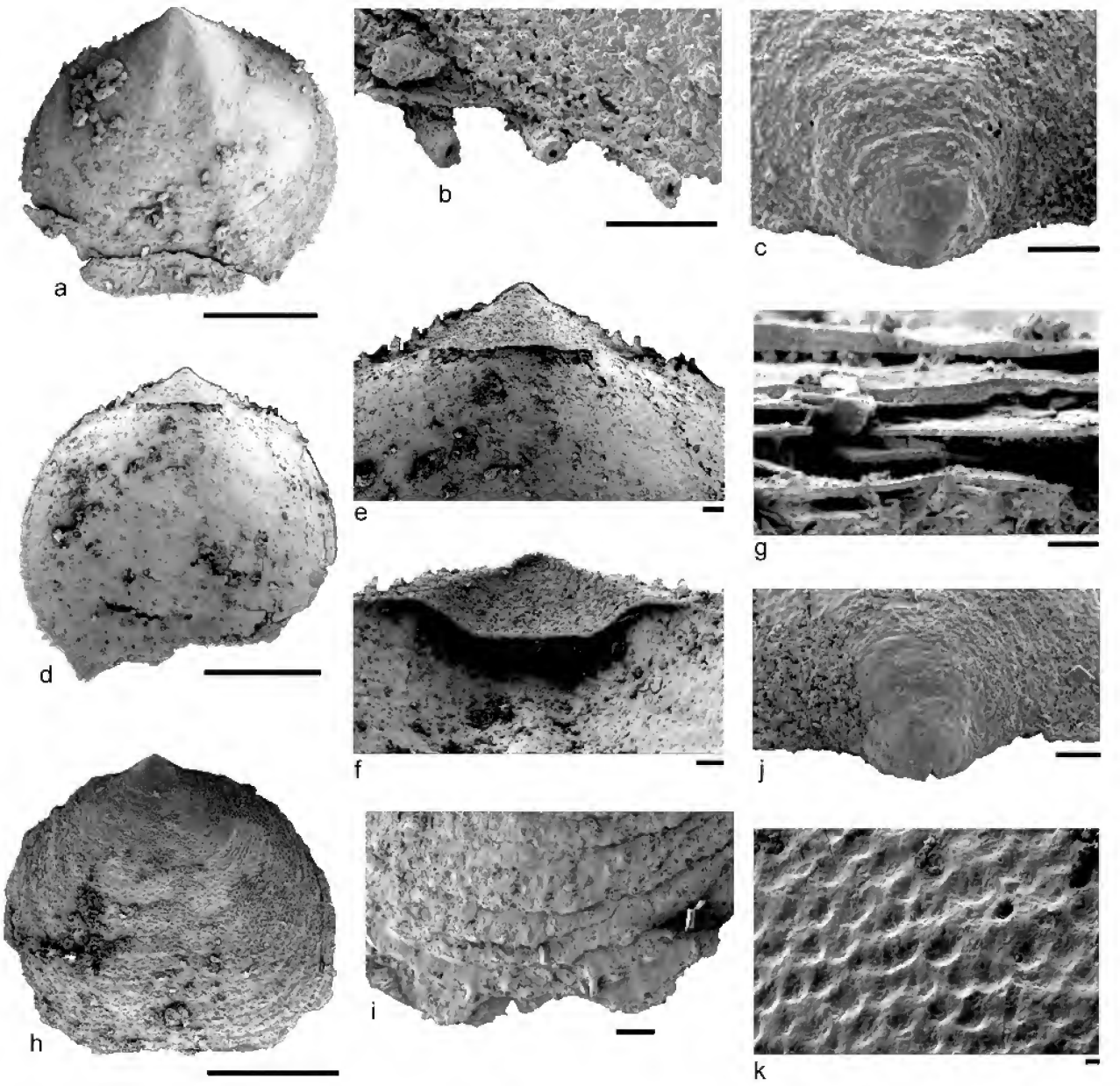

Fig. 5. *Orbaspina gelasinus* n.gen. and n.sp.: *a–g*, holotype AMF120610, dorsal valve from sample BM 14.85, external view (*a*), detail of spines along posterior margin (*b*), detail of larval shell (*c*), internal view (*d*), detail of pseudointerarea in plan view (*e*), and anterior view (*f*), detail of shell lamina along broken section of anterior margin (*g*); *h–k* paratype AMF122212, dorsal valve from sample BM 14.85: external view (*h*), detail of anterior margin showing frill-like nature of growth lamellae (*i*), deatil of larval shell (*j*), detail of post-larval shell dimpling (*k*). Scale bars = 1 mm (*a, d, h*); 100 μm (*b, c, e, f, j, i*); 10 μm (*g, k*).

uniformly narrow grooves that "articulate" with raised portion of propareas on dorsal valve pseudointerarea. Central portion of pseudointerarea strongly arcuate, lacking median plate. Transmedian and umbonal muscle scars subcircular, posterocentrally located. Other muscle scars not observed. Inner surface of plate covering pedicle track bearing shallow median groove that terminates at posterior margin of foramen around valve midlength. Foramen bounded anteriorly and laterally by low ridge. No pedicle tube observed. Vascular system not observed.

Dorsal valve convex, subcircular in outline with evenly rounded lateral margins and gently curved anterior and posterior margins. Maximum width at, or slightly anterior of, valve midlength. In lateral profile, valve highest at midlength, flattening anteriorly. Sulcate in anterior view, particularly in larger specimens. Larval shell smooth, subcircular to subrectangular, averaging 140 μm in length and 200 μm in width. Larval shell separated from post-larval shell by change in elevation and onset of post-larval shell ornament. Post-larval shell ornament of irregular concentric growth lamellae becoming better developed, occasionally frill-like, towards margins. Lamellae spaced at intervals of 50 to 250 μm, averaging 115 μm. Post-larval shell bearing numerous subcircular dimples loosely arranged in concentric rows, ranging from 20 to 40 μm, averaging 30 μm, in diameter. Short tubular hollow spines of uniform size, averaging 175 μm in length, projecting at low angle from valve surface. Spines developed on

Table 1. Average dimensions and ratios of ventral valves of *Orbaspina gelasinus* n.gen. and n.sp. Note that due to the incomplete nature of ventral valves recovered, it was not possible to obtain accurate measurements of length. The most complete ventral valve recovered (Fig. 6g) measures 2.34 mm in length. See text below for abbreviations.

	W	LI	ML	WI	FP	WP	LI/WI	WI/W
	Red Limestone							
N	1	5	8	5	5	7	5	
mean	1.29	0.17	0.05	0.84	0.57	0.45	23%	
SD		0.05	0.02	0.39	0.08	0.07	0.1	
minimum		0.1	0.03	0.38	0.45	0.35	13%	
maximum		0.23	0.7	1.4	0.67	0.54	26%	
	Grey Limestone							
N	6	9	20	11	18	12	9	3
mean	1.69	0.27	0.05	1.27	0.78	0.59	23%	72%
SD	0.36	0.06	0.02	0.3	0.18	0.23	0.05	0.13
minimum	1.3	0.18	0.01	0.85	0.45	0.4	18%	64%
maximum	2.05	0.38	0.09	1.8	1.1	1	35%	88%

lamellae, sparsely in older portions of valve, becoming more numerous and arranged in rows toward margins, including posterior margin. Spines bearing occasional, faintly developed, transverse grooves.

Dorsal valve interior with large triangular, orthocline to anacline, shelf-like pseudointerarea, extending up to 85% valve width. Median plate triangular, concave, flat-bottomed, bearing numerous, closely spaced growth lamellae. Propareas narrowly subtriangular, raised above pseudointerarea with rounded crests, also bearing numerous growth lamellae. Some specimens with two hollow spines projecting from underneath pseudointerarea into body cavity. Outside lateral and transmedian muscle scars located immediately anterior of pseudointerarea, weakly impressed, elongately suboval, extending to approximately 25% valve length. Muscle scars separated by very low, broadly rounded, indistinct median ridge, widening anteriorly, reflecting external sulcus. Median ridge occasionally forming a very short, but distinct ridge at posterior end of muscle field. Central muscle scars indistinct, located around valve midlength. Remaining muscle scars not observed. Vascular system not observed. Numerous holes, occasionally with a very low, narrow ridge around them, connect spines with valve interior, particularly around margins.

Measurements. Following the morphological measurements for organophosphatic brachiopods used by Popov & Holmer (1994: 35), the average dimensions and ratios of *Orbaspina gelasinus* n.gen. and n.sp. are given in Tables 1 and 2. All dimensions given are in millimetres. Abbreviations used are as follows: FP, point of origin of pedicle foramen from posterior margin; L, length; LI, maximum length of pseudointerarea; ML, median length of pseudointerarea; N, number of specimens measured; SD, standard deviation; W, width; WI, maximum width of pseudointerarea; WP, maximum width of pedicle track.

Discussion. Tubular hollow spines are the one diagnostic feature of the Siphonotretida uniting them as a monophyletic clade (Holmer & Popov, 2000). Although not numerous, particularly on the ventral valve, tubular hollow spines are clearly discernible on both valves of *O. gelasinus* n.gen. and n.sp. (Figs. 5a,b,h,i, 6a,b,i, 7a–f). The hollow internal spines projecting from underneath the pseudointerarea of the dorsal valve in some specimens (Fig. 7i,j) has not previously been observed in other siphonotretids. As they would have presumably been surrounded by soft tissue throughout life, their function remains unknown. Although not unique to the siphonotretids, all siphonotretids

Table 2. Average dimensions and ratios of dorsal valves of *Orbaspina gelasinus* n.gen. and n.sp.

	L	W	LI	ML	WI	L/W	LI/WI	LI/L	ML/L	WI/W
holotype	2.67	2.87	0.57	0.29	2.02	93%	28%	21%	11%	70%
	Red Limestone									
N	3	6	7	23	6	3	4	3	3	2
mean	0.89	1.32	0.32	0.28	0.96	87%	44%	34%	18%	57%
SD	0.22	0.38	0.13	0.15	0.37	0.05	0.35	0.14	0.06	0.34
minimum	0.74	0.86	0.15	0.1	0.46	83%	21%	19%	14%	34%
maximum	1.14	1.8	0.45	0.7	1.5	93%	96%	45%	25%	81%
	Grey Limestone									
N	14	16	16	61	15	12	15	10	13	22
mean	2.27	2.83	0.78	0.44	1.88	93%	36%	32%	18%	66%
SD	0.51	0.48	0.44	0.11	0.49	0.15	0.06	0.16	0.06	0.12
minimum	0.9	2.23	0.4	0.22	1.14	75%	27%	17%	10%	46%
maximum	3.04	4.02	2.23	0.8	2.83	121%	47%	73%	33%	85%

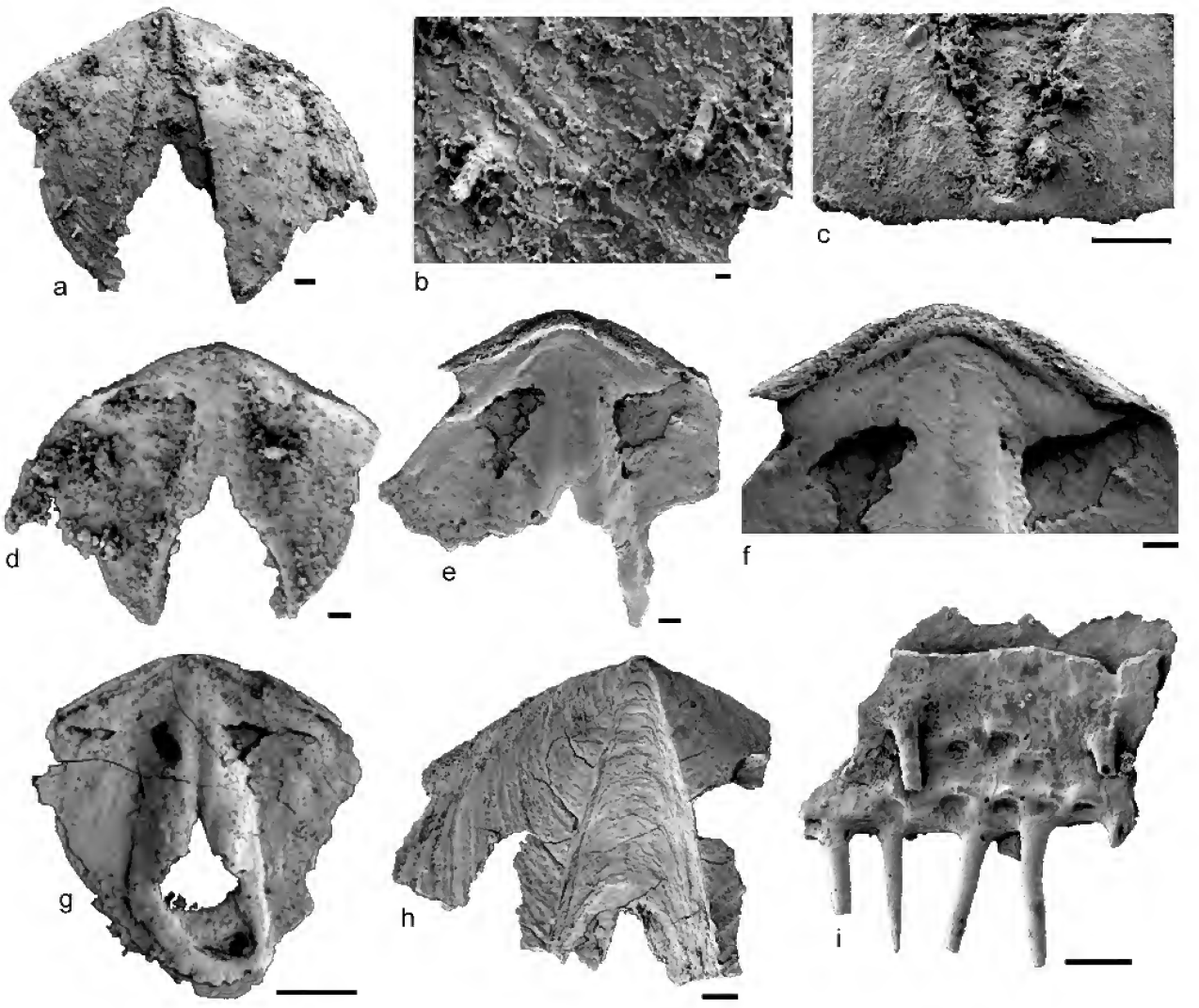

Fig. 6. *Orbaspina gelasinus* n.gen. and n.sp.: *a–d*, paratype AMF120612, ventral valve from sample BM 14.30, external view (*a*), detail of spines on anterior slope (*b*), detail of larval shell (*c*), internal view (*d*); *e, f*, paratype AMF120613, ventral valve from sample BM 14.30, internal view (*e*), detail of pseudointerarea (*f*); *g*, paratype AMF122213, ventral valve from sample BM 13.80, internal view, note the "listrum-like" plate covering the anterior portion of the pedicle track as indicated by arrow; *h*, paratype AMF122214, ventral valve from sample BM 9.90, external view showing common state of presentation of recovered ventral valves; *i*, paratype AMF122215, fragment from sample BM 9.30, external view. Scale bars = 500 µm (*g*); 100 µm (*a, c–f, h, i*); 10 µm (*b*).

possesses a smooth, unpitted larval shell (Holmer & Popov, 2000), a feature also present in *O. gelasinus* n.gen. and n.sp. (Figs. 5a,j, 6c). The shell structure of *O. gelasinus* n.gen. and n.sp. is consistent with that described by Biernat & Williams (1970) and Ushatinskaya *et al.* (1988) for other siphonotretids (Fig. 5g).

Recently, Mergl (2001a,b) documented four indeterminate post-Ordovician siphonotretids from central Bohemia, two of which were described as possessing a pitted post larval shell. Siphonotretine sp., represented by a single fragment from the Ludlow Kopanina Formation of Řeporyje, has deep, regular, closely spaced pits, somewhat similar to the pitting found on acrotretid larval shells. The spines of this species are also more numerous and erect than in *O. gelasinus* n.gen. and n.sp. The second taxon, Schizambonine sp. A, is represented by a dorsal valve fragment recovered from the Pragian Dvorce-Prokop Limestone of Klukovice. It possesses minute, scattered spines, somewhat similar to those observed on the pedicle valve of *O. gelasinus* n.gen. and n.sp. The post-larval shell pitting, however, is finer and more regular than the dimpling observed in *O. gelasinus* n.gen. and n.sp. Little is known about the internal features of these two species.

"*Siphonotreta*" *anglica* (Morris), from the Wenlock Coalbrookdale Formation of Dudley, England, was

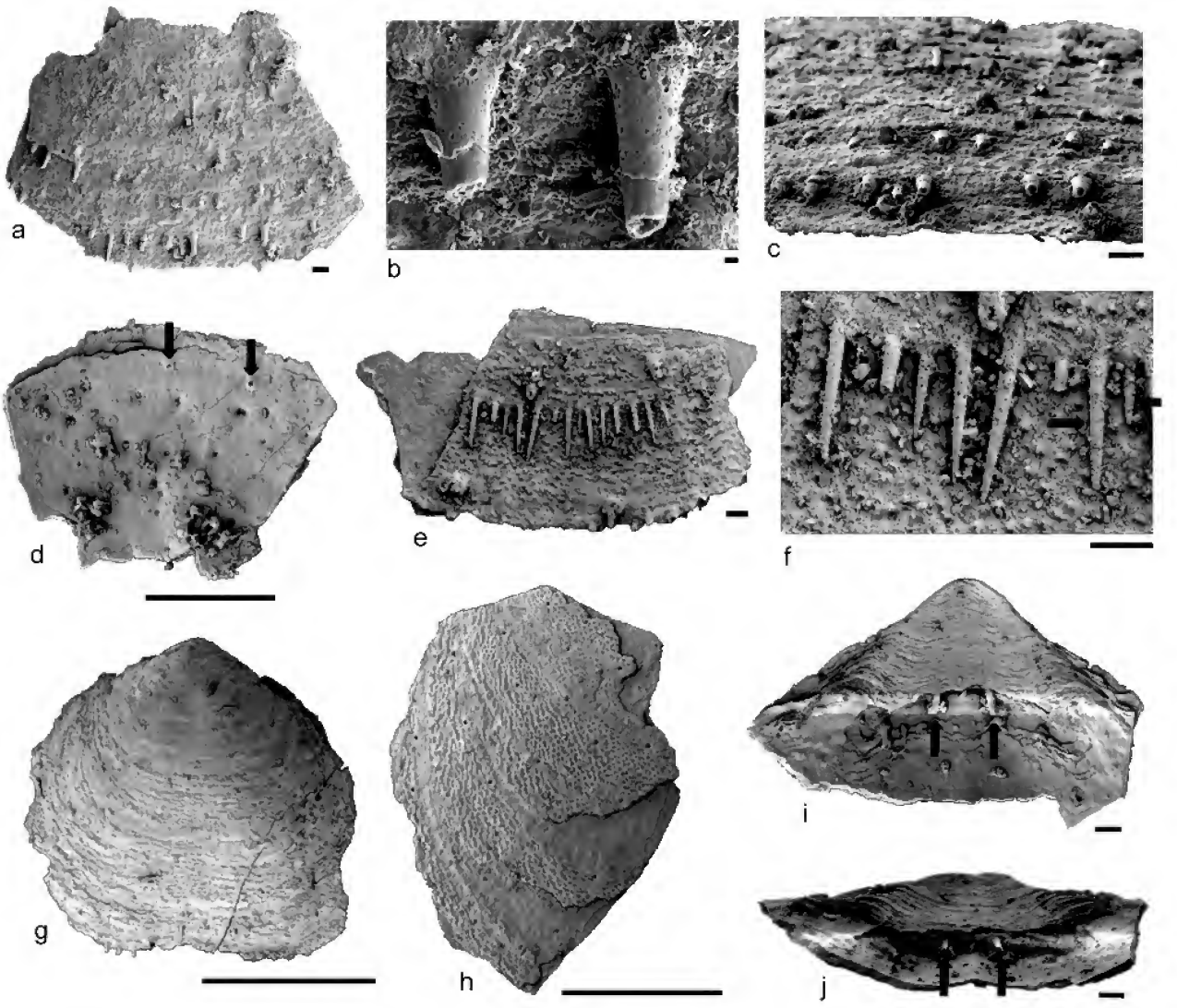

Fig. 7. *Orbaspina gelasinus* n.gen. and n.sp.; *a–d*, paratype AMF122216, fragment from sample BM 13.80, external view (*a*), detail of spines (*b*), anterior view (*c*), interior view with spine openings on internal surface indicated by arrows (*d*); *e, f*, paratype AMF122217, fragment from sample BM 14.30, external view (*e*), detail of spines with weak transverse grooves on spines indicated by arrows (*f*); *g*, paratype AMF122218, dorsal valve from sample BM 15.40, external view; *h*, paratype AMF122219, dorsal valve fragment from sample BM 11.20, external view showing well developed post-larval shell dimpling; *i, j*, paratype AMF122220, fragment of dorsal valve pseudointerarea from sample BM 14.40, with two spines projecting from underneath the pseudointerea as indicated by arrows, in plan (*i*) and anterior views (*j*). Scale bars = 1 mm (*a, d, g, h*); 100 µm (*c, e, f, i, j*); 10 µm (*b*).

described by Morris (1849: 321) as possessing spines which were "…regularly and transversely sulcated or centrated, giving the spines a beaded or jointed appearance"; a feature also noted by Davidson (1866). Some spines of *O. gelasinus* n.gen. and n.sp. bear the occasional, faintly developed, transverse groove (Fig. 7f), whereas no trace of similar grooving can be observed on any of the spines in Mergl's (2001a,b) material. "*Siphonotreta*" *anglica* also has more numerous spines and a more regular post-larval shell pitting than *O. gelasinus* n.gen. and n.sp. A comparison of internal features is not possible as these have not been described in "*Siphonotreta*" *anglica*.

ACKNOWLEDGMENTS. The authors gratefully acknowledge the enthusiastic assistance with fieldwork provided by Peter Molloy, David Mathieson, Carl Valentine, John Talent, Ruth Mawson and Graham Felton on various occasions. David Mathieson assisted with scanning electron microscopy and digital photography. Peter Molloy, Andrew Simpson and Peter Cockle provided many useful insights into Silurian conodonts. David Holloway, Museum Victoria, kindly loaned us samples of Chapman's "siphonotretid" collection. Dean Oliver skillfully drafted the figures. This project would not have been possible without the kindness and generosity of Keith Goodridge, who allowed us access to his property, "Kalinga". Ian Percival (Sydney) and Michal Mergl (Plzen) are thanked for their constructive reviews of this manuscript.

References

Aksarina, N.A., & Y.L. Pel'man, 1978. Kembriiskie brakhiopody i dvustvorchatye molliuski Sibiri. *Trudy Instituta Geologii i Geofiziki, Sibirskoye otdeleniye Akademiya Nauk SSSR* 362: 5–178 [in Russian].

Alvarez, F., & C.H.C. Brunton, 2001. Fundamental differences in external spine growth in brachiopods. In *Brachiopods Past and Present*, ed. C.H.C. Brunton, L.R.M. Cocks & S.M. Long. *Systematics Association Special Volume* 63: 108–118.

Bassett, M.G., L.E. Popov & L.E. Holmer, 1999. Organophosphatic brachiopods: patterns of biodiversification and extinction in the Early Palaeozoic. *Geobios* 32: 145–163.

Bednarczyk, W., & G. Biernat, 1978. Inarticulate brachiopods from the Lower Ordovician of the Holy Cross Mountains, Poland. *Acta Palaeontologica Polonica* 23: 293–316.

Beecher, C.E., 1891. Development of the Brachiopoda. *American Journal of Science* 41: 343–357.

Bell, C.W., 1941. Cambrian Brachiopoda from Montana. *Journal of Paleontology* 15: 193–255.

Biernat, G., & A. Williams, 1970. Ultrastructure of the protegulum of some acrotretide brachiopods. *Palaeontology* 13: 491–502.

Bischoff, G.C.O., 1986. Early and Middle Silurian conodonts from midwestern New South Wales. *Courier Forschungsinstitut Senckenberg* 89: 1–337.

Brock, G.A., 1998. Middle Cambrian articulate brachiopods from the southern New England Fold Belt, northeastern N.S.W., Australia. *Journal of Paleontology* 72: 604–619.

Carlson, S.J., 1991. Phylogenetic relationships among brachiopod higher taxa. In *Brachiopods Through Time*, ed. D.I. MacKinnon, D.E. Lee & J.D. Campbell, pp. 3–10. Rotterdam: A.A. Balkema.

Carlson, S.J., 2001. Ghosts of the past, present, and future in brachiopod systematics. *Journal of Paleontology* 75: 1109–1118.

Chapman, F., 1903. New or little known Victorian fossils in the National Museum: part II.—Some Silurian Molluscoidea. *Proceedings of the Royal Society of Victoria* 16: 60–82.

Chapman, F., 1910. A synopsis of the Silurian fossils of South Yarra and the Yarra Improvement Works. *Victorian Naturalist* 27: 63–70.

Chapman, F., 1913. New or little-known Victorian fossils in the National Museum: part XVI.—Some Silurian Brachiopoda. *Proceedings of the Royal Society of Victoria* 26: 99–113.

Chapman, F., 1914. On the palaeontology of the Silurian of Victoria. *Report of the Fourteenth Meeting of the Australasian Association for the Advancement of Science* 14: 207–235.

Chuang, S.H., 1971. New interpretation of the morphology of *Schizambon australis* Ulrich and Cooper (Ordovician siphonotretid inarticulate brachiopod). *Journal of Paleontology* 45: 824–832.

Cockle, P., 1999. Conodont data in relation to time, space and environmental relationships in the Silurian (Late Llandovery-Ludlow) succession at Boree Creek (New South Wales, Australia). *Abhandlungen de Geologischen Bundesanstalt* 54: 107–133.

Cocks, L.R.M., 1978. A review of British Lower Palaeozoic brachiopods, including a synoptic revision of Davidson's monograph. *Palaeontographical Society Monograph* 131: 1–256.

Cooper, G.A., 1956. Chazyan and related brachiopods. *Smithsonian Miscellaneous Collections* 127: 1–1245.

Davidson, T., 1866. British fossil Brachiopoda, vol III. The Silurian Brachiopoda. *Palaeontographical Society Monograph* 7: 1–88.

de Verneuil, E., 1845. Paléontologie, Mollusques, Brachiopodes. In *Géologie de la Russie d'Europe et des Montagnes de l'Oural, Systéme Jurassique: Mollusques, Lamellibranches ou Acéphales 2*, ed. R.I. Murchison, E. de Verneuil & A. Keyserling, pp. 17–395. London and Paris: John Murray and Bertrand [in French].

Dorning, K.J., 1983. Palynology and stratigraphy of the Much Wenlock Limestone Formation of Dudley, central England. *The Mercian Geologist* 9: 31–40.

Duméril, A.M.C., 1806. *Zoologie analytique ou méthode naturelle de classification des animaux*. Paris: Allais, 344 pp. [in French].

Gagel, C., 1890. Die Brachiopoden der Cambrischen und Silurischen Geschiebe im Diluvium der Provinzen Ost- und Westpreussen. *Beitrage zur Naturkunde Preussens* 6: 1–79 [in German].

Goryanskij, V.I., 1969. Bezzamkovye brakhiopody kembriiskikh i ordovikskikh otlozhenii sever-zapada Russkoi platformy. *Materialy po Geologii i Poleznym Iskopaemym severo-zapada R.S.F.S.R.* 6: 1–171 [in Russian].

Goryanskij, V.I., & L.E. Popov, 1985. The morphology, systematic position, and origin of inarticulate brachiopods with carbonate shells. *Paleontological Journal* 19: 1–11.

Hall, J., & J.M. Clarke, 1892. An introduction to the study of the Brachiopoda, intended as a hand book for the use of students. *New York State Museum Annual Report* 45: 449–616.

Harper, D.A.T., 1984. Brachiopods from the upper Ardmillan succession (Ordovician) of the Girvan district, Scotland. Part 1. *Palaeontographical Society Monograph* 136: 1–78.

Harper, D.A.T., C.H.C. Brunton, L.R.M. Cocks, P. Copper, E.N. Doyle, A.L. Jeffrey, E.F. Owen, M.A. Parkes, L.E. Popov & C.D. Prosser, 1993. Brachiopoda. In *The Fossil Record 2*, ed. M.J. Benton, pp. 427–462. London: Chapman & Hall.

Harper, D.A.T., & J.-Y. Rong, 1995. Patterns of change in the brachiopod faunas through the Ordovician-Silurian interface. *Modern Geology* 20: 83–100.

Havlíček, V., 1982. Lingulacea, Paterinacea, and Siphonotretacea (Brachiopoda) in the Lower Ordovician sequence of Bohemia. *Sborník Geologickych ved, Paleontologie* 25: 9–82.

Holloway, D.J., & P.D. Lane, 1998. Effaced styginid trilobites from the Silurian of New South Wales. *Palaeontology* 41: 853–896.

Holmer, L.E., 1989. Middle Ordovician phosphatic inarticulate brachiopods from Västergötland and Dalarna, Sweden. *Fossils and Strata* 26: 1–172.

Holmer, L.E., & L.E. Popov, 1994. Early Paleozoic radiation and classification of organo-phosphatic brachiopods. In *Brachiopods*, ed. P. Copper & J. Jin, pp. 117–121. Rotterdam: A.A. Balkema.

Holmer, L.E., & L.E. Popov, 2000. Lingulata. In *Treatise on Invertebrate Paleontology, Part H, Brachiopoda (Revised) (2)*, ed. R.L. Kaesler, pp. 30–146. Boulder and Lawrence: Geological Society of America and The University of Kansas.

Holmer, L.E., L.E. Popov, M.G. Bassett & J. Laurie, 1995. Phylogenetic analysis and ordinal classification of the Brachiopoda. *Palaeontology* 38: 713–741.

Jeppsson, L., 1997. The anatomy of the mid-early Silurian Ireviken Event and a scenario for P-S events. In *Paleontological Events: Stratigraphic, Ecological, and Evolutionary Implications*, ed. C.E. Brett & G.C. Baird, pp. 451–492. New York: Columbia University Press.

Kolobova, I.M., & L.E. Popov, 1986. K paleontologicheskoj kharakteristike anderkenskogo gorizonta srednego ordovika v Chu-ilijskikh gorakh (yuzhnyj Kazakhstan). *Ezhegodnik vsesoyuznogo paleontologicheskogo obshchestva* 29: 246–261 [in Russian].

Koneva, S.P., & L.E. Popov, 1983. Nekotorye novye lingulidy iz verkhnego kembriia i nizhnego ordovika Malogo Karatau. In *Stratigrafiya i paleontologiya nizhnego paleozoya Kazakhstana*, ed. M.K. Apollonov, S.M. Bandaletov & N.K. Ivshin, pp. 112–124. Nauka: Alma-Ata [in Russian].

Krause, F.F., & A.J. Rowell, 1975. Distribution and systematics of the inarticulate brachiopods of the Ordovician carbonate mud mound of Meiklejohn Peak, Nevada. *The University of Kansas Paleontological Contributions* 61: 1–74.

Kuhn, O., 1949. *Lehrbuch der Paläozoologie*. Stuttgart: E. Schweizerbart [in German].

Kutorga, S.S., 1848. Ueber die Brachiopoden-Familie der Siphonotretaceae. *Russisch-Kaiserliche Mineralogische Gesellschaft Verhandlungen* 1847: 250–286 [in German].

Lapworth, C., 1879. On the tripartite classification of the lower Palaeozoic rocks. *Geological Magazine* 6: 1–15.

Männik, P., & R.J. Aldridge, 1989. Evolution, taxonomy and relationships of the Silurian conodont *Pterospathodus*. *Palaeontology* 32: 893–906.

Mergl, M., 1995. New lingulate brachiopods from the Milina Formation and the base of the Klabava Formation (late Tremadoc-early Arenig), central Bohemia. *Věstník Ústředního ústavu geologického* 70: 101–109.

Mergl, M., 2000. Extinction of some lingulate brachiopod families: a new stratigraphical data from Silurian and Devonian from Bohemia. In *The Fourth Millennium International Brachiopod Congress*, ed. C.H.C. Brunton, pp. 61. London: The Natural History Museum.

Mergl, M., 2001a. Extinction of some lingulate brachiopod families: new stratigraphical data from the Silurian and Devonian of central Bohemia. In *Brachiopods Past and Present*, ed. C.H.C. Brunton, L.R.M. Cocks & S.M. Long. *Systematics Association Special Volume* 63: 345–351.

Mergl, M., 2001b. Lingulate brachiopods of the Silurian and Devonian of the Barrandian (Bohemia, Czech Republic). *Acta Musei Nationalis Prague, Series B, Historia Naturalis* 57: 1–49.

Molloy, P., & A. Simpson, 2002. Morphological variation in the Pa element of *Pterospathodus* from the Early Silurian of Boree Creek, NSW. In *IPC 2002, Geological Society of Australia, Abstracts 63*, ed. G.A. Brock & J.A. Talent, pp. 245–246. Sydney: Geological Society of Australia.

Morris, J., 1849. Note on the genus *Siphonotreta*, with a description of a new species. *Annals and Magazine of Natural History* 4: 315–321.

Pickett, J.W., 1982. The Silurian System in New South Wales. *Bulletin of the Geological Survey of New South Wales* 29: 1–264.

Popov, L.E., M.G. Bassett, L.E. Holmer & J. Laurie, 1993. Phylogenetic analysis of higher taxa of Brachiopoda. *Lethaia* 26: 1–5.

Popov, L.E., & L.E. Holmer, 1994. Cambrian-Ordovician lingulate brachiopods from Scandinavia, Kazakhstan, and South Ural Mountains. *Fossils and Strata* 35: 1–156.

Popov, L.E., K.K. Khazanovitch, N.G. Borovko, S.P. Sergeeva & R.F. Sobolevskaya, 1989. Opornye razrezy i stratigrafiya kembro-ordovikskoj fosforitonosnoj obolovoj tolshchi na severo-zapade Russkoj platformy. *AN SSSR, Ministerstvo Geologii SSSR, Mezhvedomstvennyj stratigraficheskij komitet SSSR, Trudy* 18: 1–222 [in Russian].

Popov, L.E., & J. Nõlvak, 1987. Revision of the morphology and systematic position of the genus *Acanthambonia* (Brachiopoda, Inarticulata). *Eesti NSV Teaduste Akadeemia Toimetised, Geoloogia* 36: 14–18.

Popov, L.E., & G.T. Ushatinskaya, 1992. Lingulidy, proizkhozhdenie discinid, sistematika vysokikh taksonov. In *Drevnejshie brakhiopody territorii Severnoi Evrazii*, ed. L.N. Repina & A.U. Rozanov, pp. 59–67. Novosibirsk: Obedinennyi Institut Geologii, Geofiziki i Mineralogii, Sibirskoie Otdeleniie RAN [in Russian].

Poulsen, C., 1971. Notes on an Ordovician acrotretacean brachiopod from the Oslo region. *Bulletin of the Geological Society of Denmark* 20: 265–278.

Rickards, R.B., & A.C. Sandford, 1998. Llandovery-Ludlow graptolites from central Victoria: new correlation perspectives of the major formations. *Australian Journal of Earth Sciences* 45: 743–763.

Robson, S.P., & B.R. Pratt, 2001. Cambrian and Ordovician linguliformean brachiopods from the Shallow Bay Formation (Cow Head Group), western Newfoundland. *Journal of Paleontology* 75: 241–260.

Rong, J.-Y., & D.A.T. Harper, 1999. Brachiopod survival and recovery from the latest Ordovician mass extinctions in South China. *Geological Journal* 34: 321–348.

Rowell, A.J., 1962. The genera of the brachiopod superfamilies Obolellacea and Siphonotretacea. *Journal of Paleontology* 36: 136–152.

Rowell, A.J., 1965. Inarticulata. In *Treatise of Invertebrate Paleontology, Part H, Brachiopoda (1)*, ed. R.C. Moore, pp. H260-H296. Boulder and Lawrence: The Geological Society of America and The University of Kansas Press.

Rowell, A.J., 1977. Valve orientation and functional morphology of the foramen of some siphonotretacean and acrotretacean brachiopods. *Lethaia* 10: 43–50.

Rowell, A.J., 1981. The origin of the brachiopods. In *Lophophorates: notes for a short course 5*, ed. J.T. Dutro & R.S. Boardman, pp. 97–109. Tennessee: University of Tennessee, Department of Geological Sciences.

Rowell, A.J., & W.C. Bell, 1961. The inarticulate brachiopod *Curticia* Walcott. *Journal of Paleontology* 35: 927–931.

Sarytcheva, T.G., 1960. Mshanki, Brakhiopody. In *Osnovy Paleontologii 7*, ed. Y.A. Orlov, pp. 115–324. Moscow: Akademiia Nauk SSSR [in Russian].

Schallreuter, R., 1999. Rogo-Sandstein und *jentzschi*-Konglomerat als sedimentare Leitgeschiebe. *Archiv fur Geschiebekunde* 2: 497–520 [in German].

Schindewolf, O.H., 1955. Uber einige kambrische Gattungen inartikulater Brachiopoden. *Neues Jahrbuch für Geologie und Paläontologie Monatschefte* 12: 538–557 [in German].

Sheehan, P.M., 2001. The Late Ordovician mass extinction. *Annual Review of Earth and Planetary Sciences* 29: 331–364.

Shergold, J.H., R.A. Copper, D.I. MacKinnon & E.L. Yochelson, 1976. Late Cambrian Brachiopoda, Mollusca, and Trilobita from Northern Victoria Land, Antarctica. *Palaeontology* 19: 247–291.

Sherwin, L., 1971. Stratigraphy of the Cheesemans Creek District, New South Wales. *Records of the Geological Survey of New South Wales* 13: 199–237.

Simpson, A., 1995. Silurian conodont stratigraphy in Australia: a review and critique. *Courier Forschungsinstitut Senckenberg* 182: 324–345.

Strusz, D.L., M.R. Banks, G. Bischoff, B.J. Cooper, P. Cooper, P.G. Flood, E.D. Gill, J.S. Jell, J.W. Pickett, N.M. Savage, L. Sherwin, J.A. Talent, B.D. Webby & A.J. Wright, 1972. Correlation of the Lower Devonian rocks of Australasia. *Journal of the Geological Society of Australia* 18: 427–455.

Talent, J.A., R. Mawson, A.S. Andrew, P.J. Hamilton & D.J. Whitford, 1993. Middle Palaeozoic extinction events: faunal and isotopic data. In *Event Markers in Earth History*, ed. H.H.J. Geldsetzer & G.S. Nowlan. *Palaeogeography, Palaeoclimatology, Palaeoecology* 104: 139–152.

Termier, G., & O. Monod, 1978. Inarticulate brachiopods from Cambro-Ordovician formations in western Taurus (Turkey). *Bulletin of the Geological Society of Turkey* 21: 145–152.

Ushatinskaya, G.T., 1990. The shell microstructure and secretion in the inarticulate brachiopods of the order Acrotretida. *Paleontological Journal* 24: 16–27.

Ushatinskaya, G.T., O.N. Zezina, L.E. Popov & N.V. Putivtseva, 1988. Microstructure and mineral composition of brachiopods with calcium phosphate shells. *Paleontological Journal* 22: 43–54.

Valentine, J.L., G.A. Brock & P.D. Molloy, 2003. Linguliformean brachiopod faunal turnover across the Ireviken Event at Boree Creek, central-western New South Wales, Australia. *Courier Forschungsinstitut Senckenberg* 242: 301–327.

von Helmersen, G., 1861. Die geologische Beschaffenheit des untern Narovathals und die Versandung der Narovamundung. *Bulletin de l'Academie Imperiale des Sciences de-St. Petersbourg* 3: 12–49 [in German].

Walcott, C.D., 1884. Paleontology of the Eureka District. *United States Geological Survey Monographs* 8: 1–298.

Walcott, C.D., 1897. Cambrian Brachiopoda: genera *Iphidea* and *Yorkia*, with descriptions of new species of each, and of the genus *Acrothele*. *Proceedings of the United States National Museum* 19: 707–718.

Walcott, C.D., 1908. Cambrian geology and paleontology. *Smithsonian Miscellaneous Collections* 53: 53–165.

Walcott, C.D., 1912. Cambrian Brachiopoda. *United States Geological Survey Monographs* 51: 1–872.

Williams, A., 1962. The Barr and Ardmillan Series (Caradoc) of the Girvan District, south-west Ayrshire, with descriptions of the brachiopods. *Memoirs of the Geological Society of London* 3: 1–267.

Williams, A., S.J. Carlson, C.H.C. Brunton, L.E. Holmer & L.E. Popov, 1996. A supra-ordinal classification of the Brachiopoda. *Philosophical Transactions of the Royal Society of London* 351: 1171–1193.

Williams, A., & G.B. Curry, 1985. Lower Ordovician Brachiopoda from the Tourmakeady Limestone, Co. Maye, Ireland. *Bulletin of the British Museum (Natural History), Geology* 38: 183–269.

Williams, A., & G.B. Curry, 1991. The microarchitecture of some acrotretide brachiopods. In *Brachiopods Through Time*, ed. D.I. MacKinnon, D.E. Lee & J.D. Campbell, pp. 133–140. Rotterdam: A.A. Balkema.

Wright, A.D., 1963. The fauna of the Portrane Limestone 1. The inarticulate brachiopods. *Bulletin of the British Museum (Natural History), Geology* 8: 221–254.

Manuscript received 4 June 2002, revised 3 September 2002 and accepted 5 September 2002.

Associate Editor: G.D. Edgecombe.

INSTRUCTIONS TO AUTHORS

Manuscripts must be submitted to the Editor. Authors will then liaise with a nominated Associate Editor until a work is accepted, rejected or withdrawn. All manuscripts are refereed externally.

Only those manuscripts that meet the following requirements will be considered for publication.

Submit three hard copies and one electronic file. Attach a **cover sheet** showing: the title; the name, address and contact details of each author; the author responsible for checking proofs; a suggested running head of less than 40 character-spaces; the number of figures, tables and appendices; and total word count. Manuscripts must be complete when submitted.

Electronic copy is stripped and reconstructed during production, so authors should avoid excessive layout or textual embellishments; a single font should be used throughout (Times or Times New Roman are preferred). **Tables** and **figures** should be numbered and referred to in numerical order in the text.

All copy is manipulated within a Windows (not Mac) environment using Microsoft and Adobe software. Electronic submissions should be entirely readable using the latest version of Microsoft Word. Avoid using uncommon fonts. The submitted manuscript should be printed from the most recent version of electronic copy.

A manuscript should be prepared using recent issues as a guide. There should be a **title** (series titles should not be used), **author**(s) with their institutional and e-mail addresses, an **abstract** (should be intelligible by itself, informative not indicative), **introduction** (should open with a few lines for general, non-specialist readers), **materials and methods**, **results** (usually subdivided with primary, secondary and sometimes tertiary-level headings), **discussion**, **acknowledgments** and **references**. If appropriate, an appendix may be added after references. An index may be called for if a paper is very large (>55,000 words) and contains many indexible elements.

In the **titles** of zoological works the higher classification of the group dealt with should be indicated. Except for common **abbreviations**, definitions should be given in the materials and methods section. Sentences should not begin with abbreviations or numerals. Metric units must be used except when citing original specimen data. It is desirable to include **geo-spatial coordinates**; when reference is made to them, authors must ensure that their format precludes ambiguity, in particular, avoid formats that confuse arcminutes and arcseconds. If known, authors should indicate how geo-spatial coordinates are derived, for example, from GPS, map, gazetteer, sextant, or label.

Label and specimen data should, as a minimum requirement, indicate where specimens are deposited. Original specimen data—especially that of type material—is preferred over interpreted data. If open to interpretation, cite original data between quotation marks or use "[sic]".

Rules of the International Code of Zoological Nomenclature must be followed; authors must put a very strong case if Recommendations are not followed. Authorities, including date, should be given when a specific name is first mentioned except where **nomenclature** follows an accepted standard (in which case that standard should then be cited). The publication by the authority must be included in the Reference section, unless explicit mention is made of a standard work where such information can be found. When new taxa are introduced in works having **multiple authors**, the identity of the author(s) responsible for the new name(s) and for satisfying the criteria of availability, should be made clear in accordance with recommendations in Chapter XI of the Code (1999). In the view of the Editorial Committee, a scientific name with more than two authors is unwieldy and should be avoided. **Keys** are desirable; they must be dichotomous and not serially indented. **Synonymies** should be of the short form: taxon author, year, pages and figures. A period and dash must separate taxon and author except in the case of reference to the original description. Proposed type material should be explicitly designated and, unless institutional procedure prohibits it, registered by number in an institutional collection.

Authors should retain **original artwork** until it is called for. Previously published illustrations will generally not be accepted. Artwork may be submitted either as hard copy or as **digital images**. The author, figure number and orientation must be clearly marked on each piece of artwork. Extra costs resulting from **colour** production are charged to the author. All artwork must (*a*) be rectangular or square and scalable to a width of 83 mm (one text column) or 172 mm (both text columns) and any depth up to 229 mm (the number of lines in a caption limits depth); (*b*) have **lettering** similar to 14 point upper case normal Helvetica in final print; and (*c*) have **scale bars**, the lengths of which should be given in the caption.

Hard copy submissions must meet the following requirements: (*a*) they must be no larger than A4; (*b*) the dimension of artwork should not be less than the desired final size; (*c*) **halftones** and **line-drawings** must be mounted separately; (*d*) lettering, scales and edges—especially of halftone artwork—must be sharp and straight; (*e*) photographic **negatives** can be used in production, but *positive* images are, of course, required by referees.

Halftone, colour or black and white line images may be submitted electronically once a work has been accepted for publication; all such images must be presented in a file format, such as TIFF, suitable for *Adobe Photoshop* version 5.0 or later. Halftone and colour images must be at a minimum **resolution** of 300 dpi (not higher than 400 dpi) at final size and all labelling must be sharp. Black and white line images must be at a minimum resolution of 1200 dpi at final size.

When reference is made to **figures** in the present work use Fig. or Figs., when in another work use fig. or figs.; the same rule applies to tables. Figures should be numbered and referred to in numerical order in the text.

Authors should refer to recent issues of the *Records of the Australian Museum* to determine the correct format for listing **references** and to *The Chicago Manual of Style* to resolve other matters of style.

Certain **anthropological manuscripts** (both text and images) may deal with culturally sensitive material. Responsibility rests with authors to ensure that approvals from the appropriate person or persons have been obtained prior to submission of the manuscript.

Stratigraphic practice should follow the *International Stratigraphic Guide* (second edition) and *Field Geologist's Guide to Lithostratigraphic Nomenclature in Australia.*

The Editor and Publisher reserve the right to modify manuscripts to improve communication between author and reader. Authors may make essential corrections only to final **proofs**. No corrections can be accepted less than six weeks prior to publication without cost to the author(s). All proofs should be returned as soon as possible. There are no page **charges**. Authors of a paper in the *Records* receive a total of 50 free **offprints**. Authors of a *Supplement* or *Technical Report* receive a total of 25 free offprints.

All authors must agree to publication and certify that the research described has adhered to the Australian Museum's *Guidelines for Research Practice* (www.amonline.net.au/about/research_ethics.htm)—or those of their home institution providing they cover the same issues, especially with respect to authorship and acknowledgment. Agreement can be registered by signing and returning the Editor's letter that confirms our receipt of a submitted manuscript. While under consideration, a manuscript may not be submitted elsewhere.

More information and examples are available at our website:

www.amonline.net.au/publications/

Stock no. 003R55B

RECORDS OF THE AUSTRALIAN MUSEUM 2003 Vol. 55 No. 2

CONTENTS

AUSTRALIAN MUSEUM

Publications may be purchased at the Australian Museum Shop or online at:
www.amonline.net.au/shop/